



Multi-scale Spatial Analysis of the Water-Food-Climate Nexus in the Nile Basin using Earth Observation Data

Inaugural-Dissertation

zur

Erlangung des Doktorgrades

der Mathematisch-Naturwissenschaftlichen Fakultät

der Universität zu Köln

vorgelegt von

Muhammad Saeed Ahmed Khalifa

aus Sudan

Köln 2020

Berichterstatter:

Prof. Dr. Karl Schneider

Institute of Geography, University of Cologne

Prof. Dr. Georg Bareth

Institute of Geography, University of Cologne

Prof. Dr. Lars Ribbe

*Institute for Technology and Resources Management in
the Tropics and Subtropics (ITT), TH Köln (University
of Applied Sciences)*

Tag der letzten mündlichen Prüfung: 29.05.2020

Dedication

To the new generation of Sudan who conquers fear and fights to pursue freedom, peace, and justice, and to the martyrs of the December revolution who sacrificed their lives for a new Sudan.

Acknowledgment

The Ph.D. journey has been a truly life-changing experience that enabled me to deepen my knowledge and to discover my potentialities, and it would not have been possible to accomplish without the inspiration, support, and guidance that I received from many people. Throughout the preparation of this dissertation, I have received a great deal of support and assistance from my respected supervisors. I would like to thank my supervisors, Prof. Dr. Karl Schneider, Prof. Dr. Lars Ribbe and Dr. Nadir Ahmed Elagib for generously offering their valuable time, wisdom advice and whose expertise made all the difference in this dissertation. A special thanks to Dr. Elagib for seeing in me a promising researcher and for encouraging me a few years ago to pursue a Ph.D. degree, and I am deeply indebted to Prof. Ribbe and Prof. Schneider for offering me the chance and believing in my abilities. I sincerely thank Prof. Dr. Georg Bareth for consenting to act as a second examiner of this dissertation, Prof. Dr. Bülent Tezkan for chairing the examination committee, and Dr. Wolfgang Korres for accepting to take part in the committee.

This work would not have been possible without the financial support of the Centers for Natural Resources and Development (CNRD). I am especially indebted to Dr. Rui Pedroso, Coordinator of the CNRD doctoral program (DNRD) for his continuous support throughout my Ph.D. studies. I would like to express my gratitude to all staff at the Institute for Technology and Resources Management in the Tropics and Subtropics (ITT), TH Köln, especially, Ms. Karola Schmelzer, Mr. Alexander Klein, Ms. Nora Ellen Lucidi, Mr. Joschka Thurner and Ms. Ricarda Pedroso for their continuous and unlimited support. My gratitude to my colleagues, Uyen, Teresa, Samah, Amrita, Van, Elmoiz, Nazmul, Tun, Zryab, Oscar, Asraful latif and Pedro for being such good friends and for the knowledge that we shared during our personal and scholarly interactions.

A special thanks go to my colleague, Dr. Mirja Michalscheck, for her kindness in translating the dissertation's abstract into the German language. My gratitude is extended to Dr. Wolfgang Korres for his kindness and the support and guidance that he gave me during the preparation of the scientific work of chapter 4 of this dissertation. I would like also to thank Ms. Azeb Mercha, Dr. Omer Elawad, and all staff at the Eastern Nile Technical Regional Office (ENTRO) for their kind support and for hosting me during my field work in Ethiopia. I thank Dr. Islam Sabry Al Zayed for sharing GIS data and for his kind support and Dr. Alexandra Nauditt, Eng. Abu Bakr Eltagi, and Dr. Bashir Mohammed Ahmed for the fruitful discussions.

I would like to thank all the local farmers in the Gezira Irrigation Scheme, Central Sudan, who took part in the survey conducted within the framework of this research and the block inspectors for their generous assistance during the field survey. My gratitude is also extended to many institutions in Sudan; the Gezira Scheme Board (GSB), Hydraulic Research Center (HRC), Agricultural Research Corporation (ARC), Water Research Center of the University of Khartoum, Ministry of Water Resources, Electricity and Irrigation, for providing some of the needed data. I am immensely grateful to the editors and the anonymous reviewers of the journals of Science of the Total Environment, Hydrological Sciences Journal, and Agriculture and Forest Meteorology for reviewing the earlier publication manuscripts and for their constructive remarks which helped to enhance the publications substantially.

I would also like to say a heartfelt thank you to my mother, father, sisters, and brother for always believing in me and encouraging me to follow my dreams. Last but not least to Enas, my loving and supportive wife, who has been by my side throughout the Ph.D. journey, living every single moment of it with great patience and honest advice, and without whom, I would not have had the courage to embark on this journey in the first place, and to our little flower, Yazan, for being such a good baby that past eleven months giving us a bright smile every new morning.

Table Contents

	Page
Table of contents	iv
List of figures	viii
List of tables	xii
List of abbreviations	xiii
Abstract	xv
Zusammenfassung	xvii
Chapter 1: General introduction	1
1.1. Background	2
1.2. Problem statement and motivation	2
1.3. Earth Observation for water, food, and climate: State of the art	4
1.4. Research concept and research questions	5
1.5. Structure of the dissertation	7
1.6. Research publications supporting this dissertation	10
Chapter 2: Regional context	12
2.1. The Nile River Basin	13
2.2.1. Physical setting	13
2.2.2. Water resources and water use patterns	15
2.1.3. Agriculture and food production	19
2.1.4. The Nile's transboundary conflict	21
2.2. Future dynamics and expected changes in the Nile region	23
2.3. Implications of future changes	24
2.4. Conclusion	27
Chapter 3: Sensitivity and response of vegetation to climate variability	28
Abstract	29
3.1. Introduction	29
3.2. Materials and data	32
3.2.1. Area of study and its importance	32
3.2.2. Data and methods	34
3.2.2.1 Primary productivity	35
3.2.2.2. Normalized Difference Vegetation Index	36
3.2.2.3. Precipitation	37
3.2.2.4. Temperature	37
3.2.2.5. Actual evapotranspiration (ET _a)	37

3.2.2.6. Drought index data	38
3.2.2.7. Land cover	39
3.2.2.8. Correlation of the variables and calculation of water and carbon uses efficiency	39
3.3. Results and discussion	41
3.3.1. Climate conditions during 2000-2013	41
3.3.2. Net primary productivity during 2000-2013	43
3.3.3 Variation of primary productivity and correlation with climate variability ...	44
3.3.4. Drought impact on primary productivity	47
3.3.5. Intra-annual variability of primary productivity and drought	48
3.3.6. Water Use Efficiency (WUE)	49
3.3.7. Carbon Use Efficiency (CUE)	51
3.3.8. Relevance to food security and climate change	53
3.4. Limitation and uncertainty	54
3.5. Conclusion	56
Chapter 4: Consistency of public-domain precipitation products	58
Abstract	59
4.1. Introduction	59
4.2. Data and materials	63
4.2.1. Study area	63
4.2.2. Data description	64
4.3 Methods	65
4.3.1. Data processing	65
4.3.2. Interpolation of ground-based precipitation measurements	65
4.3.3. Inter-comparison and evaluation of the precipitation products	66
4.3.4. Clustering and merging of the products	66
4.4. Results and discussion	68
4.4.1. Evaluation of gridded methods	68
4.4.2. Statistical characteristics of public-domain precipitation products	69
4.4.3. Pixel-to-pixel inter-comparison between public-domain precipitation products	71
4.4.4. Pixel-to-point validation of the public-domain precipitation products	74
4.4.5. Hierarchical Clustering and Principal Component Analyses	76
4.4.6. Sensitivity and stability of clusters	79
4.4.7. Merging of products	80
4.5. Conclusion	81

Chapter 5: Yield gap and pathways for sustainable intensification in irrigated schemes	86
Abstract	87
5.1. Introduction	87
5.2. Materials and methods	89
5.2.1. Gezira Irrigation Scheme	89
5.2.2. Data	90
5.2.3. Methods	92
5.2.3.1. Processing of gridded data	93
5.2.3.2. Calculation of the productivity gap	93
5.2.3.3. Standardization of vegetation index and classification of the administrative groups	94
5.2.3.4. Field survey	94
5.2.3.5. Statistical analysis	95
5.3. Results	95
5.3.1. Spatio-temporal variation of productivity gap	95
5.3.2. Factors controlling productivity in the scheme	100
5.3.2.1 Physical factors	100
5.3.2.2. Socio-economic factors	104
5.3.2.3. Management and field practices	104
5.4. Discussion	105
5.4.1. Satellite-based productivity gap	105
5.4.2. Yield gap of sorghum	106
5.4.3. Factors influencing agricultural productivity	106
5.5. Conclusion	108
Chapter 6: Crop vulnerability and resilience to climate in rainfed schemes	111
Abstract	112
6.1. Introduction	112
6.2. Materials and methods	115
6.2.1. Study area	115
6.2.2. Data	117
6.2.3. Processing of gridded data	119
6.2.4. Drought assessment	119
6.2.5. Analysis of regime shift, vulnerability and resilience of sorghum production	121
6.2.6. Vegetation productivity indices	122
6.2.7. Trend analysis	123

6.3. Results and discussion	123
6.3.1. Drought and wetness during the period 1941–2015	123
6.3.2. Performance of regional sorghum production during 1970–2016	126
6.3.3. Resilience and vulnerability of sorghum yield to climate during 1970-2015	126
6.3.4. Case of El Gedaref State	129
6.3.4.1. Temporal variation in climatic factors and productivity indices	129
6.3.4.2. Spatial variation in climatic and vegetation-related drought indices	129
6.3.4.3. Production level as a function of low precipitation	133
6.4. Conclusion	134
Chapter 7: Synopsis, synthesis and perspectives	136
7.1. Synopsis	137
7.2. Synthesis	137
7.3. Perspectives	140
7.4. Final remarks	143
References	145
Appendices	172
Appendix A: Chapter 2	173
Appendix B: Chapter 3	174
Appendix C: Chapter 4	177
Appendix D: Chapter 5	178
Appendix E: Erklärung	184
Appendix F: Curriculum Vitae (CV)	185

List of figures

	Page
Figure 1.1. Time series of 30-years (1989-2018) of the annual total number of publications found in the Scopus database related to the topic of using Earth observation for water, food, and climate. Different search strategy syntaxes were used to cover 5 main research focuses. The analysis was conducted on 7 October 2019	5
Figure 1.2. The conceptual framework adopted in the current research	8
Figure 2.1. Location map of the Nile Basin (a) the Nile basin with 11 riparian countries, (b) Eastern Nile basin with four main sub-basins	13
Figure 2.2. Land cover map created based on Globcover 2009 data	14
Figure 2.3. Long-term monthly average rainfall (1970-2000) over the Nile Basin. These maps are created based on the data of WorldClim (Fick and Hijmans, 2017)	16
Figure 2.4. Long-term monthly average temperature (1970-2000) over the Nile Basin. These maps are created based on the data of WorldClim (Fick and Hijmans, 2017)	16
Figure 2.5. Schematic representation of the water fluxes (inflow, evaporative losses and outflow) in the Nile Basin (Blackmore and Whittington, 2008)	17
Figure 2.6. Water use quantities (km ³ /year) in the Nile Basin countries. Water use is subdivided into agricultural, industrial and municipal uses. Data are obtained from the AQUASTAT database	20
Figure 2.7. Time series (1961-2017) of cereal crops statistics in the Nile Basin countries: (a) harvested area, (b) yield, and (c) production. Data are obtained from FAOSTAT database	21
Figure 2.8. Time series (1950-2019) of population estimation in the Nile riparian countries along with future forecasts until 2060. The future forecasts are based on three fertility projections (low, medium and high). Data of these graphs are obtained from the population division of the UN DESA (2019) database	25
Figure 2.9. Current (2005) and projected (2030 and 2050) agricultural water use in the Nile basin countries. This figure is created based on tabulated data obtained from FAO, 2011	25
Figure 3.1. Location map of the East of Africa region showing the boundaries of the two case studies (Sudan and Ethiopia) and the different land cover types located in the region. Landcover data in this map are that of MCD12Q1 product	34
Figure 3.2. The total area of each land cover in Sudan and Ethiopia as appear in the MDC12Q1 product	34
Figure 3.3. Flowchart of the methodological procedure followed in this study to correlate the inter-annual variability in NPP, CUE and WUE and their response to climate variability and drought conditions	40
Figure 3.4. Temporal and spatial variation in climate variables in the two countries considered in this study: (a) precipitation, (b) Actual evapotranspiration and (c) temperature	42
Figure 3.5. Time series of SPEI for in the study area with different time steps 1, 3, 6 and 12 months, (a) Sudan and (b) Ethiopia	43

Figure 3.6. (a) Spatial variation of the average NPP in Sudan and Ethiopia as modeled by MOD17. (b) Multiyear annual average (2000-2013) of NPP for land cover types in Sudan and Ethiopia	44
Figure 3.7. The anomaly of inter-annual NPP in different land covers in Sudan and Ethiopia. Anomalies in climate conditions (precipitation, temperature, and drought (SPEI)) prevailing in each land cover type are plotted	45
Figure 3.8. The spatial pattern of correlation between NPP and climate variables for the period 2000-2013	46
Figure 3.9. Monthly GPP, NDVI and precipitation during the wet year 2007 and the dry 2009 for croplands and grasslands in the two countries	49
Figure 3.10. Time series of WUE of the land cover types in Sudan and Ethiopia	50
Figure 3.11. Time series of CUE of the land cover types in Sudan and Ethiopia	52
Figure 3.12. Quality control of NPP data for each land cover in Sudan and Ethiopia	55
Figure 4.1. The Blue Nile Basin (BNB): (a) location and riparian countries, (b) rain gauges used in the current research and corresponding Thiessen polygons and their areas in km ² , (c) topography	63
Figure 4.2. Spatial distribution of multi-year average precipitation using four gridding methods: (a) Thiessen Polygons, (b) Inverse Distance Weighting (IDW), (c) Kriging and (d) precipitation-elevation regression	69
Figure 4.3. Multi-year (2001-2005) mean annual precipitation over the Blue Nile Basin as estimated by the 17 public-domain precipitation products and the reference datasets; i.e., Regression PP	70
Figure 4.4. Box-Whisker plots of all pixel values on monthly and annual precipitation of the 17 precipitation products and the Regression PP, showing the mean and median (middle horizontal lines and asterisks inside the boxes, respectively). The lower and upper box boundaries represent the 1st and 3rd quartiles. Outliers in pixel values are shown as isolated points below and above Whiskers.	72
Figure 4.5. Spatial distribution of the multi-year (2001-2005) mean annual precipitation over the Blue Nile Basin as depicted by 17 public-domain precipitation products and a Regression PP	73
Figure 4.6. Plots of pixel-to-point evaluation, on a monthly scale (in mm units), of precipitation of the 17 precipitation products using rain gauges data as a reference (in mm). Values of the four measures of fit, i.e., R ² , RMSE, NSE, and %BIAS are indicated. Each symbol represents one of the rain gauges used in the current validation	75
Figure 4.7. Hierarchical clustering of the 17 precipitation products with heatmaps for the annual and monthly precipitation using the multi-year average over the period 2001-2005. The connecting level shown on the left represents the relationship between the products. Heatmaps show the relative differences (scaled in unit variance) between the pixel values among the products. The grids are arranged from left as the upper left corner to right as the lower right corner of the basin (Fig. 4.1)	78
Figure 4.8. Two-dimensional plots of the two first Principal Components (PCs). The distance between the points approximates the relative similarity/dissimilarity between the products. The data used to create these plots are the grid values of the multi-year annual and monthly averages over the period 2001-2005	79

Figure 4.9. Three examples (annual, February and August) of the sensitivity analysis conducted on the precipitation products to check the stability of clusters. The multi-year average (2001-2005) of the reference dataset (Regression PP) is used to validate the results of this stability analysis. Products that are clustered together were merged to produce precipitation estimates. For the names of the products in each cluster refer to the associated table (Table 4.2)	82
Figure 5.1. Location map of the Gezira Scheme showing the Administrative Groups (AGs) and the two main irrigation canals. The source of irrigation water is Sennar reservoir at the south-eastern border of the scheme. Locations of the selected field survey blocks are shown as dots	89
Figure 5.2. Flowchart of the approach developed in the current study	92
Figure 5.3. Spatial productivity gap for the Gezira Scheme based on (a) iNDVI and (b) iFAPAR	97
Figure 5.4. Statistical measures of pixel-to-pixel productivity gap based on iNDVI (a and b) and iFAPAR (c and d) represented by Box-Whisker plot	98
Figure 5.5. Average productivity gap for the Gezira Scheme and the administrative groups: (a) time series based on iNDVI, (b) time series based on iFAPAR and (c) multi-year average over 2001-2016. The line colors in (a) and (b) correspond to the colors used for the administrative groups in Figure 5.1	99
Figure 5.6. Average yield and maximum yield of sorghum achieved by all respondent farmers in each block selected for the field survey	100
Figure 5.7. Dependence of crop productivity index (iNDVI) on the average distance of the administrative groups of the Gezira Scheme to Sennar Reservoir: (a) average seasonal iNDVI (2001–2016) and distance for each administrative group and (b) Spearman’s Rho of the correlation between the two variables	101
Figure 5.8. Areal average precipitation using CHIRPS 2.0 precipitation product: (a) over the Gezira Scheme for the years 2000–2016; (b) over the different administrative groups during 2015 and 2016; (c and d) daily precipitation over the scheme during the summer seasons of 2015 and 2016, respectively	102
Figure 5.9. Scatter plot of pixel iNDVI versus total seasonal precipitation: (a) for all years (2001–2016) and (b) multi-year average over the Gezira Scheme	102
Figure 5.10. Spatial distribution of soil properties: (a) pH, (b) organic carbon content (OCC) and (c) bulk density clipped from the original SoilGrids data to the boundaries of the Gezira Scheme. Units of OCC and bulk density are g/kg and g/m ³ , respectively	103
Figure 5.11. Pixel-to-pixel correlation between multi-year (2001–2017) average iNDVI and three soil properties: (a) pH, (b) Organic Carbon Content and (c) bulk density. Spearman’s Rho values of the correlation for each year are shown in d, e, and f for the three soil properties, respectively	103
Figure 5.12. Regression-tree detecting the most important factors that control the average sorghum yield in the Gezira Scheme	105
Figure 5.13. A conceptual framework for sustainable intensification in the Gezira Scheme showing the identified entry points and their proposed measures	109
Figure 6.1. Ranking of the top sorghum-producing countries in terms of (a) harvested area, (b) production and (c) yield. The data represent the multi-year averages (1961-2016) calculated from FAOSTAT data	115

Figure 6.2. Location map of the study area, regional states, and meteorological stations	116
Figure 6.3. Polygons represented by the meteorological stations as constructed by GIS	121
Figure 6.4. Components of the multi-criterial drought index (MCDI) for the stations under consideration obtained using the ratio of rainfall to grass reference evapotranspiration: a) Dry spell; b) Drought severity; c) Time frequency	124
Figure 6.5. Regional drought assessed by polygon-based average a) multi-criterial drought index (MCDI) compared to b) Standardized Precipitation Index (SPI)	125
Figure 6.6. Time series of particulars of mechanized sorghum farming and corresponding regime shift detection: a) Planted area; b) Harvested area; c) Area lost at harvest; d) Harvested-to-planted area ratio; e) Production; f) Yield. M = Million ...	127
Figure 6.7. The occurrence of drought and wetness resilience and vulnerability of sorghum	128
Figure 6.8. Temporal areal average growing season (a) precipitation, temperature and potential evapotranspiration (PET) and (b) UNEP aridity index (AI), c) productivity index and d) sorghum yield for El Gedaref State	130
Figure 6.9. Spatial distribution of drought zones in El Gedaref State assessed by the Standardized Multi-criteria Drought index (SMCDI) for the growing season	131
Figure 6.10. Spatial distribution of vegetation indices across El Gedaref State for the growing season (June to October): a) productivity index (iNDVI) and b) Modified Vegetation Condition Index (MVCI)	132
Figure 6.11. Percentage area of El Gedaref State under drought and/or low productivity condition as measured by SMCDI > 0.11, iNDVI < 5 and MVCI < 40%	133
Figure 6.12. Sorghum production level under drought versus low growing season (June to October) rainfall for El Gedaref State. PL is the production level and RF stands for rainfall	134

List of tables

	Page
Table 1.1. List of research publications supporting this dissertation	10
Table 1.2. Contribution of the papers to the research questions (Qs) of the current dissertation	11
Table 2.1. List of major dams in the Nile Basin with their storage capacity	18
Table 2.2. Annual water balance (2005-2010) as estimated by Bastiaanssen et. al. (2014) using remote sensing over different sub-basins of the Nile basin	20
Table 3.1. Review of some research using MOD17 data of NPP and GPP	33
Table 3.2. Specification of the data used in this study	36
Table 3.3. Categories of the SPEI scale	39
Table 4.1. List and characteristics of the 17 PPs considered in the current study	64
Table 4.2. Product clusters resulted from stability analysis on annual and monthly (February and August) time scales	83
Table 5.1. List of primary information collected for the current research through a questionnaire	91
Table 5.2. Characteristics of secondary data collected from public-domain sources and official authorities in Sudan	91
Table 5.3. Classification of the administrative groups (AGs) of the Gezira based on the standardized vegetation index (SVI) derived from z-scores of iNDVI and iFAPAR. SVI classes are obtained from Peters et. al. (2002)	96
Table 6.1. Characteristics of the gridded data used in the current study	118
Table 6.2. Drought and wetness classes for the standardized multi-criteria drought index (SMCDI)	125
Table 6.3. Summary of results of the regime shift analysis	127

List of abbreviations

AG	Administrative Group
ANPP	Aboveground Net Primary Productivity
APAR	Absorbed Photosynthetically Active Radiation
ARC	African Rainfall Climatology
BNB	Blue Nile Basin
CFA	The Cooperative Framework Agreement
CFSR	Climate Forecast System Reanalysis
CHG	Climate Hazard Group
CHG-UCSB	Climate Hazard Group, University of California, Santa Barbara
CHIRPS	Climate Hazards Group InfraRed Precipitation with Station data
CHRS-UCI	Center for Hydrometeorology and Remote Sensing, University of California, Irvine
CMORPH	Climate Prediction Center MORPHing Technique
CO ₂	Carbon dioxide
CPC	Climate Prediction Center
CUE	Carbon Use Efficiency
CRU TS	Climatic Research Unit Time-Series
CV	Coefficient of Variation
DAS	Data Assimilation System
DEM	Digital Elevation Model
DN	Digital Numbers
DR	Drought resilient
DS	Dry spell
DV	Drought vulnerable
DWD	Deutscher Wetterdienst
EO	Earth Observation
ERA	ECMWF Re-Analysis
EROS	Earth Resources Observation and Science
ET _a	Actual Evapotranspiration
FAO	Food and Agriculture Organization of the United Nations
FAPAR	Fraction of Absorbed Photosynthetically Active Radiation
FEWS NET	Famine Early Warning Systems Networks
GADM	Database of Global Administrative Areas
GEOS	Goddard Earth Observing System
GERD	Grand Ethiopian Renaissance Dam
GIS	Geographic Information System
GLDAS	Global Data Assimilation Systems
GPCC	Global Precipitation Climatology Center
GPCP	Global Precipitation Climatology project
GPCP 1DD	Global Precipitation Climatology Project, 1 degree
GPP	Gross Primary Productivity
Gwh	Gigawatt hours
ha	Hectare
HCA	Hierarchical Clustering Analysis
iFAPAR	Integrated Fraction of Absorbed Photosynthetically Active Radiation
IGBP	The International Geosphere-Biosphere Programme
iNDVI	Integrated Normalized Difference Vegetation Index
JRC	Joint Research Centre
km ³ /yr	Cubic kilometer per year (billion cubic meters per year)
LBNB	Lower Blue Nile Basin
MCDI	Multi-Criteria Drought Index
MERRA	Modern Era Retrospective-analysis for Research and Applications
MODIS	Moderate Resolution Imaging Spectroradiometer
MPP	Merged Precipitation Product
MSWEP	Multi-Source Weighted-Ensemble Precipitation
MVC	Maximum Value Composite
MVCI	Modified Vegetation Condition Index
MW	Megawatt
NASA	National Aeronautics and Space Administration
NB	Nile Basin

NBI	The Nile Basin Initiative
NCEP–NCAR	National Centers for Environmental Prediction–National Center for Atmospheric Research
NDVI	Normalized Difference Vegetation Index
NNR	Near-normal climate resilient
NNV	Near-normal climate vulnerable
NPP	Net Primary Productivity
NW Sennar	North West Sennar
OCC	Organic Carbon Content
P	Precipitation
PCA	Principal Component Analysis
PERSIANN-CDR	Precipitation Estimation from Remotely Sensed Information using Artificial Neural Networks - Climate Data Record
PERSIANN-CSS	Precipitation Estimation from Remotely Sensed Information using Artificial Neural Networks -Cloud Classification System estimation
PET	Potential Evapotranspiration
Pg C	Petagram carbon (10 ¹⁵ grams)
PGF	Princeton University Global Meteorological Forcing
PP	Public-domain Precipitation Product
QC	Quality Control
RFE	Rainfall Estimation
Rho (ρ)	Spearman's coefficients
S	Drought severity
SAI	Standardized Anomaly Index
SDGs	Sustainable Development Goals
SI	Sustainable Intensification
SMCDI	Standardized Multi-Criteria Drought Index
SPEI	Standardized Precipitation Evapotranspiration Index
SPI	Standardized Precipitation Index
SPOT	Satellite Pour l'Observation de la Terre
SRTM	Shuttle Radar Topography Mission
SVI	Standardized Vegetation Index
T	Temperature
TAMSAT	Tropical Applications of Meteorology Using Satellite Data and Ground-Based Observations
TF	Time relative frequency of drought
THRG-PU	Terrestrial Hydrology Research Group - Princeton University
TRMM	The Tropical Rainfall Measuring Mission
UBNB	Upper Blue Nile Basin
UDel	University of Delaware
UEA	University of East Anglia
UNEP AI	United Nations Environment Programme Aridity Index
USA	United States of America
USGS	United States Geological Survey
VCI	Vegetation Condition Index
WFC Nexus	Water-Food-Climate Nexus
WR	Wet resilient
WUE	Water Use Efficiency
WV	Wet vulnerable

* For an improved understanding of the text, the abbreviation might be spelled out at several places throughout the dissertation.

Abstract

Securing enough water and food for everyone is a great challenge that the humanity faces today. This challenge is aggravated by many external drivers such as population growth, climate variability, and degradation of natural resources. Solutions for weak water and food securities require holistic knowledge of the different involved drivers through a nexus approach that looks at the interlinkages and the multi-directional synergies to be promoted and increased and trade-offs to be reduced or eliminated. In particular, the interlinkages between water, food, and climate, the so-called Water-Food-Climate Nexus (WFC Nexus) is critical for the given challenge in many regions around the world such as the Nile Basin (NB). Studying the WFC Nexus synergies and trade-offs might provide entry points for the required interventions that are potential to induce positive impacts on water and food securities. However, these synergies and trade-offs are not well known due to factors such as the complexity of the interactions which involve many dimensions within and across spatial and temporal domains and unavailability of reliable ground observations that could be used for such analysis. Therefore, multidisciplinary research that encompasses different methodologies and employs datasets with adequate spatial and temporal resolutions is required.

The recent advancement in Earth Observation (EO) sensors and data processing algorithms have resulted in the accumulation of big data that are produced in rates faster than their usage in solving real challenges such as the one that is in the focus of the current research. The availability of public-domain datasets for several parameters with spatial and temporal coverage offers an excellent opportunity to discover the WFC Nexus interlinkages. To this end, the main goal of the current research is to employ EO data derived from public-domain datasets and supplemented with other primary and secondary data to identify WFC Nexus synergies and trade-offs in the NB region, taking the agricultural systems in Sudan as a central focus of this assessment. By concentrating mainly on the agricultural systems in Sudan, which are characterized by low performance and efficiency despite the huge potentials for food production, the current research provides a representative case study that could deliver helpful and transferrable knowledge to many areas within and outside the NB region.

In the current research, multi-scale analysis of the WFC Nexus synergies and trade-offs was conducted. The assessment involved investigations on a country scale as a strategic level, and on river basin, agricultural scheme (both irrigated and rainfed systems) and field scales as operational levels. On a country scale, a general analysis of the vegetation's Net Primary Productivity (NPP) and Water and Carbon Use Efficiencies (WUE and CUE, respectively) in different land cover types was carried out. A comparison between the land cover types in Sudan

and Ethiopia was conducted to understand and compare the impact of inter-annual climate variability on the NPP, WUE and CUE indicators of these different land cover types under relatively different climate regimes. The results of this analysis indicate low magnitude of the three indicators in the land cover types that are in Sudan compared to their counterparts in Ethiopia. Moreover, the response of these indicators to climate variability varies widely among the land cover types. In addition, land cover types such as forests and woody savannah represent important natural sinks for the atmospheric CO₂ that need to be protected. These observations suggest the need for effective policies that enhance crop productivity, especially in Sudan, and at the same time ensure preserving the land cover types that are important for climate change mitigation.

On a river basin scale, which represented by the Blue Nile Basin (BNB), precipitation estimation is of utmost importance, as it is not only the main source of water in the basin but also because precipitation variability is controlling food production in the agricultural systems, especially in the rainfed schemes. The high spatial and temporal variation in precipitation within the BNB suggests the need for water storage and water harvesting be promoted and practiced. This would ensure water transfer spatially from wet to dry areas and temporally from wet to dry seasons.

As a major staple cereal crop in Sudan, the performance of sorghum production in irrigated and rainfed schemes was investigated on agriculture schemes and field scales. A noticeable low and unstable sorghum yield is detected under both agricultural systems. This low performance represents a serious challenge, not only for food production but also for water availability. The current low performance was found to be controlled by many factors of physical, socio-economic and management nature. As many of these factors are closely linked, effectively addressing some of them might induce positive impacts on the other controlling factors. To conclude, the identified synergies and trade-offs of the WFC Nexus could be used as entry points to increase the efficiency of water use and bridge the crop yield gap. Even simple interventions in the field might induce positive effects to the total crop production of the agricultural schemes and water use efficiency. The increase of water availability in the river basin and improved production in the schemes would enhance the overall water and food security in the country and would minimize the need to convert land covers that are important for climate change mitigation into croplands. This paradigm shift needs to be done through a comprehensive sustainable intensification (SI) framework that is not only aimed at increasing crop yield but also targets promoting a healthy environment, improved livelihood, and a growing economy.

Zusammenfassung

Genügend Wasser und Nahrung für alle Menschen zu sichern, ist eine große Herausforderung, der sich die Menschheit heute gegenüber sieht. Diese Herausforderung wird durch viele externe Faktoren wie Bevölkerungswachstum, Klimavariabilität und die Verschlechterung der natürlichen Ressourcenbasis verschärft. Lösungen, um die geringe Wasser- und Nahrungsmittelsicherheit zu verbessern, erfordern ein ganzheitliches Wissen über die verschiedenen beteiligten Treiber durch einen Nexus-Ansatz, welcher sektorübergreifende Zusammenhänge untersucht, deren multidirektionale Synergien fördert und skaliert sowie Kompromisse reduziert oder beseitigt. Insbesondere die Zusammenhänge zwischen Wasser, Nahrung und Klima, der sogenannte Wasser-Nahrung-Klima-Nexus (Engl.: WFC Nexus), sind für die gegebenen Herausforderung in vielen Regionen der Welt, wie auch dem Nilbecken (NB), von entscheidender Bedeutung. Die Untersuchung der WFC Nexus-Synergien und Kompromisse könnte Ansatzpunkte für erforderliche Interventionen liefern, die potenziell positive Auswirkungen auf die regionale Wasser- und Lebensmittelsicherheit haben können. Diese Synergien und Kompromisse sind jedoch aktuell wenig bekannt, aufgrund von Faktoren wie der Komplexität der Wechselwirkungen, welche viele Dimensionen innerhalb und über räumliche und zeitliche Domänen umfassen sowie der Nichtverfügbarkeit zuverlässiger Beobachtungen, die für eine solche Analyse verwendet werden könnten. Daher ist eine multidisziplinäre Forschung erforderlich, die verschiedene Methoden umfasst und Datensätze mit angemessenen räumlichen und zeitlichen Auflösungen verwendet.

Die jüngsten Fortschritte bei Erdbeobachtungssensoren (EBS) und Datenverarbeitungsalgorithmen haben dazu geführt, dass sich große Datenmengen ansammeln, die schneller erzeugt werden, als sie zur Lösung realer Herausforderungen, wie derjenigen, auf die sich die aktuelle Forschung konzentriert, benötigt werden. Die neue Verfügbarkeit und Qualität öffentlich zugänglicher und relevanter Datensätze bietet eine hervorragende Gelegenheit, die WFC-Nexus-Verknüpfungen weiter zu erforschen. Zu diesem Zweck besteht das Hauptziel der aktuellen Forschung darin, EBS-Daten zu verwenden, die aus öffentlich zugänglichen Datensätzen abgeleitet und mit anderen primären und sekundären Daten ergänzt wurden, um WFC-Nexus-Synergien und Kompromisse in der NB-Region zu identifizieren, wobei die landwirtschaftlichen Systeme im Sudan im Fokus der Analyse stehen. Die landwirtschaftlichen Systeme im Sudan, zeichnen sich, trotz des enormen Potenzials für die Lebensmittelproduktion, durch geringe Leistung und Effizienz aus. Unsere Studie ist eine repräsentative Fallstudie, die hilfreiches übertragbares Wissen für viele weitere Bereiche innerhalb und außerhalb der NB-Region liefert.

In der aktuellen Forschung wurde eine mehrskalige Analyse der WFC Nexus Synergien und Kompromisse durchgeführt. Die Bewertung umfasste Untersuchungen auf Länderebene, als strategische Ebene, sowie auf der Ebene des Wassereinzugsgebiets, des landwirtschaftlichen Systems (sowohl Bewässerungs- als auch Regenwassersysteme) und der Ebene einzelner landwirtschaftlicher Flächen, als operationelle Ebene. Auf Länderebene wurde eine allgemeine Analyse der Netto-Primärproduktivität (NPP) der Vegetation sowie der Wasser- und Kohlenstoffnutzungseffizienz (WUE bzw. CUE) in verschiedenen Landnutzungstypen durchgeführt. Zusätzlich, wurde ein Vergleich zwischen den Landnutzungstypen im Sudan und in Äthiopien durchgeführt, um die Auswirkungen der jährlichen Klimavariabilität auf die NPP-, WUE- und CUE-Indikatoren dieser verschiedenen Landnutzungstypen unter relativ unterschiedlichen Klimaregimen zu verstehen und zu vergleichen. Die Ergebnisse dieser Analyse zeigen unterschiedliche Auswirkungen von Klimavariabilität auf die drei untersuchten Indikatoren und eine geringe Größenordnung der Indikatoren der Landnutzungstypen im Sudan im Vergleich zu denen in Äthiopien. Darüber hinaus stellen Ökosysteme wie Wälder und Waldsavannen wichtige natürliche und schützenswerte Senken für atmosphärisches CO₂ dar. Diese Beobachtungen legen die Notwendigkeit einer wirksamen Politik nahe, welche die Ernteproduktivität, insbesondere im Sudan steigert, gleichzeitig aber auch die für die Eindämmung des Klimawandels wichtigen Arten der Bodenbedeckung bewahrt.

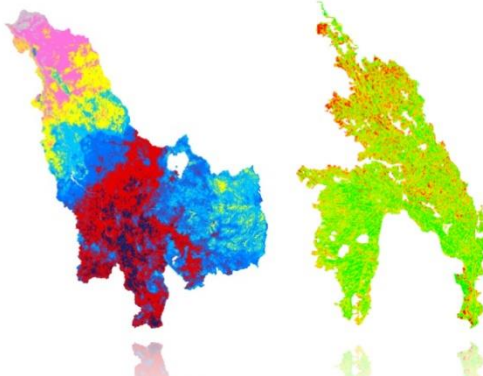
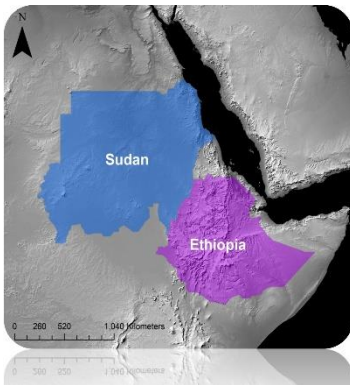
Auf der Ebene des Einzugsgebiets, das vom Blauen Nil (BNB) repräsentiert wird, ist die Niederschlagsüberwachung von größter Bedeutung, da sie nicht nur die Hauptwasserquelle im Einzugsgebiet darstellt, sondern auch die Variabilität der Niederschläge in hohem Maße die Nahrungsmittelproduktion in landwirtschaftlichen Systemen kontrolliert, vor allem im Regenfeldbau. Die starken räumlichen und zeitlichen Unterschiede in den Niederschlägen innerhalb des BNB legen nahe, dass die Wasserspeicherung und die Wassernutzung stärker gefördert und praktiziert werden müssen. Dies würde den Wassertransfer räumlich von nassen in trockene Gebiete und zeitlich von nassen in trockene Jahreszeiten sicherstellen.

Da Sorghum eines der wichtigsten Grundnahrungsmittel im Sudan darstellt, wurde die Sorghumproduktion in den Bewässerungs- und Regenfeldbausystemen im Sudan untersucht. In beiden Systemen, dem großflächigen Bewässerungs- und dem kleineren Regenfeldbausystem, wurde ein auffallend niedriger und instabiler Sorghumertrag festgestellt. Diese geringe Leistung ist nicht nur für die Nahrungsmittelproduktion, sondern auch für die Wasserverfügbarkeit eine große Herausforderung. Es wurde festgestellt, dass die derzeitige niedrige Leistung durch viele Faktoren physischer, sozioökonomischer und wirtschaftlicher Natur bedingt wird. Da viele dieser Faktoren eng miteinander verknüpft sind, wird

angenommen, dass eine wirksame Verbesserung einzelner Faktoren auch positive Auswirkungen auf die anderen Steuerungsfaktoren haben. Zusammenfassend lässt sich festhalten, dass die identifizierten Synergien und Kompromisse des WFC Nexus als Einstiegspunkte zur Steigerung der Wassernutzungseffizienz und zur Überbrückung der Ertragslücke genutzt werden könnten. Sogar einfache Eingriffe auf Feldebene könnten positive Auswirkungen auf die gesamte Ernteproduktion der regionalen landwirtschaftlichen Produktion und auf die Wasserverfügbarkeit haben. Die Erhöhung der Wasserverfügbarkeit im Wassereinzugsgebiet und die Verbesserung der Produktion der einzelnen landwirtschaftlichen Systeme würde die allgemeine Wasser- und Ernährungssicherheit im Land verbessern und die Notwendigkeit minimieren, die für die Eindämmung des Klimawandels wichtigen Ökosysteme in Ackerland umzuwandeln. Dieser Paradigmenwechsel muss durch ein umfassendes Konzept zur nachhaltigen Intensivierung (SI) erreicht werden, das nicht nur auf die Steigerung des Ernteertrags abzielt, sondern auch auf die Förderung einer gesunden Umwelt, einer verbesserten Lebensgrundlage und einer wachsenden Wirtschaft.

Chapter 1

General introduction



1.1. Background

Access to water and food is a basic right for everyone. Currently, with a world of 7.7 billion people in 2019 (UN-DESA, 2019), there are more than two billion people live in countries experiencing high water stress (UNESCO, 2019) and around two billion suffer moderate and severe levels of food insecurity (FAO et. al., 2019). Taking into consideration the planetary boundaries (Steffen et al., 2009), and the impacts of external drivers such as population growth, urbanization and climate change, the picture of the world might be worse in the future. Fostering socio-economic development and fulfilling shared goals set in the global agenda (e.g. Sustainable Development Goals, SDGs) require extensive use of natural resources (e.g. water and land). This may put such resources under great pressure in the future, especially in the areas that already suffer from natural resources scarcity and degradation. Ensuring water and food security under drivers such as climate change while preserving these resources remains a great challenge, especially in Africa (Misra, 2014; Schmidhuber and Tubiello, 2007).

Earth systems such as water, land, and climate are closely linked, and interactions and feedbacks between them are numerous. Recently, an approach that looks at the interlinkages between the different systems and sectors, the so-called the “Nexus concept”, has emerged and gained large attention from researchers, practitioners, and policy-makers (Rasul, 2014), for instance, the Water-Food-Energy Nexus. The ultimate goal of the Nexus approach is to discover potential synergies between the systems and sectors to be promoted or increased and trade-offs to be eliminated or reduced (Hoff, 2011). For the Water-Food-Climate Nexus (WFC Nexus), an improved understanding of these synergies and trade-offs is essential to better predict, adapt and mitigate the expected global climate changes and to ensure water and food availability. However, this is hindered by limited information from the ground. In this regard, information from Earth Observation (EO) could act as an alternative that can be used as an essential input for developing this understanding (Sudmanns et. al., 2019; ESA, 2015).

1.2. Problem statement and motivation

Following the Nexus thinking, an in-depth analysis of the interactions between water, food, and climate within and across spatial domains would provide insights on the potential synergies and trade-offs. These potential synergies and trade-offs are helpful to identify effective entry points to address the challenge of securing water and food under climate variability and climate change impacts. However, the interactions between the three are not

always known. One reason behind this is the complexity of the interactions and involvement of many disciplines that require using multiples datasets with adequate temporal and spatial resolutions employed in diverse methodologies. Moreover, environmental challenges are usually complex and often cross spatial scales (Yee et. al., 2012; Knol et. al., 2010), which requires comprehensive analyses that encompasses several spatial and temporal domains and involve multiple dimensions (e.g., physical, socio-economy, and governance). Lack of data with adequate spatial and temporal resolutions is particularly the main challenge in this regard. The recent advancement in EO has resulted in massive freely available datasets (Augustin et. al., 2019), which provide continuous information with different spatial and temporal resolutions for several parameters (e.g. climate variables and vegetation indices) that could be used to study the WFC Nexus. The availability of these public-domain datasets has paved the way to conduct such integrated research and to improve our understanding of the cross-cutting interactions between the systems, spatially and temporally. Still, extracting the needed information from this large amount of EO datasets is both, a great opportunity and a great challenge (Augustin et. al., 2019; Sudmanns et. al., 2019).

The Nile Basin (NB) is located in the northeastern part of Africa. The economies of the riparian countries of this basin are chiefly agricultural-based (Swain, 2011), where agriculture represents not only the main source for livelihood (Awulachew et. al., 2010), but it is the sector where most of the water withdrawals occur (Swain, 2011). Taking into consideration that complex interlinkages between water, food, and climate exist in the agricultural sector and numerous interactions take place within and across the systems, assessing the WFC Nexus in the NB will provide useful insights for this area where the impact of climate variability is a formidable challenge and closely associated with achieving water and food securities. Despite the wide acceptance and applicability of the Nexus concept, integrated and multi-scale analysis of the WFC Nexus in this region using EO data is still limited. In the NB region, relevant previous research had usually targeted one spatial scale (region, country, river basin or agricultural scheme). No previous studies have been conducted to employ these datasets in an integrated framework that crosses spatial domains. Therefore, the current study aims at orchestrating multiple EO datasets supplemented by other primary and secondary data to enhance our understanding of the synergies and trade-offs of the WFC Nexus in the NB with a special focus on Sudan. The rationale behind this special focus on Sudan will be discussed and concluded in Chapter 2, where the regional context is presented.

1.3. Earth Observation for water, food, and climate: State-of-the-art

Traditionally, the EO term is associated with satellite-based information. However, the recent usage of the term involves multiple datasets from different sources, including *in-situ* measurements (Hamm et. al., 2015; Yang et. al., 2013). The large expansion in EO has led to an accumulation of big data that are characterized by 5 Vs (Lynch, 2008): (1) extreme volume, (2) a wide variety of form, (3) require high velocity of data processing, (4) need to deal with the veracity of data uncertainty, and (5) need to be turned into value. Many operational missions and platforms provide measurements of different variables related to water, food, and climate. The number of public-domain products that can be used for the WFC Nexus assessment is increasing. For instance, within the framework of the current research, the author was able to identify more than 40 different precipitation products that are free and publicly available. Reviews on the satellite missions, platforms and derived data and indices that could be used to study the water cycle components, vegetation status and climate are available in many studies (Fritz et. al., 2019; Huang et. al., 2018; Sheffield et. al., 2018; Sun et. al., 2018; Xue and Su, 2017; Guo et. al., 2015; Thies and Bendix, 2011; Kidd, 2001).

During the last few decades, the usage of EO datasets for multiple purposes experienced a large increase (Tomás and Li, 2017). We conducted a scoping review using the Scopus publication database (www.scopus.com) to study the trend and focus of publications related to the topic of using EO for water, food, and climate. This review was confined to the last 30 years (1989-2018), the period which noticed the largest increase in the number of publications dealt with this topic. To identify relevant studies, potential keywords have been listed and five search syntaxes were formulated (Fig. 1.1). The results of this review show a noticeable increase in the number of studies published every year, especially during the years post-2000. The total number of retrieved publications, which has any of the five research focuses adopted in the review, is 940,522 study. Compared to EO for climate (focus 5) and EO for food (focus 4), EO for water shows a noticeable lower total number of publications (448,673, 340,891 and 140,617, respectively). Using EO for monotopic (water, food or climate) is more common than integrated “nexus” studies that consider the three (Fig. 1.1). Only a small number of publications used the term WFC Nexus in combination with any of the EO-related keywords (e.g. remote sensing, and satellite). These results indicate a gap in the research that focuses on utilizing EO for WFC Nexus.

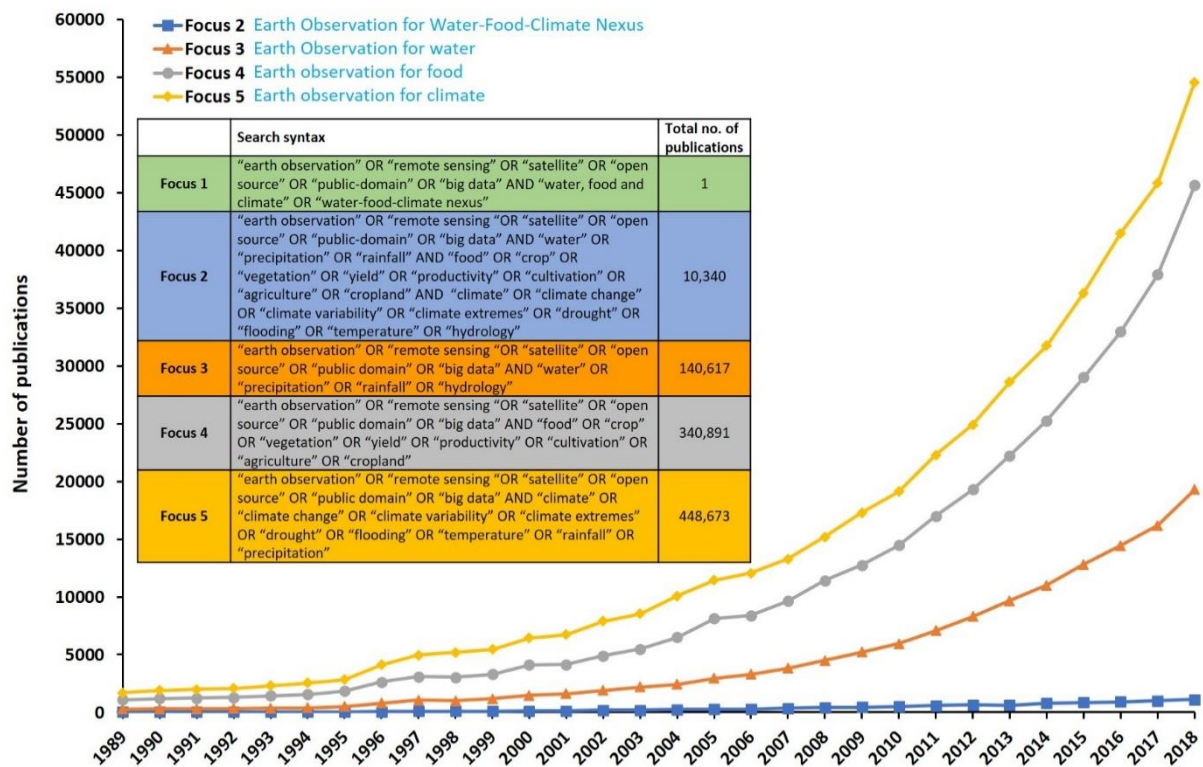


Fig. 1.1. Time series of 30-years (1989-2018) of the total number of publications retrieved by the Scopus database, which are related to the topic of using Earth observation for water, food, and climate. Different search strategy syntaxes were used to cover 5 main research focuses. The analysis was conducted on 7 October 2019.

Examples of previous studies conducted in the NB region that employed EO datasets to understand water, food and/or climate include, among others, estimating of water balance (Gleason et. al., 2018; Seyoum, 2018; Abera et al., 2017; Bastiaanssen et. al., 2014; Senay et. al., 2014, 2009), detecting water stress (Elnmer et. al., 2018), assessment of Water Use Efficiency (WUE) in irrigated schemes (Al Zayed et. al., 2016, 2015), monitoring of vegetation conditions (Teferi et. al., 2015; Meroni et. al., 2014; Tadesse et. al., 2014; Lenney et. al., 1996), the impact of drought on vegetation productivity (Bayissa et. al., 2019; Gidey et al., 2018), and implications of agricultural and water policies (Al Zayed and Elagib, 2017). To the best of our knowledge, no previous study has been conducted to identify and quantify synergies and trade-offs of the WFC Nexus in the NB using EO and following a multi-scale approach.

1.4. Research concept and research questions

The subject of WFC Nexus is a multidisciplinary subject that encompasses multiple disciplines and may require investigation to be conducted at different spatial and temporal domains. As mentioned earlier, this complexity requires multidisciplinary research that uses

different types of data and several methodologies. Therefore, the current research is an “integrated” analysis that amalgamates diverse types of data in several methodologies to investigate the WFC Nexus within and across different spatial scales. The integration in the current research involves:

- **Multidiscipline inclusion:** The current research includes several disciplines such as water resources management, agriculture, climate, remote sensing, socio-hydrology, and science-policy interaction.
- **Data integration:** Using different types of data of primary (obtained through a field survey) and secondary origins (public-domain EO datasets and ancillary data).
- **Methods integration:** Involving multiple methods, including spatial correlation, time series analysis, data validation, and field survey mission supplemented by statistical analysis and modeling.
- **Spatial multi-scale:** The synergies and trade-offs of the WFC Nexus are investigated within and across several spatial domains in a nested approach. These spatial domains are (i) Country scale: taking Sudan and Ethiopia as a case study for the NB region, (ii) River basin scale: considering the Blue Nile Basin (BNB) as a basic unit for water management and as one of the most important water and food production spots in the two riparian countries, i.e. Sudan and Ethiopia, (iii) Agricultural schemes: targeting the two main agricultural systems in the BNB (i.e. irrigated and rainfed) and (iv) field scale: aiming to detect the most influential factors on crop yield of sorghum as an example of the main staple crops in the basin.

Based on the above background, the knowledge gaps regarding WFC Nexus in the NB has been identified. Within the current study, five research questions need to be answered. These questions are:

- Q1.** How consistent are public-domain precipitation products, as an example for EO datasets?
- Q2.** How to employ EO data for WFC Nexus analysis?
- Q3.** What is the current status and trend of performance of water use and main food crops in the agricultural sector in the NB?
- Q4.** Can EO datasets detect nexus synergies and trade-offs in the Nile Basin?
- Q5.** How to convert nexus knowledge into action?

To summarize the different components of the current research, a conceptual framework is established (Fig. 1.2). The focus of the current research is subdivided into two main levels: (i) strategic level, which consists mainly of the country scale, and (ii) operational level, which comprises of the river basin, agricultural scheme and agricultural field scales. For each of these scales, specific objectives were proposed based on the identified knowledge gap. The ultimate cross-cutting objective is to identify synergies and trade-offs of the WFC Nexus within and across the selected spatial scales that could be used as entry points to enhance water and food security under a variable climate. The expected outcomes of the current research are:

- Assessment of the consistency of some EO datasets that potential to be used for spatial analysis of the WFC Nexus.
- Analysis of the interactions between water, food and climate systems within and across different spatial scales.
- Assessment of the spatio-temporal variation of agricultural productivity and the main controlling factors.
- Evaluation of the current status and trend of agricultural performance in some of the main irrigated and rainfed schemes.
- Identification of potential synergies and trade-offs between water, food, and climate
- Diagnosis of entry points to promote or increase WFC Nexus synergies and reduce or eliminate trade-offs

1.5. Structure of the dissertation

This dissertation consists of seven chapters. Along with introductory and conclusion chapters, five chapters are dealing with the five research questions listed in the previous section (Section 1.4).

Chapter 1 - Introduction: This chapter provides an overview of the focus problem of the current research. Besides, it provides information about the objectives and research questions of the research. Moreover, an overview of this dissertation is supplied, how is it subdivided?, supporting publications by the researcher and how each of the research questions is covered in each of these publications.

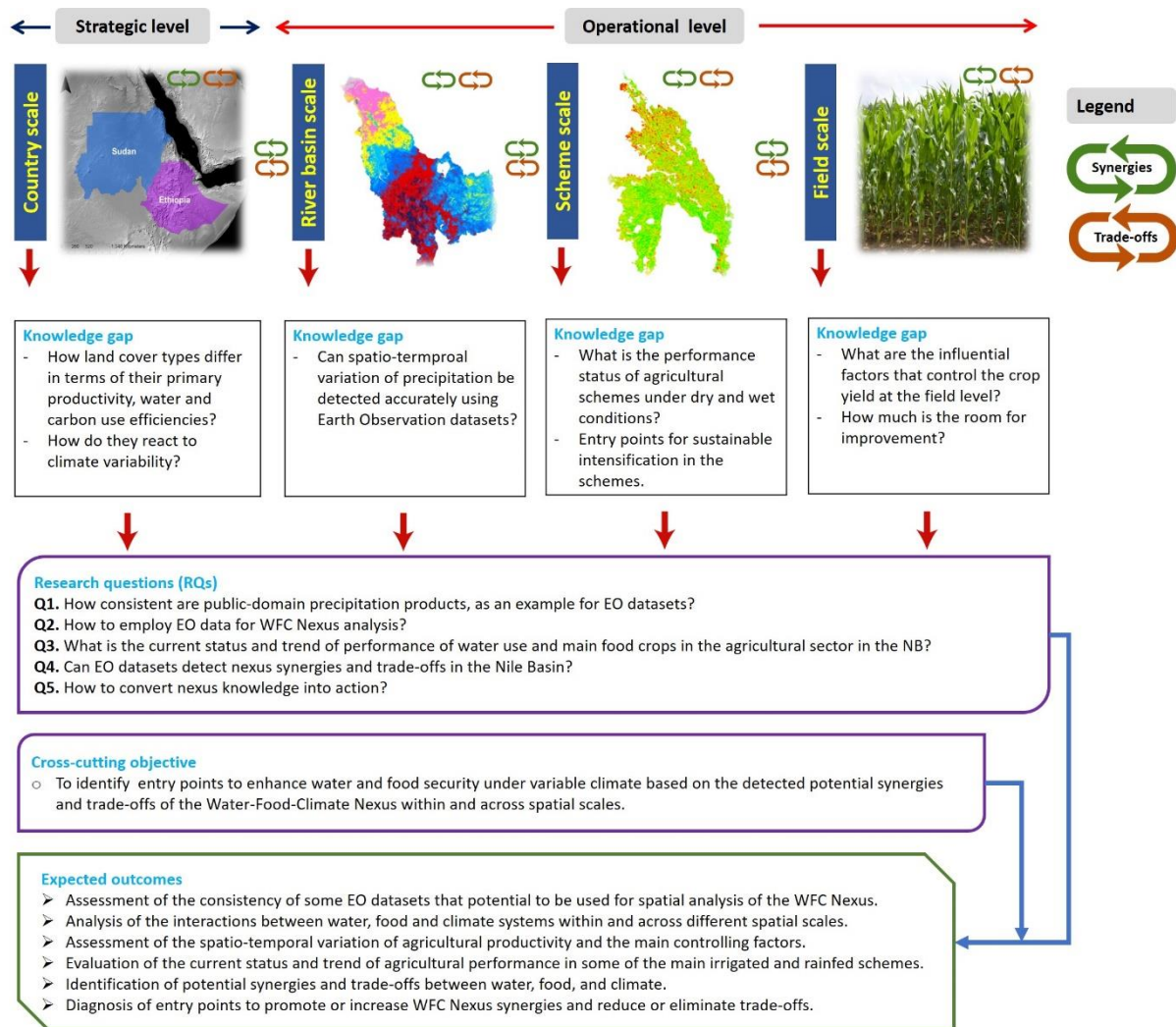


Fig. 1.2. The conceptual framework adopted in the current research.

Chapter 2 - Regional context: In this chapter, a general overview of the geographical setting of the NB and the current patterns of water uses and agricultural production in the riparian countries is provided. It concludes and delivers information on the rationale behind selecting Sudan for the subsequent analyses.

Chapter 3 - Sensitivity and response of vegetation to climate variability: This chapter compares the behavior and response of different land cover types in Sudan and Ethiopia under climate variability. This comparison is helpful to identify the resistivity and response of the studied land cover types in terms of their Net Primary Productivity (NPP), Water Use Efficiency (WUE) and Carbon Use Efficiency (CUE), as important indicators for ecosystem function. Such analysis is important to detect the variation of the different land cover types in terms of these indicators and to recognize how they react to climate variation.

Chapter 4 - Consistency of public-domain precipitation products: Usually a river basin is considered as the basic unit water resources management. As precipitation is the main source for water in many sub-basins in the NB, it is crucial to estimate it and detect its spatio-temporal variation accurately. In this part, the Blue Nile Basin (BNB), which is a transboundary basin shared between Sudan and Ethiopia was selected as a case study to recognize the spatial and temporal variation of precipitation, as detected by 17 Public-domain Precipitation Products (PPs). This basin is the most important region for water and food security for both riparian countries, as it is the main source of water resources in the NB region. In addition, it accommodates major irrigated and rainfed agricultural schemes, among which some were selected for the subsequent analysis of WFC Nexus in the current research (chapters 5 and 6).

Chapter 5 - Yield gap and pathways for sustainable intensification in irrigated schemes: The Gezira Irrigation Scheme in central Sudan, irrigated from the Blue Nile river, was targeted to study the socio-hydrological determinants of agricultural productivity. Combining EO data, field survey and statistical modeling, the most important factors controlling the crop yield of sorghum (the main staple crop in the country) were detected. The synergies and trade-offs identified within the WFC Nexus were used to build a framework for Sustainable Intensification (SI) in the scheme, as a potential approach to provide more food while preserving a healthy environment and promoting improved livelihood and growing economy.

Chapter 6 - Crop vulnerability and resilience to climate in rainfed schemes: As the main source for food production in the NB region, an assessment of the rainfed system is included in the current research. The major area for mechanized sorghum production, located in the central and eastern parts of Sudan was studied using different methodologies to detect the resilience and vulnerability of sorghum production in dry and wet years. El Gedaref state was selected for further spatial and temporal analysis using multiple EO datasets including remote sensing and models.

Chapter 7 - Synopsis, synthesis, and perspectives: The major observations and findings of the current research are summarized in this chapter. Moreover, the identified synergies and trade-offs within and across spatial scales are listed. In this last chapter, lessons learned and transferability are discussed. In addition to recommendations for policymakers, researchers and local farmers, topics for future studies are suggested.

1.6. Research publications supporting this dissertation

This dissertation is supported by four journal articles and one book chapter (Table 1.1). Among the journal articles, three have been published in peer-reviewed journals and one is submitted to a journal for a possible publication. All the published articles have undergone at least two blind reviews. The relative contribution of each publication in answering the research questions is provided in Table (1.2).

Table 1.1. List of research publications supporting this dissertation.

Spatial Scale	Chapter	Corresponding publication
Region	Chapter 2 Regional context	<i>Nile basin</i> 1. Khalifa, M. , Thomas, S., Ribbe, L., 2020. The Nile River Basin, in: Schmandt, J., North, G., Ward, G., Kibaroglu, A., (eds). Sustainability of engineered rivers in arid lands: Challenge and Response. Cambridge University Press (In preparation).
Country	Chapter 3 Sensitivity and response of vegetation to climate variability	<i>Sudan and Ethiopia</i> 2. Khalifa, M. , Elagib, N.A., Ribbe, L., Schneider, K., 2018. Spatio-temporal variations in climate, primary productivity and efficiency of water and carbon use of the land cover types in Sudan and Ethiopia. <i>Science of the Total Environment</i> , 624, 790–806.
River basin	Chapter 4 Consistency of public-domain precipitation products	<i>Blue Nile Basin</i> 3. Khalifa, M. , Korres, W., Saif, S., Elagib, N.A., Baez-Villanueva, O.M., Basheer, M., Ayyad, S., Ribbe, L., Schneider, K., 2020., Consistency of public-domain precipitation products: coupling traditional evaluation approaches with data mining techniques (Submitted).
Agricultural scheme and field	Chapter 5 Yield gap and pathways for sustainable intensification in irrigated schemes	<i>Irrigated system</i> 4. Khalifa, M. , Elagib, N.A., Bashir, M.A., Ribbe, L., Schneider, K., 2020. Exploring socio-hydrological determinants of crop yield in under-performing irrigation schemes: Pathways for sustainable intensification. <i>Hydrological Sciences Journal</i> , 55 (2), 153-168.
	Chapter 6 Crop vulnerability and resilience to climate in rainfed schemes	<i>Rainfed system</i> 5. Elagib, N.A., Khalifa, M. , Rahma, A.E., Babker, Z., Gamaledin, S.I., 2019. Performance of major mechanized rainfed agricultural production in Sudan: Sorghum vulnerability and resilience to climate since 1970. <i>Agricultural and Forest Meteorology</i> , 276–277.

Table 1.2. Contribution of the publications to the research questions (Qs) of the current dissertation.

No.	Publication title	Research questions*				
		Q1	Q2	Q3	Q4	Q5
1	The Nile River Basin					
2	Spatio-temporal variations in climate, primary productivity and efficiency of water and carbon use of the land cover types in Sudan and Ethiopia					
3	Consistency of public-domain precipitation products: coupling traditional evaluation approaches with data mining techniques					
4	Exploring socio-hydrological determinants of crop yield in under-performing irrigation schemes: Pathways for sustainable intensification					
5	Performance of major mechanized rainfed agricultural production in Sudan: Sorghum vulnerability and resilience to climate since 1970					

Legend



No coverage of research question



Partial coverage of research question

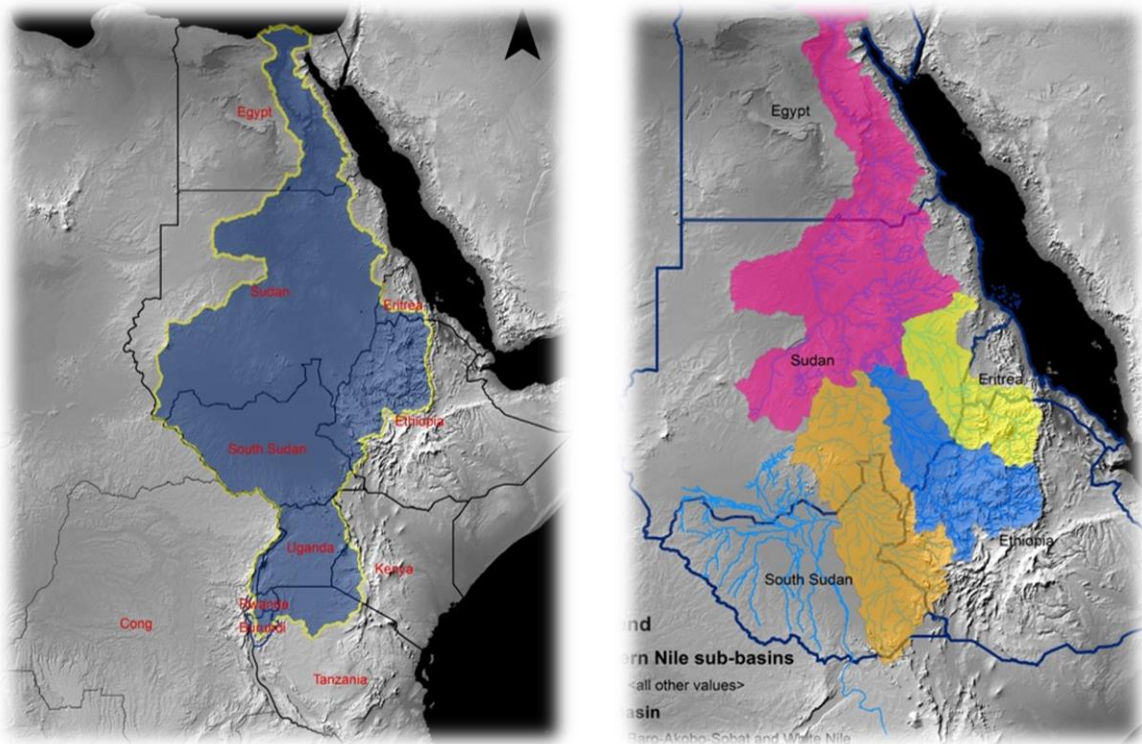


Full coverage of research question

* Research questions are listed in section 1.4.

Chapter 2*

Regional Context



Based partially on:

Khalifa, M., Thomas, S., Ribbe, L., 2020. The Nile River Basin, in: Schmandt, J., North, G., Ward, G., Kibaroglu, A., (eds). Sustainability of engineered rivers in arid lands: Challenge and Response. Cambridge University Press (In preparation)

* List of data sources used in the current chapter can be found in the appendix A: Table S2.1

2.1. The Nile River Basin

2.1.1. Physical setting

The Nile Basin (NB) is one of the largest transboundary basins all over the world. It occupies an area around 10% of the total area of the Africa continent (Barnes, 2017). With a total length of 6,695 km, the River Nile is the longest in the world. The NB is shared between 11 countries, namely, Burundi, Congo, Egypt, Eritrea, Ethiopia, Kenya, Rwanda, South Sudan, Sudan, Tanzania and Uganda (Fig. 2.1a). The two main tributaries of the Nile river, the Blue Nile and the White Nile originate, respectively, from the Ethiopian Highlands and the Equatorial Lakes. These two major tributaries meet at Khartoum, the capital of Sudan, to form the main Nile river which flows northwards through northern Sudan and then to Egypt to drain into the Mediterranean Sea. The Eastern Nile basin consists of four main sub-basins, namely, Tekeze-Atbara-Setit, Blue Nile, Main Nile and Baro-Akobo-Sobat and White Nile (Fig. 2.1b).

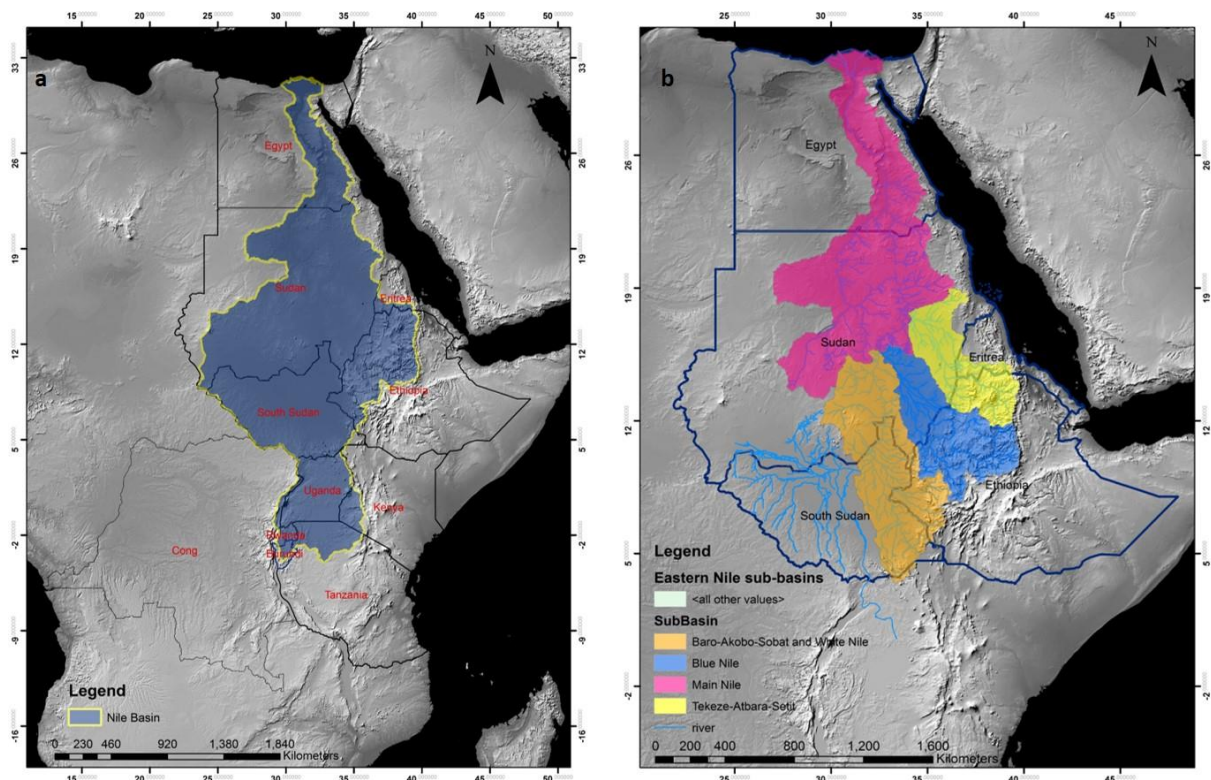


Fig. 2.1. Location map of the Nile Basin: (a) the Nile basin with 11 riparian countries, (b) The Eastern Nile Basin with four main sub-basins. Sources of data: boundaries of the countries: GADM, River basin boundaries: delineated using SRTM Digital Elevation Model, relief background: Natural Earth Data.

According to the estimates of the Population Division of the United Nations Department of Economic and Social Affairs (UN DESA), the current (2019) total population of the 11 riparian countries of the Nile is around 0.54 billion people. Among all of the riparian countries, Ethiopia,

Egypt and Congo have the largest population with estimates of 115, 102, and 95 million people, respectively. Within the NB countries, there are six cities with a population of 3 million inhabitants or more. Only Cairo (Egypt) is classified as a megacity – with a population of over 10 million people. Other large cities such as Kinshasa (Congo), Khartoum (Sudan), and Alexandria (Egypt) exhibit the typical characteristics of megacities. These include large peri-urban populations at their fringes, with dominant illegal settlements and inadequate housing, sanitation, and other essential services. Other features of megacities include traffic congestion, water, and air pollution, smog, unemployment, lack of open spaces, and very high population densities.

The NB has diverse land cover types (Fig. 2.2). Most of the area in the basin is bare lands, which represent around 28% of the total area of the basin. Bare lands extend in the northern arid and semi-arid regions, mainly in Egypt and northern Sudan. Forests, shrublands, grasslands, and croplands cover vast areas in the basin. While large irrigated croplands are in Egypt (Delta) and central Sudan, rainfed agriculture characterizes the eastern, central, and southern countries of the basin, where precipitation is higher. Savannas, grasslands, shrublands, and forests are located mostly in the central part of the NB. The basin wetlands are concentrated in two areas, namely, the Equatorial Lakes region and the Sudd area in South Sudan. The Nile Delta north of Egypt, once an area of natural wetlands, has now been almost entirely converted into agricultural lands.

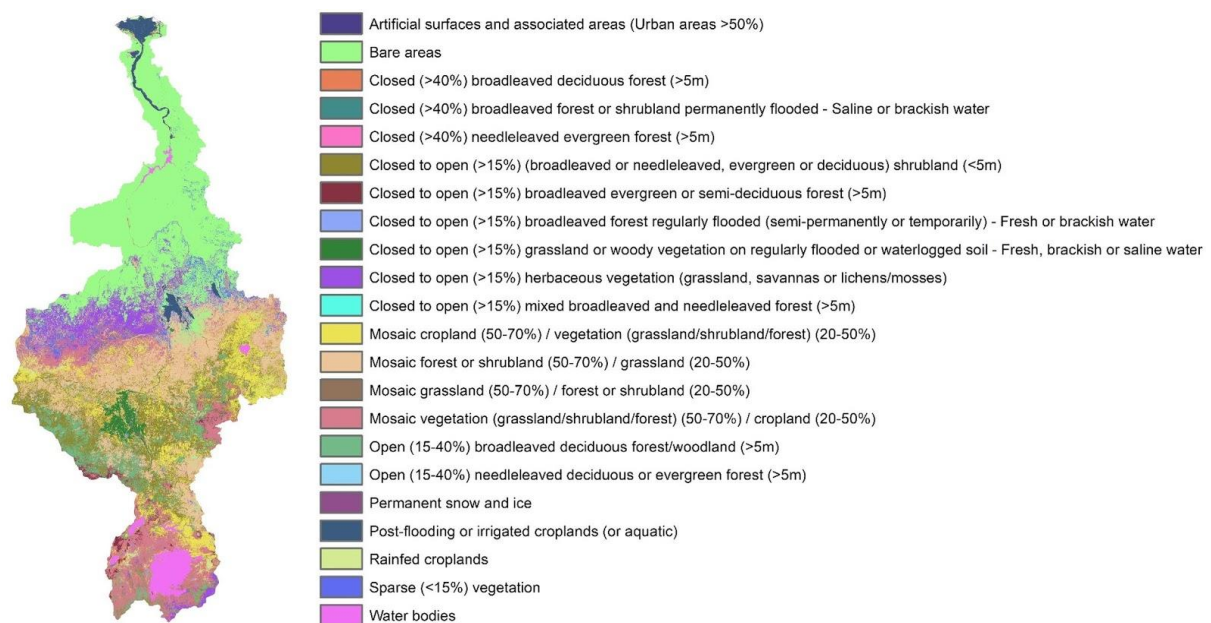


Fig. 2.2. Land cover map created based on Globcover 2009 data.

The NB is characterized by large spatial and temporal variations in climate conditions, for instance, precipitation and temperature. Spatially, the northern regions of the basin receive negligible precipitation (Fig. 2.3) and characterized by high temperatures (Fig. 2.4). High precipitation occurs generally in the eastern (Ethiopian highlands) and southern (Equatorial lakes) regions of the basin. The average monthly precipitation ranges between 0 and 450 mm. While the basin receives low amounts of rain from November to April, except in some locations in the Equatorial Lakes, the main rains fall during the period from June to October (Fig. 2.3). The average monthly temperature ranges between 1°C and 35.5 °C.

2.1.2. Water resources and water use patterns

As mentioned earlier, the river Nile originates in two main regions; the Ethiopian highlands (Lake Tana) and the equatorial lakes (Lakes Victoria, Kyoga, and Albert), which are the sources of the two major tributaries of the Nile, the Blue Nile and White Nile rivers, respectively (Fig. 2.5). The main tributaries of the Blue Nile river are Rahad and Dinder, which originate in the Ethiopian highlands and join the Blue Nile river upstream Khartoum. Several major tributaries are contributing to the White Nile, namely, Bahr el Jabal, Bahr el Gazal, Baro, Pibor and Sobat rivers. Compared to the high seasonality of the water flow in the Blue Nile river, the White Nile is regulated by the large Sudd swamp in South Sudan. The only major tributary of the Main Nile (downstream of the confluence of the Blue Nile and the White Nile) is Atbara/Tekeze river, which contributes around 12 km³ per year. The historical flow of the Nile is 84 km³ as measured at the High Aswan dam in Egypt (Sutcliffe and Parks, 1999), from which, approximately 62% is contributed by the Blue Nile river (Amdihun et al., 2014).

As an adaptation measure against insufficient water availability and to offer water for food and energy production, several dams were built on the Nile tributaries during the last decades. The existing major water control structures are listed in Table (2.1). Sediments resulting from soil erosion taking place at the upstream parts of the NB represent a serious problem for water management of the reservoirs in the basin. For instance, some of the dams in Sudan, i.e. Sennar, Roseries, and Khashm El Girba have lost more than 60% of their original storage capacities (Ahmed, 2004; Williams, 2009; Shahin, 1993). An increasing trend of 5% in the sediment yield during 1980-2009 is detected (Gebremicael et al., 2013). An X-ray analysis coupled with cluster assessment and balance modeling conducted by Ali et. al. (2017) on the sediments in the Roseires reservoir (in Sudan) and the potential source areas in the Upper Blue Nile Basin (UBNB) showed that some sub-basins in Ethiopia are the main sediment source areas of sediments accumulated in the reservoir.

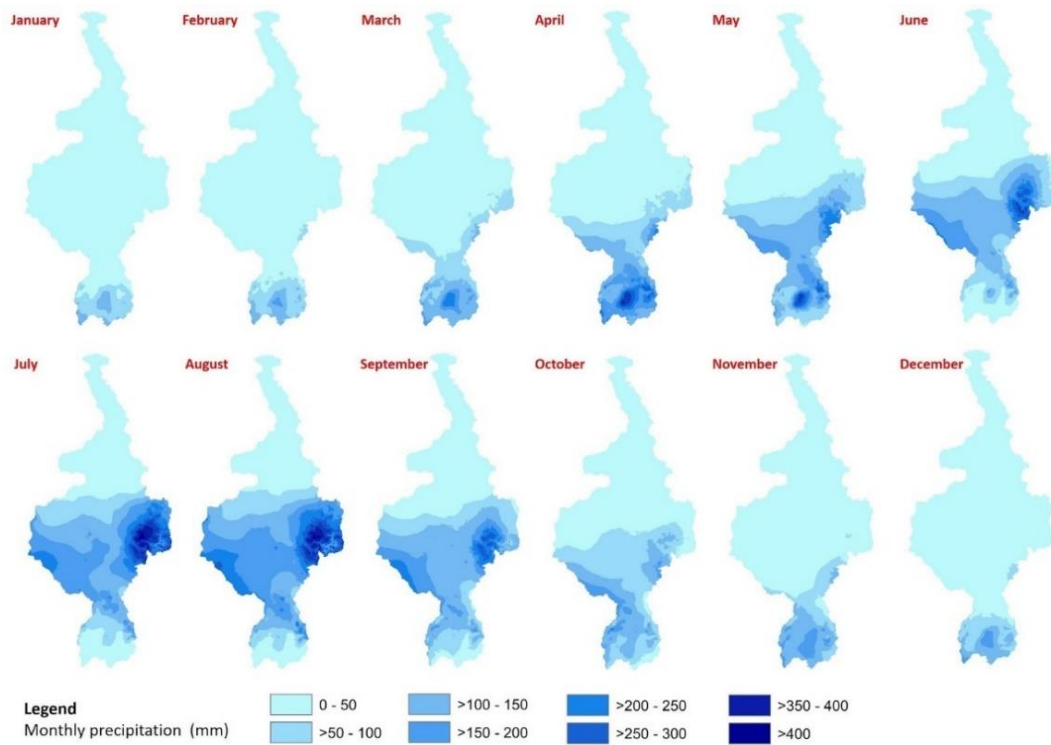


Fig. 2.3. Long-term monthly average precipitation (1970-2000) over the Nile Basin. These maps are created based on the data of WorldClim (Fick and Hijmans, 2017).

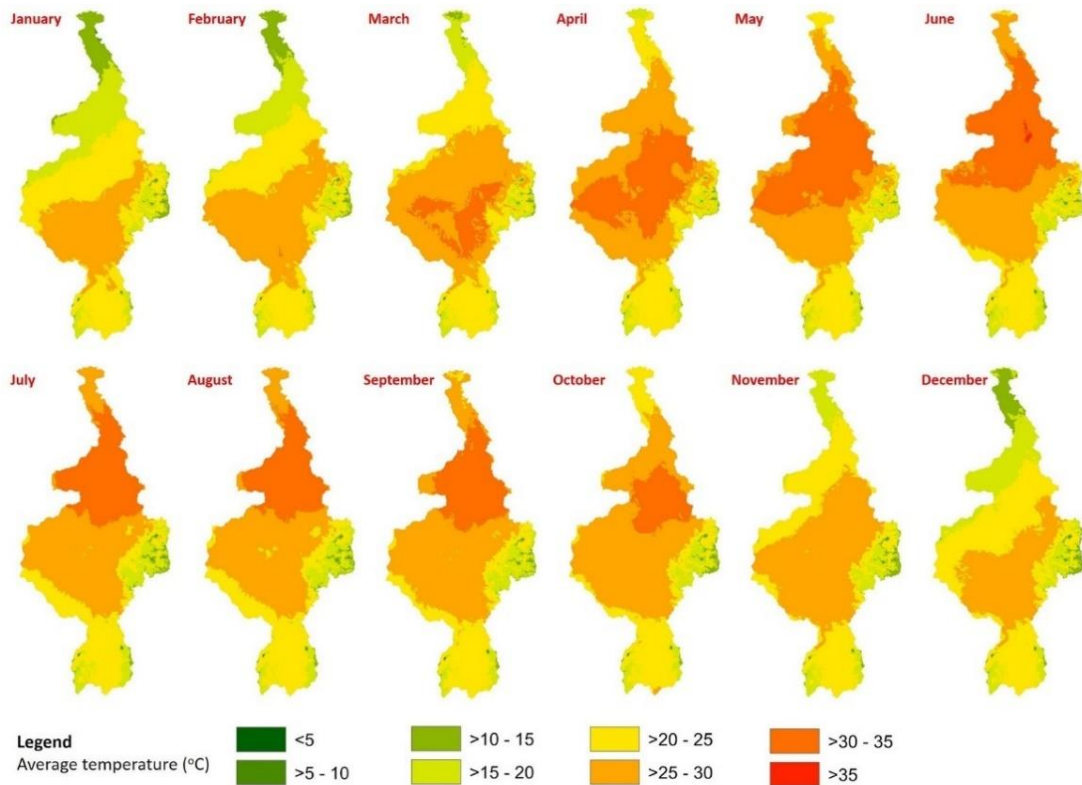


Fig. 2.4. Long-term monthly average temperature (1970-2000) over the Nile Basin. These maps are created based on the data of WorldClim (Fick and Hijmans, 2017).

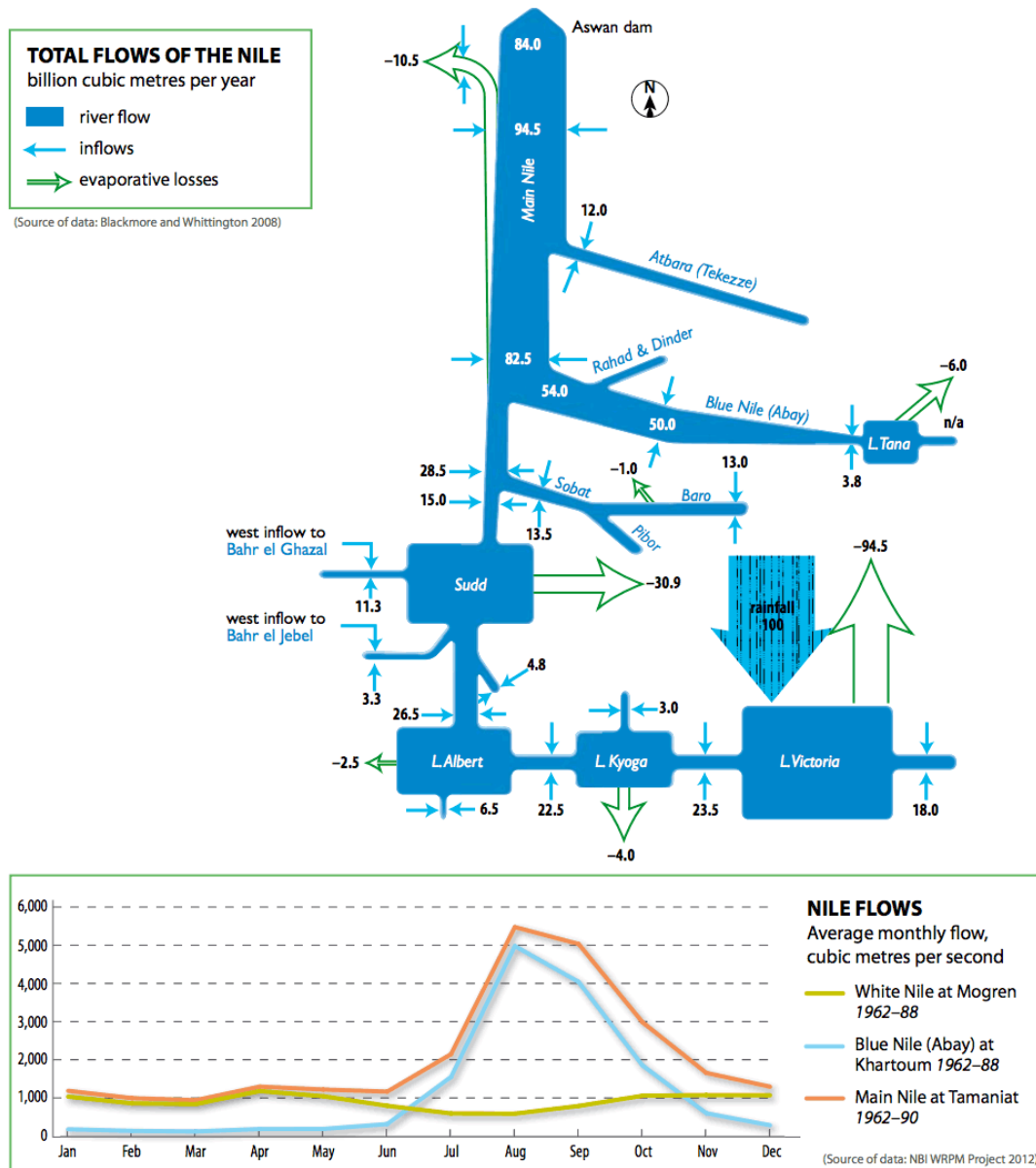


Fig. 2.5. Schematic representation of the water fluxes (inflow, evaporative losses, and outflow) in the Nile Basin and annual flow pattern of the major Nile tributaries (Blackmore and Whittington, 2008).

An estimated, 3% (95,926 km²) of the Nile’s open water is in the form of lakes. Notable large lakes include Victoria, Kyoga, Albert, George, Edward, and Tana. The lakes are primarily located in the Equatorial Lakes Plateau region. The only major lake in the desert biome is Lake Nasser/Nubia, which resulted from the damming of the Nile at Aswan. The lakes in the basin have various functions, including acting as a habitat for aquatic plant and animal species, buffering the discharge of outflowing rivers against seasonal extremes, and acting as a trap for sediments from the headwater areas. Natural lakes and artificial reservoirs show large evaporative losses. For instance, approximately 94.5, 30.9 and 10.5 km³ of water are evaporated annually from Lake Victoria, Sudd swamps and Aswan dam, respectively.

Table 2.1. List of major dams in the Nile Basin with their storage capacity.

No.	Country	Dam	Storage capacity (km ³)
1	Egypt	Aswan Low Dam	5
2		Aswan High Dam	162
3	Sudan	Merowe	12.5
4		Jebel Awlia	3.5
5		Sennar	0.9
6		Roseries	3
7		Khashm Al Girba	1.3
8		Upper Atbara and Setit Dam Complex	2.7
9	Ethiopia	Grand Renaissance Dam (GERD)	74 (under construction - 2019)
10		Mendaia	15.9
11		Tekeze	9
12		Megech	1.8
13		Rib	0.2
14	Uganda	Owen falls	80

In addition to surface waters, the NB countries have considerable groundwater resources occurring in localized and regional basins. Groundwater is an important resource, supporting the social and economic development of the Nile riparian countries and making an important contribution to the water and food security in the region. The degree to which it is relied upon varies from country to country, but commonly it is the most important source for drinking water, especially for rural communities in the basin. The main groundwater aquifers in the NB are (1) Victoria artesian aquifer, (2) Congo hydrogeological artesian aquifer, (3) Upper Nile artesian aquifer, (4) Volcanic rock aquifers, (5) Nubian sandstone aquifer system, and (6) Nile Valley aquifer.

Using multiple remote sensing data validated with ground measurement of different water balance components, Bastiaanssen et. al., 2014 has estimated the water balance in 15 sub-basin in the NB over the period from 2005 to 2010. According to this study, while the total precipitation falls over the basin is 2013 km³/yr, the total evapotranspiration is around 1987 km³/yr (Table 2.2), which implies that most of the available water in the NB is lost by evapotranspiration process. The contribution of the upstream sub-basins to the flow of the ones

located at downstream differs widely. Inter-basin transfer of surface water and groundwater between the sub-basins is a small fraction compared to the other water balance components.

According to the data of AQUASTAT, agriculture is the largest water consumer in the NB countries compared to the industrial and municipal uses (Fig. 2.6). For instance, agriculture accounts for nearly 96% of the total water use in Sudan. The annual irrigation requirement rate varies widely in the NB countries, and it ranges between nearly 8000 m³/ha in Kenya and Uganda up to 13,700 m³/ha in the arid and semi-arid regions in Sudan (Awulachew et. al., 2012). Egypt and Sudan alone account for around 82% (87.26 km³) of the total agricultural water withdrawal in the basin. The current agricultural, industrial and municipal water uses in countries such as Burundi, Rwanda, South Sudan, Eritrea are very small (Fig. 2.6).

2.1.3. Agriculture and food production

Agriculture is the main source of livelihood for most of the population and the main contributor to the Gross Domestic Product (GDP) (approximately 20%) and accounts for around 40% of all employment in the NB (Appelgren et. al., 2000). The basin has large arable lands, from which around 8 million hectares is potential for irrigation (FAO, 2005). Sudan alone has approximately 105 million ha of arable land, and only 17% of this large area is currently utilized. Rainfed and irrigated agriculture are both practiced in the basin. However, the rainfed system is dominating the agricultural lands. While only 3.8% (on average) of the total arable land in the Nile's sub-Saharan countries is irrigated, this percentage is a bit higher in Sudan and it reaches 100% in Egypt (Oestigaard, 2012), where precipitation is negligible. Cereal crops are dominating the cultivated land in the basin, and among all the NB countries, Sudan and Ethiopia have the largest cereal harvested area (Fig. 2.7a), with nearly 9.5 and 9.2 million ha, respectively (NBI, 2012). The yield of cereal crops shows high variability among the Nile riparian countries. Egypt stood out and exhibits higher cereal yield compared to the other countries (Fig. 2.7b). This high yield results in higher total production of cereal crops in Egypt compared to other countries with a large harvested area such as Sudan (Fig. 2.7c). Land grabbing by foreign countries and large companies is a big issue in some of the NB countries. According to a review conducted by Rulli et. al., (2013), land grabbed in four of the NB countries, namely, Congo, Sudan, Ethiopia, and Tanzania accounts for more than 33% of the total global grabbed lands. According to the same study, land grabbing is associated with large water withdrawal. The average withdrawal of blue water estimated to be around 3.18 km³ in these four countries, which represents 27.8% of the total average of the globally grabbed blue water.

Table 2.2. Annual water balance (2005-2010) as estimated by Bastiaanssen et. al. (2014) using remote sensing over different sub-basins of the Nile basin.

Abbreviations: P = precipitation, ET = actual evapotranspiration, I = interception, GW = groundwater, SW = surface water, ΔS = change in storage.

Sub-basin	Inflow (km ³ /yr)	P (km ³ /year)	ET+I (km ³ /yr)	Net GW interbasin (km ³ /yr)	Net SW interbasin (km ³ /yr)	ΔS (km ³ /yr)	Outflow (km ³ /yr)
Main Nile 1	36	2	19	4	1	-0.09	14
Main Nile 2	55	3	16	4	1	-0.22	36
Main Nile 3	79	51	71	4	1	0.10	55
Tekeze- Atbara	0	121	105	1	2	1.19	12
Main Nile 4	87	4	6	4	2	-0.07	79
Blue Nile	0	299	237	5	6	1.54	50
Lower White Nile	25	122	14	-11	-7	-0.25	25
Bahr el Ghazal	0	435	446	-3	-10	1.00	1
Sudd	35	162	201	-9	-6	-1.25	12
Baro-Akobo-Sobat	0	242	232	-1	0	-1.17	13
Albert - Bahr al Jabal	33	90	91	-2	-1	-0.08	35
Victoria Nile	28	100	93	3	5	-0.56	28
Semliki - Lake Albert	0	78	72	0	0	0.43	5
Lake Victoria	5	246	208	6	8	2.00	28
Kagera	0	57	52	0	0	0.78	5
Nile	-	2013	1987	5	2	3	14

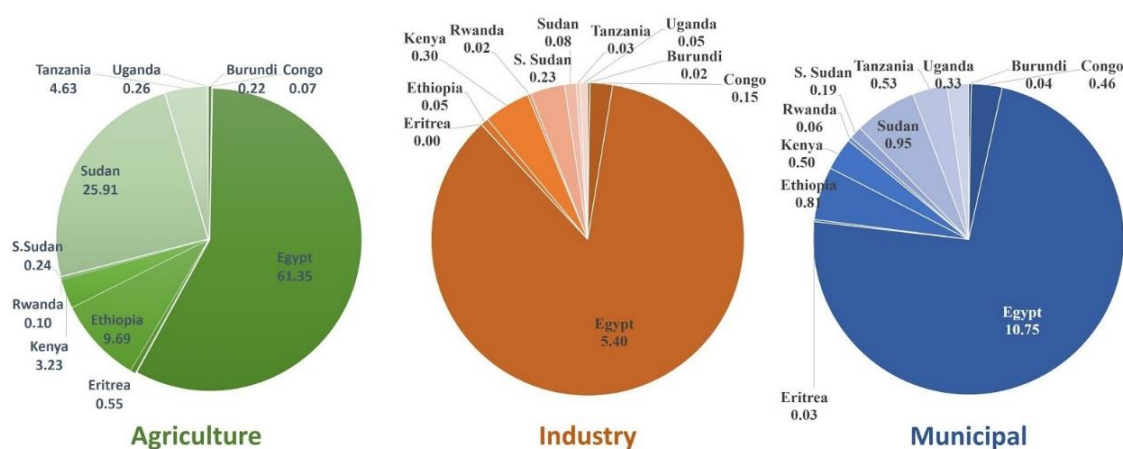


Fig. 2.6. Water use quantities (km³/year) in the Nile Basin countries. Water use is subdivided into agricultural, industrial and municipal uses. Data are obtained from the AQUASTAT database.

The main hydropower dams that are currently in operation are the High Aswan and Merowe dams (on the main Nile river), Rosaries and Sennar (on the Blue Nile river), Khashm El Girba and Atbara and Setit Complex (on Atbara river), Tekeze (on Tekeze river) and Gebel Aulia (on the White Nile). Currently, Ethiopia is building the Grand Ethiopian Renaissance Dam (GERD), only 20 kilometers away from the borderline with Sudan. The dam, once completed, will produce a peak of 6,000 megawatts of power, and store 74 km³ of water in its reservoir (Dessu, 2019), making it the largest hydropower dam in Africa. The GERD consists of a 1.8 km high gravity dam and a 5 km rockfill saddle dam (Abteu and Dessu, 2019).

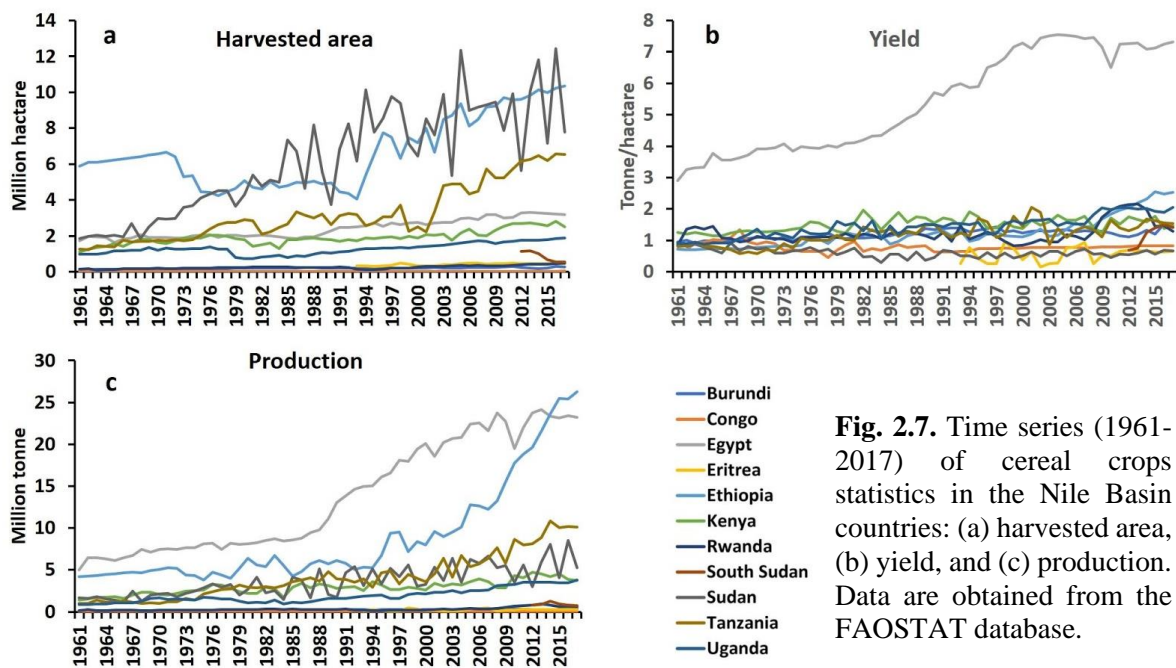


Fig. 2.7. Time series (1961-2017) of cereal crops statistics in the Nile Basin countries: (a) harvested area, (b) yield, and (c) production. Data are obtained from the FAOSTAT database.

2.1.4. The Nile’s transboundary conflict

The use of the Nile waters has for decades been monopolized by the downstream countries, i.e. Egypt and Sudan, that claim ‘historic right’ over the waters, thus, building tensions among the riparian countries. The upstream countries which are the source of the water have been alienated for long from significantly using the Nile waters. Also, none of the past treaties and agreements dealing with the use of the Nile waters – most of them signed during the colonial period - involved all the riparian countries and they did not deal equitably with the interests of these riparian countries. These agreements and treaties did not consider a comprehensive view of the impact of water development on the basin social and biophysical environment and to distribute the shares of water properly between the riparian countries. Due to the need for socio-economic development in the upstream countries, they have recently demanded de-monopolizing the Nile water use by Egypt and Sudan (Ashton, 2002).

Despite the long history of conflicts and tension over the Nile waters, yet, there is no a basin-wide agreement ratified by all riparian states. The 1929 Anglo-Egyptian Treaty gave Egypt the right to veto any project in the NB, as agreed upon by Britain and Egypt, to protect the British cotton interests in the Nile Valley. The 1959 bilateral agreement increased Sudan's and Egypt's water allocation to be 55.5 and 18.5 km³, respectively, and stipulated that any increase in water yield should be divided equally amongst them. Besides excluding the upstream riparian countries, this agreement stated that, if any of the other riparian countries need to make significant use of the Nile water, it should send a request to Egypt and Sudan who reserve the ultimate decision on approving the request or not (Salman, 2012). The international water law promotes reasonable and equitable use of water for the current and future users, increase access, share benefits, and encourage broad participation. At present, The Nile Basin Initiative (NBI) is operating as the transitional institutional mechanism after the Technical Cooperation Committee for the Promotion of Development and Environmental Protection of the Basin (TECCONILE). Since 1999, the Nile countries are participating in the NBI, which serves as a framework for managing transboundary trade-offs and opportunities such as sharing hydropower benefits, stronger integration in agriculture markets and exploiting opportunities for regional trade. The Cooperative Framework Agreement (CFA) was introduced in 2010 by the NBI to allow for a more equitable distribution of ownership on the Nile between the riparian countries. The CFA contains 45 articles clearly defining the intention, utilization, sustainability, optimization, benefit-sharing and cost-sharing principles of the Nile riparian states. Burundi, Ethiopia, Kenya, Rwanda, Tanzania, and Uganda signed the agreement, but Egypt and Sudan insisted on mentioning protecting the current use and the ownership that they held.

The need for socio-economic development in the Nile countries under the conditions of inadequate cooperation and lack of a comprehensive agreed-upon framework for water use in this transboundary basin are the driving forces that lead some of the basin's counties to take unilateral actions. The case of GERD in Ethiopia is the most recent example. On April 2, 2011, the Ethiopian government started construction of the GERD (Kimenyi and Mbaku, 2015). The Bureau of Reclamation of the United States originally surveyed and suggested the dam construction in 1956 and 1964, but Ethiopia only submitted a final design in November 2010. The GERD will store 74 km³ of water and produce 6000 megawatts (MW) of electricity (Kimenyi and Mbaku, 2015). This large dam might significantly affect the hydrology of the Blue Nile River and consequently the Main Nile that reaches Egypt. Egypt is afraid that the GERD might decrease the Nile share of water that reaches its territories, especially during the reservoir filling period. Ethiopia has ignored Egypt's claims to comply with the 1959 Bilateral

Agreement between Egypt and Sudan. Egypt has also used the 1929 Anglo-Egyptian Treaty as a basis of vetoing any projects occurring along the Nile river.

The water conflict in the Nile is not confined only to the riparian countries. Due to the need for socio-economic development in the riparian countries of the Nile and the plentiful of natural resources (e.g. water, hydropower potentiality, and arable land) in some of these countries, the region has attracted large international investments. For example, the push for modernization and development in Ethiopia opened doors for international actors such as the China Gezhouba Group, Voith Hydro Shanghai, and Salini Costruttori who awarded commissions for the construction of the GERD. Vast fertile lands in Sudan and South Sudan are grabbed by China, Russia, the Gulf States, and other international players. Because of their interests, these regional and international players put further stress not only hydrologically but also politically along the Nile, as its fertility is sought after by neighboring regions sometimes at the expense of the locals.

2.2. Future dynamics and expected changes in the Nile region

Based on future forecasts of UN DESA (2019), the total number of populations in the NB countries is expected to increase significantly (Fig. 2.8). The medium variant scenario exhibit values of 0.73 and 1.20 billion people for the two horizon years 2030 and 2060, respectively. While the low variant scenario forecasts a total population of 0.69 and 1.06 billion by 2030 and 2060, respectively, the high variant scenario expects a population of 0.72 and 1.36 billion people for the two years, respectively. This expected large increase in the population of the riparian countries would, consequently, put great pressure on the limited water resources of the Nile. Environmental problems in the NB are expected to intensify in the future. For instance, Onencan et. al., 2016, stated that there is high confidence that the basin will suffer from severe shifts in biome distribution, compounded water stress, degradation of marine life and reduced crop productivity. In particular, climate change impacts could affect the basin seriously. While studies investigated the temperature change in the basin are quite consistent in predicting a warming trend during the 21st century, studies focused on the precipitation change exhibit inconsistency in their predictions. A review conducted by Barnes (2017) showed that most of the studies on temperature change expect an increasing trend over the NB of values ranging between 0.3-0.6 °C per decade based on the A2 and B1 emission scenarios. On the other hand, some studies on precipitation forecast an increasing trend, while others predict a significant reduction in precipitation levels. Due to the high diversity in climatic conditions in the basin,

the impact of climate change might have different consequences on the different parts of the basin, spatially and temporally (Degefu and He, 2015).

Studies on some sub-basins (e.g. UBNB) reported that hot and dry years are more frequent and this trend seems to continue in the future and consequently may lead to chronic water scarcity in the NB (Coffel et al., 2019). The expected increase in temperature will induce an increase in the potential evapotranspiration by 7.8% in some headwater sub-basins (Worqlul et al., 2018). Climate changes in the UBNB sub-basin, which represents the primary headwater area for the main Nile, could affect the water availability in the downstream countries, i.e. Sudan and Egypt, especially due to their sensitivity to the variability of runoff from this headwater area (Kim et al., 2008). Moreover, the forecasted climate changes in some of the sub-basins in the Blue Nile region would increase the mean annual sediment yield by 2050 by around 16.3% for scenario A2 and 14.3% for scenario B2 (Adem et al., 2016).

As estimated by FAO (2011), the total agricultural water withdrawal in the NB is 99.19 km³ (2005). This figure is expected to increase significantly to reach 107.02 km³ and 114.77 km³ by the years 2030 and 2050, respectively. The irrigated schemes in Sudan and Egypt are assumed to be the main source for this major increase in water withdrawal in the NB (Fig. 2.9). Although increasing irrigation efficiency is believed to save substantial amounts of water, some researchers assume that this saved water is insufficient to meet the future water demand in the basin (Mutsch et al., 2017). Using the Water Evaluation and Allocation and Planning (WEAP) model, McCartney et al. (2012) investigated the impact of future development of irrigation and hydropower in Ethiopia and Sudan on the system of the BNB. Their results indicate that the total water storage in Ethiopia will increase to 167 km³. Irrigation is expected to increase up to 13.8 and 3.8 km³ in Sudan and Ethiopia, respectively. The annual hydropower generation in Ethiopia is expected to increase to 31,297 gigawatt hours (Gwh).

2.3. Implications of future changes

As shown earlier, the large increase in population in the future and the need to foster socio-economic development in the riparian countries will be the main drivers for increasing demand for the main key services, i.e. water, food and energy in the NB region. This substantial increase in demand will put natural resources under great pressure to satisfy these ever-increasing demands. On the other hand, drivers such as climate change and degradation of natural resources are expected to diminish the available natural resources in the basin.

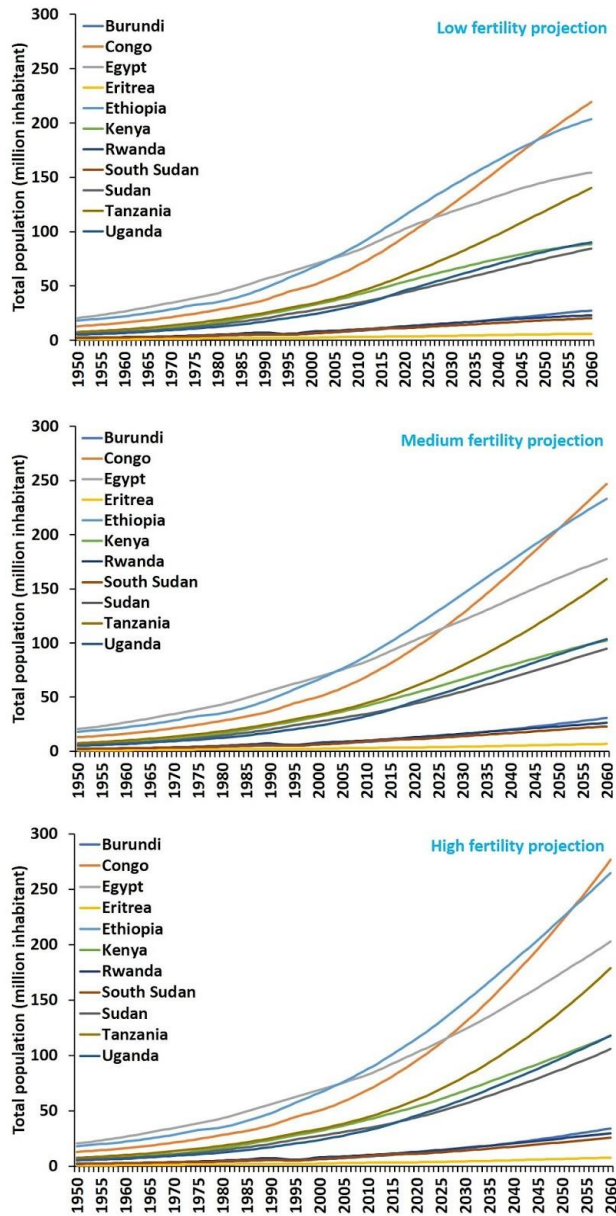


Fig. 2.8. Time series (1950-2019) of population estimation in the Nile riparian countries along with future forecasts until 2060. The future forecasts are based on three fertility projections (low, medium and high). Data of these graphs are obtained from the population division of the UN DESA (2019) database.

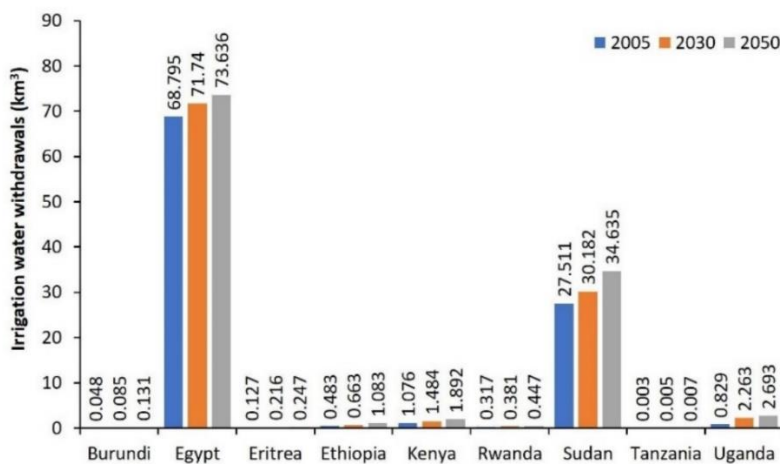


Fig. 2.9. Current (2005) and projected (2030 and 2050) agricultural water use in the Nile basin countries. This figure is created based on tabulated data obtained from FAO, 2011.

Climate change is believed to affect the way the water resources are managed in the NB. Despite the conflicting results between the studies conducted to forecast the future of precipitation in the basin, there is a wide acceptance that climate extremes such as droughts and floods will be more intense and frequent in the future. This calls for measures that enable better adaptation of the local people and require proper policies for better preparedness against such extreme events. A striking example of the expected impacts of climate change on the NB is forecasted for the Delta region in Egypt. Despite its relatively small area (~2.5% of Egypt's area), this area is highly populated, and it represents the most important area for food production in Egypt. This area is highly vulnerable to sea-level changes due to climate changes. It is estimated that a 1-meter rise of sea level would cause a loss of 4,500 km² and displace around 6.1 million people in the Nile Delta (NBI, 2012).

Although engineering the Nile river has several positive impacts to secure water, food, and energy in the basin, many negative impacts such as changes in the hydrological regime, might occur due to these projects, and this might intensify the transboundary conflict. For example, Ethiopia's construction of the GERD modernizes the energy sector and provides a clean and sustainable source of energy to Ethiopia, but it might have impacts on the agricultural activities and water security in Egypt and Sudan, especially during the dam's filling period. It is projected that the dam is going to reduce flow into Aswan High Dam by 25% (Connif, 2017), causing 2 billion US\$ in economic losses and about 1 million farmers and workers to be unemployed (Lazarus, 2018). The Aswan High Dam currently irrigates around 840,000 ha along the Nile Valley (Heinz, 1983) and produces almost half of the country's electricity (Abu-Zeid and El-Shibini, 1997). Taking into consideration the high demand for water in Egypt and the limited other sources of water in this country combined with the lack of cooperation between the riparian countries, some researchers argue that the transboundary conflict over the Nile water will be escalating during the 21st century (Keith et. al., 2013; Rahman, 2012). To minimize the GERD impacts on Sudan and Egypt during the filling period, a synchronized dam operation between the three countries is needed (Abteu and Dessu, 2019). Hence, cooperation and communication between the Nile riparian countries is a must. As reported by many researchers (e.g. Basheer et. al., 2018; Wheeler et. al., 2016), the benefits gained from the Nile waters could be maximized if a cooperative approach is followed between the riparian countries. Potential solutions for Egypt to overcome the problem of water shortage includes developing unconventional water resources such as desalination of seawater, re-use of treated wastewater, water-saving technologies, artificial groundwater recharge, inter-basin water transfer and virtual water trade (Ashour et. al., 2019; Yihdego et. al., 2017).

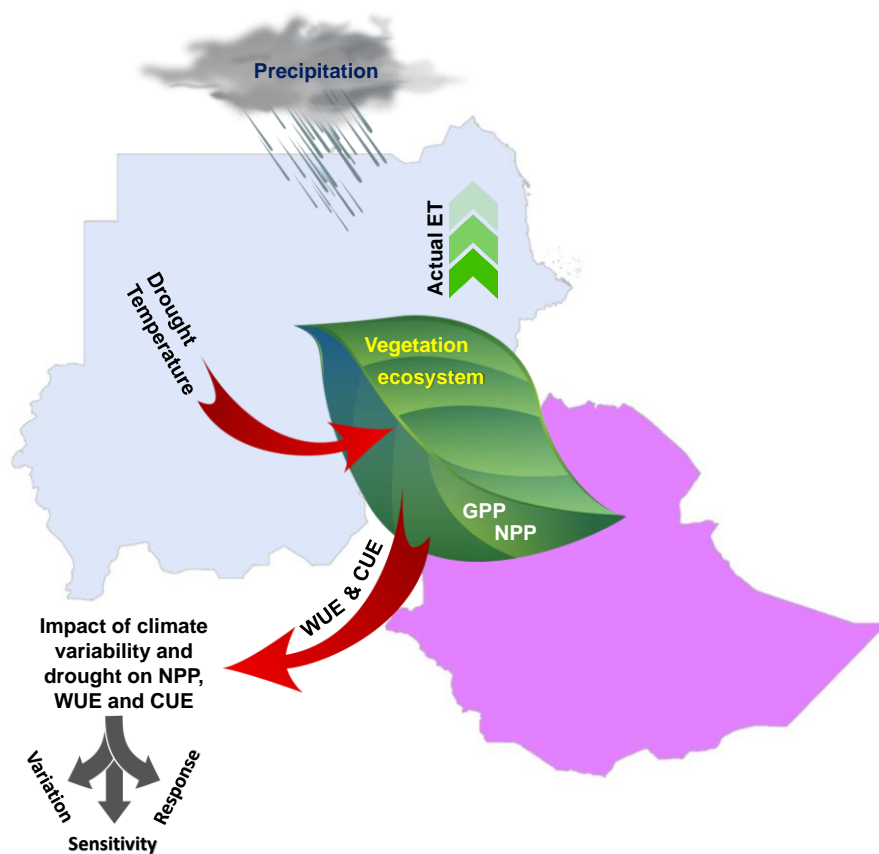
As found by McCartney et al. (2012), the large increase in water storage in Ethiopia and irrigation water in Sudan and Ethiopia would affect the current river regime. These developments are expected to decrease the river flow at the Ethiopia-Sudan border from 45.2 to 42.7 km³ and at Khartoum from 40.4 to 31.8 km³. Despite the significant reduction in the river flow at Khartoum, regulating the flow all over the year - as a result of the GERD - would provide Sudan with a continuous flow of water throughout the year compared to the current seasonal flow that peaks during the rainy season (Fig. 2.5), enabling Sudan to have more cropping seasons that could help to secure food in the country. Additionally, it might decrease the sediment yield, which accumulates in the downstream dams (Ali et al., 2017), and consequently, slows down the capacity loss of these dams and decrease the operation and sediment removal costs in the major irrigation schemes.

2.4. Conclusion

Based on the above background on the regional context, it can be emphasized that the agriculture systems in the NB are important for achieving food security and their serious implications on water security, as the major water consumer in the basin. As stated earlier, following a cooperative approach between the riparian countries and sharing benefits beyond the political boundaries would maximize the benefits gained from the use of natural resources, especially water. In terms of potentials for water and arable land, Sudan can be at the heart of such a regional cooperative approach that aims at fulfilling water and food security in the region. Despite these large potentials for water and food production, Sudan is currently struggling to ensure water and food security for its people. This could be attributed to multiple factors, i.e., endemic poverty, long history of political instability and military conflicts, ineffective policies, inefficient use of natural resources and environmental challenges. An essential step towards improving water and food securities in Sudan and the NB, in general, is to discover entry points for action and to highlight where an intervention could induce a large positive impact. Therefore, the current research focuses mainly on Sudan for the WFC Nexus analysis to derive some conclusions and convey some key messages that could be helpful for local farmers, research community and policy-makers who work on issues related to water and food security, climate change and sustainability of natural resources. Given the huge potential for food production in Sudan, the key messages obtained from Sudan's case might have implications beyond the country's boundaries and could be transferred to similar cases within and outside the NB region.

Chapter 3

Sensitivity and response of vegetation to climate variability



Based on:

Khalifa, M., Elagib, N.A., Ribbe, L., Schneider, K., 2018. Spatio-temporal variations in climate, primary productivity and efficiency of water and carbon use of the land cover types in Sudan and Ethiopia. *Science of the Total Environment*, 624, 790–806.

Abstract

The impact of climate variability on the Net Primary Productivity (NPP) of different land cover types and the reaction of NPP to drought conditions are still unclear, especially in Sub-Saharan Africa. This research utilizes public-domain data for the period 2000 through 2013 to analyze these aspects for several land cover types in Sudan and Ethiopia, as examples of data-scarce countries. Spatio-temporal variations in NPP, Water Use Efficiency (WUE) and Carbon Use Efficiency (CUE) for several land covers were correlated with variations in precipitation, temperature, and drought at different time scales, i.e. 1, 3, 6 and 12 months using Standardized Precipitation Evapotranspiration Index (SPEI) datasets. WUE and CUE were estimated as the ratios of NPP to actual evapotranspiration and NPP to Gross Primary Productivity (GPP), respectively. The results of this study revealed that NPP, WUE, and CUE of the different land cover types in Ethiopia have higher magnitudes than their counterparts in Sudan. Moreover, they exhibit higher sensitivity to drought and variation in precipitation. Whereas savannah represents the most sensitive land cover to drought, croplands and permanent wetlands are the least sensitive ones. The inter-annual variation in NPP, WUE, and CUE in Ethiopia is likely to be driven by a drought of a time scale of three months. No statistically significant correlation was found for Sudan between the inter-annual variations in these indicators with drought at any of the time scales considered in the study. Our findings are useful from the viewpoint of both food security for a growing population and mitigation to climate change as discussed in the present study.

3.1. Introduction

Net Primary Productivity (NPP) is defined as the amount of atmospheric carbon that is captured by plants and transformed into biomass (Zhao and Running, 2010). The total amount corresponding to the photosynthesis process is called Gross Primary Productivity (GPP). The difference between NPP and GPP is referred to as respiration (Ardö, 2015), which is the amount of carbon previously assimilated by the plant and subsequently used for maintenance of the biomass or growth. Monitoring of the variability in primary production is critical because NPP provides vital services for human survival (Ardö, 2015). Reduction in NPP potentially jeopardizes food security and may increase global warming since a reduction in NPP might decrease the available carbon sinks (Zhao and Running, 2010). While the spatial variation of NPP depends on vegetation type, soil, climate conditions, and human activities, its temporal variation depends mostly on the variability of climatic factors (Li et. al., 2016). Several climate factors control the NPP, such as temperature, precipitation and shortwave solar radiation (Li et

al., 2016). Temperature and precipitation have more influence on NPP in arid and semi-arid areas while solar radiation is the main controlling factor in humid and semi-humid areas (Liu et al., 2015). Temperature plays a role in raising NPP (Zhao and Running, 2010). Although the period from 2000 through 2009 was the warmest decade in the records since 1880 (NOAA, 2016), Zhao and Running (2010) found that global NPP has declined by 0.55 petagram carbon (Pg C) during the same decade. They suggested that a drying trend in the southern hemisphere was the main driver for this reduction. There has been a debate regarding these findings as to whether there was a decrease in NPP or whether this decrease was due to artifacts from the applied model (Samanta et. al., 2011; Zhao and Running, 2011). If NPP is affected by climate as suggested in that model; then, NPP should have decreased during this period (Medlyn, 2011).

Ecosystems differ in their responses to climate variability (Knapp and Smith, 2001). Different plant species respond differently to drought conditions based on their physiological and structural characteristics, to prevent loss of water (Van Der Molen et. al., 2011). Understanding how vegetation types respond to drought and climate variability can lead to more efficient management of these land covers and can, in turn, assist significantly in securing water and food in the future. Many studies have been conducted on this matter, yet, most of them have focused on the climate driver of the NPP variation on a global scale (e.g. Huang et al., 2016; Liu et. al., 2015). Recent analyses have found that semi-arid areas are the major controllers of the global NPP variation (Huang et al., 2016; Ahlström et. al., 2015). However, it is important to examine whether the same pattern of NPP found by Zhao and Running (2010) on a global scale also applies to regional and local scales (Chen et. al., 2013). Different patterns may reveal when zooming into a local scale. Drought is expected to be more severe in the future (Ault et. al., 2014). Therefore, it is important to investigate the effect of drought on primary productivity and efficiency of the land cover types in terms of water and carbon use. Analysis of these interactions at regional and national levels is useful and provides essential information for land cover management and climate policy-making (Peng et. al., 2017; Liu et. al., 2015). Recently, a country scale analysis of the relationship between NPP and drought was published by Peng et al. (2017). The data used in their work was that of Moderate Resolution Imaging Spectroradiometer (MODIS) NPP and the Standardized Precipitation Evapotranspiration Index (SPEI) for drought. They found that countries show different trends in NPP for the period 2000 to 2014, and only 35 countries accounted for more than 90% of the global NPP.

Continentially, Africa has witnessed an increase in NPP during the same period, i.e. from 2000 through 2009, by 0.189 Pg C, and this is mostly due to decreased vapor pressure deficit

(Zhao and Running, 2010). The African ecosystems produce around 20% of the total global NPP (Ciais et. al., 2011), and a large fraction of the inter-annual variability in the global carbon cycle is due to ecological processes on the African continent (Williams et. al., 2007). Monitoring the variation in vegetation productivity, WUE and CUE, and correlating this variation with climate variability for large areas is a challenge, particularly against the backdrop of the given limitations of ground data, especially in the countries of Sub-Saharan Africa, where ground weather stations are few and sparsely distributed.

Water Use Efficiency (WUE) and Carbon Use Efficiency (CUE) are useful indicators for the assessment of the pattern of water use and carbon sequestration by the plants. WUE is defined as “The rate of carbon uptake per unit of water lost” (Tang et. al. 2014), and it can be calculated differently according to the purpose of the investigation (Ito and Inatomi, 2012). For this research, WUE is defined as the amount of water evaporated for every g carbon/m² of NPP produced, i.e. NPP/ET_a , where ET_a is the actual evapotranspiration (Kuglitsch et al., 2008). The CUE is defined as a ratio of NPP to GPP. The old conception of the CUE is that it ideally equals 0.5 (Zhang et. al. 2009; De Lucia et al. 2007). However, CUE should not be considered as a constant value since the photosynthesis is primarily governed by the Absorbed Photosynthetically Active Radiation (APAR) and respiration by temperature. Several researchers noted that CUE might vary depending on climate factors (e.g. precipitation and temperature) and geographical location (Zhang et. al., 2009). Plants are considered carbon sinks, and examining the variability of CUE is useful in climate change and CO₂ emissions studies (Chen et. al., 2013). A better understanding of WUE and CUE results in better management of ecosystems (Tang et. al., 2014; Zhang et. al., 2009).

Variability in primary productivity affects food availability and food security directly, while the magnitude of primary production is directly related to the carbon cycle (Zhao et. al., 2005). However, the lack of continuous ground observation hinders the long-term analysis of the dynamics of vegetation development. Luckily, many public-domain sources nowadays provide continuous spatial climate observations and productivity estimates. The use of many of these datasets provides some indication and knowledge about their uncertainty and reliability. These datasets also provide a reproducible analysis of the impact of climate variation on primary productivity. The general availability of these public-domain data sources provides a unique opportunity for examining the climate-plant productivity relationship. Such types of data are receiving increasing attention nowadays. In comparison with climatic variables, only a few number of public-domain databases are offering data on primary productivity. Many studies

used the publicly available product of MODIS satellite of primary productivity (MOD17) to detect the variability of primary productivity as well as WUE and CUE of land cover types or entire ecosystems and their association with climate conditions. For a summary of the most important studies, refer to table (3.1). To the best of our knowledge, apart from the study of Peng et. al. (2017) which detected the impact of drought on NPP on a country scale for the whole globe, no previous comprehensive study was conducted to bridge the knowledge gap on the response of NPP, WUE and CUE of different landcover types to drought and climate variability in Sub-Saharan Africa. In this study, inter-annual variations in climate conditions and drought with different time scales for the period from 2000 through 2013 were correlated with inter-annual variation in NPP, WUE, and CUE in various land cover types in Sudan and Ethiopia. The two selected countries are examples of East Africa countries with severe data-scarcity, despite their high vulnerability to climate variation and food insecurity. The outcome of such a spatio-temporal study would be useful for better land cover management in the studied countries.

3.2. Materials and Data

3.2.1. Area of study and its importance

East Africa is one of the most challenging areas for managing natural resources due to many complex factors. It is a region highly vulnerable to climate change impacts (Abebe, 2014). Moreover, most of the countries in this region are considered among the least developed countries, with a high and rapidly rising population (UNECA, 2016), consequently putting more pressure on the natural resources in the future. With an area of about 3 million km², Sudan and Ethiopia are a good example of land use types in this region (Fig. 3.1). The two countries together are characterized by great diversity in land covers, including savannas, permanent wetlands, croplands, shrublands, and forests. Accordingly, they show significant spatial variation in climate conditions, ranging from hyper-arid in northern Sudan to the humid conditions in some parts of the Ethiopian highlands. These features make the two countries particularly suitable for our research. Most of the area in Sudan is bare or sparsely vegetated land (62% of the total area). These areas are mainly located in the northern half of the country (Fig. 3.1). In Sudan, grassland is the dominant land cover type, covering around 20% of the total area. In Ethiopia, open shrublands represent the largest land cover type, covering approximately 27.6% of the total area. Woody savannas, grasslands, and croplands also represent important ecosystems in Ethiopia in terms of area (Fig. 3.2).

Table 3.1. Review of some research used MOD17 data of NPP and GPP

Author(s)	Scale	Time period	Main objective(s)	Main findings
Huang et. al. (2016)	global	2000-2013	To examine the impact of drought on inter-annual variability on NPP	NPP is highly controlled by drought, and semi-arid ecosystems play an important role in the inter-annual variability on a global scale.
Li et. al. (2016)	global	2000-2014	To study the climate factors affecting NPP variability and its feedback to actual evapotranspiration (ET_a).	NPP is correlated positively with ET_a , and it responds differently in the northern and southern hemispheres according to dominant climate factors in each hemisphere.
Ahlström et. al. (2015)	global		To figure out the role of semi-arid ecosystems in the trend and variability of land CO_2 sinks.	The trend and variability of the global land CO_2 sinks are largely derived by variation in temperature and precipitation variation occurring over semi-arid ecosystems.
Ardö (2015)	Africa	2000-2010	To compare primary production data coming from remote sensing and dynamic vegetation models.	GPP estimations derived from remote sensing data (i.e. MOD17) are higher than those derived from dynamic vegetation models, while NPP estimations are lower. When validated against ground-based data, both estimations show a significant positive correlation.
Liu et. al. (2015)	China	2000-2011	To assess the WUE of ecosystems and their response to drought	Drought has an impact on WUE, and the response of WUE to drought is variable among ecosystem types and geographic location and climate conditions.
Abdi et. al. (2014)	Sahel region, Africa	2000-2010	To estimate and analyze the supply and demand of NPP in the Sahel countries.	The demand for NPP was increased at an annual rate of 2.2%, but with a near-constant supply. The major increase in demand is for food requirements.
Tang et. al. (2014)	global	2000-2013	To investigate the WUE of different ecosystems and to study their variation and trends.	WUE varied greatly among ecosystem types and ecosystems located under different climate conditions. Recent changes in land cover led to a decline in global WUE.
Zhang et. al. (2014)	Lower Mekong Basin	2000-2011	To assess the effect of drought on vegetation productivity	Droughts with varied intensities have different impacts on ecosystems, which show variation in response to drought.
Chen et. al. (2013)	global	1997-2009	To analyze the impact of drought on NPP	NPP and drought are positively correlated in arid regions, while boreal (sub-arctic) areas show a negative correlation, and some areas show no correlation.
Zhao and Running (2010)	global	2000-2009	To detect the trend of NPP and its relation to drought	A global reduction trend in the average NPP is detected for the investigated period. The main driving force of this reduction is drought.
Zhang et. al. (2009)	global	2000-2003	To investigate the pattern of CUE (GPP/NPP) in different ecosystems, geographical and climate conditions.	CUE varies considerably based on ecosystem type, geographical location, and climate conditions and it is not a constant value.
Turner et. al. (2006)	global	2000-2004	To evaluate the performance of MOD17 products across different biomes and compare it to 9 Eddy covariance flux towers data.	MOD17 data provide a good source to capture the response of the general trend of primary productivity, but it shows overestimations in low productivity locations and underestimations in high productivity locations.

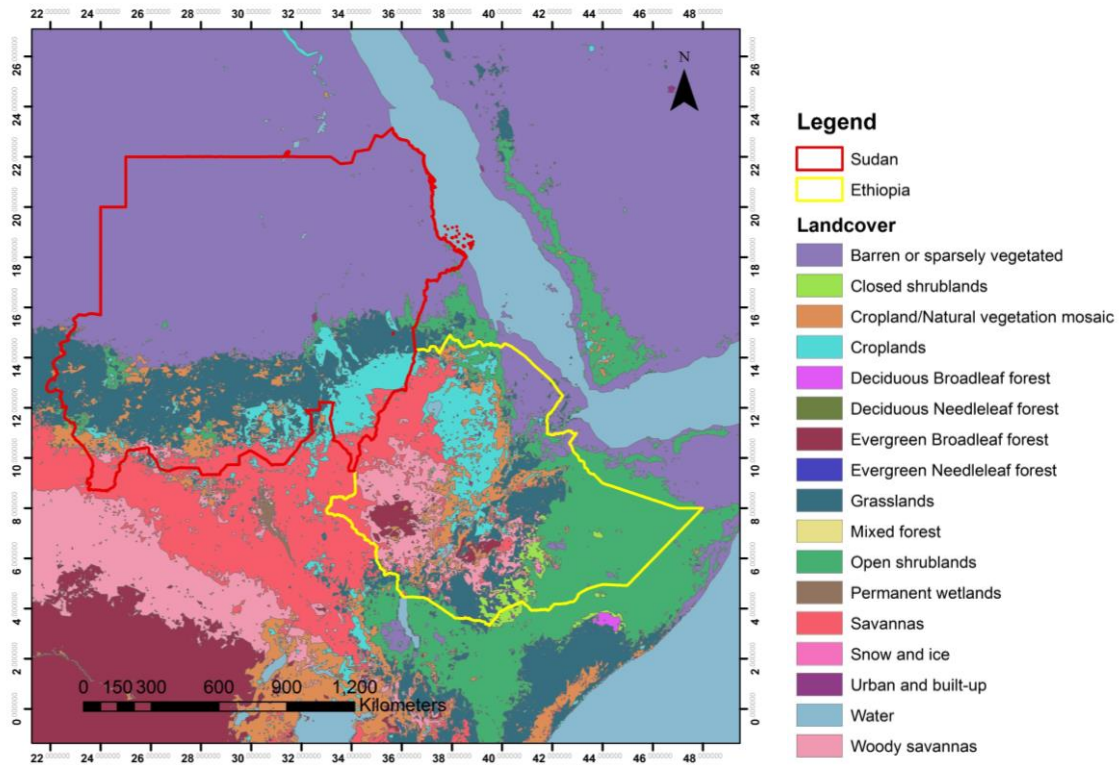


Fig. 3.1. Location map of the study area showing the boundaries of the two case studies (Sudan and Ethiopia) and the different land cover types located in the region. Landover data in this map are that of MCD12Q1 product.

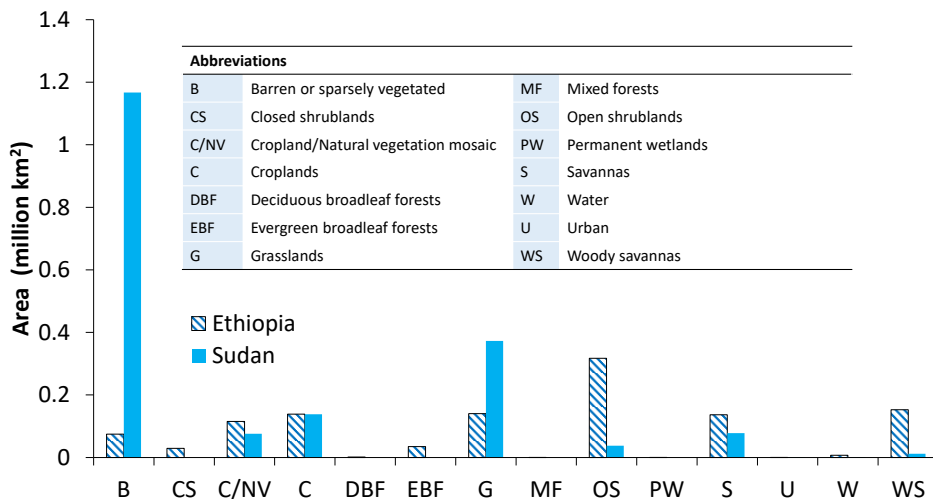


Fig. 3.2. The total area of each land cover in Sudan and Ethiopia as appears in the MDC12Q1 product.

3.2.2. Data and Methods

Using data acquired from public-domain sources offers a solution for such a data-scarce region. Along with land cover data, time series of the NPP, GPP, Normalized Difference Vegetation Index (NDVI), precipitation, evapotranspiration, temperature and Standardized Precipitation Evapotranspiration Index (SPEI), were used in this analysis (Table 3.2). All these

data were derived from public-domain sources for a time frame extending from 2000 through 2013. Most of the remote sensing datasets used in this study are recent products and available only for the years after 2000, for instance, the NPP, GPP, and ET_a from MODIS. The selection of the period (2000-2013) was mainly controlled by the availability of the data from different sources for the same period. On the other hand, many studies dealt with the same subjects were conducted for somehow a similar period. We choose the period to be consistent with these researches to facilitate the comparison of the findings. Moreover, as mentioned earlier, the period between 2000-2009 was the hottest on the global record and therefore these years are very interesting from the NPP point of view. In this study, the data processing was carried out using ArcGIS 10.3 software.

3.2.2.1. Primary productivity

Primary productivity data were obtained from MOD17 product (Zhao et al., 2005), which provides NPP and GPP data (in $g\ carbon\ m^{-2}$) from MODIS satellite. MODIS is one of the sensors on NASA's Earth Observing System (EOS) satellites. It provides continuous global monitoring data of primary productivity with a spatial resolution of 1 km and at a temporal resolution of 8-day, monthly and annual intervals. MOD17 version 55 data of annual estimates of NPP and GPP were downloaded from the Numerical Terradynamic Simulation Group website. Invalid values were removed from the raster files; then, each raster file was multiplied by a scale factor of 0.1 to restore the original NPP and GPP values, as instructed in the metadata file of this dataset. Lastly, using the “extract by mask” tool in ArcGIS, separate raster time series of NPP and GPP were produced for each of the two countries, i.e. Sudan and Ethiopia.

With limited available ground data in comparison with MOD17 data, validation of MODIS data is a challenge (Zhao et. al., 2005). Numerous studies were conducted to compare the MOD17 data with field measurements. A detailed overview of the performance of this product is beyond the purpose of this research. Nevertheless, it is worth mentioning for instance that Turner et. al. (2006) used Eddy flux towers to validate MOD17 data and found that MOD17 show no overall bias when compared with towers data. They found, however, that MOD17 data tend to overestimate primary productivity in the low productivity areas and underestimate it in high productivity areas. Zhao et. al. (2005) made many enhancements in the main inputs of this dataset and reported on correlation analyses between MOD17 and ground-based data. Ardö (2015) compared MOD17 NPP with Aboveground NPP (ANPP) data collected from ground measurements in 35 sites in Sudan. While, they found a strong correlation between the multi-year average MOD17 NPP and the ANPP ($r = 0.80$, $RMSE = 135\ g$), but also reported a

systematic over-estimation of MOD17 NPP, which is regarded to the fact that the ANPP only considers aboveground biomass.

Table 3.2. Specification of the data used in this study

Dataset	Source	Reference	Temporal resolution	Spatial resolution	Dissemination website	Performance
Net Primary Productivity (NPP)	MOD17	Zhao et al., 2005	Annual	1 km	http://www.ntsug.umt.edu	Differ from field measurements by 28%
Gross Primary Productivity (GPP)	MOD17	Zhao et al., 2005	Monthly	1 km	http://www.ntsug.umt.edu	
Precipitation (P)	CHIRPS	Funk et al., 2015	10-day composite	5 km	http://earlywarning.usgs.gov/fews/datadownloads/Global/CHIRPS%202.0	CHIRPS correlations with gridded ground precipitation data are with $R > 0.75$ in many areas of the world
Actual Evapotranspiration (ETa)	MOD16	Mu et al., 2007; Mu et al., 2011	Monthly	1 km	http://www.ntsug.umt.edu/project/mod16	The correlation coefficient between MOD16 and tower data is 0.86 (Mu et. al., 2011)
Normalized Difference Vegetation Index (NDVI)	e-MODIS NDVI, Famine Early Warning Systems Network (FEWS NET)	-	10-day composite	0.25 km	http://earlywarning.usgs.gov/fews/datadownloads/East%20Africa/eMODIS%20NDVI	
Temperature (T)	University of Delaware (UDel)	Willmott and Matsuura, 2001	Monthly	50 km	http://www.esrl.noaa.gov/psd/data/gridded/data.UDel_AirT_Precip.html#detail	
Drought index	Standardized Precipitation Evapotranspiration Index (SPEI)		Monthly	50 km	http://www.sac.csic.es/spei	
Land cover	MCD12Q1	-	-	0.5 km	https://lpdaac.usgs.gov/dataset_discovery/modis/modis_products_table/mcd12q1	

3.2.2.2. Normalized Difference Vegetation Index (NDVI)

Data on the NDVI were obtained from the website of the Famine Early Warning Systems Networks (FEWS NET). This dataset was developed by the U.S. Geological Survey (USGS) Earth Resources Observation and Science (EROS) Center. The data used herein were 10-day composite data with a spatial resolution of 250 m. The raw NDVI images processing involved: (i) eliminating the invalid values, as per instruction of the product documentation; (ii)

converting the digital numbers (DNs) provided in the raster files to NDVI values, using the formula $NDVI = (DN - 100) / 100$; (iii) using “extract by mask” tool to create separate NDVI data for each country from the original tiles of East Africa; (iv) aggregating 10-day composite data into monthly time steps, using Maximum Value Composite (MVC) method (Holben 1986), which selects the maximum value for each pixel from the three 10-day composite images. Integrated NDVI (iNDVI) for the cultivation season was used as a proxy for accumulated biomass (Field et. al., 1995; Prince and Goward, 1995). It was calculated as a summation of the NDVI for June – October, which represents the main growing season in the region (Elagib, 2014; 2015).

3.2.2.3. Precipitation

In the current study, we used Climate Hazards Group InfraRed Precipitation with Station data; CHIRPS (Funk et. al., 2015) version 2.0 with a spatial resolution of 0.05° . Processing of precipitation data for this research included aggregation of the original 10-day composite data into monthly and annual data. Then, extract by mask tool in GIS was used to produce a time series of precipitation for Sudan and Ethiopia. CHIRPS product is a gridded precipitation dataset, which is developed by the United States Geological Survey (USGS) to provide high-quality precipitation data to be used for early warning missions and drought monitoring. Blending remote sensing estimations with in-situ data from climate stations, including stations in Sudan and Ethiopia, results in good reliability of this dataset (Funk et. al., 2015).

3.2.2.4. Temperature

A temperature product developed by the University of Delaware (UDel) was used in this investigation. UDel provides gridded monthly air temperature data with a spatial resolution of 0.5° for the whole globe (Willmott and Matsuura, 2001). This dataset covers the period from 1901 to 2014. Data of UDel product uses observations from ground weather stations. The last version (V4.01) of this dataset was used herein. As with the previous datasets, monthly temperature data were also processed and time series rasters were produced for each country over the study period and later aggregated to annual averages.

3.2.2.5. Actual evapotranspiration (ET_a)

Only a few public-domain sources provide data on actual evapotranspiration (ET_a). For this study, MOD16A2 product was used. MOD16A2 is a monthly ET_a dataset offered by a NASA/EOS project. It provides global evapotranspiration data using input data from MODIS satellite. The data come in a 1 km spatial resolution and at 8-day, monthly and annual temporal

resolution. This product uses an ET algorithm developed by Mu et. al. (2007) and improved by Mu et. al., (2011) to calculate ET_a based on the Penman-Monteith equation (Monteith, 1965). MOD16 provides a special product for the Nile basin which is the one used herein. This product overcomes the problem encountered by the regular MOD16A2 datasets of not considering deserts, which is one of the major ecosystems in the region. Processing of MOD16A2 raw data considered excluding invalid values by removing the pixels of these values and restoring the original ET_a values from the DN. Separate raster time series were created for Sudan and Ethiopia. This product was validated using ground data by several researchers. Some researchers found an inconsistency between MOD16 ET and ground data. For instance, Ramoelo et. al. (2014) used ET_a data for savanna and woodland ecosystems between two eddy covariance flux towers in South Africa and MOD16 ET_a . Their analysis showed that due to parameterization of the Penman-Monteith model and flux tower measurement errors, MOD16 underestimates ET_a by 2-7 mm per 8 days. In contrast, Tang et. al. (2015) found a good agreement between MOD16 ET_a and eddy covariance and large aperture scintillometer measurements in north and northwest China. Validation studies of this product over East Africa are few. Al Zayed et. al. (2016) have validated MODIS ET_a (MOD16A2) among other satellite-based ET_a estimation methods using field-scale water balance over the Gezira scheme in central Sudan. They found that, on a regional scale, MOD16A2 is one of the more useful operational products, yet, MOD16 algorithm tended to overestimate (underestimate) low (high) ET_a values. Despite the observed differences between the ground measurements and MOD16, this product provides essential knowledge on the water cycle and its interaction with environmental changes (Mu et. al., 2007). It provides easily accessible information for areas with limited surface data like the region of Sub-Saharan Africa.

3.2.2.6. Drought index data

Because drought is a slow phenomenon that develops over a long time without precipitation (Wilhite and Glantz, 1985; Gillette, 1950), drought indices that take different timescales into account are very useful for drought assessment. Incorporating different time scales in the assessment of drought impact is widely used (Potopová et. al., 2015). In the current investigation, we used the Standardized Precipitation Evapotranspiration Index (SPEI) developed by Vicente-Serrano et al. (2010). With a spatial resolution of 0.5° and a monthly time step. SPEI calculation requires precipitation and temperature data to account for the difference between precipitation and potential evapotranspiration (PET), i.e. a simple water balance. SPEI is a multi-scalar index that allows comparison of drought severity over different

time scales and across space. For the SPEI scale ranges refer to Table (3.3) As SPEI is a standardized variable, it can be compared with other SPEI values over time and space. The most widely used time steps are 1, 3, 6, 12 and 24 months, denoted by SPEI01, SPEI03, SPEI06, SPEI12, and SPEI24, respectively (Chen et. al., 2013). In the current investigation, we used SPEI01, SPEI03, SPEI06 and SPEI12.

Table 3.3. Categories of the SPEI scale

Class	SPEI value
Extremely wet	≥ 2.00
Severly wet	1.5 to 1.99
Moderately wet	1.00 to 1.49
Normal	0.99 to -0.99
Moderately drought	-1.00 to -1.49
Severe drought	-1.50 to -1.99
Extreme drought	≤ -2.00

3.2.2.7. Land cover

In the current research, MCD12Q1 land cover dataset (Friedl et al., 2010) provided by the Land Processes Distributed Active Archive Center (LP DAAC) was used. This product provides annual land cover data for the whole globe with a spatial resolution of 1 km for the period spanning 2001 to 2012. The latest land cover data (version 51) was used herein, with land cover classification scheme of the International Geosphere-Biosphere Programme (IGBP). The global land cover layer was processed to generate separate land cover classes layers for each country.

3.2.2.8. Correlation of the variables and calculation of water and carbon uses efficiency

The NPP and climate elements were standardized according to Kraus (1977) to analyze the inter-annual variability of the Standardized Anomaly Indices (SAIs). Before standardization, the data from all variables were tested for normality using the Shapiro-Wilk test (Ghasemi and Zahediasl, 2012; Shapiro and Wilk, 1965). Employing an online calculator (Dittami, 2009), the data were found to be normally distributed. For each variable, the SAI was calculated as: {value – average (2000 – 2013)} / standard deviation (2000 – 2013). The annual average of each climate variable for each land cover class was calculated using the functions of the GIS environment. Figure 3.3 shows the procedure followed in this study to correlate the variation in the annual NPP and climate indices. This procedure was used for all land cover classes and each year using the non-parametric Spearman's coefficients (ρ , rho), with the aid of XLSTAT V.19.4

software (Addinsoft, 2017). Croplands and grasslands were considered in the analysis of the impact of climate variability on food production on a monthly time step for two selected years (2007 and 2009) representing a wet and dry year, respectively (Elagib, 2013; Sulieman and Elagib, 2012). For the two years, 10-day composite NDVI data were summed for the five cultivation months (June -October), and the seasonal iNDVI was used as a proxy of vegetation productivity as explained before. Annual average WUE and CUE were calculated for each land cover type as the ratios of NPP to ET_a and NPP to GPP, respectively.

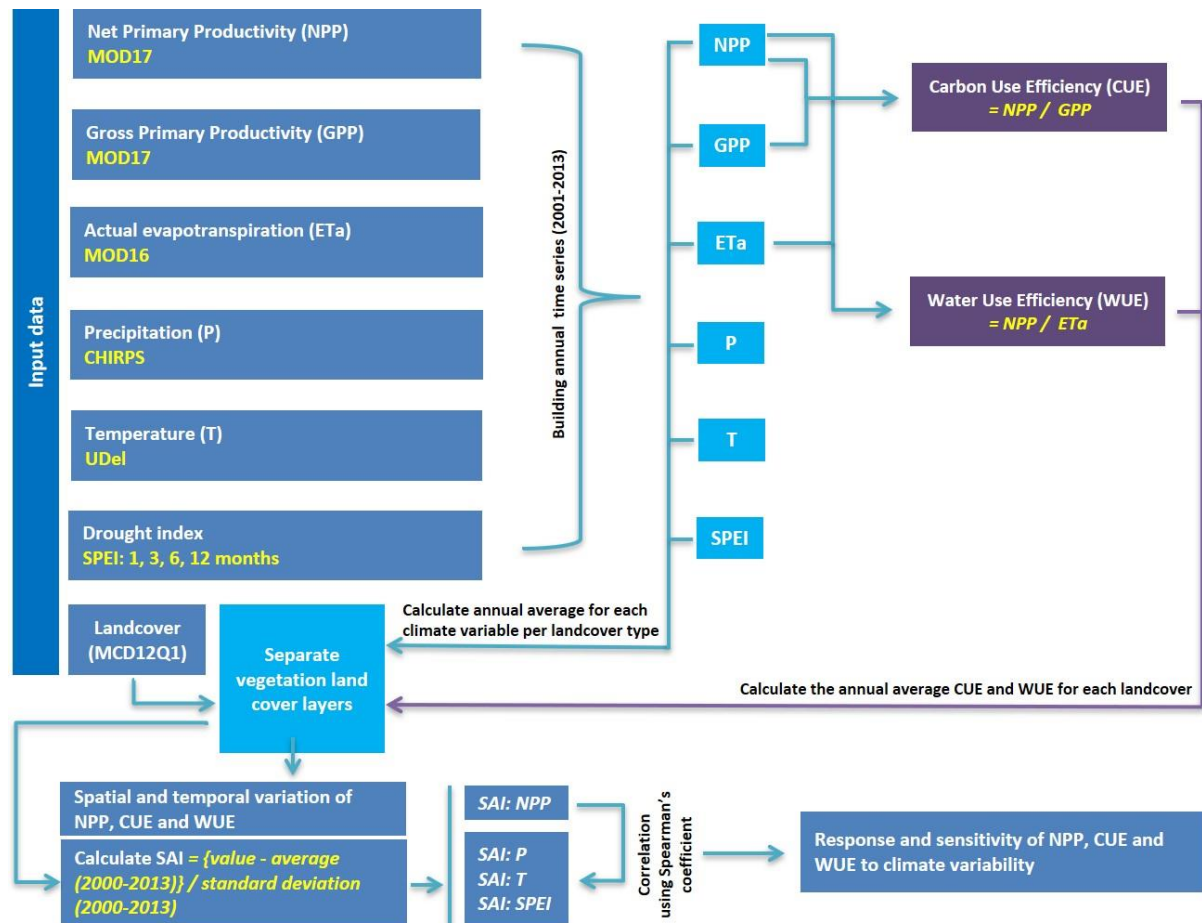


Fig. 3.3. Flowchart of the methodological procedure followed in this study to correlate the inter-annual variability in NPP, CUE and WUE and their response to climate variability and drought conditions.

3.3. Results and discussion

3.3.1. Climate conditions during 2000-2013

In general, precipitation in Sudan is much less than in Ethiopia. Temporally, precipitation shows some variation from year to year in both countries (Fig. 3.4a). The year with the lowest precipitation in Sudan was 2004, recording 180.3 mm. For the period 2000-2013, the average total annual precipitation is 227.9 mm and the Coefficient of Variation (CV) is 0.13 for Sudan. As for Ethiopia, the corresponding values are 808.8 mm and 0.08 (Fig. 3.4a). The results on average precipitation obtained from CHIRPS are comparable with the 1970-2000 averages, i.e., 225.5 mm and 799.1 mm for Sudan and Ethiopia, respectively, as estimated using WorldClim (Fick and Hijmans, 2017). Most of the vegetation in Sudan is found on an east-west belt located in the southern part of the country and characterized by precipitation amounts between 250-500 mm and rarely above 1000 mm. Large areas of the northern part of Sudan receive less than 250 mm per year. As for Ethiopia, the annual precipitation is on average more than 2000 mm, with the highest precipitation occurring in the western part while the lowest precipitation is recorded in the northeastern and southeastern portions of the country.

In the study area, the timing of precipitation is very important to understand the vegetation development. Sudan and Ethiopia are relying mostly on rainfed agriculture for domestic food production. The rainy season and growing season are identical, and they extend between June and October. Even in Sudan, where irrigated agriculture is widely practiced, the main growing season timing remains the same, especially in the large irrigated schemes (e.g. Gezira and Rahad). This is because the water supply in these schemes is highly dependent on the River Nile flow which is highly variable due to the seasonal variability in precipitation.

On average, most of Sudan shows an annual ETa of less than 500 mm. The southern part displays ETa up to 1500 mm. Some of the irrigated agricultural schemes (e.g. Gezira) in central Sudan show an average ETa between 500 mm and 1000 mm. The country's annual average of ETa is 204.4 in Sudan and 530.2 mm in Ethiopia (Fig. 3.4b). Spatial variation in ETa takes the same pattern as that of precipitation. The highest ETa values are of water bodies, e.g. Lake Tana in Ethiopia (Fig. 3.4b).

The 14-year annual average temperature is 28.1 °C in Sudan and 23.1 °C in Ethiopia. During the study period, the highest average temperature detected for each country was 29.0 °C in Sudan in 2010 and 23.5 °C in Ethiopia in 2009. Regionally, the center of Sudan is the area characterized by the highest temperature (Fig. 3.4c).

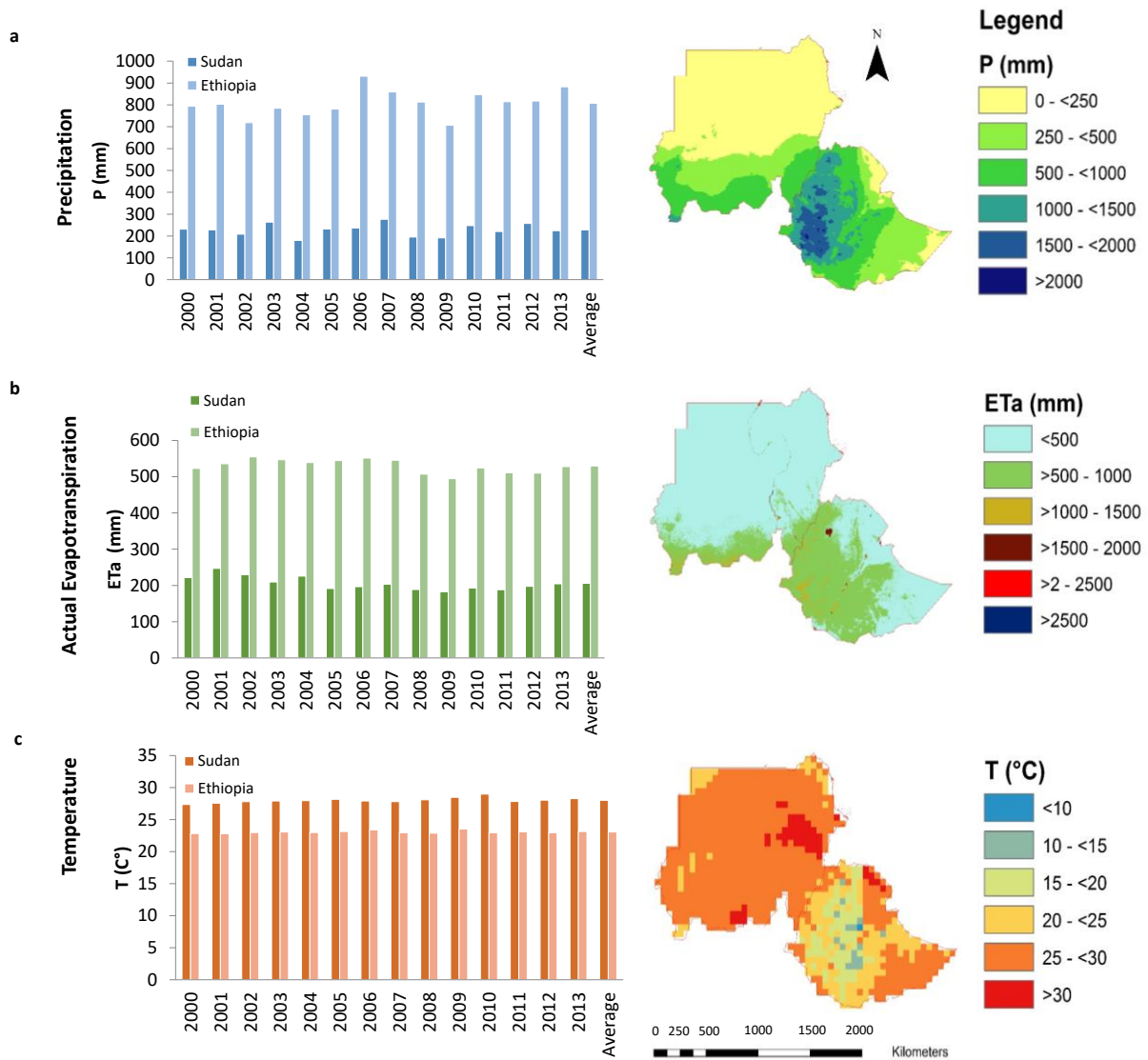


Fig. 3.4. Temporal and spatial variation in climate variables in the two countries considered in this study: (a) precipitation, (b) actual evapotranspiration and (c) temperature.

On a monthly time scale, the most severe droughts in the region during the study period occurred in 2004, 2005 and 2009 (See Appendix B: Fig. S3.1). During these years, Sudan was affected by moderate to severe drought, while moderate drought conditions prevailed during only a few months in these years in Ethiopia. Based on the annual data (Fig. 3.5a and b), Sudan was affected by a moderate drought in 2009, while the rest of the years were normal. Ethiopia experienced normal moisture conditions during the same period.

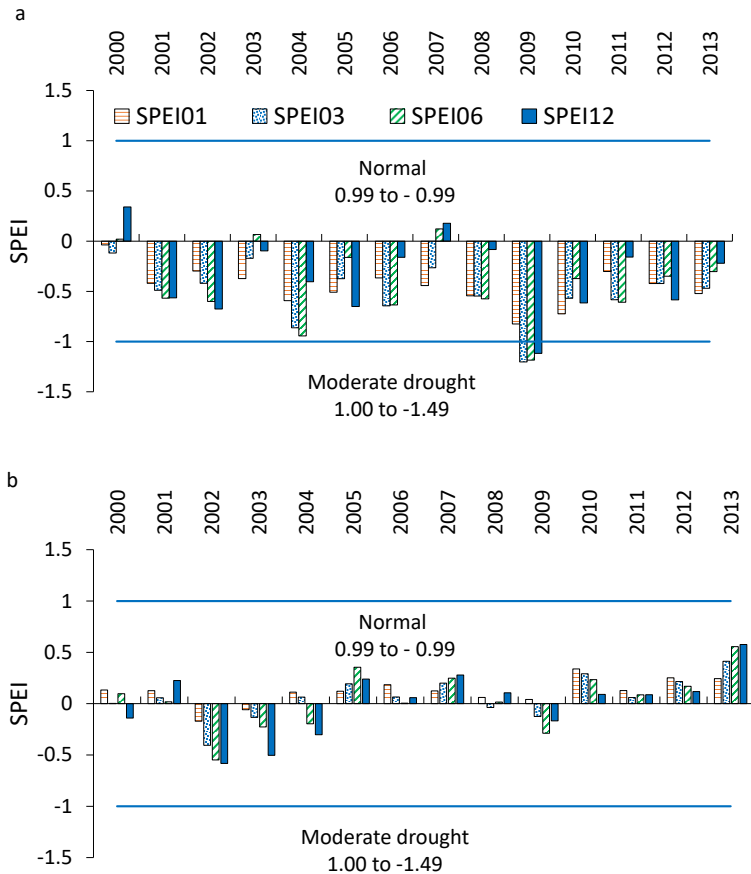


Fig. 3.5. Time series of SPEI for in the study area with different time steps 1, 3, 6 and 12 months, (a) Sudan and (b) Ethiopia.

3.3.2. Net primary productivity during 2000-2013

Spatially, the highest NPP values in Sudan are found along the southeastern and southwestern borders of the country where most of the savannas are located (Fig. 3.6a). The majority of the northern parts of the country are barren areas with too low NPP rates compared to the vegetated areas within the country. In Ethiopia, the highest NPP values characterize the middle part of the country that is covered mostly by woody savannas and evergreen broadleaf forests (Fig. 3.6b). The areas with the lowest NPP rates are located in the northeastern part of the country which is mostly barren, sparsely vegetated or covered by open shrublands. The annual average NPP is 87.24 and 501.92 g carbon for Sudan and Ethiopia, respectively. All of the land covers in Ethiopia show higher NPP than their correspondents in Sudan. This could be attributed to the higher precipitation and larger areas of the vegetation landcover types in Ethiopia compared to Sudan. On average, evergreen broadleaf forests and woody savannas in Ethiopia show the highest annual NPP, with NPP values of 1279.5 and 845.3 g Carbon/m², respectively.

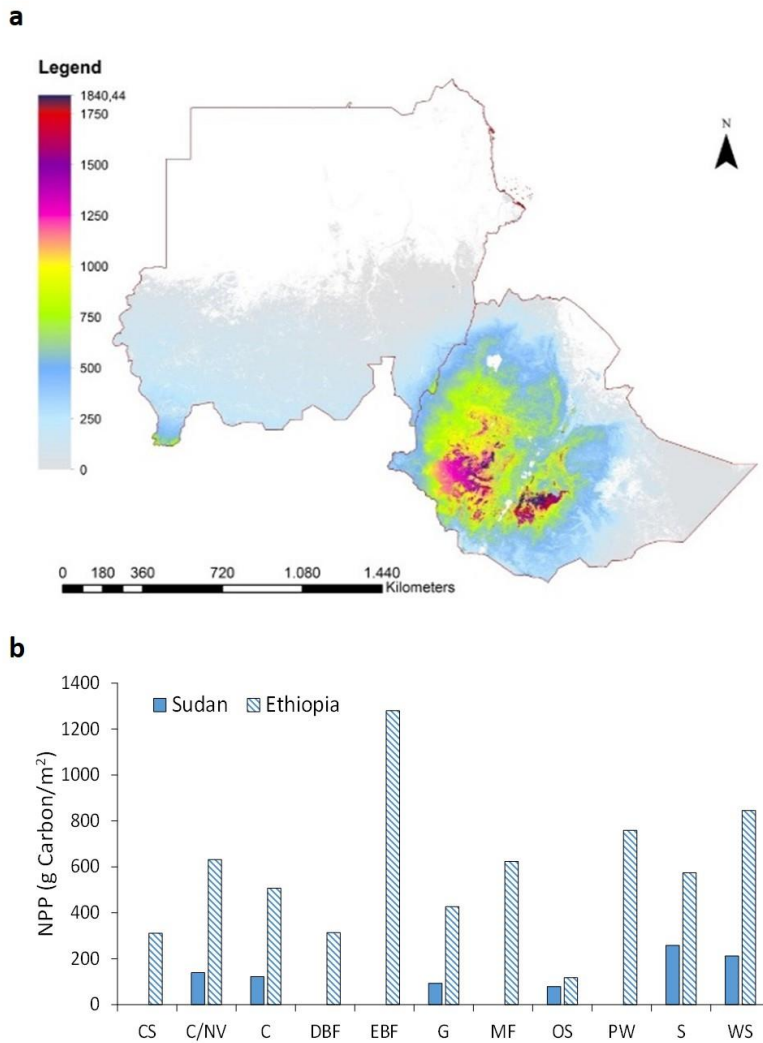


Fig. 3.6. (a) Spatial variation of the average NPP in Sudan and Ethiopia as modeled by MOD17. (b) Multiyear annual average (2000-2013) of NPP for land cover types in Sudan and Ethiopia. Abbreviations for names of land cover types can be found in figure 3.2.

3.3.3. Variation of primary productivity and correlation with climate variability

Throughout the period from 2000 to 2013, the NPP displayed high inter-annual variability in both countries. In Sudan, most of the land cover types showed negative anomalies during the years 2000-2008 (Fig. 3.7a). The year 2007 was an exception, probably because it was a year with relatively high precipitation. The last five years (2009-2013) witnessed an increase in NPP of all land cover types. NPP for the year 2002 was associated with the largest decline for all land covers. The drought effect in two successive years (2001 and 2002) is likely to be the reason behind this considerable decrease in NPP. In comparison with Sudan, some land covers in Ethiopia displayed positive NPP anomalies during the first years of the study period, mainly due to the high precipitation. From the data, the impact of drought of 2002 in some land cover types (e.g. closed shrublands, croplands mixed forest and savannas) was notable as NPP in these land covers showed negative anomalies.

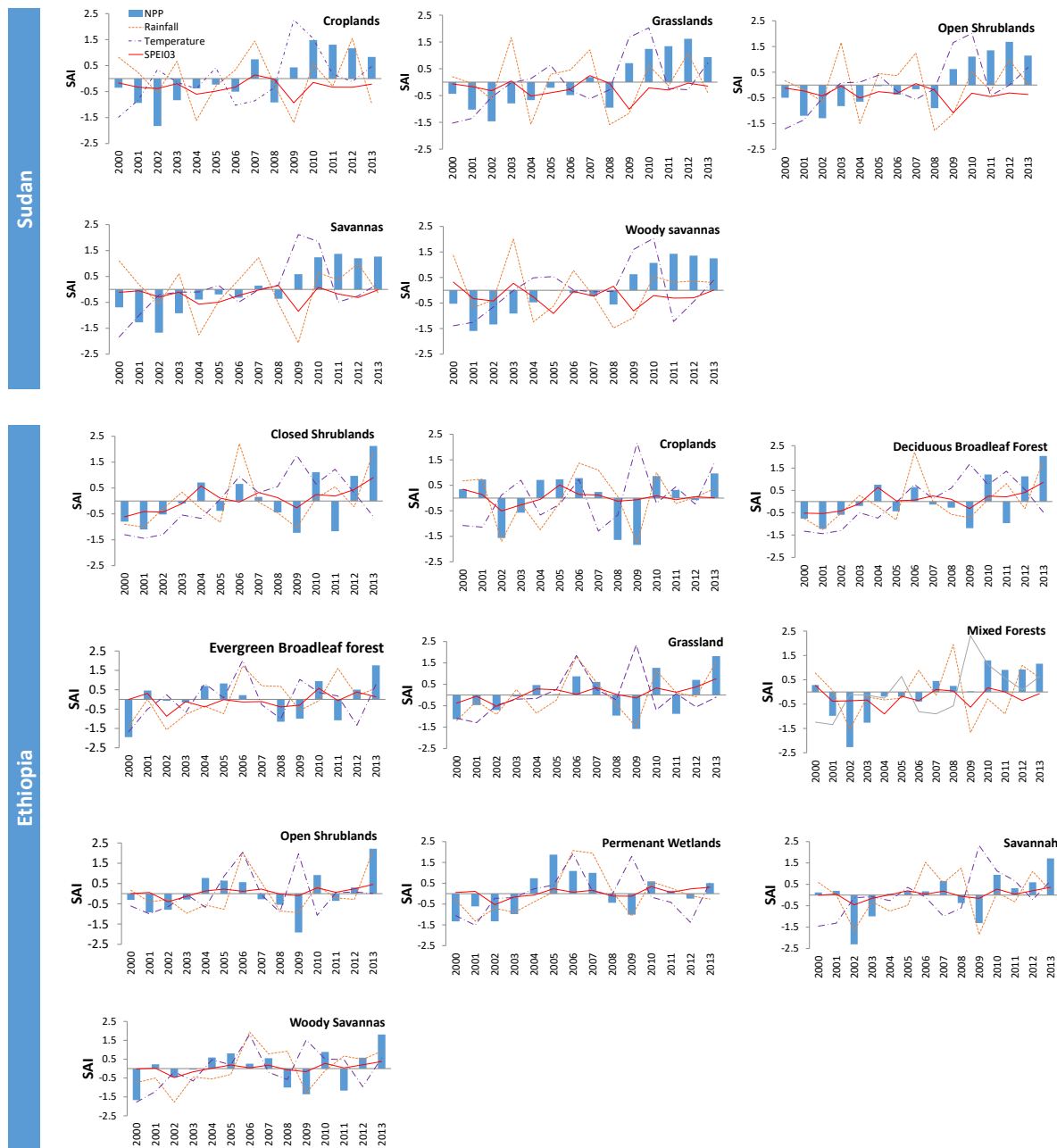


Fig. 3.7. The anomaly of inter-annual NPP in different land covers in Sudan and Ethiopia, with the anomalies in climate conditions (precipitation, temperature, and drought (SPEI)) prevailed in each land cover type are plotted.

As mentioned earlier, many drivers regulate the inter-annual variability of NPP. In arid and semi-arid areas, such as the study area, patterns of precipitation and temperature are likely to be the most important climatic factors, but the interactions of these climatic factors on vegetation activities are complex (Li et. al., 2016). From the analysis, it can be noted for Ethiopia that the variability in NPP is influenced directly by the variability in precipitation (Fig. 3.7). This is manifest by the in-phase response of NPP to changes in precipitation and by Spearman’s ρ (See Appendix B: Fig. S3.2). Among all land cover types in Ethiopia, grasslands

revealed the strongest correlation ρ value ($\rho = 0.82$, $p = 0.05$). While the correlation with closed shrublands, croplands, deciduous broadleaf forests, grasslands, and permanent wetlands were significant, the correlation for evergreen broadleaf forests, mixed forests, open shrublands savannas, and woody savannas was statistically insignificant. In Sudan, the correlation was statistically insignificant at $p = 0.05$ (See Appendix B: Fig. S3.3). Zhang et. al., (2014) listed many biotic and abiotic factors (e.g. soil properties, nutrient availability, and temperature) to be responsible for the lack of immediate response of NPP to the current-year precipitation. Spatially, the highest correlation between NPP and precipitation is detected in the eastern and southern Ethiopia (Fig. 3.8). Spearman's ρ in these areas is more than 0.6. These areas are dominated by croplands, grasslands, and savannas. Only small spots in the central (El Gedaref and Blue Nile states) and western parts of Sudan exhibited ρ values more than 0.6. The central part of Sudan is characterized by extensive croplands (both irrigated and rainfed agriculture). However, the correlation between NPP and precipitation in these areas was statistically insignificant. Statistical analysis showed no significant correlation between the inter-annual variation in mean annual temperature and NPP for all land covers in both countries. Several land cover types showed an insignificant correlation between the inter-annual variation in temperature and NPP (Fig. 3.8). Lack of correlation between temperature and inter-annual variability in NPP in arid and semi-arid regions were detected in some parts of the world, as reported by Liang et al. (2015) for China. These findings may suggest that the land cover types in Ethiopia are more sensitive to variation in precipitation than those characterizing Sudan. However, since this analysis was conducted on only an annual basis, further analysis of the varying seasonal effects on vegetation development is deemed imperative to draw a more solid conclusion.

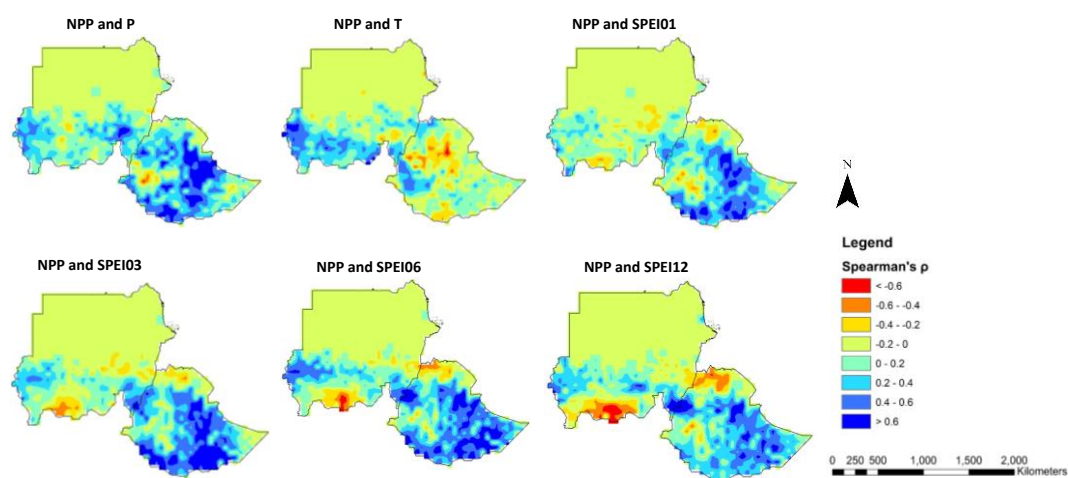


Fig. 3.8. The spatial pattern of correlation between NPP and climate variables for the period 2000-2013.

3.3.4. Drought impact on primary productivity

Drought affects the annual NPP in the land covers of Sudan and Ethiopia differently. While all land cover types in Ethiopia show a positive significant correlation ($p = 0.05$) between NPP and drought severity, no statistically significant correlation was detected for Sudan. Lack of correlation between annual NPP and the SPEI was also found by Peng et al. (2017) for many countries (e.g. Indonesia, Philippines, and Malaysia). Correlating SPEI at different time scales (1, 3, 6, and 12 months) with NPP anomalies, we found the highest correlation with the annual NPP anomalies for SPEI03 in Ethiopia. Thus, drought events on a time scale of 3 months largely control NPP in this country. This high correlation is detected spatially. Large areas in Ethiopia showed a statistically significant correlation between NPP and SPEI03 compared to other drought time steps (Fig. 3.8). Savannas also showed a very strong positive correlation between NPP anomalies and SPEI at a time step of three months ($\rho = 0.93$, $p = 0.05$). Open shrublands in Ethiopia seem to be more sensitive to drought as their NPP showed a strong positive correlation with a drought of one month (SPEI01) ($\rho = 0.84$, $p = 0.05$). The NPP for croplands and permanent wetlands displayed the weakest relationship with SPEI03 ($\rho = 0.66$ and 0.63 respectively, $p = 0.05$). This relatively lower correlation suggests that these two land covers are less sensitive to drought than the other land covers due to agricultural management (e.g. irrigation) and/or sufficient water supply from tributaries or groundwater. Evergreen broadleaf forests seem to be quite resistant to drought since their inter-annual NPP variation showed a moderate correlation with SPEI ($\rho = 0.54$ with SPEI01, $p = 0.05$). Deeper rooting (Song et. al., 2017) and access to larger water stores in soils and groundwater could be a reason. All of the land cover types in Sudan showed no statistically significant correlation between their annual NPP anomalies and SPEI at any of the SPEIs.

The total NPP in the dry year 2009 increased by 20.1% in Sudan and decreased in Ethiopia by 11.4% from the 14-year country's average (2000-2013). The increase of NPP in dry years is reported in many areas around the world, for example in Northeast China (e.g. Sun et. al, 2016; Liu et. al, 2015; Pei et. al, 2013) and Phoenix, USA (Frolking, 1997). Generally, there are three potential causes of this phenomenon (Yang et. al., 2016; Liu et. al., 2015; Pei et. al., 2013). These causes are (i) the association of the increase in temperature with drought, (ii) the memory effect of the previous year drought on the current year NPP and (iii) the characteristics of drought. In the case of the dry year 2009 in Sudan, it seems that all these factors are playing a role in this increase. It can be explained partly by the notable increase in the annual temperature in this year (Fig. 3.7), which was the hottest in the record (Sulieman and Elagib, 2012).

Temperature is an important factor in this regard, as it plays a key role in the plant respiration process contributing to increasing NPP (Zhao and Running, 2010). In particular, mild drought when coupled with high temperature might increase the NPP (Sun et. al., 2016). This is because an increase in temperature during the drought period might partly offset the decrease of NPP induced by water deficit (Liu et. al., 2015). In contrast, the dry year of 2004 witnessed a decrease in the average temperature from the multi-year average which might contribute to the decrease in the annual NPP. On the other hand, the drought of the previous year might have an impact on the NPP of the current year, a phenomenon called the memory effect (Yang et. al., 2016). This effect is notable in the dry year of 2002, where the NPP was decreased significantly, probably by the cumulative effect of the drought of 2002 and the drought of 2001. The relatively better drought condition in 2008 probably weakens the drought impact of 2009. The timing of drought is also an important factor determining the response of NPP and the crop yield (Elagib, 2015). NPP has different responses to droughts that occur during different seasons of the year. In the case of Northeast China, while spring drought has an insignificant impact on the vegetation NPP, autumn drought leads to a larger reduction in NPP (Liu et. al., 2015). Froelich, (1997) found that late summer drought in Phoenix increased NPP by about 20% due to reduced respiration. A careful analysis of drought characteristics in Sudan showed that, while the intensity of drought in 2009 was stronger than that of other dry years (e.g. 2002), the timing of drought during the beginning of the season (e.g. July) was stronger in the other years than in 2009, and the spatial extent of the drought was lesser in 2009. According to Bussmann et. al., (2016), the optimum sowing date for rainfed agriculture in the main agriculture area in Sudan is the 8th of July. Drought at the sowing period is very critical and could lead to a significant decrease in crop yield. A mild drought during July-August could lead to a significant drop in cereal crop yield in the country (Elagib, 2013). This resulted in a relatively higher NPP in many land covers (e.g. croplands and shrublands) in July 2009, which is less by 33% from the NPP of the same month in the wet year, 2007. It is not realistic to attribute the increase of NPP in the dry year of 2009 to only one factor. As shown in this case, this increase is probably caused by the combined effects of temperature, the memory effect, and the drought characteristics. This conclusion goes in line with the findings of Pei et. al., (2013).

3.3.5. Intra-annual variability of primary productivity and drought

Results of monthly GPP and NDVI for croplands and grasslands showed the same temporal pattern in 2007 and 2009. GPP and NDVI start to increase remarkably at the beginning of the rainy season (i.e. June) as shown in Fig. 3.9. The average NDVI showed lower values during

the drought year 2009 in both countries and for both types of land covers. A strong correlation was found between the monthly NDVI and monthly GPP for the two land covers in both countries (See Appendix B: Fig. S3.4). The drought condition of 2009 reduced both the monthly NDVI and GPP during the rainy months. The reduction in the NDVI was more noticeable in Sudan as compared to Ethiopia. Accordingly, the decline in NDVI for croplands and grasslands in 2009 compared to 2007 were 16.9 and 14.9% in Sudan and 7.1 and 16.1% in Ethiopia, respectively. Statistical correlation between the intra-annual variations in GPP with precipitation, temperature, and SPEI revealed a weak correlation for croplands and shrublands in both countries. The highest correlation between GPP and SPEI03 was detected for Sudan with Spearman's ρ of 0.58 and 0.59 for croplands and shrublands, respectively.

3.3.6. Water Use Efficiency (WUE)

The magnitude of WUE varies depending on the magnitudes of NPP and actual evapotranspiration. The national multi-year average WUE for Sudan is lower ($0.24 \text{ g C kg}^{-1} \text{ H}_2\text{O}$) as compared to that for Ethiopia ($0.74 \text{ g C kg}^{-1} \text{ H}_2\text{O}$) due to low NPP production and high evapotranspiration for the former. Literature shows comparable values for the Ethiopian average WUE and the national average WUEs of China ($0.79 \text{ g C kg}^{-1} \text{ H}_2\text{O}$) as reported by Liu et. al. (2015), and for the southern United States ($0.71 \text{ g C kg}^{-1} \text{ H}_2\text{O}$) as indicated by Tian et. al. (2010), but higher values for the global average ($0.92 \text{ g C kg}^{-1} \text{ H}_2\text{O}$).

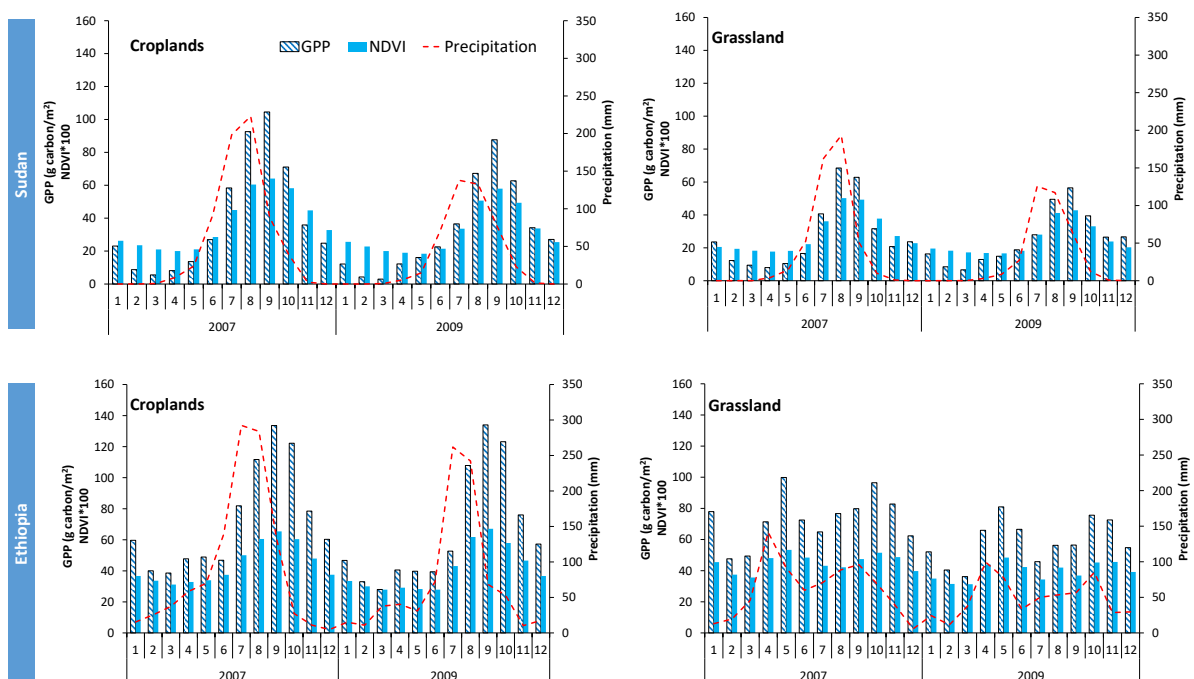


Fig. 3.9. Monthly GPP, NDVI, and precipitation during the wet year 2007 and the dry 2009 for croplands and grasslands in the two countries.

Large variations in WUE are evident for different land cover types due to differences in carbon uptake and water consumption (Liu et. al., 2015). This dissimilarity is mainly due to physiological differences and climate conditions (Tang et. al., 2014). Variations are also noticeable for the same land cover types under different climate conditions in Sudan and Ethiopia. Generally, all the land cover types in Ethiopia show higher WUE than their counterparts in Sudan (Fig. 3.10). For instance, savannas show an average WUE of $0.31 \text{ g C kg}^{-1} \text{ H}_2\text{O}$ in Sudan but $0.75 \text{ g C kg}^{-1} \text{ H}_2\text{O}$ in Ethiopia. In Ethiopia, evergreen forests have higher WUE than deciduous forests. This is in agreement with forests in similar latitudes (Tang et. al., 2014). Among all the land cover types in the region, evergreen broadleaf forests and woody savannas exhibit the highest average WUE. They displayed an average WUE of 1.4 and $1.07 \text{ g C kg}^{-1} \text{ H}_2\text{O}$, respectively.

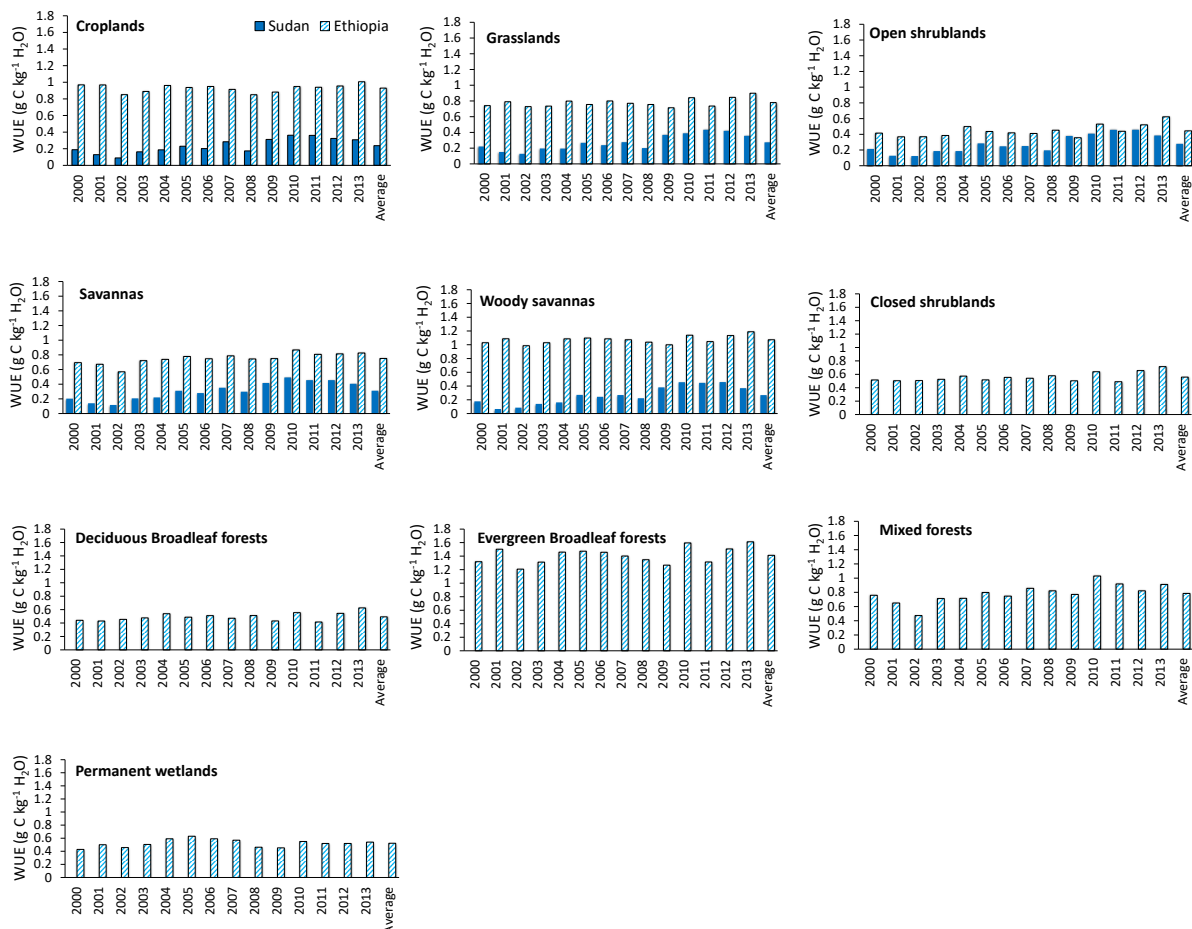


Fig. 3.10. Time series of WUE of the land cover types in Sudan and Ethiopia.

In Sudan, the highest WUE is that of Savannas, which shows an average value of $0.31 \text{ g C kg}^{-1} \text{ H}_2\text{O}$. WUE of open shrublands, grasslands, and croplands are 0.278 , 0.274 and $0.236 \text{ g C kg}^{-1} \text{ H}_2\text{O}$, respectively. WUE shows a great inter-annual variation in the region during the study period. In Sudan, it displays a positive anomaly during the period 2009-2013. This increase is

detectable for all land cover types and is due to an increase in NPP and a decrease in evapotranspiration. When the inter-annual variation in WUE was correlated with SPEI, the land cover types in Sudan exhibited no significant correlation (See Appendix B: Fig. S3.5). Most of the land covers in Ethiopia show the strongest correlation between annual NPP and SPEI01 and SPEI03 (See Appendix B: Fig. S3.6). This might reflect a high degree of sensitivity of the land covers found in Ethiopia to drought compared to those found in Sudan. A negative correlation between variations in WUE and drought is typical for arid areas (Huang et. al., 2017).

In the current study, the drought of 2009 induced an increase in WUE in most land cover types in Sudan. The highest increase in this year is detected in woody savannas with a percentage of up to 42.2% of the multi-year average WUE in Sudan. An increase in precipitation in arid and semi-arid areas may induce a larger increase in NPP than in evapotranspiration (Liu et. al., 2015). Though, the response of WUE to drought is not so clear (Liu et. al., 2015), many studies (e.g. Dong et. al., 2011; Tian et. al. 2011; Reichstein et. al., 2002) reported an increase in WUE due to drought. The increase in WUE under drought results mainly from internal stomata mechanisms that work to reduce water losses as a measure of adaptation to water stress (Reichstein et.. al. 2002). In contrast, all the land cover types in Ethiopia showed a decrease in the same year in WUE for all the land cover types. The largest drop (13.3%) was in permanent wetlands when compared to the multi-year average WUE. These observations suggest different responses of WUE under different climate conditions.

3.3.7. Carbon Use Efficiency (CUE)

In comparison with CUE for Sudan, CUE in Ethiopia shows less inter-annual variability for most land cover types. This could be attributed mainly to the high precipitation in Ethiopia since where precipitation is high, CUE usually shows a constant value (Zhang et. al., 2009). However, statistical analysis showed an insignificant correlation between variation in CUE and precipitation for most land covers. As with WUE, CUE also increased during the years 2009 - 2013 in Sudan. The lowest CUE was found in 2005 and 2006 (Fig. 3.11) as dry years exhibit high respiration (Metcalf et. al., 2010) and low NPP.

All of the land cover types in Sudan display much lower CUE values than their counterparts in Ethiopia (Fig. 3.11), mostly due to higher temperature inducing higher respiration (Shaver et al. 2000) in Sudan compared to Ethiopia. In turn, this suggests a larger release of CO₂ rate from the land cover types in Sudan, or in other words, land cover types in Ethiopia uptake more CO₂. Generally, net CO₂ is released through respiration where the climate is dry and warm and is uptaken where the climate is cool and moist (Ahlström et. al., 2015). CUE exhibits a great

variation among the vegetation land cover types. Croplands in Ethiopia show the highest annual average CUE (0.59) among all land cover types in the region. Open shrublands show the lowest CUE among all land covers, giving annual CUE of 0.27 and 0.35, respectively for Sudan and Ethiopia. While the inter-annual variation in CUE in Sudan's land covers show insignificant correlation with drought (See Appendix B: Fig. S3.7), land covers in Ethiopia are positively correlated with SPEI, giving highest Spearman's ρ values with SPEI1 and SPEI03 for most land covers (See Appendix B: Fig. S3.8). These local-scale results support the previous global-scale findings by Zhang et. al. (2009) and DeLucia et al. (2007).

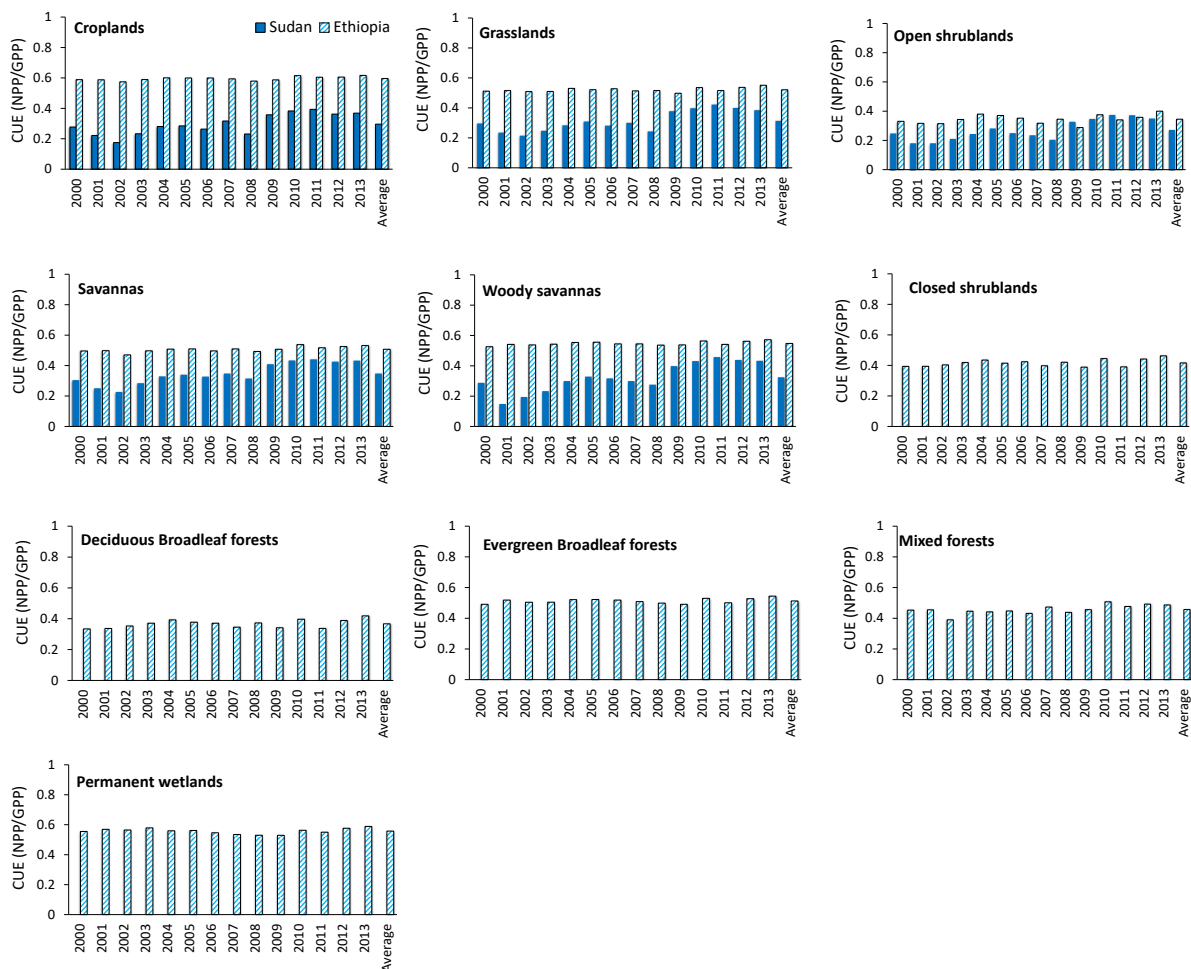


Fig. 3.11. Time series of CUE of the land cover types in Sudan and Ethiopia.

The multi-year average of CUE is about 0.50 for Ethiopia, which is close to the global average of 0.52 (Zhang et. al., 2009), and within the realistic range of CUE for Africa, i.e. 0.45 to 0.60 (Amthor, 2000). In contrast, the average CUE for Sudan (0.31) is much lower than both the global and the continental averages. This result indicates higher respiration from the land cover types in Sudan compared to the same land cover types in Ethiopia. One of the major conclusions of these findings is that, future climate change might impact the efficiency of land cover types as sinks for atmospheric carbon by affecting carbon sequestration capacity (Xiao

et. al., 2013). However, large uncertainty is expected in estimating CUE for Africa because of uncertainty in estimating vegetation productivity in the continent in addition to the relatively limited field measurements in comparison with other continents (Ardö, 2015; Valentini et. al. 2014).

3.3.8. Relevance to food security and climate change

As mentioned earlier, the decrease in NPP may affect food security and increase global warming (Zhao and Running, 2010). From a food security perspective, NPP is key for food production. The ability of the plant to assimilate atmospheric CO₂ and convert it into biomass is of supreme importance for food production. Increasing NPP will consequently increase crop yield. Cereal crops such as sorghum, millet, and wheat are the main staple crops in Sudan and Ethiopia. The two countries are facing gaps between the demand and supply in these crops. Any additional reduction in the current yield values (in kilogram/hectare) or the cultivated area would widen this gap and consequently put the food security of the country in danger. Drought may affect the crop yield and may also have a negative impact on the suitability of areas for rainfed agriculture, which is also considered as a loss. According to the data from the Food and Agriculture Organization of the United Nations (FAOSTAT, 2017), many years in the investigation period exhibit a decrease in the cereal crop yield and the cultivated area. For instance, the dry year of 2002 witnessed a reduction in the yield of cereal crops and the cultivated area from the multi-year average (2000-2013). The drop in crop yield and the cultivated area is about 15.8% and 11.5% in Sudan and 11.8% and 23.8% in Ethiopia, respectively. This reduction is comparable to the decrease in NPP in croplands in 2002 in both countries. Consequently, a drop in the total production of cereal crops by 25.6% and 33.9% in Sudan and Ethiopia, respectively, were reported. More in-depth analysis is needed to detect the impact of drought on the crop yield. Crop models such as WEAP-MABIA (Jabloun and Sahli, 2012), AquaCrop (Vanuytrecht et. al., 2014.) and Cropsyst (Stöckle et. al., 2003) are very useful for such analysis. The impact of drought on suitability for rainfed agriculture could provide a clue on the contribution of drought in reducing the cultivated area in the overall decrease in food production.

From a climate change perspective, vegetation represents an important sink for atmospheric CO₂. High CUE of a landcover means that vegetations in this landcover are more efficient in assimilating CO₂. In this direction, the land cover types in Sudan are less efficient than the landcover in Ethiopia in this process. The findings of the current CUE analysis emphasize the importance of some natural vegetation such as permanent wetlands, evergreen broadleaf forests

savanna and woody savannas in mitigating climate change. Especially in Ethiopia, these land covers exhibit high CUE values. This high CUE indicates that the vegetation in these land covers have a higher ability for CO₂ assimilation, which is very important to reduce the CO₂ in the atmosphere and consequently contributing to climate change mitigation. The noticeable increase in CUE in all landcover types in Sudan is a positive sign showing an enhancement of the efficiency of these landcover types during the last years of the current analysis. Under the climate change threat, conserving these landcover types is important. Analysis of the landcover changes should be addressed since it is responsible for a large share of global greenhouse gases emission (Smith et. al., 2014). Converting natural land covers into cultivated lands to ensure food security should be optimized, taking into consideration also the consequences of/on climate change. Sustainable intensification in the existing croplands, especially in developing countries, is very crucial to ensure increased food production while maintaining the sustainability of natural resources and mitigating climate change (Campbell et. al., 2014). To conclude, understanding how NPP responds to climate variability can lead to more efficient management of these land covers and can, in turn, assist significantly in securing food and reducing the impacts of climate change. Improved land use management is crucial to strengthen the ability of the countries to address food security and climate change.

3.4. Limitation and Uncertainty

Public-domain data based on remote sensing and models can provide outstanding spatial and temporal coverage of primary productivity and climate, especially in data-scarce regions. Nevertheless, all these data sources have inaccuracy and uncertainty. One major drawback of using these data in the current research was the lack of ground-based data of NPP, WUE, and CUE to validate the findings. All the studies reviewed so far, however, note this as the greatest challenge.

MOD17 NPP data come with a quality control dataset (QC), where QC is measured in percentage of the number of days with poor quality of data (due to clouds) from the total number of days in the growing season. In MOD17 algorithm, the data with poor quality are artificially filled with Fraction of Absorbed Photosynthetically Active Radiation (FAPAR) and Leaf Area Index (LAI); thus, higher QC values represent lower quality (Ardö, 2015). In the current research, processing of these QC data for the study area revealed lower QC values for most land cover types in Sudan (Fig. 3.12) because Sudan is drier than Ethiopia and, hence, with less cloud frequency. This suggests MOD17 NPP data as being more reliable for Sudan than for Ethiopia. The croplands type is an exception since it exhibited a better QC for Ethiopia, perhaps

due to their occurrence mostly in areas with higher precipitation and, hence, high frequency of occurrence of clouds. Evergreen broadleaf forests in Ethiopia represent the land cover with the least reliable data (QC of about 58% of days). Open shrublands exhibited the best QC for both countries because they are located mostly in areas with low precipitation and less occurrence of cloud, hence, their NPP data could be considered more reliable in comparison with those for other land cover types. The overall mean QC is 24% for Sudan and 32% for Ethiopia.

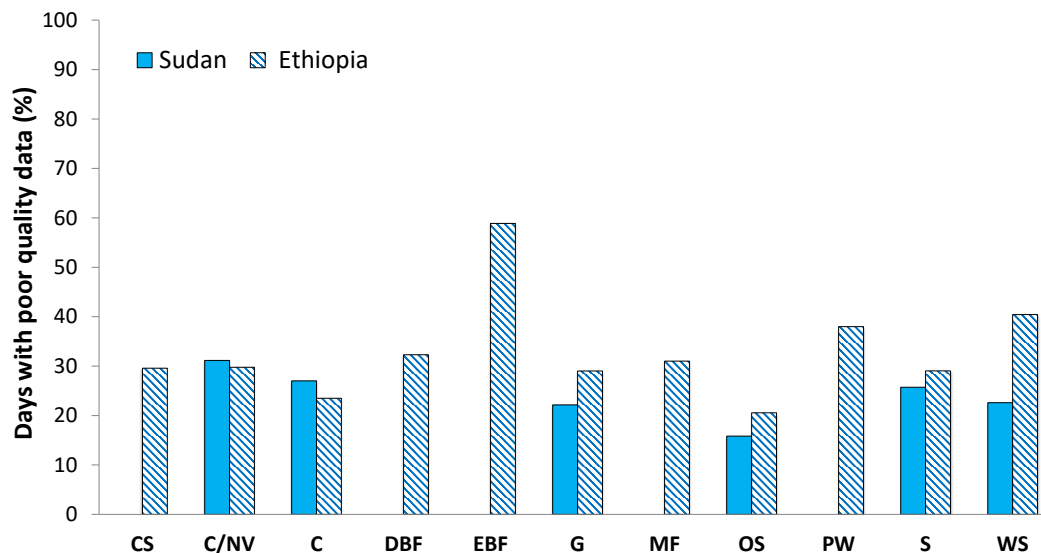


Fig. 3.12. Quality control of NPP data for each land cover in Sudan and Ethiopia.

There are tens of public-domain precipitation products available online. According to many literature, these products have different accuracies and their performance could be quite different. Generally, the overall accuracy using remote sensing precipitation estimations in water accounting is about 82% (Karimi and Bastiaanssen, 2015). Many studies were conducted to check the performance of CHIRPS along with other public-domain precipitation products in many areas in Sudan and Ethiopia. Hence, a literature review was conducted to detect the performance of CHIRPS in the study area in order to detect the degree of uncertainty in precipitation estimations using this product. According to Funk et. al., 2015, CHIRPS exhibits the lowest bias than the other products. This high accuracy is, in part, due to the inclusion of ground station data in producing it. Several in-depth performance studies showed that, this product has greater accuracy in the study area than the other public-domain precipitation products. Although CHIRPS has a high performance, there is still some uncertainty in this product. Compared to other precipitation products, CHIRPS shows the highest Pearson correlation of coefficient of 0.61-0.79 and the lowest bias and mean absolute error when compared with ground station data (Bayissa et. al., 2017; Gebremicael et. al., 2017). According to the Gebremicael et. al. (2017), a percent bias (PBIAS) in CHIRPS of -8% is estimated. The

mean error of this product is quite low compared to other products. A mean error of about -27.9 mm in some locations in the study area is estimated (Bayissa et. al., 2017). Given the potential error in this product, uncertainty in precipitation estimations presented in the current study using CHIRPS needs to be taking into consideration.

Some studies found that, WUE calculated on a global scale using remote sensing data to be consistent with tower measurements (Tang et. al., 2014). However, calculating WUE and CUE using public-domain data may involve a high degree of uncertainty. Lack of ground data with good spatial coverage makes it impossible to validate the regional WUE and CUE estimates for this study. The currently available data are suitable only for analyzing the NPP, WUE, and CUE for various land cover types but not for different plant species. It will be useful to detect the NPP, WUE, and CUE across species if more detailed data are available. Results from this analysis should be interpreted with caution though, as the relationship between primary productivity and climate variability only hold if other factors remain constant (e.g., management, technology, and crop variety).

Nevertheless, these datasets are very valuable to understand the spatial and temporal patterns of the NPP, WUE, and CUE of land cover types in data-scarce areas like the region of Sub-Saharan Africa. Besides, they enable the investigation of the relationship between land covers and climate processes, a type of information that is not available for many areas around the world. Such understanding, in turn, is useful to understand interactions of land use, land cover and ecosystem management.

3.5. Conclusion

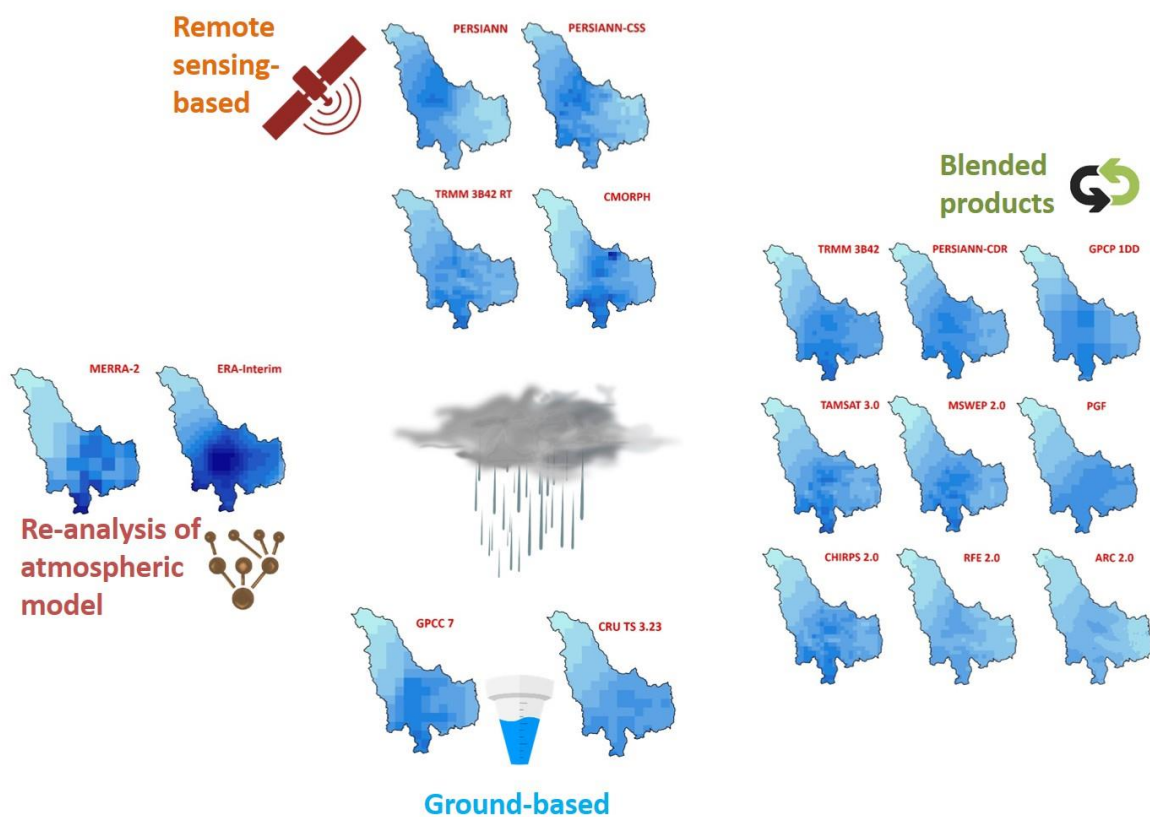
In this study, we provide new insights into the interaction between land cover types and climate in two countries in Sub-Saharan Africa. Results of the current research confirm that NPP responds differently among different land cover types and among the same land cover types located in different climate conditions. The variation of NPP in the region is primarily driven by climate variation. The last few years of the study period (2009-2013) showed positive NPP anomalies in all vegetation land cover types in Sudan. This was mainly induced by the recent recovery of precipitation. The current analysis revealed that a moderate drought, such as that of 2009, leads to reduced annual NPP, and vice versa for the wet year 2007. Drought decreases the growing season iNDVI of the croplands and grasslands remarkably in both countries. Low iNDVI reflects low productivity and results in negative effects on food production.

There is a strong positive correlation between the inter-annual variability of NPP and drought severity of three months, i.e. SPEI03, in most of the vegetation land cover types in Ethiopia, but no statistically significant correlation was found between the two indices for Sudan. This suggests that land cover types in Sudan are more resistant to drought than those present in Ethiopia. In Ethiopia, savannas are the most sensitive land cover to drought in the time step of three months while croplands and permanent wetlands are the least sensitive land cover types.

Analysis of WUE and CUE is often performed for short periods and individual plants or small plots (Zhang et al., 2009). However, this study offered spatio-temporal analysis of both indicators. The results of this analysis showed that all land cover types in Ethiopia have higher WUE and CUE than their counterparts in Sudan, thus reflecting the prevalent climate conditions in each country. WUE and CUE displayed differences in magnitude among the land cover types. They also respond differently to climate conditions and drought severity. Despite the limitation and uncertainty encountered in using public-domain data, the current study provided a useful analysis of using these data for monitoring and analyzing NPP, WUE and CUE and their interaction with climate variables on a country scale. Moreover, this analysis provides an essential understanding of the interactions between ecosystem productivity and efficiency and climate variability. The findings of the current research could be considered as a basis for further analysis of the impact of climate variability on food production. They also provide essential information for the critical role some land cover types play as sinks for atmospheric carbon dioxide and, therefore, for climate change studies.

Chapter 4

Consistency of public-domain precipitation products



Based on:

Khalifa, M., Korres, W., Saif, S., Elagib, N.A., Baez-Villanueva O.M., Basheer, Ayyad, S., M., Ribbe, L., Schneider, K., 2020. Consistency of public-domain precipitation products: coupling traditional evaluation approaches with data mining techniques (Submitted).

Abstract

The efficient use of water requires understanding its spatial and temporal availability and pattern of use. However, in-situ measurements of the components of the hydrological cycle are often unavailable. This is particularly the case for precipitation. In this respect, Public-domain Precipitation Products (PPs) represent an alternative source of information. Nonetheless, precipitation estimates by PPs show discrepancies in spatial and temporal domains; thus, in-depth analyses of similarities and differences of these products is imperative to provide accurate precipitation estimations for water applications. We introduce and test a novel approach for evaluating the performance of PPs. This approach couples traditional evaluation methods (pixel-to-point and pixel-to-pixel) with data mining techniques (Hierarchical Clustering and Principal Component Analyses). It was used to assess the performance of 17 PPs over the Blue Nile Basin (BNB) for the period 2001-2005 on monthly and annual scales. A sensitivity analysis was carried out to test the affinity of the studied PPs. The analysis results were used to guide assimilating several PPs to create Merged Precipitation Products (MPPs). Results exhibit considerable differences between the studied PPs. Noticeable spatial and temporal discrepancies were found between the 17 PPs on the one hand and between PPs and rain gauge data on the other hand. Data mining techniques proved to be useful in detecting similar and dissimilar PPs. Given their advantages over traditional methods, these techniques should be used routinely in PPs assessment. The findings of the current research provide helpful insights to advance the use of PPs in water resources applications.

4.1. Introduction

Water monitoring is crucial for hydrological, ecological, and development purposes. Due to population growth and climate change, water has become increasingly scarce in many parts of the world (Kummu et. al., 2016; Liu et. al., 2017). Therefore, decision-makers are required to adopt immediate, efficient and sustainable management practices to meet current and future human development and environmental water demands. However, the lack of ground-based data is one of the main challenges that hinder good practices of water management (McDonnel, 2008). Effective management of water resources requires continuous monitoring and an accurate estimation of the spatio-temporal patterns of different components of the hydrological cycle such as precipitation, evapotranspiration, runoff, and water storage changes (Ayyad et. al., 2019; Cosgrove and Loucks, 2015; Fernández-Prieto et. al., 2012; Su et. al., 2010; Sun et. al., 2018). In most regions of the world, water availability is directly linked to precipitation

amount and seasonality (Dinku et. al., 2007; Ligaray et. al., 2015; Noy-Meir, 1973). Variations in the spatio-temporal patterns of precipitation can cause environmental hazards such as floods and droughts, which have direct socio-economic impacts (Brown and Lall, 2006), and often result in loss of lives and infrastructure. For example, Masih et. al., (2014) reported that during 1965-2012, drought events affected ~67 million people over Ethiopia, bringing an estimated economic loss of above 92 million US\$ and a death toll of more than 400,000. These numbers emphasize the need for accurate precipitation data to support decision-making, especially in areas vulnerable to high climate variability such as the Nile Basin (Bastiaanssen et al., 2014; Beyene et. al., 2010; Cao et. al., 2018b).

Traditionally, precipitation has been measured using in-situ rain gauges (Gabriele et. al., 2017; Kidd, 2001). However, the accuracy in the characterization of precipitation, when only ground-based measurements are used, depends largely on the density and distribution of the rain gauge network (Shaghaghian and Abedini, 2013). While radar data can provide a spatially distributed estimation of precipitation (Yoon et. al., 2012), rain gauges are considered the most reliable source of precipitation measurements at the point scale (Villarini et. al., 2008) and they still required for calibration and validation purposes. Despite that, the rain gauges are sensitive to environmental conditions (Michelson, 2004), and the accuracy of their records has to be controlled (Levy et. al., 2017). However, in many regions (especially in developing countries), rain gauges are sparsely distributed (Kaba et. al., 2014), and their number is decreasing (Sun et al., 2018). Rain gauges are sensitive to environmental conditions (Michelson, 2004), and the accuracy of their records needs to be checked (Levy et. al., 2017). A dense network is expensive and hard to maintain, hindering an accurate spatial representation of the precipitation patterns, especially in high altitude areas. Systematic under-catch of gauge measurements (Beck et. al., 2019), unsystematic errors such as gaps in time series (Woldesenbet et. al., 2017), latency in data availability, in addition to inaccessibility of data are additional challenges that limit the use of rain gauge data in many regions of the world (Montesarchio et. al., 2015; Thiemig et. al., 2012). In Africa, the implementation of an adequate rain gauge network is challenging because of driver factors such as the desired accuracy and the cost of implementation, maintenance and data collection (Pardo-Igúzquiza, 1998).

The recent technological development in sensors, algorithms and new satellite missions designed to measure environmental processes, have enabled the opportunity to derive gridded precipitation estimates. This has enabled the opportunity to account for the spatial distribution of precipitation (Kidd, 2001; Zambrano-Bigiarini et. al., 2017), thus providing data which is

otherwise often not feasible to obtain. The public-domain policy of these products has encouraged the use of their datasets for different applications such as drought assessment (Agutu et. al., 2017; Gao et. al., 2018; Sahoo et. al., 2015; Zambrano-Bigiarini et. al., 2019), flood forecasting (Tekeli et. al., 2017), hydrological modeling (Kite and Pietroniro, 1996; Siddique-E-Akbor et. al., 2014), water balance studies (Bastiaanssen et. al., 2014; Karimi, et. al., 2013), among others.

A wide range of sensors, input data, and estimation algorithms are used to produce these Public-domain Precipitation Products (PPs) (Sun et. al., 2018). Accuracy of the PPs estimation can be affected by climatological of catchment-specific factors such as elevation (Ayehu et. al., 2018; Dinku et. al., 2018; Habib et. al., 2012; Hirpa et. al., 2010). Hence, the accuracy of the PPs in representing the spatio-temporal precipitation patterns varies greatly depending on the region. Although some studies have reported an overall accuracy as high as 95% (Karimi and Bastiaanssen, 2015), the accuracy of these PPs might vary at different temporal scales and geographic settings (Baez-Villanueva et. al., 2018).

Traditionally, the PPs are evaluated by comparing their estimates with in-situ measurements, for example, (i) using a pixel-to-point analysis, where the rain gauge data are compared to the estimates of the respective grid-cells of the PPs (Bai and Liu, 2018; Burton et. al., 2018; Cao et. al., 2018; Gebrechorkos et. al., 2018; Thiemig et. al., 2012); (ii) using a pixel-to-pixel approach, which compares a gridded version of the rain gauge data with the corresponding grid-cell of the PPs product (Amitai et. al., 2009; Bajracharya et. al., 2015; Chen et. al., 2014; Saber et. al., 2016). Additionally, the evaluation of PPs could be carried out indirectly by using the PPs to force a hydrologic model and evaluate the simulated discharge with streamflow observations (Beck et. al., 2017; Casse et. al., 2015; Chintalapudi et. al., 2014; Trambly et. al., 2016; Voisin et. al., 2007). In some cases, there are no enough ground-based data to evaluate these products; and therefore, information on the performance of the different PPs can be assessed through a cross-correlation analysis (Salih et. al., 2018). Such inter-comparison would provide the relative differences in precipitation between the different PPs and might shed some light on their similarities and differences. Given the large number of data that needs to be handled in such evaluation approaches using grid-cells values, data mining techniques, such as Hierarchical Clustering Analysis (HCA) and Principal Components Analysis (PCA) can be effective in reducing effort and time needed to assess these big data (Lever et. al., 2017; Zhang et. al., 2017).

Since all PPs have advantages, limitations, and uncertainties, merging different PPs may provide a better estimation for precipitation (Baez-Villanueva et. al., 2020; Bastiaanssen et. al., 2014; Peña-Arancibia et. al., 2013; Xie et. al., 2003). However, most of the available merging algorithms are complex to implement, and their performance normally improves when increasing the number of rain gauges (Baez-Villanueva et. al., 2020). Therefore, merging products over extremely data-scarce regions such as the Nile Basin remains a challenge. To this end, simple merging methods, like the one followed in the current research, would benefit massively from the comprehensive assessment that couples traditional evaluation methods with data mining techniques suggested herein.

Many previous studies have been conducted to evaluate the performance of PPs over the Blue Nile Basin (BNB) (e.g. Abera et. al., 2016; Mekonnen and Disse, 2018; Romilly and Gebremichael, 2011). For a summarized review of some of these studies, the reader is referred to Appendix C (Table S4.1). These studies have focused only on the upstream part (Upper BNB: UBNB) of the basin, with few exceptions that targeted the lower BNB (Lower BNB: LBNB) (e.g. Basheer et. al., 2018), and only a limited number of PPs were evaluated. These studies have evaluated the PPs products performance through a direct comparison with rain gauge data to assess their ability to represent the precipitation patterns (Thiemig et. al., 2012). This approach is limited over data-scarce regions because there is no enough data to implement an informative evaluation (Bastiaanssen et. al., 2014). It is worth to mention here that the number of rain gauges in operation over the BNB is decreasing (not shown).

Therefore, the objectives of the current research are: (i) to detect the similarities and differences between 17 PPs over the BNB at monthly and annual temporal scales using mean annual precipitation values through a pixel-to-pixel inter-comparison and data mining techniques, and to cluster them into groups based on their similarities; (ii) to evaluate the performance of these PPs over the BNB using rain gauge data; and (iii) to evaluate the applicability of this integrated analysis of PPs in guiding simple merging procedures of PPs. The merging exercise aims at creating Merged Precipitation Products (MPPs) to improve the precipitation estimation, as a potential solution to improve precipitation estimation of PPs over data-scarce regions. The present analysis aims to advance the current understanding of the performance of PPs over the BNB, as an example of data-scare regions. To the best of our knowledge, such a comprehensive investigation at the given scale integrating traditional evaluation approaches with data mining techniques has not been conducted so far, neither for the BNB nor any other river basins.

4.2. Data and Materials

4.2.1. Study area

The BNB is a transboundary river basin shared by Ethiopia and Sudan (Fig. 4.1a). The basin has an area of about 307,177 km², of which around two-thirds are located in Ethiopia (UBNB) and the rest is in Sudan (LBNB). Whereas the UBNB is characterized by complex topography, the LBNB is relatively flat. The BNB contributes to nearly 62% of the total streamflow of the Nile River (Amdihun et al., 2014), and is crucial for food and hydropower production (Allam and Eltahir, 2019; Elagib et. al., 2019; Wheeler et. al., 2016). The rainfed and irrigated agricultural schemes in the basin produce a large fraction of the annual domestic food production of Ethiopia and Sudan (Awulachew et. al., 2012; Elagib et. al., 2019).

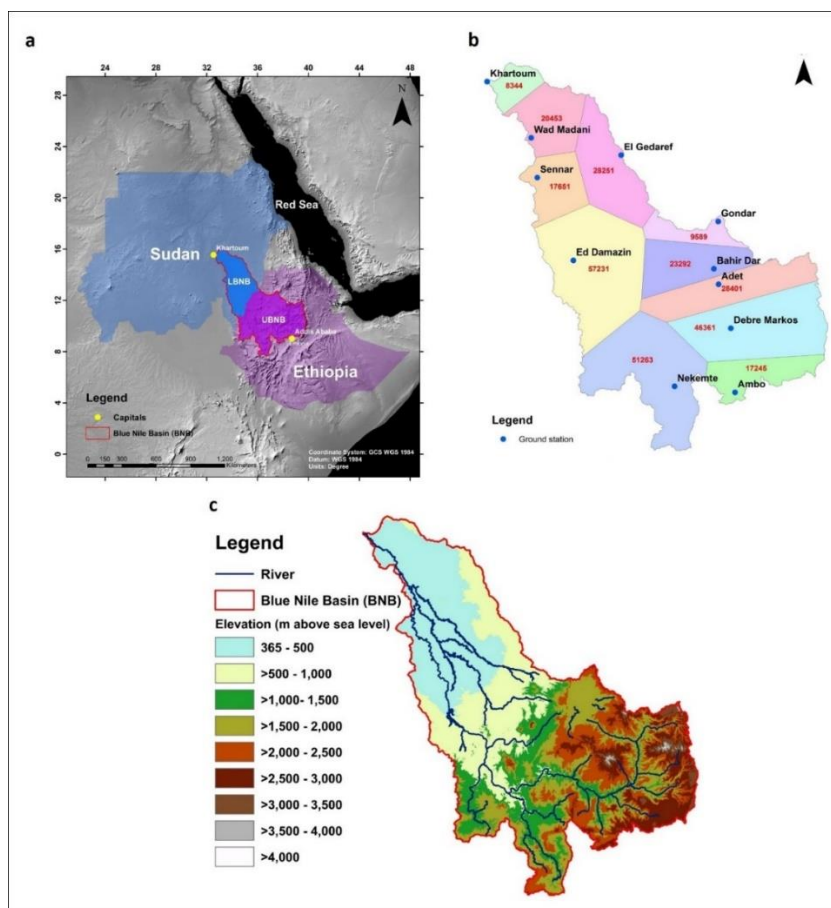


Fig. 4.1. The Blue Nile Basin (BNB): (a) location and riparian countries, (b) rain gauges used in the current research and corresponding Thiessen polygons and their areas in km², (c) topography.

The BNB is the main source of water for the Gezira irrigation scheme - one of the largest irrigated schemes in the world with an area of around 0.88 million hectares (World Bank, 1990). Precipitation in the BNB is difficult to predict (Cheung et. al., 2008; Meze-Hausken, 2004) and

highly variable in time and space (Beyene et. al., 2010; Conway, 2000). The intra-annual and inter-annual variability of precipitation has a direct impact on rainfed agriculture, and also on irrigated agriculture as a result of reduced river flows under drought conditions (Kim et. al., 2008; Siam and Eltahir, 2017). The rainy season in the basin is relatively short and lasts for only five months (from June to October). The mean annual precipitation in the basin varies from ~120 mm at the outlet of the basin in Khartoum (in the LBNB) to more than 2000 mm in some parts of the UBNB (Roth et. al., 2018).

4.2.2. Data description

Based on a detailed literature review, we identified 17 PPs particularly important for the BNB. Comprehensive reviews of available PPs can be found in the literature (e.g. Kidd, 2001; Sun et. al., 2018). PPs are typically categorized based on their spatial resolution and input data, which are some of the main factors that determine their performance (Vergara et. al., 2013). For the current analysis, the 17 selected PPs have been categorized into four groups: (1) ground-based; (2) remote-sensing-based; (3) blended; and (4) PPs based on re-analysis of atmospheric models. Although some researchers such as Sun et. al., (2018) have grouped all the satellite-related products into one category, even if they contain information from rain gauges, we preferred to separate the purely remote sensed PPs from those blended with rain gauge data. The 17 selected PPs and their main characteristics are listed in Table 4.1. For a full description of each PP, the reader is referred to the corresponding literature of each product. The full names of the products selected in this study are defined in the list of abbreviations (pages xiii – xiv).

Table 4.1. List and characteristics of the 17 PPs considered in the current study

	Product name	Provider	Product category*				Spatial resolution **	Temporal resolution**	Period of record	Reference(s)
			a	b	c	d				
1	GPCC 7	DWD	x				0.5°	Monthly	1901-2013	Schneider et al., (2015)
2	CRU TS 3.23	UEA	x				0.5°	Monthly	1901-2014	Harris et al., (2014)
3	PERSIANN	CHRS-UCI		x			0.25°	Annual	2000-present	Hsu et al., (1997)
4	PERSIANN-CCS	CHRS-UCI		x			0.04°	Annual	2003-present	Hong et al., (2004)
5	TRMM 3B42 RT	NASA		x			0.25°	Daily	1998-2019	Huffman et al., (2007)
6	CMORPH	CPC, NOAA		x			0.25°	Daily	2002-present	Joyce et al., (2004)
7	ARC 2.0	CPC, NOAA			x		0.1°	Daily	1983-present	Novella & Thiaw, (2013)
8	CHIRPS 2.0	CHG			x		0.05°	Annual	1981-present	Funk et al., (2015)
9	GPCP-1DD	GPCP			x		1.0°	Daily	1996-present	Huffman et al., (2001)
10	MSWEP 2.0	JRC, EC			x		0.1°	3-hourly	1979-2017	Beck et al., (2019)
11	PERSIANN-CDR	CHRS-UCI			x		0.25°	Annual	1983-present	Ashouri et al., (2015)
12	PGF 1.0	THRG- PU			x		0.25°	Daily	1984-2008	Sheffield et al., (2006)
13	RFE 2.0	CPC, NOAA			x		0.1°	Daily	2001-present	Xie & Arkin, (1996)
14	TAMSAT 3.0	UoR			x		0.0375°	Daily	1983-present	Maidment et al., (2017)
15	TRMM 3B42	NASA			x		0.25°	Daily	1998-2019	Huffman et al., (2007)
16	MERRA-2	NASA				x	0.5° × 0.625°	Hourly	1980-present	Gelaro et al., (2017)
17	ERA-Interim	ECMWF				x	0.75°	Monthly	1979-2019	Dee et al., (2011)

* Precipitation product categories: (a) ground-based; (b) remote sensing-based; (c) blended and (d) based on re-analysis of atmospheric models.

** These are the spatial and temporal resolution of the precipitation products considered in the current study. However, some of these products might have different versions with various characteristics.

The performance of the 17 PPs was evaluated from 2001 to 2005 over the BNB except for PERSIANN-CSS and CMORPH, which's data start from 2003 and 2002, respectively. The study period was determined mainly because of the availability of rain gauge data (2001-2005) included in the product records. Time series from 11 rain gauges distributed across the BNB (Fig. 4.1b) were obtained from the Sudan Meteorological Authority (SMA) and the Eastern Nile Technical Regional Office (ENTRO) at the monthly temporal scale. The same rain gauge data have been used in previous studies (e.g. Basheer and Elagib, 2018; Elagib, 2014b, 2013; and Wheeler et. al., 2016). The availability of rain gauge data over the BNB is a great challenge because (i) this region has a sparse network of rain gauges; (ii) the time series contains several missing values (Woldesenbet et. al., 2017); and (iii) the inexistent data sharing policies between the riparian countries of the Nile basin due to the transboundary conflict. It is worth mentioning that most of the PPs considered in this study use precipitation measurements from rain gauges to correct their estimates, i.e. the products from the ground-based and blended PPs categories. A common understanding is that such products have better performance compared to other PPs that do not include rain gauge data (e.g. purely remote sensing-based PPs).

A Digital Elevation Model (DEM) from the Shuttle Radar Topography Mission (SRTM) as shown in Figure 1c was obtained from the Consultative Group for International Agricultural Research-Consortium for Spatial Information (<https://cgiarcsi.community/data/srtm-90m-digital-elevation-database-v4-1>). This SRTM DEM covers the globe with a resampled version of 250 m. The DEM was used to delineate the boundaries of the BNB and to develop one of the reference precipitation datasets, as will be explained later in Section 4.3.2.

4.3. Methods

4.3.1. Data processing

Raster files for the 17 PPs were downloaded from their dissemination websites and processed in a Geographic Information System (GIS) environment using ArcGIS 10.3 software (ESRI, 2014). Since the present study focuses on monthly and annual time steps, the PPs with finer temporal resolution were aggregated into monthly and annual raster maps. For simplicity, we calculated and produced mean annual and mean monthly precipitation raster files for each PP, and these raster files were further used in the evaluation and merging processes.

4.3.2. Interpolation of ground-based precipitation measurements

One of the main drawbacks of the pixel-to-point evaluation is the assumption that a point-based measurement is representative of a grid-cell area. Therefore, we implemented different

interpolation algorithms to account for the spatial variability of precipitation within the grid-cells. These interpolation techniques are (i) Thiessen polygons (Fig. 1b); (ii) Inverse Distance Weighting (IDW); (iii) Ordinary Kriging; and (iv) a regression-based procedure. These four methods were implemented using ArcGIS 10.3 software. As described in Mmbando et al., (2018), we used the elevation from the SRTM DEM for the regression-based procedure as the independent variable to account for the gradient of precipitation related to elevation, while the rain gauge data was used as the dependent variable. This method assumes that there is a linear relationship between elevation and precipitation. However, this relationship may not be linear in reality, which may lead to bias if the elevation range of the model is not representative of the elevation range that needs to be predicted. The four interpolated products were evaluated to select the interpolation scheme that derived the best spatial precipitation patterns. The best performing interpolated product as identified and used as a reference for the performance evaluation of the PPs and MPPs.

4.3.3. Inter-comparison and evaluation of the precipitation products

We evaluated the 17 PPs through a pixel-to-pixel analysis using descriptive statistics. Box-Whisker plots of all pixel values of the PPs provide useful insights about mean, median, 1st and 3rd quartiles, minimum and maximum values. For the pixel-to-pixel evaluation, four performance indices were considered herein; namely, Coefficient of Determination (R^2), Root Mean Square Error (RMSE), Nash Sutcliffe Efficiency (NSE), and Percent Bias (%Bias). These indices were calculated using the HydroGOF package (Zambrano-Bigiarini, 2011) in the R Project for Statistical Computing programming language (R Core Team, 2008). Additionally, rain gauge datasets were used to evaluate the performance of the PPs through a pixel-to-point comparison. We used the same performance indices to detect and quantify the discrepancies between PPs and rain gauge measurements.

4.3.4. Clustering and merging of the products

To study the similarities and differences of PPs, HCA and PCA were conducted using the grid-cell values of the multi-year monthly and annual means. HCA is a classification method that enable clustering datasets into homogenous groups based on their similarities. It offers a way to infer inter-relationships between several datasets instead of analysing them in pairs (Zolfaghari et. al., 2019). In order to detect the relationship between the different PPs using their grid-cell values, reducing their dimensionality while preserving most of the information in data could be highly effective way to understand these products. PCA is a common and widely used approach to minimize the complexity of large datasets while retaining trends and

patterns (Lever et. al., 2017). To this end, PCA was applied to the grid-cell data with the Singular Value Decomposition (SVD). The first two components, which usually explain most of the variance in the data (Jolliffe and Cadima, 2016), were plotted against each other in two-dimensional plots to show the location of the PP points, and hence, the approximate distances between the PPs.

The products were aggregated to a unified 0.25° spatial resolution - the most common resolution in the studied PPs - to enable a fair comparison among them. Herein, the grid-cell values were used as inputs to the HCA and PCA. For the HCA, we followed an agglomerative (bottom-up) approach to group the PPs into distinct clusters, and the Euclidean distance with average linkage was used as a distance metric. The relationships between PPs on monthly and annual time steps were visualized using dendrograms and heatmaps. The HCA and PCA were performed using the ClustVis platform (Metsalu and Vilo, 2015).

The HCA algorithms do not automatically pre-specify the number of clusters (k) (Kimes et. al., 2017; Sebastiani and Perls, 2016; Yim and Ramdeen, 2015). Therefore, it offers an opportunity for further analysis of the characteristics and relationships of the PPs and their clusters by changing k (Kimes et. al., 2017). The goal of using HCA herein was to explore the PPs affinity rather than providing a rigid clustering of the PPs. This is in line with the recommendation of Bratchell (1989), but adapted for the current case. Finally, a sensitivity analysis was carried out by varying k in the HCA. This sensitivity analysis allows identifying the unstable PPs within clusters (Zappia, 2019), and therefore, exploring the PPs similarities and differences. Such an analysis is not possible in other non-nested clustering methods such as K-mean method (Kimes et. al., 2017). The k range used herein was chosen to be a few steps above and below an optimum k . This was decided to avoid over-fitting the model, since the higher the k , the less variance the new clusters could explain (Zambelli, 2016). The optimum k was determined at the mid-point of the longest branch in the resulting dendrogram, a common but inflexible method (Langfelder et. al., 2008). This threshold was then validated and refined by applying the Elbow method (Thorndike, 1953), which assumes that the optimum k is the lowest k that explains most of the variance in the data (Song et. al., 2018). The Elbow method was implemented using a script in R programming language developed by Anand (2019).

The results of HCA and PCA analyses were used to facilitate the merging of the PPs. To merge the products that were grouped in the same cluster, we computed the median value for each grid-cell using all PPs within each cluster. We selected the median as it is less affected by extreme values compared to the mean (Driscoll et. al., 2000; Manikandan, 2011). The calculated

median values for all grid-cells were used to produce gridded MPPs with the same unified spatial resolution of 0.25° of the original PPs on annual and monthly time steps. To validate these newly created products, the multi-year mean (2001-2005) of MPPs was compared against the estimations of the reference datasets and the deviation was quantified using %BIAS.

4.4. Results and discussion

4.4.1. Evaluation of gridding methods

A visual inspection of the gridded precipitation datasets using the four interpolation schemes (presented in Section 4.3.2) revealed large differences in the spatial distribution of precipitation over the BNB (Fig. 4.2). The Thiessen polygons method is simple to implement but resulted in a blocky pattern that does not reflect the spatial distribution of precipitation in the basin. This occurred because Thiessen polygons method assumes that a certain rain gauge is representative of its area of influence. Therefore, using Thiessen polygons method might lead to systematic errors, especially over data-scarce regions. Given the limited number of rain gauges available for the current study, this method did not result in an accurate spatial representation of precipitation. Although IDW and Kriging methods showed similar spatial distribution of precipitation, the resulted grid-cell values vary widely among the two. The results of IDW and Kriging methods depend on the distribution of rain gauges, which are typically installed at areas of accessible altitudes, while the mountainous areas with higher precipitation values are often unequipped with rain gauges. Hence, IDW and Kriging methods failed to represent annual precipitation higher than 2000 mm, which are expected to prevail in some regions in the Ethiopian highlands. The regression-based procedure seems to produce better spatial representation compared to the other three methods. The correlation between precipitation and elevation on a monthly time step has R^2 of up to 0.83 (at a significant level $p < 0.01$). The mean annual precipitation over the BNB exhibited an estimation of 877 mm, less by around 10% compared to the results obtained by Bastiaanssen et. al., (2014). The difference between the two estimations can be a result of the different periods considered in both studies. Therefore, the precipitation-elevation regression product was selected as the reference ground-based dataset (hereinafter referred to as Regression PP) and was used to evaluate the PPs performance. Our conclusion on the regression method goes in line with the findings of Goovaerts (2000), where the linear regression between elevation and precipitation outperforms other interpolation methods such as IDW and Thiessen polygons.

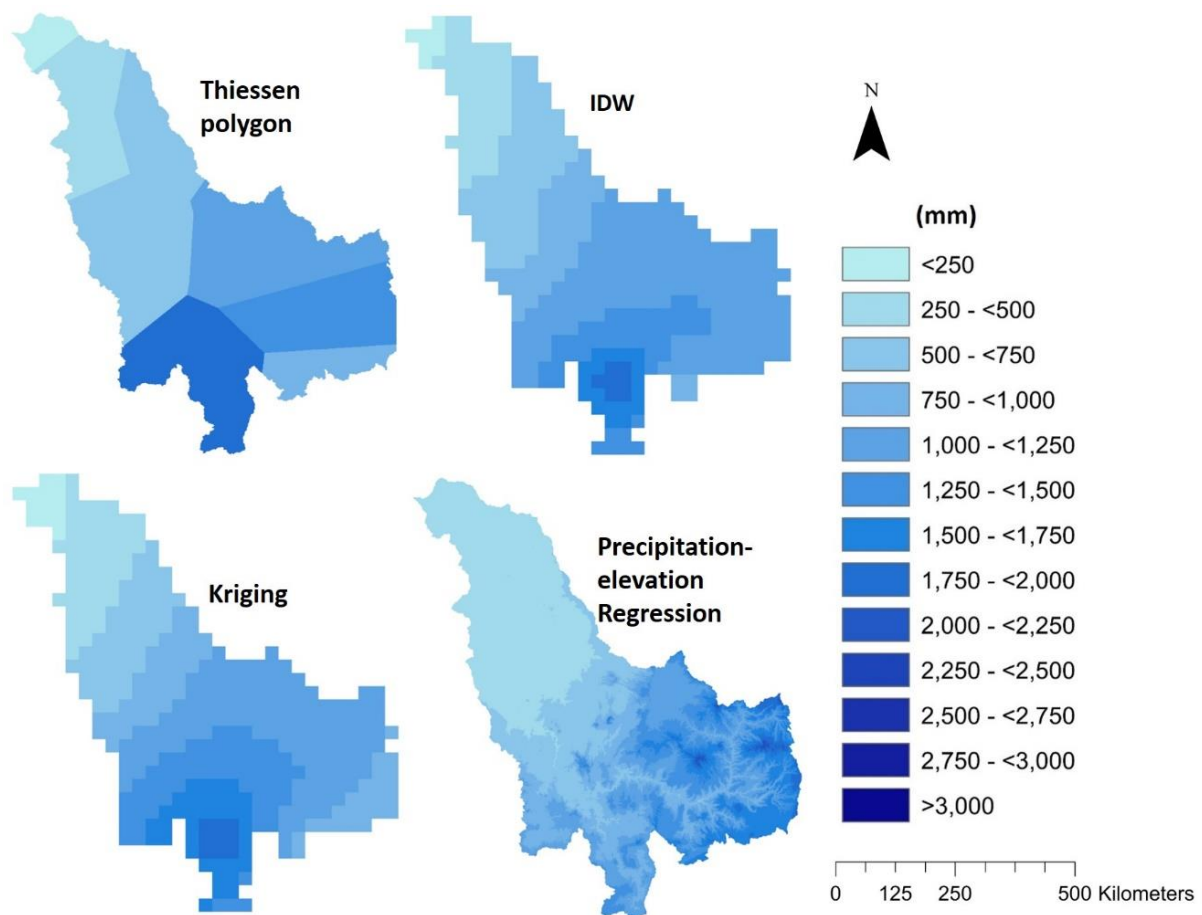


Fig. 4.2. Spatial distribution of multi-year average precipitation using four gridding methods: (a) Thiessen Polygons, (b) Inverse Distance Weighting (IDW), (c) Kriging and (d) precipitation-elevation regression.

4.4.2. Statistical characteristics of public-domain precipitation products

The evaluated PPs exhibit variations in their mean annual precipitation (2001-2005) over the BNB (Fig. 4.3) ranging from 660 mm (ARC 2.0) to 1734 mm (ERA-Interim), while the mean annual precipitation based on the Regression PP was 877 mm. Previous studies estimated the mean annual precipitation in the BNB; for instance, Bastiaanssen et al., (2014) reported 978 mm for the years 2005-2010, while Hilhorst et. al., (2011) reported 1042 mm for 1960-1990. Compared to the other PPs, Re-analysis products; i.e., ERA-Interim and MERRA-2, show higher mean annual precipitation (Fig. 4.3). This observation is supported by the results reported by Sun et. al., (2018) who conducted an analysis of 30 different PPs on a global scale and found a similar tendency of Re-analysis PPs to overestimate precipitation. Conversely, ARC 2.0 and RFE 2.0 show the lowest mean precipitation estimates, especially over the UBNB. The largest difference from the mean annual value calculated using Regression PP was recorded by ERA-Interim, MERRA-2, ARC 2.0 and RFE 2.0 (100.6%, 25.9 %, -23.7%, and -15.9%,

respectively). CRU TS 3.23 and CHIRPS 2.0 display the lowest deviation from the values estimated by Regression PP with 7.9% and 11.6%, respectively.

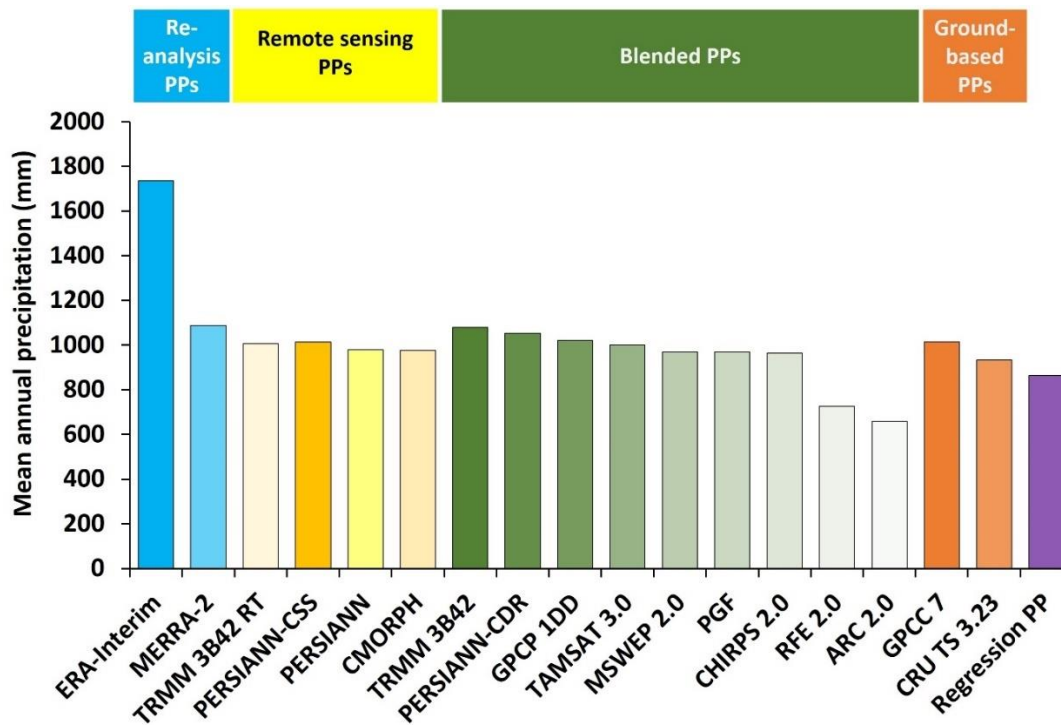


Fig. 4.3. Multi-year (2001-2005) mean annual precipitation over the Blue Nile Basin as estimated by the 17 public-domain precipitation products and the reference datasets; i.e., Regression PP.

The PPs show different dispersions of the grid-cell values on a monthly and annual time scales. On the annual temporal scale, the grid-cell values generally range from 47 mm to more than 3200 mm (Fig. 4.4). ARC 2.0 (a blended PP) show the lowest dispersion and the lowest maximum value compared to the other products. ERA-Interim and MERRA-2 (atmospheric re-analysis PPs) display higher dispersion in the grid-cell values and the highest maxima compared to the other products (Fig. 4.4). Notably, the PPs that belong to the same category and are generated from rain gauge data show different dispersion in the grid-cell values (GPC7.0 and CRU TS 3.23). The blended products; i.e. ARC 2.0, CHIRPS 2.0, GPCP 1DD, MSWEP 2.0, PGF, RFE 2.0, TAMSAT3.0, and TRMM 3B42 display relatively less variability among each other compared to the variability within other product categories (Fig. 4.4).

The median and mean, as measures for central tendency, show large differences between all PPs (Fig. 4.4). For instance, while the median and mean values of ERA-Interim and MERRA-2 exhibit the highest values compared to the Regression PP, ARC 2.0 showed the lowest mean and median values among all PPs. The differences detected in the dispersion of the grid-cell values of the PPs on an annual basis were also observed at the monthly temporal scale (Fig.

4.4). Analyzing the distribution of the grid-cell values at the monthly scale, we noticed that the PPs show different behaviour in terms of seasonality and precipitation distribution. For example, whereas many products show less dispersion over dry months (i.e. January), products such as CMORPH and TRMM 3B42 RT exhibit outliers (generally, are those values lying outside 1.5 times the interquartile range) of around 100 mm in several months. ERA-Interim and MERRA-2 show a larger data range compared to the other products during dry months (November - May). The higher precipitation values of ERA-Interim and MERRA-2 compared to the Regression PP and the other PPs are also noticeable in most months (Fig. 4.4). This observation suggests that precipitation overestimation is an inherited characteristic in these two products. Overestimation of precipitation by Re-analysis PPs could be attributed to their inefficiency in representing convective precipitation (Hu et al., 2016) compared, for instance, to satellite-based PPs, which are better in detecting convective precipitation (Paola et. al., 2012). The low annual precipitation level of ARC 2.0 can be attributed to the lower estimation of monthly precipitation, in the wet months (June, July, and August).

4.4.3. Pixel-to-pixel inter-comparison between public-domain precipitation products

A pixel-to-pixel inter-comparison of the PPs allows detecting and quantifying similarities and differences between the PPs at the grid-cell level. Discrepancies between the 17 PPs were detected at the monthly and annual scales. On the annual scale, some PPs show some similarities. For instance, ARC 2.0 and RFE 2.0 scored R^2 of 0.96, RMSE of 90.4 mm, NSE of 0.91 and %BIAS of 6.9%; CHIRPS 2.0 and MSWEP 2.0 achieved R^2 of 0.93, RMSE of 126.8 mm, NSE of 0.92 and %BIAS of -4.5%. The similar performances of ARC 2.0 and RFE 2.0 is because the two PPs are produced using a similar approach in blending satellite estimates with rain gauge data and comparable input datasets (Maidment et. al., 2017). On the contrary, many PPs show no or low agreement with each other. For instance, the correlation results of two of the remote sensing-based PPs; i.e., PERSIANN and PERSIANN-CSS, with most of the other PPs show no or weak correlation. Although PERSIANN-CDR is produced using the same algorithm as PERSIANN and PERSIANN-CSS, this product exhibit a better correlation with the other PPs compared to its sister products. This is mainly due to the use of rain gauges data to correct the bias of PERSIANN-CDR (Ashouri et. al., 2015).

On the monthly temporal scale, the correlation between the PPs is weaker than that detected at the annual scale, especially during the dry months. This might be because small differences of precipitation over dry months can have large impacts on the performance of the product. However, the four performance indices show relatively similar behaviour between the

individual PPs as those detected at the annual scale. Most of the PPs display similar spatial patterns of precipitation, with a decreasing precipitation gradient from south to north (Fig. 4.5). The weak agreement between PPs, as indicated by the four measures of goodness-of-fit, suggests that using these PPs at the monthly and annual scales may derive different results for many water applications (e.g. water balance and drought characterization).

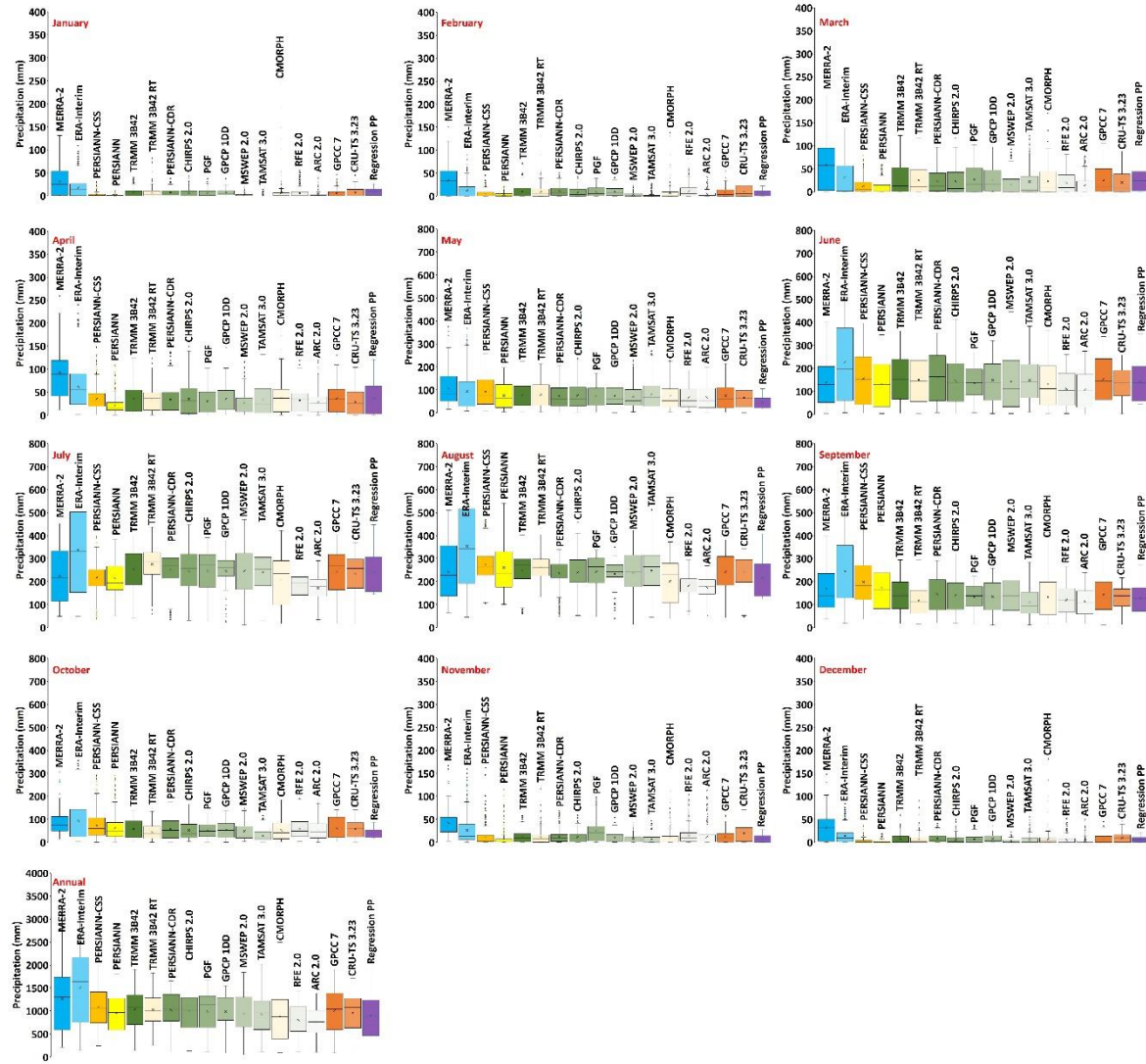


Fig. 4.4. Box-Whisker plots of all pixel values on monthly and annual precipitation of the 17 precipitation products and the Regression PP, showing the mean and median (middle horizontal lines and asterisks inside the boxes, respectively). The lower and upper box boundaries represent the 1st and 3rd quartiles. Outliers in pixel values are shown as isolated points below and above Whiskers.

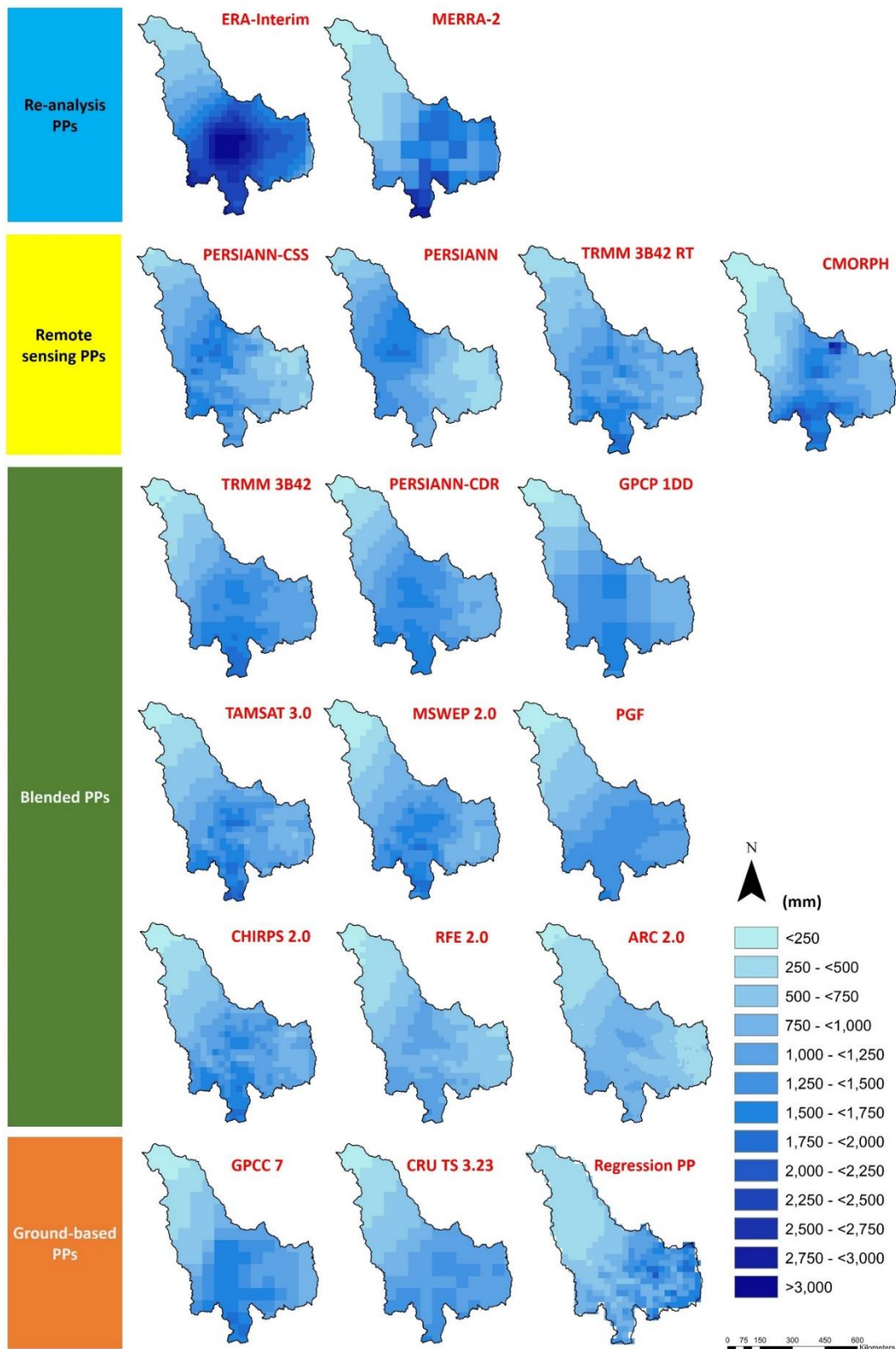


Fig. 4.5. Spatial distribution of the multi-year (2001-2005) mean annual precipitation over the Blue Nile Basin as depicted by 17 public-domain precipitation products and a Regression PP.

4.4.4. Pixel-to-point evaluation of public-domain precipitation products

The PPs exhibit varying performances when evaluated against rain gauge data (pixel-to-point evaluation) at the monthly and annual temporal scales. Figure 4.6 shows the monthly correlation results from 2001 through 2005. These correlations display that the measures of the performance indices range between $R^2 = 0.44$ and 0.89 , $RMSE = 37$ mm and 102.9 mm, $NSE = -1.7$ and 0.87 , and $\%BIAS = -60.8\%$ and 37.5% . As mentioned earlier, some of the PPs are only based on rain gauge data (i.e., GPCC 7.0 and CRU TS 3.23), and others blend different types of information (e.g. CHIRPS 2.0, MSWEP and ARC 2.0). Although it is only logical to expect a strong correlation between these PPs and rain gauge data if the PP used the same rain gauge that are being used in the evaluation, as mentioned earlier, this was not fully true as some of these PPs exhibit low correlation levels. While GPCC 7.0 show the best performance among all the PPs considered in the current research ($R^2 = 0.98$, $RMSE = 36.96$ mm, $NSE = 0.87$, and $\%BIAS = -5.3\%$), CRU TS 3.23 reveal a moderate performance ($R^2 = 0.79$, $RMSE = 52.03$ mm, $NSE = 0.68$, and $\%BIAS = -8.8\%$), and ARC 2.0 show a lower performance ($R^2 = 0.72$, $RMSE = 71.20$ mm, $NSE = -0.20$, and $\%BIAS = -60.80\%$).

When evaluated with the R^2 , the decrease in performance of PPs follows this order: GPCC 7.0 > CHIRPS 2.0 > TRMM 3B42 > TAMSAT 3.0 > CMORPH > CRU TS 3.23 > GPCP 1DD > PERSIANN CDR > MSWEP > PGF > ERA-Interim > RFE 2.0 > ARC 2.0 > TRMM 3B42 RT > MERRA-2 > PERSIANN CSS > PERSIANN. The two worst performing PPs using NSE were ARC 2.0 and RFE 2.0 with negative values that ranged between -1.7 and -0.2 reflecting a noticeable underestimation of precipitation. Based on RMSE, PERSIANN and ERA-Interim exhibit the largest error compared to the rain gauges, with RMSE values of 84 mm and 103 mm, respectively.

While two of the remote sensing-based PPs; i.e., PERSIANN and PERSIANN CSS, show the worst performance ($R^2 = 0.44$ and 0.5 , $RMSE = 88.46$ mm and 80.29 mm, $NSE = 0.25$ and 0.26 , $\%BIAS = 14.30\%$ and -6.30% for the two products, respectively), CMORPH exhibit better performance ($R^2 = 0.82$, $RMSE = 48$ mm, $NSE = 0.79$, and $\%BIAS = -7.6\%$). Several blended PPs were better off (e.g. CHIRPS 2.0, TRMM 3B42, TAMSAT 3.0). The good performance of TRMM 3B42 RT compared to the other remote sensing products is remarkable. The strongest correlation in the blended group was identified for CHIRPS 2.0 ($R^2 = 0.88$, $RMSE = 38.18$ mm, $NSE = 0.87$, and $\%BIAS = -3.2\%$), and TRMM 3B42 ($R^2 = 0.87$, $RMSE = 40$ mm, $NSE = 0.85$, and $\%BIAS = 2.7\%$). A good performance of these PPs was found in many other regions around the world (Duan et. al., 2016; Habib, et. al., 2012; Luo et. al., 2019).

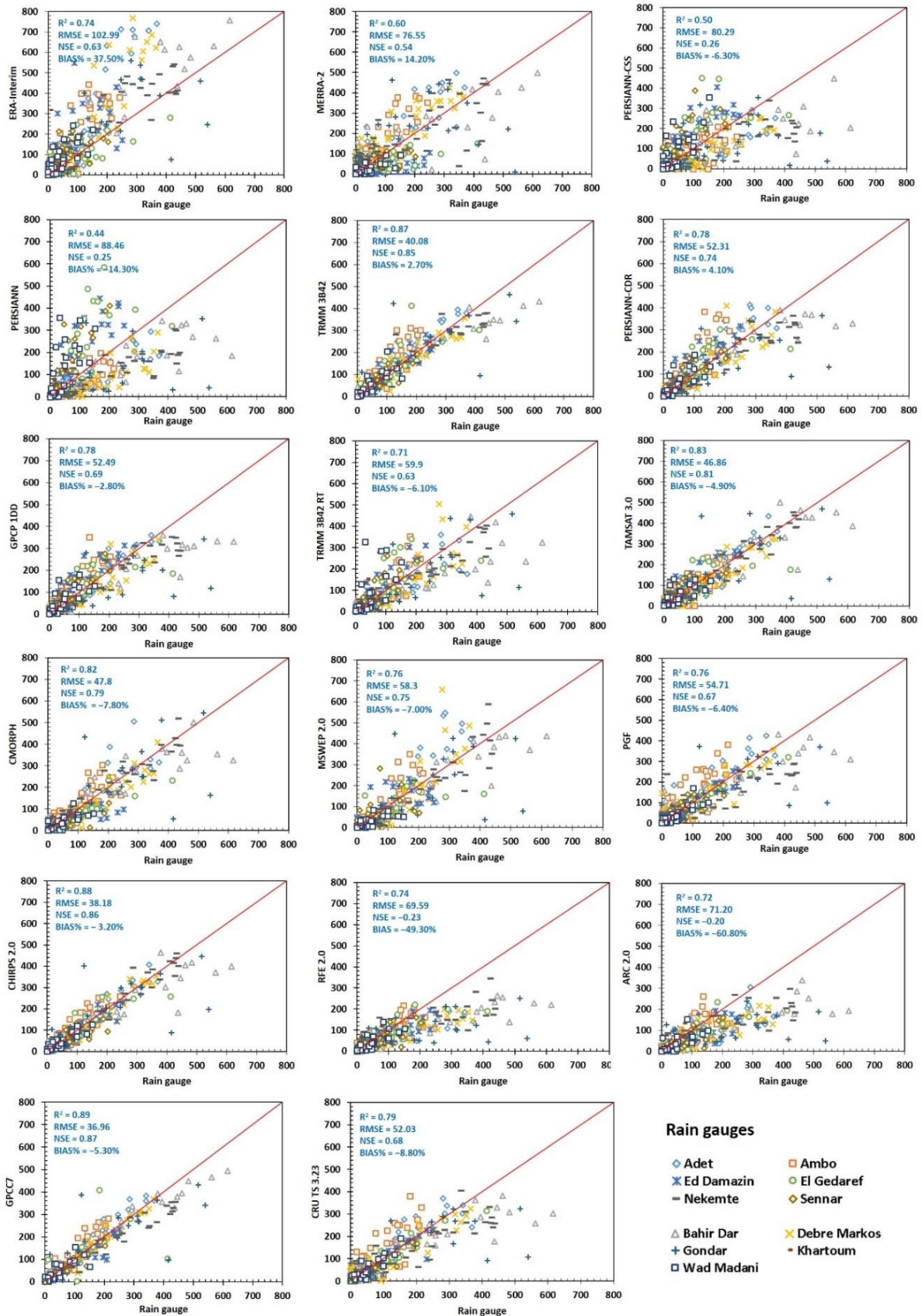


Fig. 4.6. Plots of pixel-to-point evaluation, on a monthly scale (in mm units), of precipitation of the 17 precipitation products using rain gauges data as a reference (in mm). Values of the four measures of fit, i.e., R^2 , RMSE, NSE, and %BIAS are indicated. Each symbol represents one of the rain gauges used in the current validation.

The improved performance of the PPs of this category is due to the inclusion of precipitation data from rain gauges in their algorithms, which might include also some of the rain gauges used in the current evaluation. For example, the calibration TRMM 3B42 with rain gauge data has enhanced its performance compared to the TRMM 3B42 RT product. From the results of the evaluation of the PPs with gauge data, most of the algorithms that were used to create the ground-based and blended PPs have benefited from incorporating ground estimations. This is evidenced by the relatively high R^2 and NSE values and the lower RMSE and %BIAS compared to the values corresponding to the satellite-based and atmospheric re-analysis PPs (Fig. 4.6). However, not all blended products show high performance. For instance, RFE 2.0, ARC 2.0 display a lower correlation with rain gauges data on monthly and annual scales over the BNB (Fig. 4.6). The different performances detected herein among these PPs indicate relative differences in benefiting from including rain gauge in their algorithms and could be attributed partially to the interpolation techniques used to produce each of the two PPs (Chen et. al., 2017). Considering the four performance indices; i.e. R^2 , RSME, NSE, and %BIAS, it can be concluded that CHIRPS 2.0 and TRMM 3B42 products benefited the most from the inclusion of ground-based data, a conclusion that agrees with previous studies reported high performances of CHIRPS 2.0 in the Nile Basin (Ayehu et. al., 2018).

The PPs that show the lowest BIAS% are GPCP 1DD, TRMM 3B42, and CHIRPS 2.0 with values of 2.8, -2.7, and -3.2%, respectively. On the other hand, MERRA-2 and ERA-Interim exhibit the largest positive %BIAS of 14.3% and 37.5%. A systematic overestimation of precipitation by ERA-Interim and MERRA-2 is detected, as most of the points lie above the 1:1 line. This systematic overestimation increases with precipitation amount. In contrast, the scatter points of the plot of REF 2.0 and ARC 2.0 versus rain gauge data fall below the 1:1 line indicating underestimating of precipitation amounts by these products compared to the rain gauge data and exhibit the largest negative %BIAS of -49.3% and -60.8% for the two products, respectively.

4.4.5. Hierarchical Clustering and Principal Component Analyses

Results of HCA and PCA revealed similar affinity/differences of the PPs as those shown in the cross-correlation evaluation (see Section 4.3). The connection level between each product/cluster of products on the left side of the dendrograms (Fig. 4.7) exhibits the relative relationship between the PPs at the grid-cell level; i.e. the products that are connected first are much similar to each other compared to the products that connect at higher levels. For instance, GPCC 0.7 and PGF in January, and CHIRPS 2.0 and TAMSAT 3.0 in September could be

considered as the most similar PPs in terms of their grid-cell values. On the contrary, MERRA-2 and ERA-Interim, and PERSIANN and EPRSIANN-CSS are the PPs with most dissimilarities compared to other products in January and September, respectively. The quantitative differences between the PPs are scaled using unit variance (using means and standard deviations) and shown graphically using heatmaps. MERRA-2 and ERA-Interim show substantial higher positive differences (red shades) in the heatmaps at the annual and monthly (for several months) scales. These results reflect higher precipitation in these PPs compared to the others. The dark blue color for ARC 2.0, RFE 2.0, and MERRA-2 in July, for instance, indicates lower precipitation estimates in these products compared to other PPs. Apart from MERRA-2, ERA-Interim, ARC 2.0 and RFE 2.0 products, which display different estimations from the other products, all products exhibit better affinity in their precipitation estimation in the dry months compared to wet months. The findings of PCA goes in line with those found using both the pixel-to-pixel comparison and the HCA reported earlier. For instance, in a two-dimensional plot, the first and second PCs showed that the same examples mentioned above; i.e. MERRA-2 and ERA-Interim in January, and PERSIANN and PERSIANN-CSS in September, are located far away from the points of the other PPs (Fig. 4.7), reflecting their difference compared to other PPs. The location of the plotted points approximates the similarities and differences between the studied PPs.

The results of data mining techniques do not only support the findings of the traditional evaluation methods but also show an advantage over the traditional methods in identifying discrepancies between the PPs in a graphical form, i.e. heatmaps, dendrograms, and PCA plots. The graphical representation in heatmap offers an opportunity to discover where the products differ and quantify these differences. In addition to the simplicity of applying the data mining techniques using scripts and online tools, such as ClustVis, the ability of such algorithms to handle large datasets at once is remarkable. This ability would advance the routines of comparing different PPs. Additionally, the outstanding offer of minimizing the complexity in big datasets while preserving information regarding variation between the products as shown by the results of PCA is notable. These results indicate that the application of data mining techniques can be beneficial when evaluating several PPs performance over extremely data-scarce regions.

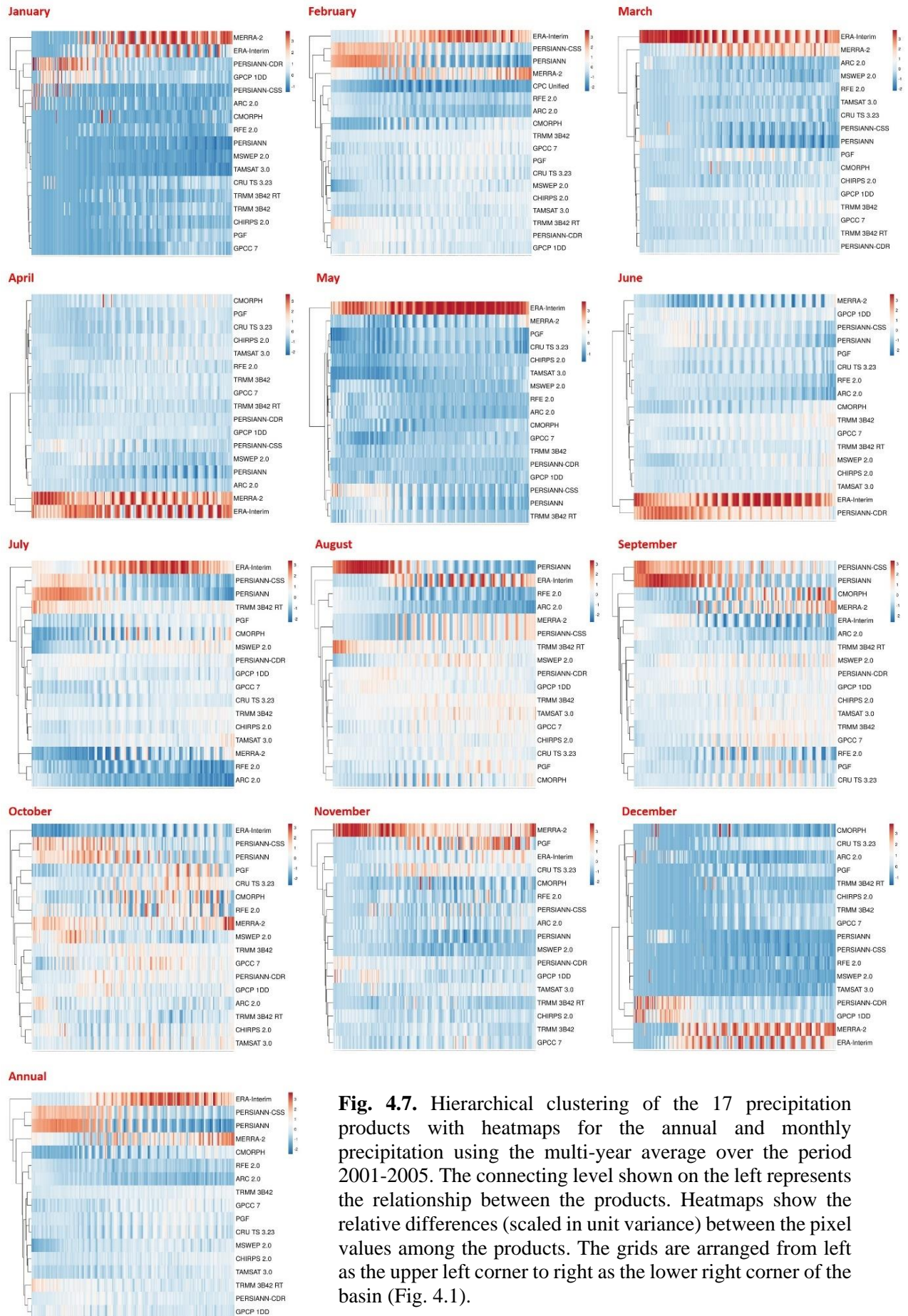


Fig. 4.7. Hierarchical clustering of the 17 precipitation products with heatmaps for the annual and monthly precipitation using the multi-year average over the period 2001-2005. The connecting level shown on the left represents the relationship between the products. Heatmaps show the relative differences (scaled in unit variance) between the pixel values among the products. The grids are arranged from left as the upper left corner to right as the lower right corner of the basin (Fig. 4.1).

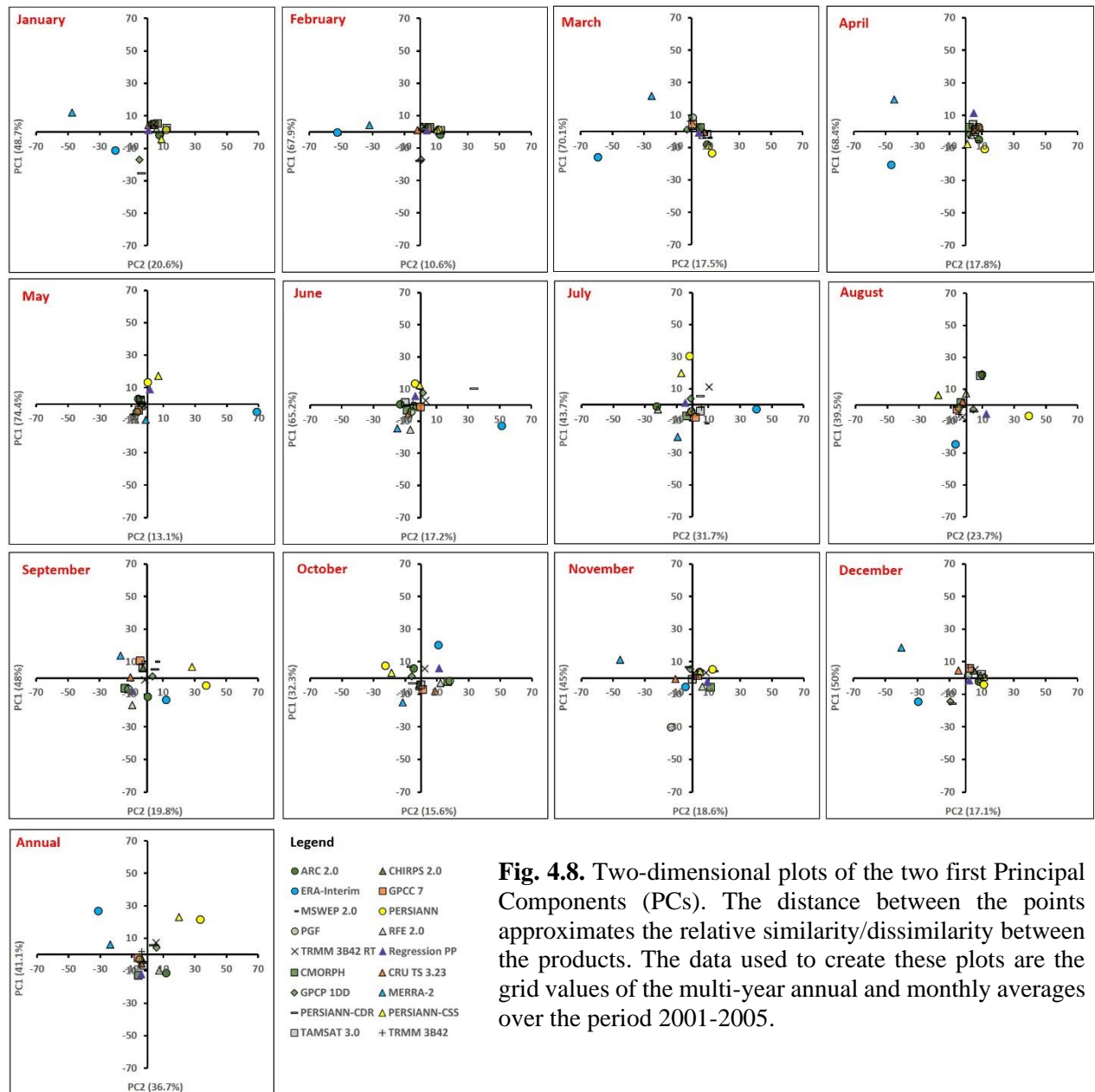


Fig. 4.8. Two-dimensional plots of the two first Principal Components (PCs). The distance between the points approximates the relative similarity/dissimilarity between the products. The data used to create these plots are the grid values of the multi-year annual and monthly averages over the period 2001-2005.

4.4.6. Sensitivity and stability of clusters

Based on the Elbow method, four clusters were determined to be the optimum k . Therefore, a sensitivity analysis was conducted on the products by creating 2-7 clusters. To illustrate examples for the analysis of clusters stability, results on annual time step along with those for February and August (as examples for dry and wet months, respectively) are presented in Figure 4.9. At the annual scale, the most dissimilar PP was ERA-Interim, as it is isolated immediately from the other 16 PPs when two clusters are created (Fig. 4.9, Table 4.2). The separation of the products from the 17 PPs group, when 2-7 clusters were created, follows this order: (i) ERA-Interim, (ii) PERSIANN and PERSIANN-CSS, (iii) MERRA-2, (iv) CMORPH, (v) RFE 2.0 and ARC 2.0, (vi) TRMM 3B42 RT, PERSIANN-CDR, and GPCP 1DD. The association of

the products grouped in clusters 3, 6 and 7 indicates a relative similarity of these PPs compared to their affinity to other ones. In particular, the association of RFE 2.0 and ARC 2.0, when five clusters are created, supports the close similarity of these two products, as reported earlier. Generally, all the PPs that are grouped in the same cluster could be considered, to some extent, to be more related compared to the other PPs that are grouped in a different cluster. This observation is emphasized by the results of the HCA and PCA.

At the monthly temporal scale, MERRA-2 and ERA-Interim split first when two clusters are created in the dry months (November – May) and wet months (July – October), respectively. The sensitivity analysis conducted herein was useful to identify the months in which precipitation estimate deviates the most between the PPs. For example, PGF was separated into an isolated cluster in February and November, suggesting that most of the differences that are detected in this product from the other PPs could be attributed to its precipitation estimates over these two months. Such findings are helpful for data providers to improve their data estimation.

4.4.7. Merging of products

The results of the MPPs displayed varying performance when compared to the Regression PP estimates (Fig. 4.9). For instance, at the annual scale, the deviation between the multi-year mean precipitation between the MPPs (bars in the figure) and the estimates of the reference dataset (horizontal line in the figure) ranged from -20.7% to 53.7% . In many cases, creating MPPs by merging all the PPs of cluster 1 resulted in precipitation estimates relatively close to that estimated using the Regression PP dataset (horizontal line). For instance, the mean annual values estimated with the MPPs of the first cluster deviates by only -0.6% to -3.8% from that estimated using Regression PP. This characteristic could be seen in the annual temporal scale and in most of the individual months (Fig. 4.9).

The relatively good performance of the MPPs that were created by merging the products of the first cluster could be attributed mainly to the exclusion of the most dissimilar PPs. Moreover, merging different PPs might enable capturing additional information compared to the individual PPs, and hence, providing more accurate input data for water resources application (Abera et al., 2016; Peña-Arancibia et al., 2013). For example, merging the annual PERSIANN and PERSIANN-CSS, which were grouped in the same cluster (cluster 3), was found to result in a better precipitation estimate compared to their original precipitation estimates. This is also true for the precipitation estimates of the same two products when compared with those of many other PPs (e.g. ERA-Interim (cluster 2), MERRA-2 (cluster 4) and RFE 2.0 and ARC 2.0 (cluster 6)), as shown in Figure 4.9. However, merging PPs which

were grouped in the same cluster does not always result in better precipitation estimates perhaps, because such products agree in their precipitation estimates but still be biased. For example, cluster 5 in the case of the annual time step and cluster 4 in the case of August resulted in poor estimates of the annual precipitation compared to other clusters. The deviations found in the two above-mentioned cases are, respectively, -20.8% and -23.2% from the mean annual precipitation as estimated by the Regression PP (Fig. 4.9). These two clusters include ARC 2.0 and RFE 2.0, which displayed an underestimation of precipitation when compared to the reference data (Figs. 4.6 and 4.7).

At the grid-cell level, merging PPs on the annual scale display better performance than the monthly scale and in dry months compared to wet months. Generally, MPPs exhibit %BIAS up to 40.4% on an annual scale. While, %BIAS ranges from 4.8% to 7.9% for the first cluster on an annual scale, it showed values from -0.1% to -10.7% and from 96% to 97.8% , in February and August, respectively. These results indicate that merging PPs that are grouped in the first cluster, i.e. after separating the most dissimilar PPs, result in an enhanced estimation of precipitation at the annual scale compared to the monthly scale, especially for the wet months. This could be attributed to the large discrepancies found using HCA, between the studied PPs during wet months at different grid-cells (See Section 4.4.5 and Figure 4.7). Therefore, the merging of different PPs should be done carefully by considering the performance of the individual PPs spatially and temporally, as low performing products may worsen the precipitation estimation of the MPPs.

4.5. Conclusion

This study provided an analysis of 17 selected PPs over the BNB using traditional evaluation approaches and data mining techniques; thus, providing an innovative contribution to the field of PPs in the BNB and other similar data-scarce regions. First, this research has evaluated and compared 17 PPs commonly used in water resources research and development projects, usually without prior evaluation. Second, the methodological approach suggested in the current study on utilizing data mining techniques proved to be effective, easier and more informative than the traditional evaluation methods. Finally, this research displayed an innovative approach to investigate the potential for creating improved precipitation estimates using simple merging methods based on the results of comprehensive analysis of PPs. Even though there are several merging methods available nowadays, our approach is easier to implement and the procedure is straightforward.

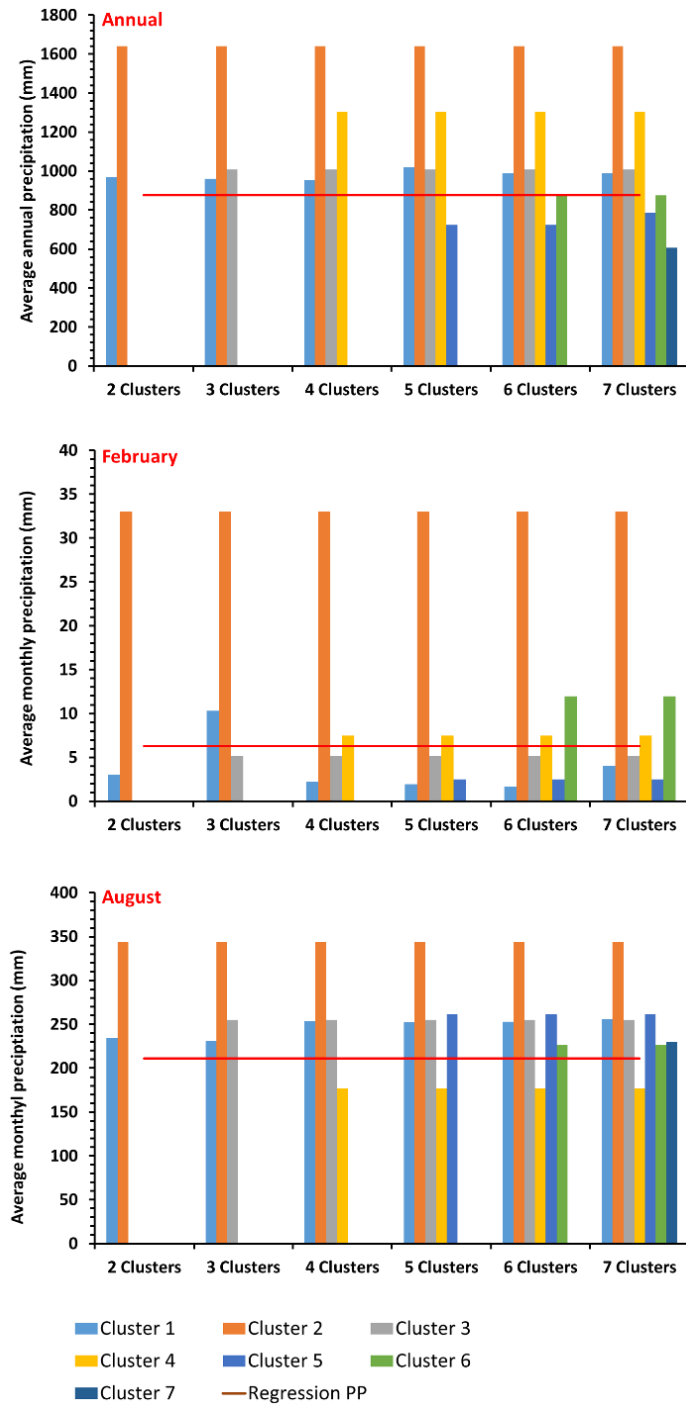


Fig. 4.9. Three examples (annual, February and August) of the sensitivity analysis conducted on the precipitation products to check the stability of clusters. The multi-year average (2001-2005) of the reference dataset (Regression PP) is used to validate the results of this stability analysis. Products that are clustered together were merged to produce precipitation estimates. For the names of the products in each cluster refer to the associated table (Table 4.2).

Table 4.2. Product clusters resulted from stability analysis on annual and monthly (February and August) time scales.

Annual							
	Cluster 1	Cluster 2	Cluster 3	Cluster 4	Cluster 5	Cluster 6	Cluster 7
2 clusters	PERSIANN, PERSIANN-CSS, MERRA-2, ARC 2.0, RFE 2.0, CMORPH, GPCC7, TRMM 3B42, TRMM3B42 RT, CRU TS 3.23, PGF, MSWEP 2.0, CHIRPS 2.0, TAMSAT 3.0, GPCP 1DD, PERSIANN-CDR	ERA Interim					
3 clusters	MERRA-2, ARC 2.0, RFE 2.0, CMORPH, GPCC7, TRMM 3B42, TRMM3B42 RT, CRU TS 3.23, PGF, MSWEP 2.0, CHIRPS 2.0, TAMSAT 3.0, GPCP 1DD, PERSIANN-CDR	ERA Interim	PERSIANN PERSIANN-CSS				
4 clusters	ARC 2.0, RFE 2.0, CMORPH, GPCC7, TRMM 3B42, TRMM3B42 RT, CRU TS 3.23, PGF, MSWEP 2.0, CHIRPS 2.0, TAMSAT 3.0, GPCP 1DD, PERSIANN-CDR	ERA Interim	PERSIANN PERSIANN-CSS	MERRA-2			
5 clusters	CMORPH, GPCC7, TRMM 3B42, TRMM3B42 RT, CRU TS 3.23, PGF, MSWEP 2.0, CHIRPS 2.0, TAMSAT 3.0, GPCP 1DD, PERSIANN-CDR	ERA Interim	PERSIANN PERSIANN-CSS	MERRA-2	ARC 2.0, RFE 2.0		
6 clusters	GPCC7, TRMM 3B42, TRMM3B42 RT, CRU TS 3.23, PGF, MSWEP 2.0, CHIRPS 2.0, TAMSAT 3.0, GPCP 1DD, PERSIANN-CDR	ERA Interim	PERSIANN PERSIANN-CSS	MERRA-2	ARC 2.0, RFE 2.0	CMORPH	
7 clusters	GPCC7, TRMM 3B42, CRU TS 3.23, PGF, MSWEP 2.0, CHIRPS 2.0, TAMSAT 3.0,	ERA Interim	PERSIANN PERSIANN-CSS	MERRA-2	ARC 2.0 RFE 2.2	CMORPH	TRMM3B42 RT, GPCP 1DD, PERSIANN- CDR
February							
	Cluster 1	Cluster 2	Cluster 3	Cluster 4	Cluster 5	Cluster 6	Cluster 7
2 clusters	ERA-Interim, PERSIANN, PERSIANN-CSS, ARC 2.0, RFE 2.0, CMORPH, GPCC7, TRMM 3B42, TRMM3B42 RT, CRU TS 3.23, PGF, MSWEP 2.0, CHIRPS 2.0, TAMSAT 3.0, GPCP 1DD, PERSIANN-CDR	MERRA-2					
3 clusters	ERA-Interim, PERSIANN, PERSIANN-CSS, ARC 2.0, RFE 2.0, CMORPH, GPCC7, TRMM 3B42, TRMM3B42 RT, CRU TS 3.23, MSWEP 2.0, CHIRPS 2.0, TAMSAT 3.0, GPCP 1DD, PERSIANN-CDR	MERRA-2	PGF				
4 clusters	ERA-Interim, PERSIANN, PERSIANN-CSS, ARC 2.0, RFE 2.0, CMORPH, GPCC7, TRMM 3B42, TRMM3B42 RT, CRU TS 3.23, MSWEP 2.0, CHIRPS 2.0, TAMSAT 3.0,	MERRA-2	PGF	GPCP-1DD PERSIANN-CDR			
5 clusters	ERA-Interim, PERSIANN, ARC 2.0, RFE 2.0, CMORPH, GPCC7, TRMM 3B42, TRMM3B42 RT, CRU TS 3.23, MSWEP 2.0, CHIRPS 2.0, TAMSAT 3.0,	MERRA-2	PGF	GPCP-1DD PERSIANN-CDR	PERSIANN-CSS		
6 clusters	PERSIANN, ARC 2.0, RFE 2.0, CMORPH, GPCC7, TRMM 3B42, TRMM3B42 RT, CRU TS 3.23, MSWEP 2.0, CHIRPS 2.0, TAMSAT 3.0,	MERRA-2	PGF	GPCP-1DD PERSIANN-CDR	PERSIANN-CSS	ERA-Interim	
7 clusters	PERSIANN, ARC 2.0, RFE 2.0, CMORPH, GPCC7, TRMM 3B42, TRMM3B42 RT, CRU TS 3.23, MSWEP 2.0, CHIRPS 2.0, TAMSAT 3.0	MERRA-2	PGF	GPCP-1DD PERSIANN-CDR	PERSIANN-CSS	ERA-Interim	ARC 2.0, TAMSAT 3.0, CPC Unified, PERSIANN, MSWEP 2.0
August							
	Cluster 1	Cluster 2	Cluster 3	Cluster 4	Cluster 5	Cluster 6	Cluster 7
2 clusters	MERRA-2, PERSIANN, PERSIANN-CSS, CPC Unified, ARC 2.0, RFE 2.0, CMORPH, GPCC7, TRMM 3B42, TRMM 3B42 RT, CRU TS 3.23, PGF, MSWEP 2.0, CHIRPS 2.0, TAMSAT 3.0, GPCP 1DD, PERSIANN-CDR	ERA-Interim					
3 clusters	MERRA-2, CPC Unified, ARC 2.0, RFE 2.0, CMORPH, GPCC7, TRMM 3B42, TRMM 3B42 RT, CRU TS 3.23, PGF, MSWEP 2.0, CHIRPS 2.0, TAMSAT 3.0, GPCP 1DD, PERSIANN-CDR	ERA-Interim	PERSIANN, PERSIANN-CSS				
4 clusters	MERRA-2, CPC Unified, ARC 2.0, RFE 2.0, CMORPH, GPCC7, TRMM 3B42, TRMM 3B42 RT, CRU TS 3.23, PGF, MSWEP 2.0, CHIRPS 2.0, TAMSAT 3.0, GPCP 1DD, PERSIANN-CDR	ERA-Interim	PERSIAAN, PERSIANN-CSS	ARC 2.0, RFE 2.0			
5 clusters	MERRA-2, CMORPH, GPCC7, TRMM 3B42, CRU TS 3.23, PGF, MSWEP 2.0, CHIRPS 2.0, TAMSAT 3.0, GPCP 1DD, PERSIANN-CDR	ERA-Interim	PERSIAAN, PERSIANN-CSS	ARC 2.0, RFE 2.0	TRMM 3B42 RT		
6 clusters	CMORPH, GPCC7, TRMM 3B42, CRU TS 3.23, PGF, MSWEP 2.0, CHIRPS 2.0, TAMSAT 3.0, GPCP 1DD, PERSIANN-CDR	ERA-Interim	PERSIAAN, PERSIANN-CSS	ARC 2.0, RFE 2.0	TRMM 3B42 RT	MERRA-2	
7 clusters	GPCC7, TRMM 3B42, CRU TS 3.23, PGF, MSWEP 2.0, CHIRPS 2.0, TAMSAT 3.0, GPCP 1DD, PERSIANN-CDR	ERA-Interim	PERSIAAN, PERSIANN-CSS	ARC 2.0, RFE 2.1	TRMM 3B42 RT	MERRA-2	CMORPH

Despite the usefulness of PPs, especially for data-scarce regions such as the BNB, the current analysis revealed great variations between the studied PPs, which could potentially lead to varying results in water resources application, for instance, drought characterization, water balance estimation, and hydrological modeling. Therefore, a comprehensive analysis is required before employing any PPs in those applications. The results of the current research highlighted that there are still variations between the selected PPs over the BNB for the analysed period. The variation at the grid-cell level was quantified using descriptive statistics; i.e. pixel dispersion and central tendency of the grid-cell data, and analysed through a pixel-to-pixel comparison. The direct correlation of these PPs with rain gauges data (pixel-to-point) revealed the degree of proximity of these PPs to in-situ measurements. Among the individual PPs, GPCC 7.0, CHIRPS 2.0 and TRMM 3B42 showed the highest performance at the monthly scale when the PPs were correlated directly with the rain gauges data (pixel-to-point). Two of the remote sensing-based PPs, i.e. PERSIANN and PERSIANN-CSS, exhibited the poorest performance. CMORPH revealed the best performance among the studied remote sensing-based products.

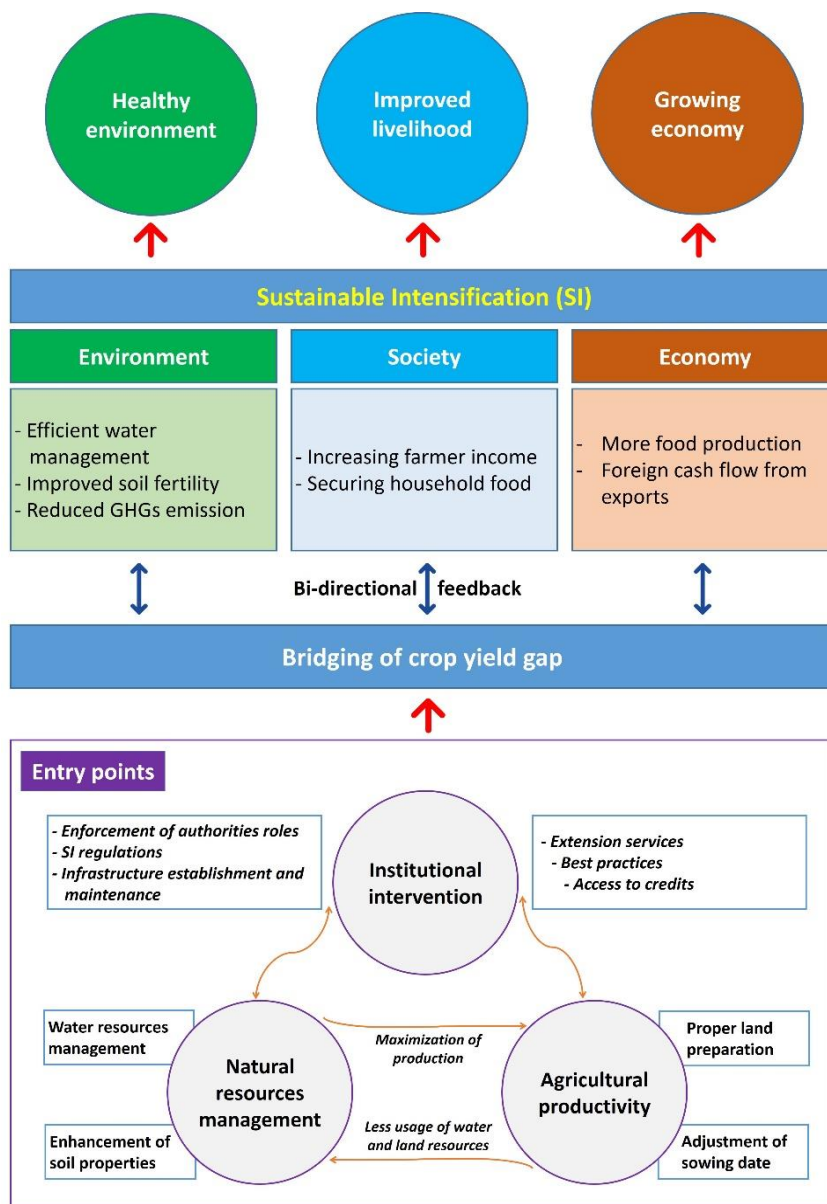
A limitation of the pixel-to-point evaluation conducted herein is the limited number of rain gauges and the unavailability of a dataset that is independent of all the selected PPs. This is particularly true for two groups of the selected PPs; i.e. purely ground-based, and blended categories. However, due to the limited available rain gauges in this data-scarce areas, several previous studies (Basheer et. al., 2018; Sahlu et. al., 2017) have used data from non-independent rain gauges to validate some of these PPs. Despite the inclusion of rain gauge data in the composition of several PPs, we provided evidence that even such products might not reveal a strong correlation with rain gauge data, which could be related to the interpolation process. However, this remains an open question to be analysed in further research.

Results of data mining techniques, i.e. HCA and PCA, identified the similarities and dissimilarities between the 17 PPs. These results confirm the findings obtained using traditional approaches and suggest the usefulness of data mining approaches in such evaluations. Given their simplicity and their ability to handle big datasets from different PPs at the same time, provision of graphical representation of the difference between PPs, and their feasibility to conduct a sensitivity analysis of products, these techniques should gain more attention in assessing the performance of PPs.

The merging of different PPs showed, in many cases, the potential for generating improved precipitation estimates compared to those of the original PPs. For example, the MPP that was created by combining the PPs that were clustered in the first group at the annual scale, deviates

only by -0.6% to -3.8% from the reference data. However, the performance of MPP is dependent, largely, on the PPs being merged, their underlying characteristics such as spatial resolution and source of data, as many MPPs showed large deviations from the reference dataset. Given the results emerging from the proposed merging approach, we recommend testing it over different geographical settings and, perhaps, testing more other PPs. This research direction might result in the development of a simple operational approach to improve the PPs performance.

Yield gap and pathways for sustainable intensification in irrigated schemes



Based on:

Khalifa, M., Elagib, N.A., Bashir, M.A., Ribbe, L., Schneider, K., 2020. Exploring socio-hydrological determinants of crop yield in under-performing irrigation schemes: Pathways for sustainable intensification. *Hydrological Sciences Journal*, 55 (2), 153-168.

Abstract

Understanding the human–water–food–climate nexus is central to achieving sustainable intensification (SI) in agriculture. This research uses a socio-hydrological approach to understand the underpinning for implementing SI in the Gezira Irrigation Scheme, Sudan, by integrating vegetation indices derived from remote sensing, ancillary, gridded soil, and precipitation data, supplemented by interviews with 393 farmers. The productivity gap was estimated as the difference between the potential and actual productivities. Based upon data on farmers' socio-economic status and field practices, a regression tree model was built to determine the factors that control the sorghum yield. The model revealed that the financial status of farmers and access to water are the most influential factors on sorghum yield. A conceptual framework that elucidates SI and its bi-directional feedback to the environment, society and the economy is proposed. Implementing SI in the scheme has implications on water and food security in Sudan and beyond its borders.

5.1. Introduction

In the Anthropocene, human activities induce large global environmental changes (Steffen et. al., 2007). Among all these activities, agriculture is the largest driver of such changes in this new geological epoch (Rockström et. al., 2017; Kuyper and Struik, 2014). Agriculture is an important pillar for the achievement of Sustainable Development Goal (SDG) 2 on eradicating hunger and securing food for an ever-growing population (Rockström et. al., 2017). Despite the recent improvement in agricultural productivity, undernourishment and hunger still affect millions of people (Webb et. al., 2018; Powledge, 2010). Even in scenarios of modest economic growth, the future global demand for food will require agricultural production to increase by 50% by the year 2050 as compared to 2013 (FAO, 2017). It is expected that the increasing demand for food will aggravate environmental impacts (Tilman, 1999). Providing more food with limited water and land resources while ensuring the sustainability of resource use is a great challenge to future development (Davis et. al., 2016; Steffen et. al., 2015).

Coping strategies to address this challenge, such as (1) closing the yield gap for the already existing croplands, (2) reducing food waste, (3) managing diet behavior, and (4) enhancing the efficiency of resource use, have the potential to double the agricultural production while minimizing the negative environmental impacts (Foley et. al., 2011). The approach of sustainable intensification (SI) of agriculture in already cultivated lands is promising (Burke et. al., 2017; Davis et. al., 2016), as it emphasizes preserving the land for the coming generations

(Davis et. al., 2016). Intensification of agriculture to tap the unused potential in existing agricultural schemes, especially in underperforming ones, is the best choice to address the challenge of future food security (Pradhan et. al., 2015; Finger, 2011; Foley et. al., 2011). A paradigm shift towards SI would change the position of agriculture from being one of the largest drivers of global environmental change to becoming a key contributor toward a more sustainable environment (Rockström et. al., 2017). A key research issue in this context is to quantify the potential of SI for increasing food production and to develop suitable intervention strategies to reap the benefits of this potential. The issue at hand has a spatio-temporal as well as natural and socioeconomic dimensions.

In order to develop pathways for SI, it is crucial to analyze the interactions between humans and hydrological systems and, consequently, their impacts on water and food production. Socio-hydrology (Sivapalan et. al., 2012) is a science that emphasizes understanding the bi-directional perspective of interactions and feedbacks between humans and water at long time scales (Blair and Buytaert, 2016). This paradigm has the potential to lead to a new understanding of human–water interactions (Pande and Savenije, 2016), which may result in more sustainable solutions to the challenges ahead.

In Sub-Saharan Africa in particular, suitable data and knowledge to address these dimensions are scarce, while the need to improve crop yield is particularly important for food security (Pretty et. al., 2011). Agricultural production in the irrigation sector is a particularly relevant field of research for investigating the concept of socio-hydrology and to explore pathways for SI. In this regard, the Gezira Irrigation Scheme in Sudan is a suitable model to investigate. The scheme plays a major role in the food security of the country, with the main season extending from June to October (Elagib, 2015, 2014) and the dominant crop being sorghum (See Appendix D: Fig. S5.1).

Against this background, an integrated approach that uses multi-data to analyze the productivity gap, its temporal and spatial variation and the controlling factors affecting the sorghum yield in the scheme provides useful insights into potential pathways for SI in the Gezira Scheme and other irrigation schemes that are facing similar challenges. Therefore, the main objectives of this research are: (1) to understand the spatial and temporal variations of the productivity gap in the summer seasons in the Gezira Irrigation Scheme; (2) to detect the most important factors controlling the yield of sorghum in the scheme; and (3) to identify underpinnings and entry points to SI policies for the scheme.

5.2. Materials and methods

5.2.1. Gezira Irrigation Scheme

The Gezira Irrigation Scheme lies in the flat area located to the south of the confluence of the Blue Nile and the White Nile in central Sudan (Fig. 5.1). This scheme was chosen for the current research since it is considered a model for most irrigation schemes in Sudan (Osman et. al., 2017). With a total command area of around 0.88×10^6 ha (World Bank, 1990), the scheme is considered the largest irrigation scheme in the world under one administrative body (Bicciato and Faggi, 1995). In recent years, the scheme has greatly deteriorated due to multiple and complex factors. Currently, it suffers from low irrigation efficiency (Mohamed et. al., 2010), low crop yield (Mahgoub et. al., 2017) and several problems in the irrigation system (See Appendix D: Fig. S5.2). Using remote sensing, Al Zayed and Elagib (2017) detected tens of canals with water spillover in the Gezira Irrigation Scheme, thus reflecting inefficient water distribution and over-supply of irrigation water.

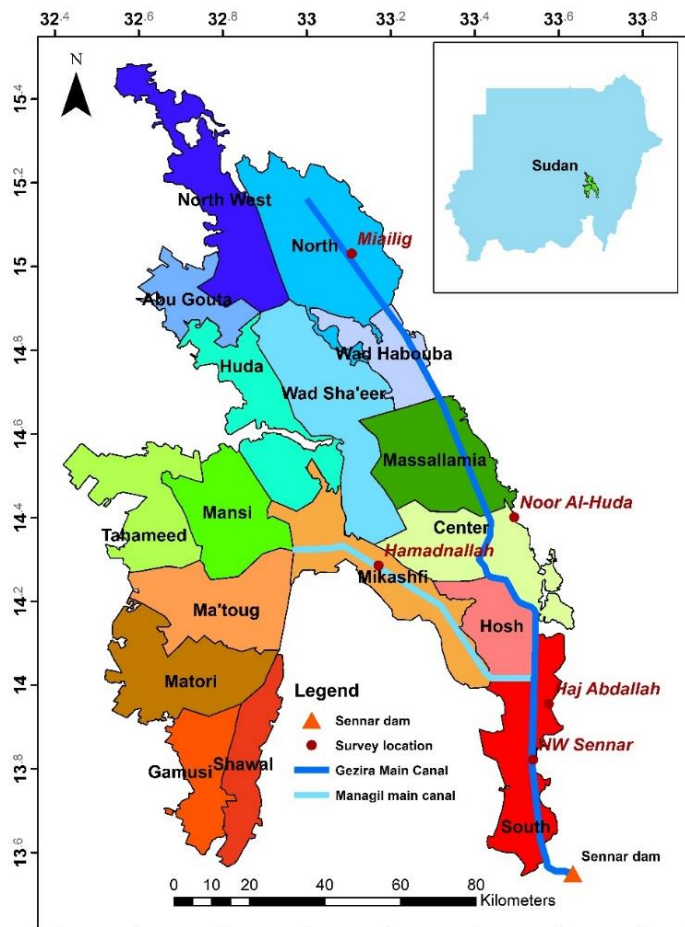


Fig. 5.1. Location map of the Gezira Scheme showing the Administrative Groups (AGs) and the two main irrigation canals. The source of irrigation water is Sennar reservoir at the south-eastern border of the scheme. Locations of the selected field survey blocks are shown as dots.

Whereas sorghum, cotton, and groundnuts are the main crops being cultivated during the summer season (June–October), wheat and chickpea are the main winter season (November–April) crops (See Appendix D: Fig. S5.3). Beside these main crops, vegetables are also cultivated on a smaller scale. As shown in Fig. 5.1, the scheme is divided into 18 administrative groups (AGs), each group is subdivided into smaller units called blocks (Adam et. al., 2002). Water is supplied to the scheme from the Sennar Reservoir, which is located to the southeast of the scheme, through two main open canals, namely Gezira and Managil (Fig. 5.1). With an annual discharge of 6–7 km³ of water to the scheme (Al Zayed and Elagib, 2017), the Gezira Irrigation Scheme consumes around one-third of the total share of the Nile water allocated to Sudan according to the Nile Treaty of 1959 between Sudan and Egypt. Hence, the current underperformance of the scheme is not only affecting the food security in Sudan but has also implications on achieving water security goals (SDG 6: to ensure availability and sustainable management of water and sanitation for all).

5.2.2. Data

Within the framework of the current integrated research, diverse primary and secondary data were used. Primary data were collected through interviews with farmers in different blocks of the Gezira Scheme. These data focus mainly on socio-economic information and field management practiced by the farmers who cultivate sorghum (Table 5.1). Secondary data were obtained from the official authorities in Sudan. Agricultural statistics of crops, i.e. cultivated area, crop type and crop yield, and the quantity of water discharged from Sennar Reservoir to the scheme were obtained from the Gezira Scheme Board and the Ministry of Water Resources, Irrigation, and Electricity, respectively.

Gridded data were obtained from public-domain sources (Table 5.2). Two types of remote sensing data were used as a proxy for vegetation productivity, namely the Normalized Difference Vegetation Index (NDVI) from the Moderate Resolution Imaging Spectroradiometer (MODIS) satellite, and the Fraction of Absorbed Photosynthetically Active Radiation (FAPAR) from the Satellite Pour l'Observation de la Terre (SPOT-Vegetation). These two datasets are widely used to quantify productivity levels of vegetation and to monitor vegetation dynamics in many areas around the world. Examples of such studies include the Gezira Scheme (Al Zayed and Elagib, 2017; Al Zayed et. al., 2015, 2016), Sudan and Ethiopia (Khalifa et. al., 2018), the Horn of Africa region (Meroni et. al., 2014), Europe (Kowalik et. al., 2014) and Finland (Wang et. al., 2004).

Table 5.1. List of primary information collected for the current research through a questionnaire.

Socio-economy	Age Level of education Years of experience in farming Source of income Number of household members
Farm information	Size Location along tertiary canal
Pre-sowing land preparation	Date of land preparation Use of machinery Pre-sowing land watering
Sowing	Sowing date Seed density (rate) Crop variety
Irrigation	Method of irrigation: furrow, basin First irrigation (days after sowing) Number of applications
Fertilizers	Number of applications Timing of application (days after sowing) Applied quantity
Yield	Average achieved yield Maximum achieved yield during previous seasons

Table 5.2. Characteristics of secondary data collected from public-domain sources and official authorities in Sudan. NDVI: Normalized Difference Vegetation Index; FAPAR: Fraction of Absorbed Photosynthetically Active Radiation; OCC: Organic Carbon Content. AGs: Administrative Groups. GSB: Gezira Scheme Board; MOWIE: Ministry of Water Resources, Irrigation, and Electricity; MODIS: Moderate Resolution Imaging Spectroradiometer; CHG-UCSB: Climate Hazard Group, University of California, Santa Barbara.

Category	Data type	Spatial resolution	Temporal resolution	Time period	Provider	Link to data	
Ancillary data	Crop	- Cultivated areas	Scheme	Seasonal*	2000-2016	GSB	-
		- Crop yield	AGs.	Seasonal*	2015-2016		
	Water	- Daily water discharge from Sennar Dam	Scheme	Daily	2015-2016	MOWIE	-
Remote sensing data	NDVI		250 m	Dekadal	2001-2016	MODIS	https://earlywarning.usgs.gov/fews
	FAPAR		1000 m	Dekadal	2001-2016	VITO - Copernicus Global Land Service	https://land.copernicus.eu/global/
	Precipitation		0.05°	Daily	2001-2016	CHG-UCSB	http://chg.geog.ucsb.edu/data/chirps/
Soil data	pH OCC Bulk density		250 m	-	-	Soil Grids	https://soilgrids.org/

* Summer season (June to October)

Soil properties and nutrient availability are the major biophysical constraints to crop yield in Africa (Tittone and Giller, 2013). Variables such as pH, Organic Carbon Content (OCC) and bulk density are among the most studied soil properties that affect crop yield (Quan and Liang, 2017; Reichert et. al., 2009; Dam et. al., 2005; Bauer and Black, 1994). For our research, spatially distributed data of pH, OCC, and bulk density were obtained from the SoilGrids project (see Table 5.2).

Gridded precipitation data were obtained from the Climate Hazards Group InfraRed Precipitation with Station data (CHIRPS), where CHIRPS 2.0 is a blended product that includes precipitation estimation from remote sensing merged with in situ measurements (Funk et. al., 2015). This product is considered one of the best performing public domain products over the East Africa region (Lemma et. al., 2019; Gebrechorkos et. al., 2018; Bayissa et. al., 2017).

5.2.3. Methods

Humans should be considered as a main component of the hydrological system (Pande and Sivapalan, 2017). Therefore, to explore pathways for implementing SI in the Gezira Irrigation Scheme, our research follows an integrated approach to highlight the interactions between the socioeconomic status of farmers and their field management practices on the one hand, and water resources and climate on the other hand. Figure 5.2 provides a graphical representation of the approaches adopted in this study in view of the data obtained as described in Section 5.2.2. Along with recognizing the intensity and spatio-temporal variation of the productivity gap in the scheme, two main approaches were followed to detect the most important factors that affect the agricultural productivity in the Gezira Irrigation Scheme. First, a spatial correlation was conducted to detect the effect of physical drivers (e.g. precipitation and soil characteristics). Second, a regression-tree model was built to determine the most influential socio-economic and management drivers. The results of these assessments were used to identify some entry points for SI in the scheme.

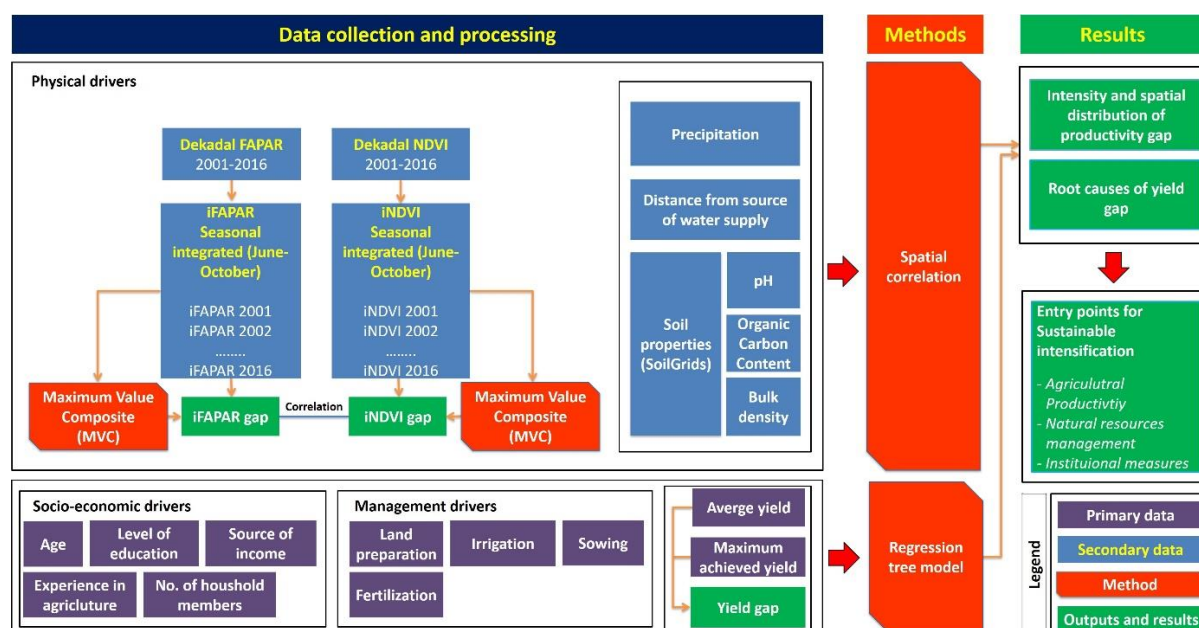


Fig. 5.2. Flowchart of the approach developed in the current study.

5.2.3.1. Processing of gridded data

Gridded data of NDVI, FAPAR, soil properties, and precipitation were processed using ArcGIS 10.3 software (ESRI, 2014). The NDVI and FAPAR raster files were processed as per instruction of the product documentation. In line with the approach followed by many researchers (e.g. Al Zayed and Elagib, 2017; Panda et. al., 2010), a threshold value NDVI and FAPAR of 0.25 was considered to differentiate between the vegetation and non-vegetation pixels. Raster files on NDVI, FAPAR and soil variables (pH, OCC, and bulk density) were clipped to the boundaries of the Gezira Irrigation Scheme.

5.2.3.2. Calculation of the productivity gap

The productivity gap was calculated as the difference between the potential/attainable productivity and actual productivity. Integrating NDVI and FAPAR values over the growing season serves as a proxy for the actual vegetation productivity throughout the season (Meroni et. al., 2014; Lobell, 2013.). Integrated NDVI (iNDVI) and integrated FAPAR (iFAPAR) were produced following the approach described by Field et. al. (1995), Prince and Goward (1995) and Al Zayed et. al. (2015, 2016) over the growing season months from June to October. Using the Maximum Value Composite (MVC) method (Holben, 1986), the maximum value for each pixel in the iNDVI and the iFAPAR images within 2001–2016 were selected to generate maximum iNDVI and maximum iFAPAR images, respectively. The maximum value that was extracted from the time series was used as a proxy for the potential productivity of the given pixel. However, this maximum productivity itself might be below the potential productivity at that given pixel. The productivity gap for each year within the investigation period was calculated as a percentage difference between the iNDVI and iFAPAR in a given year and the maximum iNDVI and iFAPAR for the data period (2001–2016), respectively:

$$iNDVI_{gap} = 100 - (iNDVI_{(y)} / iNDVI_{Max} \times 100) \dots\dots\dots (5.1)$$

$$iFAPAR_{gap} = 100 - (iFAPAR_{(y)} / iFAPAR_{Max} \times 100) \dots\dots\dots (5.2)$$

where subscript (y) denotes the individual year.

Using Equations (5.1) and (5.2), maps of the productivity gap were produced for all years over the data period. A special focus was put on the two successive years of 2015 and 2016 as they show distinctive variation in productivity and precipitation level based on the satellite-derived data. The collected data on sorghum yield were used to estimate the yield gap as the

difference between the maximum yield achieved by the farmer during the previous years and the average yield obtained by the same farmer in the 2017/18 summer season.

5.2.3.3. Standardization of vegetation index and classification of the administrative groups

This study used the Standardized Vegetation Index (SVI) and the corresponding classifications according to Peters et. al. (2002) which are based on estimating z-scores. The purpose of this SVI classification is to study the performance of the AGs of the Gezira Irrigation Scheme relative to the overall scheme performance using the proxy for productivity. To this end, the Shapiro-Wilk W-test for normality (Shapiro and Wilk 1965) was first employed to check the normal distribution of the iNDVI and iFAPAR time series before calculating the SVIs. Then, the z-scores for all pixels of the Gezira Irrigation Scheme and a corresponding average z-score for each AG were calculated. Peters et. al. (2002) suggested the following classes based on the z-scores: very poor (0–0.05), poor (0.05–0.25), average (0.25–0.75), good (0.75–0.95) and very good (0.95–1). Without an independent reference dataset, it is difficult to prefer one of the two vegetation indices, i.e. iNDVI and iFAPAR, against the other. However, due to the higher resolution of the iNDVI data compared to that of iFAPAR (i.e. 250 m versus 1000 m), the iNDVI was used instead in the correlation analysis with the independent variables, i.e. precipitation, the distance between the AG and the Sennar Reservoir and soil characteristics.

5.2.3.4. Field survey

Taking into consideration the large area of the scheme (0.88×10^6 ha), conducting a field survey for the whole scheme to collect data on crop yield, socio-economic conditions of farmers and field practices was not feasible within the scope of this research. Based on the general pattern of productivity, which varies from south to north across the scheme (Al Zayed et. al., 2015), five blocks that reflect this spatial variation were selected for the interviews. The selected blocks (Fig. 5.1) were North West (NW) Sennar and Haj Abdallah (southern region), Noor Al-Huda and Hamdnallah (central region) and Miallig (northern region). A total of 393 farmers – distributed in the five selected blocks – were randomly selected for the interviews, while ensuring the variations in the socio-economic status of the farmers and the geographical distribution between the farms (See Appendix D: Section S5.4). Most of the respondent farmers (two-thirds) had completed only primary education and were aged 40–60. Around half of the respondents had only one source of income derived from in-farm activities. The other portion of the farmers also had off-farm income, including governmental or private jobs, next to their in-farm jobs. Some researchers argue that farmers who have other off-farm sources of income

have relatively better economic status than those who are dependent only on in-farm income (BIRTHAL et. al., 2014; IbrahIM et. al., 2013).

The field survey took place during the period from December 2017 to February 2018. The interview questions were designed based on consultation with 27 experts from the fields of agriculture and water resources management in Sudan. These questions focused on the most important factors affecting the sorghum yield in the Gezira Irrigation Scheme. A list of the types of data collected during the interviews with farmers is presented in Table 5.1. The interview questions were tested first on a small sample of five farmers to check their comprehension of the questions and to estimate the average time needed for each interview. Consequently, the interview questions were modified before conducting the final, longer interviews.

5.2.3.5. Statistical analysis

Spearman's rho (ρ) was used in this investigation to measure the strength of the correlation between iNDVI/sorghum yield and the influential factors. Correlation between the average sorghum yield with the individual socio-economic and field practices factors was performed using regression-tree modeling (Breiman et. al., 1984). Regression-tree models have been found to be informative and more appropriate for detecting the relationship and interaction between the variables in such analyses compared to the traditional linear regression (Lobell et. al., 2005).

5.3. Results

5.3.1. Spatio-temporal variation of the productivity gap

Although the two satellite-based vegetation indices, i.e. iNDVI and iFAPAR, exhibit similar spatial and temporal variation of vegetation productivity across the Gezira Irrigation Scheme, the results of the F-test (not shown) indicate a significant difference between the two population variances. Based on the SVI values, the AG categories obtained according to their productivity levels are given in Table 5.3. The classification of the AGs based on the iNDVI- and iFAPAR-derived SVIs are comparable. While the best performing AGs are Shawal (iNDVI SVI = 0.98) and Hosh (iFAPAR SVI = 0.97), the worst AG is North West, showing iNDVI SVI = 0.05 and iFAPAR SVI = 0.03. On the scheme-wide scale, a large spatial and temporal variation in the productivity gap is detected. Spatially, the northern part of the scheme shows a higher gap level compared to the southern, central and western parts (Fig. 5.3). The average productivity gap over the Gezira Irrigation Scheme for the period 2001–2016 is around 32% and 24%, with a standard deviation of 19.03 and 14.03, based on iNDVI and iFAPAR, respectively (Fig. 5.4). On the AG scale, the largest productivity gap is found in the northern AGs. In some locations

of the northern part of the scheme (e.g. North West AG), the productivity gap in some years (e.g. 2015) is more than 90%. Using iNDVI, West, Abu Gouta and North show the largest average gaps among all the AGs, i.e. with averages of 40%, 37% and 35%, respectively (Fig. 5.5a). The same AGs exhibit the largest gaps using iFAPAR (Fig. 5.5b), but with a lower magnitude of 34%, 27% and 28%, respectively. Using iFAPAR systematically leads to lower productivity gap estimates as compared to iNDVI (Fig. 5.5c). Temporally, the years 2002 and 2015 show the largest productivity gaps, and this high gap is detected in most of the AGs. The lowest productivity gap is found for 2003, with scheme average gaps of 21% and 13% for iNDVI and iFAPAR, respectively (Fig. 5.5a and b).

The productivity gap varied strongly for the two successive years 2015 and 2016 (Figs. 5.3, 5.4 a and c). The results indicate an average gap for the scheme for these two years of 47% and 36%, respectively, using iNDVI and 32% and 17%, respectively, using iFAPAR. At the AG level, the productivity gaps estimated by iNDVI and iFAPAR show a highly significant correlation ($\rho = 0.93$, $P < 0.01$). Using iNDVI for the year 2015, Tahameed and Abu Gouta exhibit the highest gaps among the AGs, with averages of 56% and 51%, respectively, while for 2016, there is a noticeable reduction in the productivity gaps to 34% and 30%, respectively (Fig. 5.5a and b).

Table 5.3. Classification of the administrative groups (AGs) of the Gezira based on the standardized vegetation index (SVI) derived from z-scores of iNDVI and iFAPAR. SVI classes are obtained from Peters et. al. (2002).

Administrative group (AG)	SVI class using iNDVI		SVI class using iFAPAR		SVI classes		
	SVI	Class	SVI	Class	From	To	SVI Class
Abu Guta	0.16	Poor	0.11	Poor	0	0.05	Very poor
Center	0.86	Good	0.95	Good	0.05	0.25	Poor
Gamusi	0.67	Average	0.40	Average	0.25	0.75	Average
Hosh	0.84	Good	0.97	Very good	0.75	0.95	Good
Huda	0.24	Poor	0.25	Average	0.95	1	Very good
Mansi	0.80	Good	0.94	Good			
Masallamia	0.44	Average	0.60	Average			
Ma'toug	0.89	Good	0.49	Average			
Matouri	0.66	Average	0.81	Good			
Mikashfi	0.71	Average	0.58	Average			
North	0.18	Poor	0.30	Average			
North West	0.05	Poor	0.03	Very poor			
Shawal	0.98	Very good	0.58	Average			
South	0.32	Average	0.55	Average			
Tahameed	0.36	Average	0.43	Average			
Wad Habouba	0.12	Poor	0.16	Poor			
Wad Sha'eer	0.13	Poor	0.17	Poor			

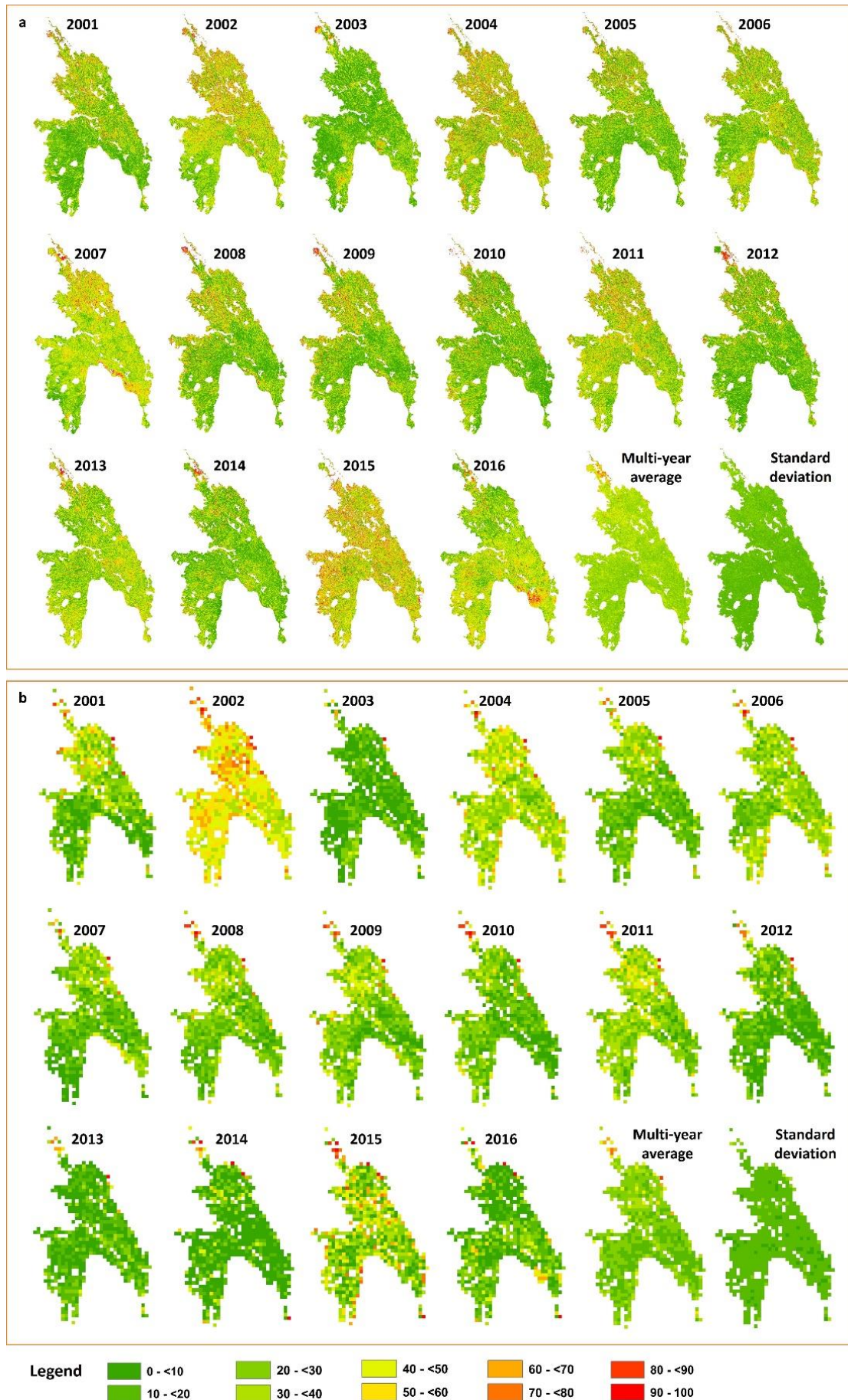


Fig. 5.3. Spatial productivity gap for the Gezira Scheme based on (a) iNDVI and (b) iFAPAR.

Based on the results of the standardized iNDVI discussed above, the five blocks selected for field surveys are located within AGs of poor, average and good productivity (Table 5.3). Thus, these five blocks have the potential to reflect the spatial variation in productivity. As shown in Fig. 5.6, the results of the farmers’ responses for the blocks located in the southern and central parts of the scheme, i.e. North West Sennar, Haj Abdalla and Hamadnalla, show a higher average yield of sorghum than for the northern part (Mialig block). Considering the five blocks where ground surveys were taken, the average yield of sorghum in the summer season of 2017/18 is 431 kg/ha. This average sorghum yield is significantly lower than the yield reported by Bashir et. al., (2015) in experimental controlled plots in Gezira; they reported a yield of 2000–4000 kg/ha in the seasons of 1998/1999.

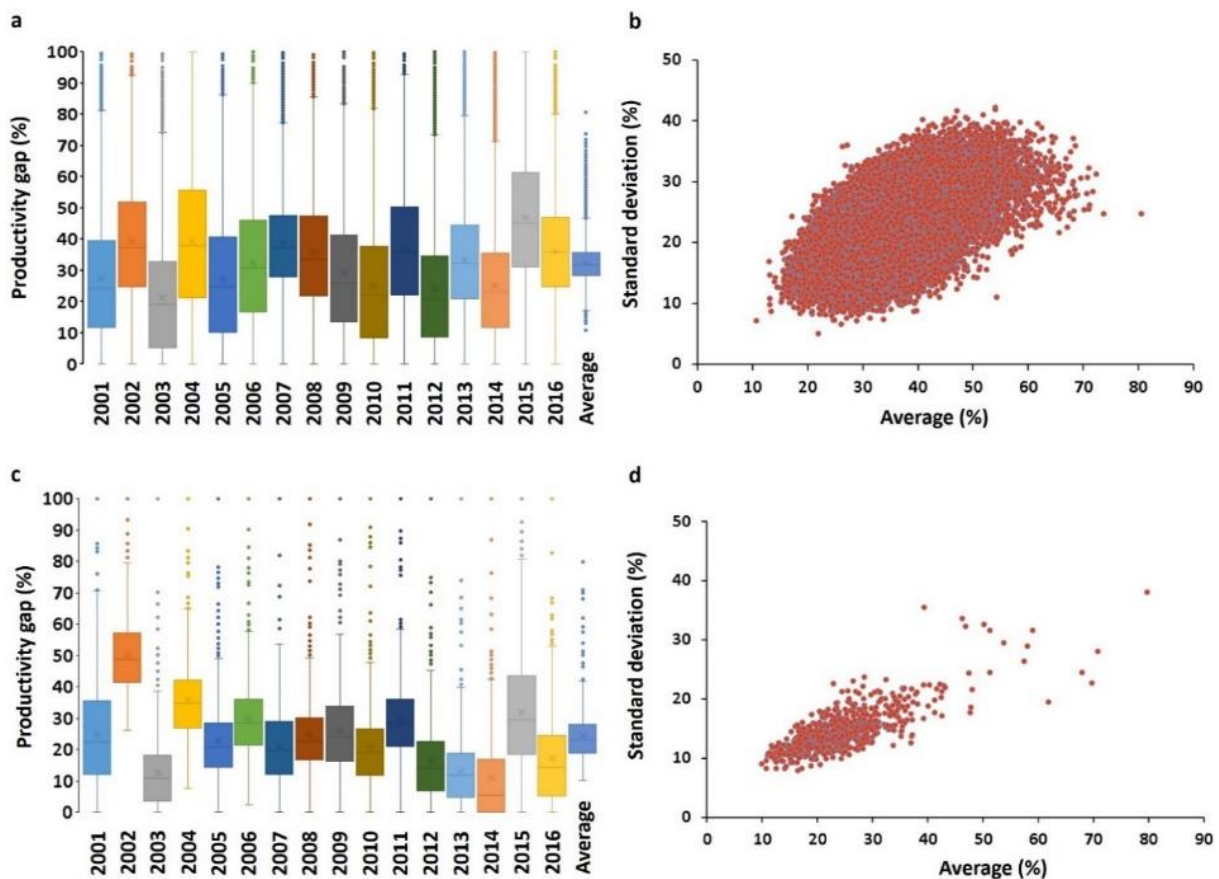


Fig. 5.4. Statistical measures of pixel-to-pixel productivity gap based on iNDVI (a and b) and iFAPAR (c and d) represented by the Box-Whisker plot.

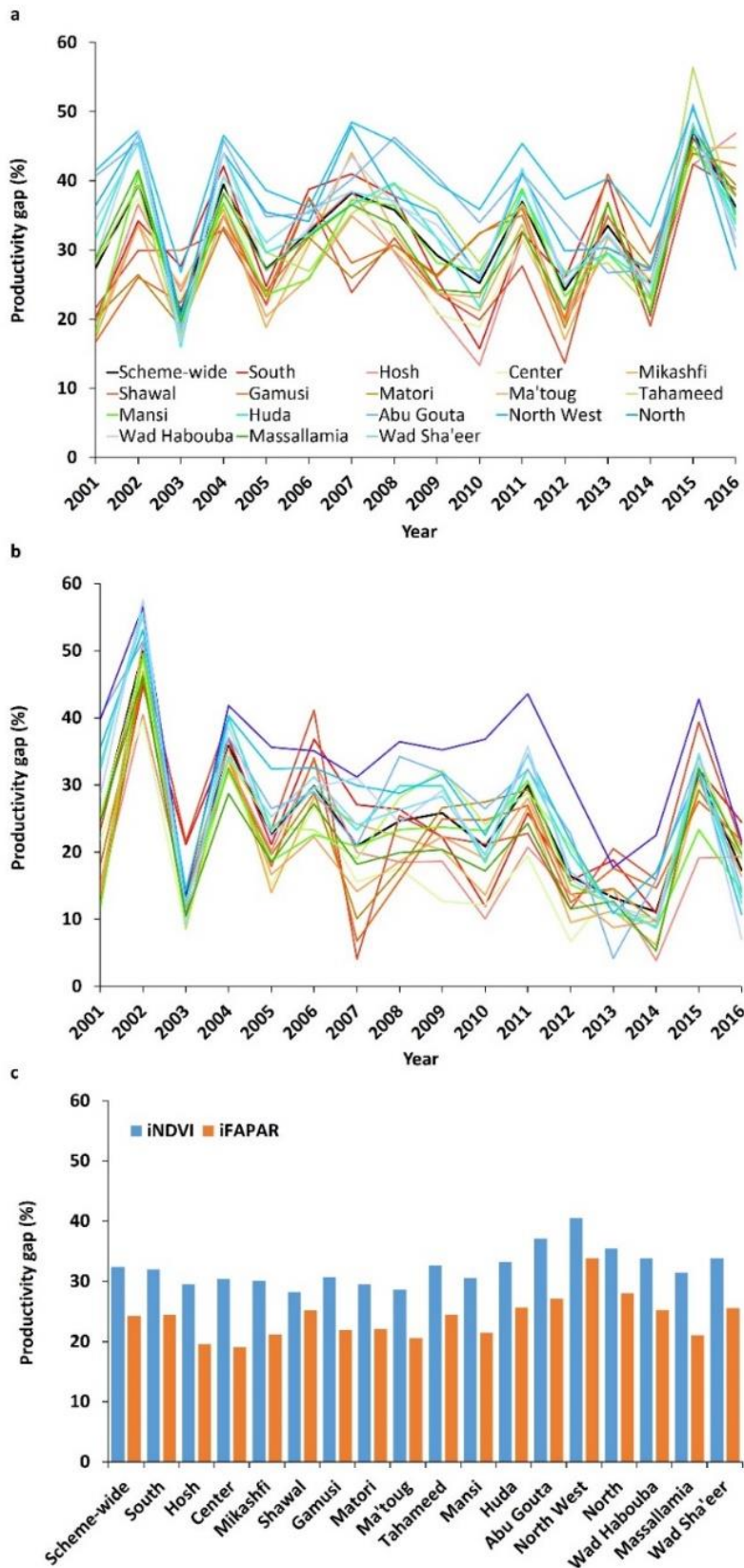


Fig. 5.5. Average productivity gap for the Gezira Scheme and the administrative groups: (a) time series based on iNDVI, (b) time series based on iFAPAR and (c) multi-year average over 2001-2016. The line colors in (a) and (b) correspond to the colors used for the administrative groups in Figure 5.1.

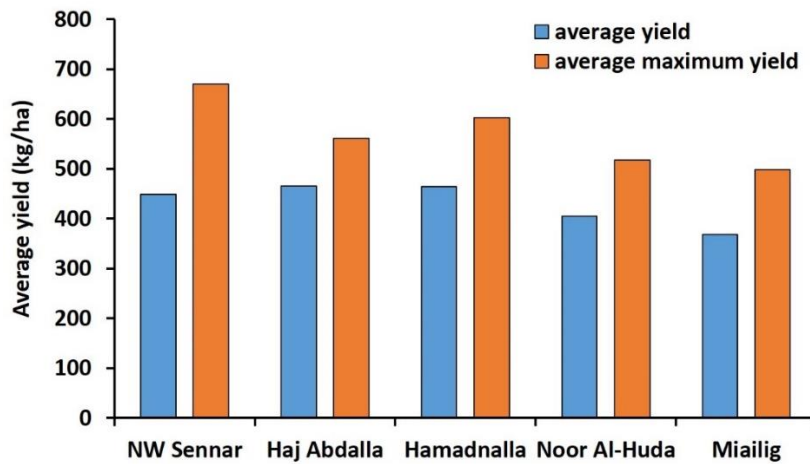


Fig. 5.6. Average yield and maximum yield of sorghum achieved by all respondent farmers in each block selected for the field survey.

5.3.2. Factors controlling productivity in the scheme

5.3.2.1. Physical factors

A negative correlation of the average iNDVI and the distance from the center of the AG to the source of water supply, i.e. Sennar Reservoir, is detected (Fig. 5.7). The sorghum yield in the selected field survey sites is found to be negatively correlated with the location of the farmland along a tertiary canal (scheme-wide: -0.56 , $p < 0.01$ and AG-wide: $\rho = -0.36$ to -0.598 , $p < 0.01$). Water shortage at the end stage of sorghum development, i.e. after mid-September, is striking in the Gezira Irrigation Scheme. Farms located at the head of the tertiary canals have the advantage of better access to water as compared to the farms located at the tails of these canals. The latter are either left without water or face water shortages. In view of the farmers' responses, the overall average sorghum yield of all farms located at the head of the tertiary canals is higher than that for farms located at the tail, i.e. 504 kg/ha vs 328 kg/ha. Detailed analysis of the location along the tertiary canals revealed a correlation with other irrigation-related factors, namely the frequency of irrigation and the sowing date.

Although the Gezira Irrigation Scheme receives a substantial amount of precipitation, this quantity is not fully accounted for in scheduling irrigation for the scheme (Al Zayed et. al., 2016). The analysis of annual precipitation data shows that the highest iNDVI and iFAPAR occur during wet years (e.g. 2014), whereas dry years, such as 2002, 2004 and 2015, show the lowest iNDVI and iFAPAR (Fig. 5.4a and c). The years 2015 and 2016, taken as examples with below- and above-average precipitation (Fig. 5.8a), respectively, according to Elagib (2015) show higher rainfall in the southern AGs than in the northern ones (Fig. 5.8b), and similarly in the southern AGs than in the northern ones (Fig. 5.8b). Whereas total precipitation of only 42.8

mm was received during June and July 2015, a larger amount of 145.5 mm was recorded during the same period in 2016 (Fig. 5.8c and d). Analysis of the water supply data at the beginning of the season shows that the water released from Sennar Reservoir remained almost the same during the two years. Productivity was also higher for the year 2016. Using the yearly data over 2001–2016, the correlation of the time series of iNDVI and precipitation reveals a ρ value of 0.48 ($p < 0.01$), as shown in Figure (5.9a). A relatively higher correlation with ρ of 0.61 ($p < 0.01$) is obtained when the multi-year average is considered (Fig. 5.9b).

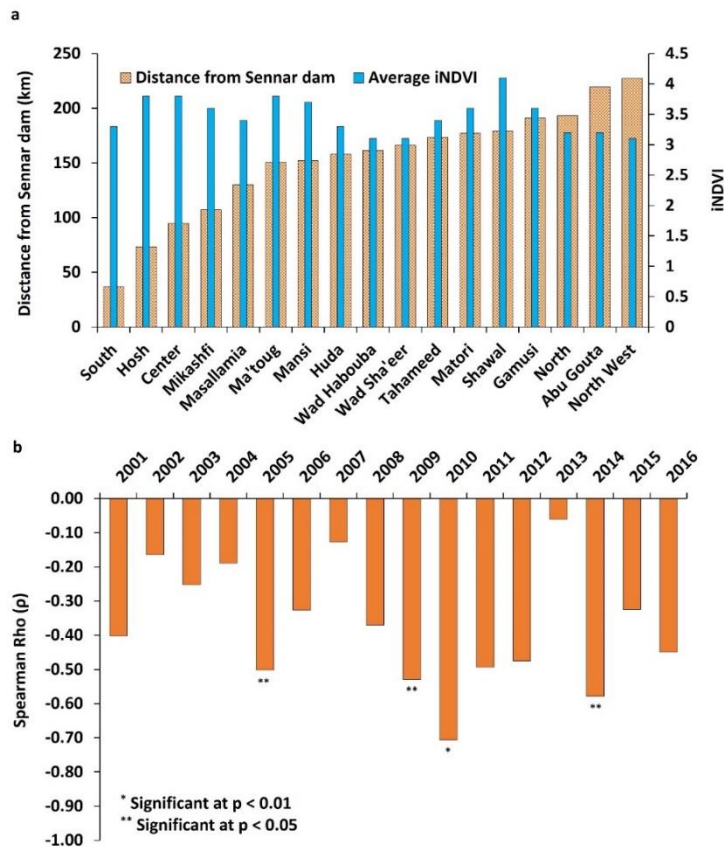


Fig. 5.7. Dependence of crop productivity index (iNDVI) on the average distance of the administrative groups of the Gezira Scheme to Sennar Reservoir: (a) average seasonal iNDVI (2001–2016) and distance for each administrative group and (b) Spearman’s Rho of the correlation between the two variables.

The spatial distribution of soil properties (pH, OCC and bulk density) in the Gezira Irrigation Scheme exhibits large variation (Fig. 5.10). The pH values indicate that alkaline soils ($pH > 7$) are dominant in the scheme. While soils with the highest alkalinity (up to 9.8) and large bulk density characterize the northern part of the scheme, the highest OCC values are found in the central AGs. A negative correlation between iNDVI and pH and bulk density can be found whereas a positive correlation can be detected between iNDVI and OCC (Fig. 5.11 a–c)). A significant correlation between iNDVI and the three soil properties is found for most of the year-to-year investigations (Fig. 5.11 d–f).

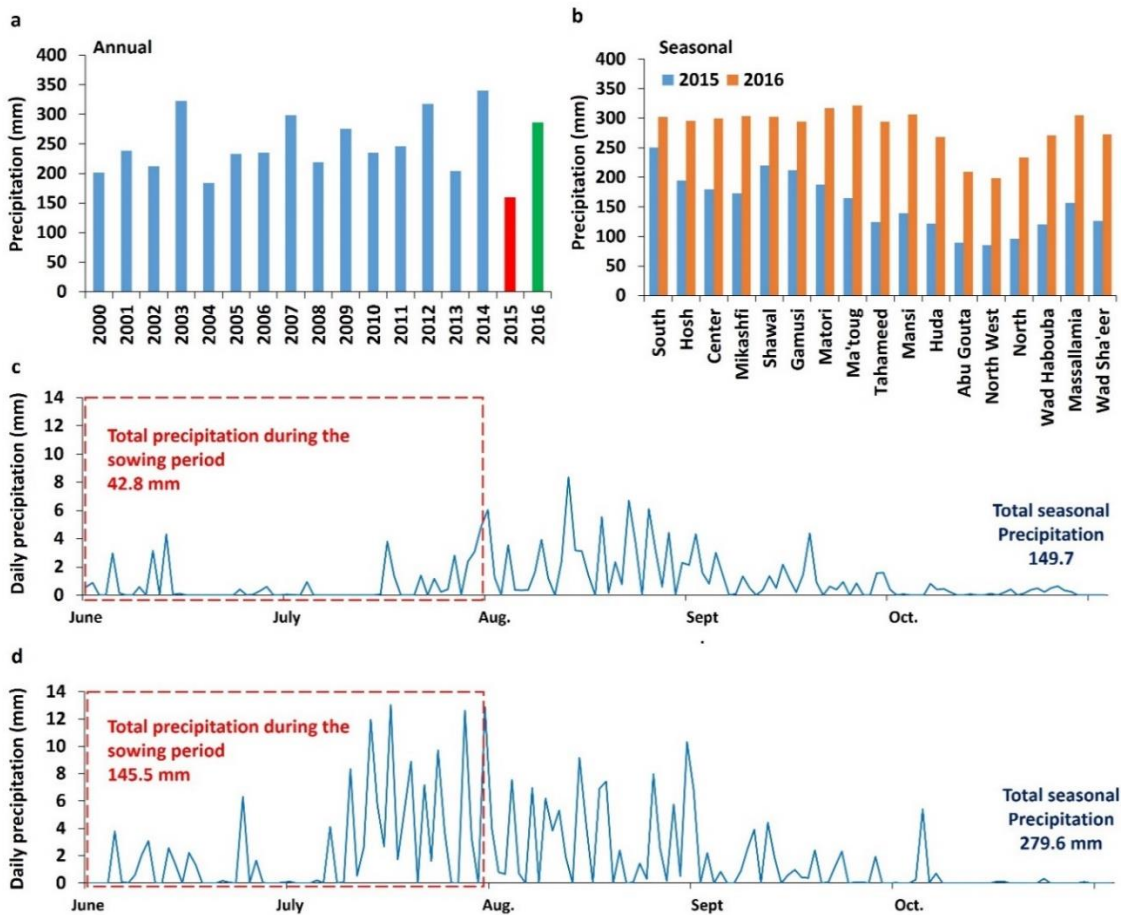


Fig. 5.8. Areal average precipitation using CHIRPS 2.0 precipitation product: (a) over the Gezira Scheme for the years 2000–2016; (b) over the different administrative groups during 2015 and 2016; (c and d) daily precipitation over the scheme during the summer seasons of 2015 and 2016, respectively.

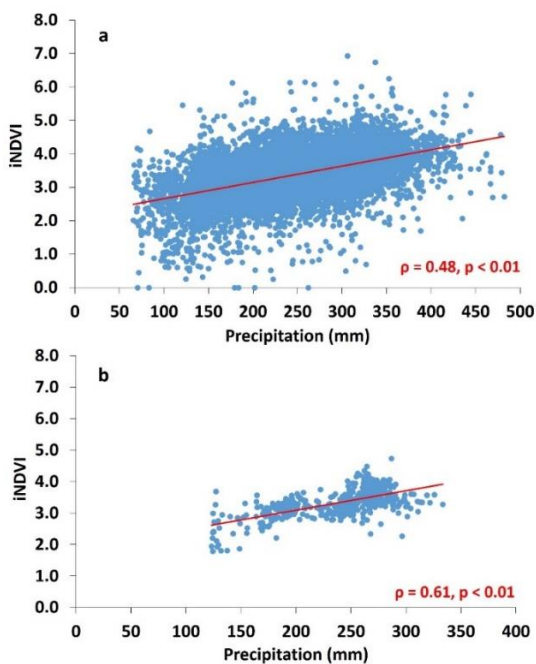


Fig. 5.9. Scatter plot of pixel iNDVI versus total seasonal precipitation: (a) for all years (2001–2016) and (b) multi-year average over the Gezira Scheme.

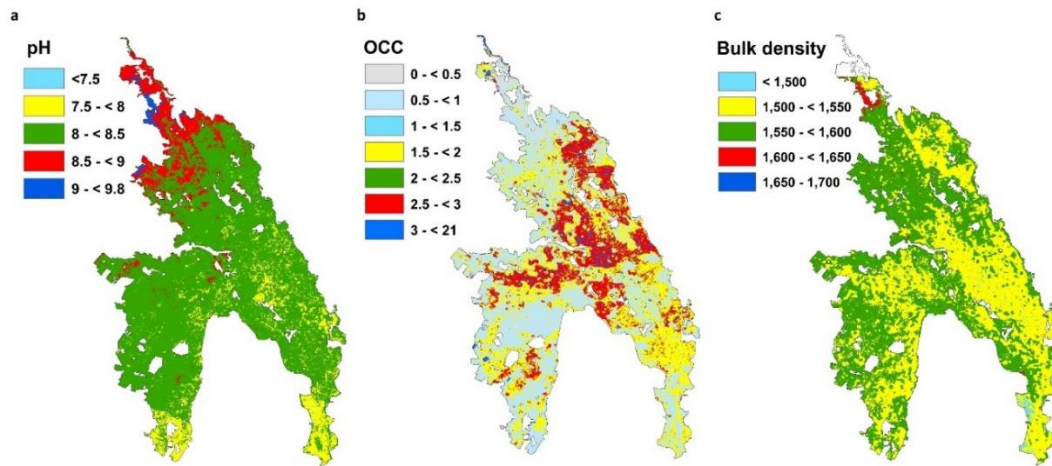


Fig. 5.10. Spatial distribution of soil properties: (a) pH, (b) organic carbon content (OCC) and (c) bulk density clipped from the original SoilGrids data to the boundaries of the Gezira Scheme. The units of OCC and bulk density are g/kg and g/m³, respectively.

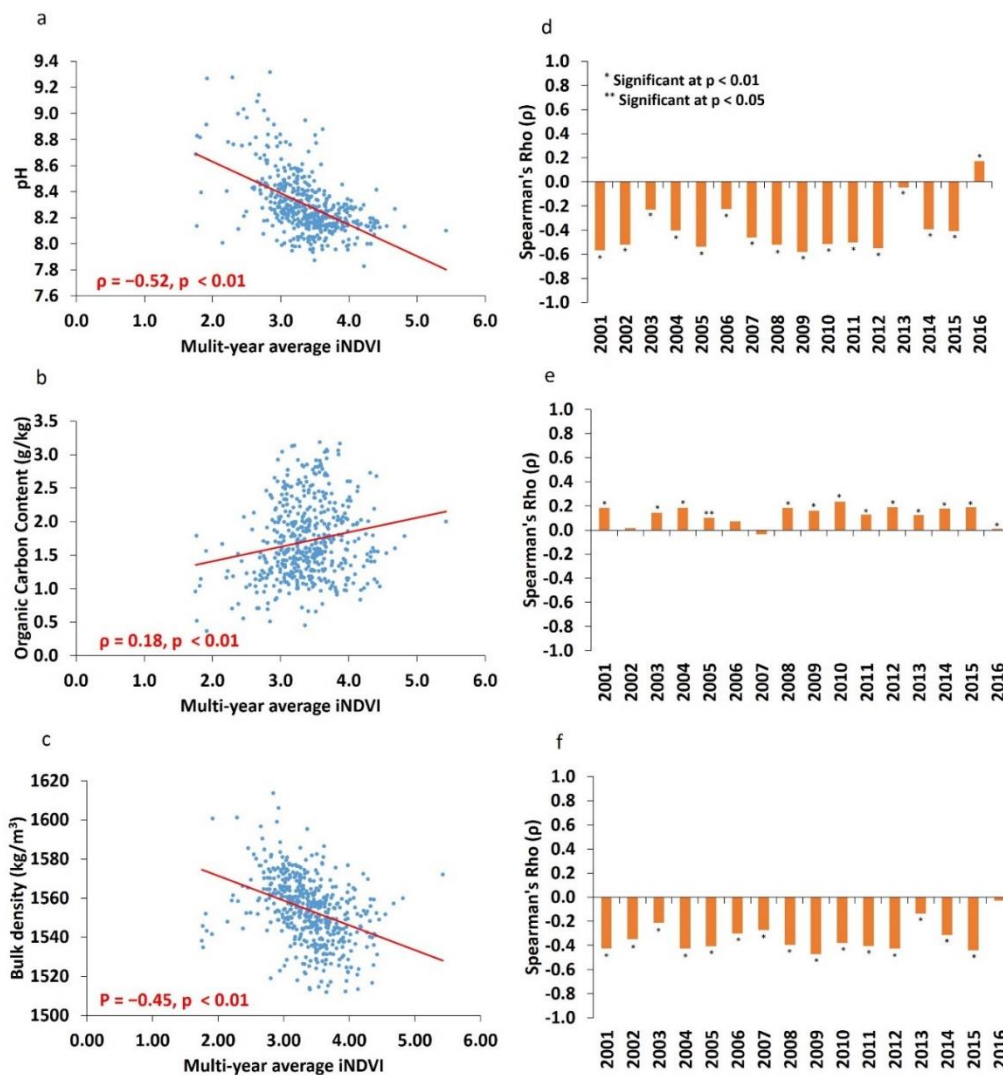


Fig. 5.11. Pixel-to-pixel correlation between multi-year (2001–2017) average iNDVI and three soil properties: (a) pH, (b) Organic Carbon Content and (c) bulk density. Spearman's Rho values of the correlation for each year are shown in d, e, and f for the three soil properties, respectively.

5.3.2.2. Socio-economic factors

The analysis of the field survey data collected from the five selected blocks shows that many socio-economic factors are correlated with the sorghum yield. On a scheme-wide level, there is a strong positive correlation between the average sorghum yield and the source of income of the respondent farmers ($\rho = 0.62$, $p < 0.01$). At the block-wide level, the correlation coefficient ranges from 0.48 to 0.69. Furthermore, a positive correlation is detected between sorghum yield and the number of household members ($\rho = 0.12$, $p < 0.05$) and the farm size ($\rho = 0.16$, $p < 0.01$).

5.3.2.3. Management and field practices

It is found in this study that the sorghum yield is controlled by several management factors and field practices. The correlation between the sorghum yield and timing of land preparation is significantly negative ($\rho = -0.22$, $p < 0.01$). In many cases, the results of the interviews show that farmers who start their preparation in June are able to achieve a relatively higher yield of sorghum (474.8 kg/ha on average) than those who prepare their fields later (412.6 kg/ha on average).

Statistical analysis of the collected data on the sowing date and average yield shows a significant negative correlation ($\rho = -0.22$, $p < 0.01$) between the two variables. Ideally, the first irrigation is usually conducted immediately after seeding. However, some of the respondent farmers delay the first irrigation to as long as two weeks, mainly due to the unavailability of water in the irrigation canals. This delay, in turn, has a negative impact on the sorghum yield; thus, delayed timing of the first irrigation is found to reduce the sorghum yield ($\rho = -0.16$, $p < 0.01$). This result is in line with the finding of Elagib (2015). The scheme-wide correlation between the sorghum yield and frequency and quantity of fertilization is positive ($\rho = 0.40$, $p < 0.01$ and $\rho = 0.47$, $p < 0.01$, respectively).

Regression-tree modeling of all the field survey data on the scheme-wide scale revealed two most influential factors to the sorghum yield during the summer season of 2017/18 to be the source of income (as a proxy for financial condition) and the location of the farm along the tertiary canal (Fig. 5.12).

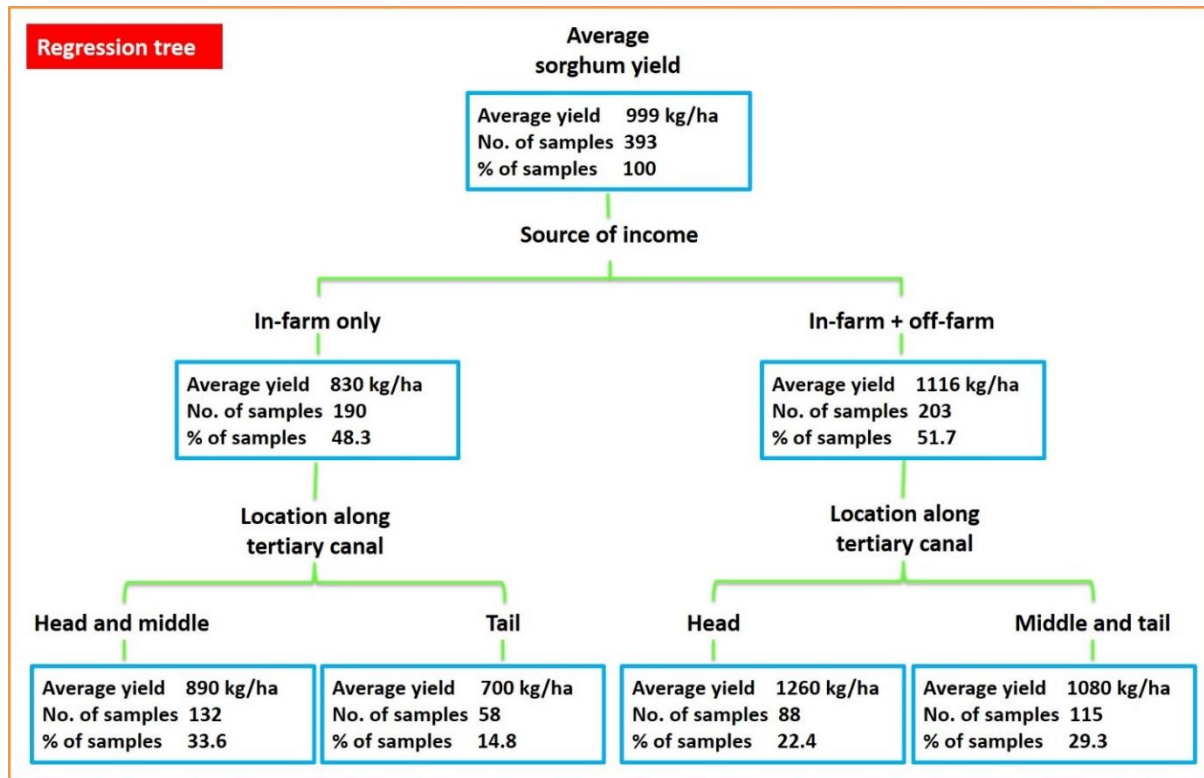


Fig. 5.12. Regression-tree detecting the most important factors that control the average sorghum yield in the Gezira Scheme.

5.4. Discussion

5.4.1. Satellite-based productivity gap

The correlation between the two vegetation indices, iNDVI and iFAPAR, indicates that the two indices are independent (See Appendix D: Section S5.2). The difference in the results of the two vegetation indices in estimating the productivity gap can be attributed mainly to differences in the characteristics of the NDVI and FAPAR data, especially in the spatial resolution. Therefore, one would assume that the higher resolution of NDVI data makes the corresponding result on the productivity gap more accurate for spatial analysis than those estimated using FAPAR, which has a coarser resolution.

The noticeable variation in SVI across the northern and southern AGs is in line with the earlier findings by Al Zayed et. al. (2015) on the spatial variation of the Modified Vegetation Condition Index (MVCI) across the scheme. These results further support the correctness of the selection of AGs, which aimed to represent a wide-range of AG performance. Moreover, the wide productivity gap indicates a large potential to increase crop productivity in the scheme.

Given the large spatial resolution of the pixels for the two different products (NDVI and FAPAR), different crops may exist within each pixel. Correlation of sorghum yield with iNDVI and iFAPAR at the AG level reveals no significant correlation. This lack of correlation is mainly due to the mismatch in spatial scale between the remote sensing and the reported yield data. Based upon our local knowledge and field surveys, we inspected iNDVI and iFAPAR values for some known sorghum fields scattered across the scheme. The variation in productivity of these fields reflects the scheme's low and high productivity in 2015 and 2016, respectively. While the cultivated area of sorghum remained almost the same, the yield of sorghum varied between the two years. These observations suggest that sorghum is the dominant crop and, thus, the variation in its yield can be considered as the largest driver of the productivity gap at the AG level for the summer seasons of 2015 and 2016 (See Appendix D: Section S5.3).

5.4.2. Yield gap of sorghum

Taking into account the experimental sorghum yield that was achieved by Bashir et. al. (2015) in the Gezira Irrigation Scheme (as referred to in Section 5.3.1), one can infer that the maximum achieved yield found herein is much lower than the potential yield of sorghum. This indicates further that the gap in sorghum yield is much higher (at least 3 times more) than the yield gap estimated by considering the farmer's maximum achieved yield. This result suggests that, based on the average yield estimated in the current investigation, the yield gap of sorghum in the Gezira Irrigation Scheme may reach 78–89% when a potential yield of 2000–4000 kg/ha is considered. However, estimating the yield gap based on the maximum yield that is achieved by the farmers seems more realistic, considering the actual spatio-temporal differences in the environmental (e.g. climate), socio-economic status (e.g. level of income) and field management practices (e.g. sowing date and fertilization). The yield gap of sorghum reported in the present analysis provides field-based evidence in support of the productivity gap identified from the satellite-based vegetation indices.

5.4.3. Factors influencing agricultural productivity

The significant correlation between iNDVI/sorghum yield and some physical, socio-economic and management factors in the Gezira Irrigation Scheme indicates that many agents are playing a role in the detected variation of sorghum yield in the scheme. The interdependence between many of the studied factors (See Appendix D: Fig. S5.10) indicates that addressing one of them might have impacts on the others. The negative correlation between the vegetation productivity and the distance from water source confirms an uneven distribution of water across the scheme and between the upstream and downstream AGs, as noted by previous studies (e.g.

Al Zayed and Elagib, 2017; Al Zayed et. al., 2015, 2016; Woldegebriel et. al., 2012; Bashir et. al., 2011). It also indicates inequality in access to water among the farmlands that share the same tertiary canal. Multiple factors contribute to this inequality in access to irrigation water, including weed growth and sedimentation in the irrigation canals, improper maintenance and collapse of many of the irrigation control systems, and the fragmentation of authorities responsible for regulating the water distribution (Woldegebriel et. al., 2012). In this regard, the significant correlation between precipitation and iNDVI, as reported herein, stresses the role precipitation could play in determining productivity if accounted for in the irrigation scheduling (Al Zayed et. al., 2015). The correlations between iNDVI and some soil properties, i.e. pH, OCC and bulk density, and between sorghum yield and the number and quantity of fertilizer applications emphasize the importance of soil properties in determining spatial variations in productivity in the scheme. These results suggest that measures towards ameliorating the soil characteristics, especially in the northern part of the scheme, could help increase productivity and, thereby, bridge the productivity gap. The use of organic manure and chemical fertilizers may enhance soil properties by enriching the OCC and mineral content of the soil and adjusting the pH, all of which could increase the crop yield (Ge et. al., 2018; Dong et. al., 2012; Holloway et. al., 2001).

The significant correlation between sorghum yield and several socio-economic and management factors indicates that these factors are as important as physical factors in determining the sorghum yield. For instance, the role of a farmer's financial status in the determination of the sorghum yield in the Gezira Irrigation Scheme is remarkable (Fig. 5.12). Farmers with multiple financial sources, i.e. in-farm and off-farm, generate more income and are, therefore, able to invest in adequate agricultural inputs (machinery, enhanced seed varieties, and fertilizers), which enhance the sorghum yield. Furthermore, the positive correlation between sorghum yield and the number of household members indicates that bigger families are more productive due to the larger labor force, and can generate higher total income, which helps with more farming investments. This finding is in line with the results found by Hassan (2015) in Darfur, Western Sudan.

Field practices and agricultural management also contribute to the variation in the sorghum yield in the Gezira Irrigation Scheme. In particular, weed growth is considered one of the main factors resulting in the drop in sorghum yield (Peerzada et. al., 2017). Pre-sowing watering is one of the important strategies to constrain the growth of weeds during the season (Oshunsanya, 2013; Erkossa et. al., 2006). However, due to the unavailability of water for irrigation during

the period from March to May, pre-sowing watering of the fields is not practiced in the Gezira. Apparently, the location of the farm along a tertiary canal governs the access to water, thus greatly affecting the crop yield. Ishag et. al. (2007) found a similar effect of farm location along tertiary canals on the yields of cotton and wheat in some locations in the Gezira Irrigation Scheme.

In this research, a significant correlation has been found between the sowing date and average yield. Such a result confirms earlier findings by Ishag et. al. (2007) regarding the association of early sowing (mid-July or earlier) with higher sorghum yield. Although water availability plays a crucial role in determining the sowing date, many non-physical factors, such as availability of seeds, fertilizers, and machinery, force farmers to postpone the sowing dates (Bussmann et. al., 2016). The scheme-wide correlation between sorghum yield and the frequency and quantity of fertilization emphasizes the role of soil management in increasing the yield.

5.5. Conclusion

Based on our analysis, several entry points for SI in the Gezira Irrigation Scheme could be identified. These entry points could be grouped into three main categories, as suggested by Schut et. al. (2016) but adapted to the situation in the Gezira Irrigation Scheme: (1) agricultural productivity, (2) natural resources management, and (3) institutional measures. The main aim of the SI measures included in these entry points is to bridge the crop yield gap, which consequently promotes a healthy environment, improved livelihood for the farmers and a growing economy (Fig. 5.13). Positive impacts on the environment, society, and the economy can feedback to SI measures. For instance, the expected positive impact of increasing crop yield on the farmer's income constitutes additional revenues that could be used to enhance both their livelihood and that of their families and the farming conditions in terms of machinery, fertilizers and simple in situ rainwater harvesting techniques. Policies promoting SI should take into consideration the impact on the environment. For example, an adequate level of fertilization is believed to help overcome the problem of unfavorable soil properties in some areas within the scheme. Nevertheless, it is imperative that appropriate levels of fertilizers that are safe for water resources be used, thus emphasizing the important role of authorities in monitoring and enforcing relevant regulations. Since sustainability rests on three pillars: the environment, the economy and the social dimensions (Barbier, 2013), SI has to address these dimensions and may not be limited in scope to increasing the food production and minimizing the negative environmental impacts (Kotu et. al., 2017; Schut et. al., 2016; Robinson et. al., 2015).

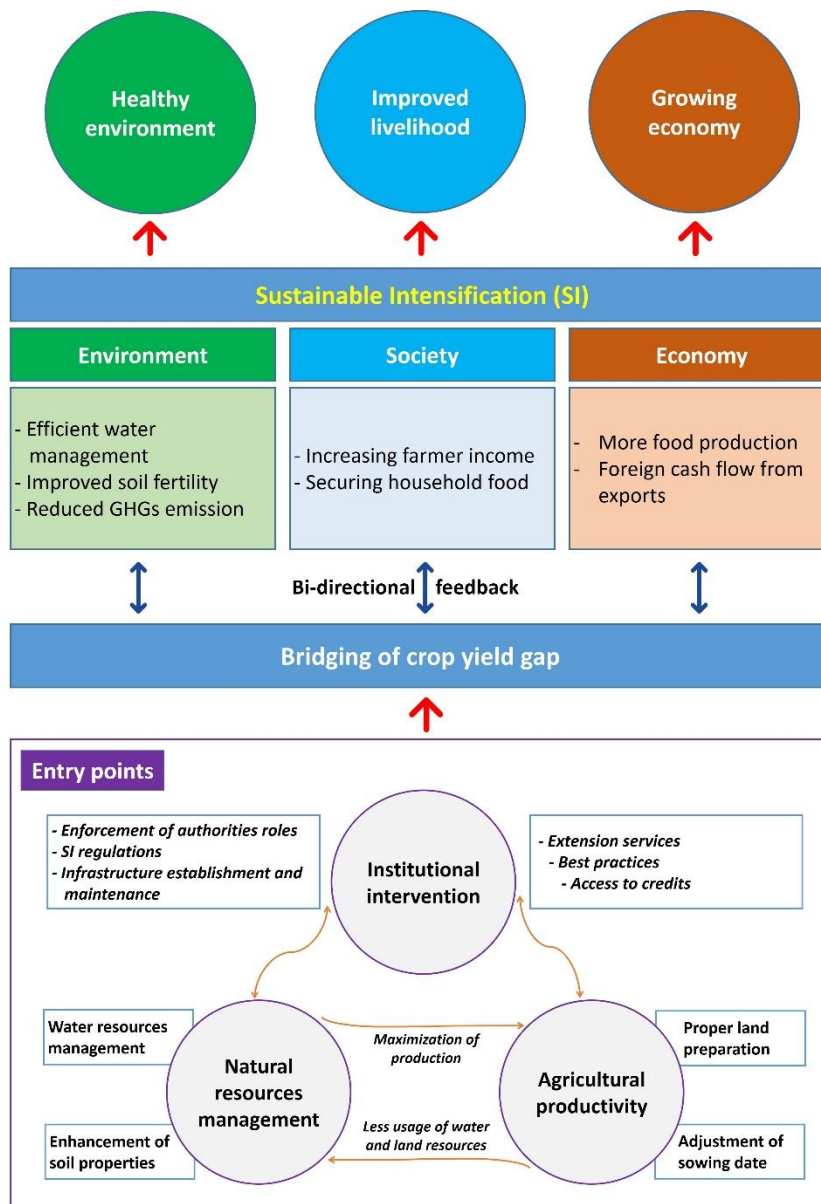


Fig. 5.13. A conceptual framework for sustainable intensification in the Gezira Scheme showing the identified entry points and their proposed measures.

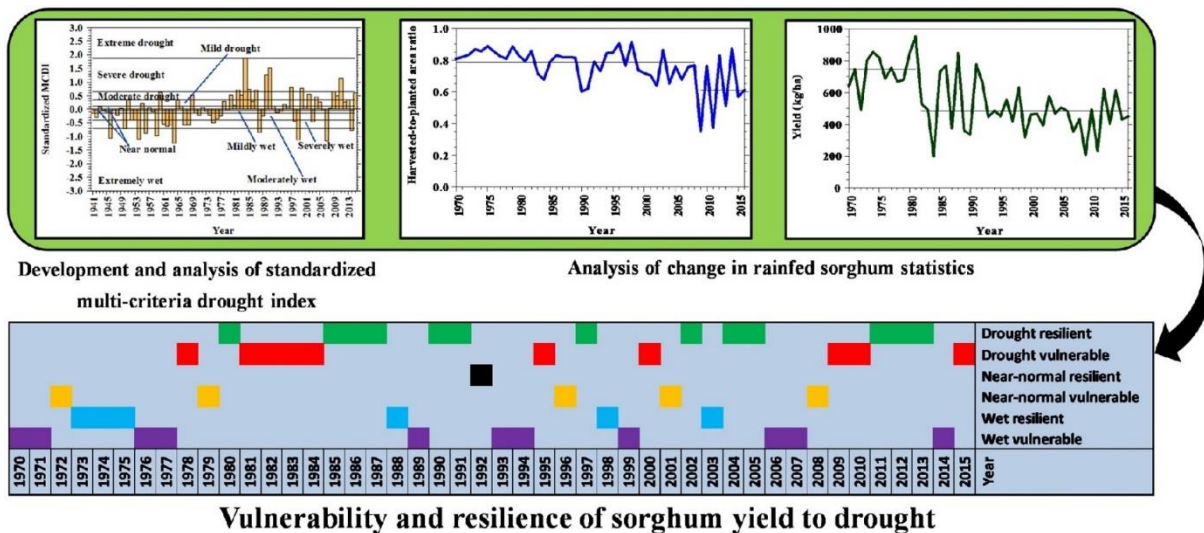
It also has to integrate social and economic systems (Loos et al. 2014). Therefore, it is important to recognize that any particular practice or measure of SI cannot succeed in isolation but only in consideration of the whole system (Thompson, 2007). Such an integrative approach enables discovering synergies and trade-offs of the human–water–food–climate nexus which, in turn, helps to identify feedback mechanisms between measures for agriculture intensification and the sustainability pillars.

Despite the obvious consequences of implementing SI policies in the Gezira Irrigation Scheme for more than 100000 farmers across the scheme and their families and the benefits that could be gained for Sudan, it has several implications beyond the borders of the country. Firstly, as stated by Elagib et. al. (2019), with an area of nearly 12% of the global harvested

area of sorghum, Sudan produces only 5.4% of the total global sorghum production. Thus, bridging the yield gap in the agricultural schemes in Sudan would provide a good contribution to the global sorghum production without depleting additional natural resources (e.g. water and land). As the yield gap is a common phenomenon that is widespread among crops around the world, the methodological approach followed herein, and the interactions highlighted between the different controlling factors will help address the challenge of full utilization of hidden potentials in such underperforming agricultural schemes. As already mentioned, this scheme alone consumes around one-third of the total share of Sudan from the Nile water and around 8% of the historical average Nile flow (84 km³: Sutcliffe and Parks, 1999), as measured at Aswan Dam in Egypt. Al Zayed et. al. (2015) detected both a low and a decreasing trend in irrigation efficiency since 1993/94 in the Gezira Irrigation Scheme. This low efficiency suggests the need for water saving in the scheme. In particular, oversupply and leakage of water from the irrigation canals need to be quantified and reduced or eliminated. Attempting to improve the irrigation efficiency in the Gezira Irrigation Scheme may have its positive implications on balancing supply and demand in the Eastern Nile basin. Lastly, the lessons learned from the Gezira Irrigation Scheme case towards implementing SI could be transferred to similar underperforming irrigation schemes around the world, to contribute to enhancing global water and food securities.

Chapter 6

Crop vulnerability and resilience to climate in rainfed schemes



Based on:

Elagib, N.A., **Khalifa, M.**, Rahma, A.E., Babker, Z., Gamaledin, S.I., 2019. Performance of major mechanized rainfed agricultural production in Sudan: Sorghum vulnerability and resilience to climate since 1970. *Agriculture and Forest Meteorology*, 276–277, 107640.

Abstract

Food security in the African Sahel has frequently been threatened by climate variability and change. A large part of the farming system in the arid and semi-arid region of Sudan is heavily rainfed, with sorghum representing the major crop. This study sheds light on the performance of sorghum production in the major mechanized sector in Sudan since 1970. Despite a significant extensification of the mechanized cultivated area of sorghum, a drastic loss of area at harvest took place during 1970-2016. The sorghum production showed both increases and decreases in the average over time besides high year-to-year variability. Synchronous with the above findings, a significant steady decline of sorghum yield occurred from the 1970s level (744.3 kg/ha) to 476.6 kg/ha since 1982. Based on the ratio of growing season precipitation to reference evapotranspiration, a Standardized Multi-Criteria Drought Index (SMCDI) for the period 1941-2015 was introduced using three drought characteristics, namely drought severity, dry spell and time relative frequency of drought. There occurred 23 mild to extreme droughts and 17 mild to extreme wet cases over the period 1970-2015. Aggregation of the SMCDI with “climatic” sorghum yield revealed highly variable performance of this crop. Accordingly, 26 vulnerable and 20 resilient sorghum yield years were discernible under drought, near normal or wet conditions due to a combination of factors not only climate, i.e. physio-geographic, socio-economic and institutional factors. Apart from the regional analysis, one representative state was also selected for further in-depth spatio-temporal assessment of the SMCDI, integrated Normalized Difference Vegetation Index (iNDVI), Modified Vegetation Condition Index (MVCI), sorghum yield, precipitation, and reference evapotranspiration data over the period 2001-2014. The results also underscored the spatio-temporal and local-scale vulnerability of the farming system under study to climate variability. Such findings urge for interventions in the mechanized rainfed sorghum farming system to enable improvement of its performance, drought vulnerability reduction, development of alternatives, and achievement of food security.

6.1. Introduction

By 2050, the world will need to increase the agricultural production by 60–110% to meet the increasing demand for food (Ray et al., 2013). Consequently, this will put more pressure on resources such as water, land, and energy. Increasing agricultural production will be one of the greatest challenges to face humanity in the near future (Godfray et al., 2010; Licker et al., 2010). Among the many dimensions of this challenge, water availability for food production has become most critical (Ferreles et al., 2011). If agricultural activities must grow substantially to

meet future demand for food of increasing populations while ensuring the sustainability of natural resources (e.g. water and land), agricultural expansion is not an option but rather strategies that consider, for instance, closing the yield gaps on underperforming lands and increasing the cropping efficiency are imperative (Foley et. al., 2011; Godfray et. al., 2010). Compared to the large increase in agricultural productivity in many parts of the world during the last decades, the level of agricultural production in many African countries is still low (Pretty et. al., 2011). According to a review conducted by Schmidhuber and Tubiello (2007) of the potential impacts of climate change on food security, poorest regions, such as sub-Saharan Africa, encounter, and will continue to encounter, dramatic fluctuation and reduction in food production and supplies (stability) as a result of climate fluctuations (droughts and floods). Realizing the impacts of climate change to date on food availability can avail the efforts made to anticipate future effects (Lobell et. al., 2011).

Rainfed agriculture plays a crucial role in the food supply in many regions around the world (Devendra, 2012; Rockstrom et. al., 2010; Lal, 2008). This farming system accounts for around 75% of the total global cropland area (Bradford et al., 2017), and will continue to play this essential role in food production in the future (Rockstrom et al., 2010). For instance, it is argued that more than 75% of future food security in the Nile Basin could be achieved through rainfed agriculture with supplementary irrigation (Siderius et. al., 2016). In many cases, however, rainfed systems across the world are characterized by lower crop yield levels compared to irrigated systems (Chapagain and Good, 2015; Elagib, 2014; Rockstrom et. al., 2010). This low yield is mainly due to the direct impact of climate on water availability (Valverde et. al., 2015; Elagib, 2014; Asseng and Pannell, 2013; Sultan et. al., 2013; Al-Bakri et. al., 2011). Mechanization of the farming activities has been introduced in the rainfed sector as a strategy to improve productivity. For instance, mechanization of farming is found to be the main source for increasing the efficiency of rice cultivation among smallholder farmers in Kenya (Mlengera et. al., 2015).

Sorghum is the fifth main cereal crop for millions of people around the globe (Iqbal et. al., 2010; Tuinstra, 2008). In many regions, sorghum is cultivated under rainfed systems, where the direct connection between crop growth and climate affects the sustainability of sorghum production and jeopardizes the food security for millions of people (Kukal and Irmak, 2018; Gebrekiros et. al., 2015; Sultan et. al., 2013; Chipanshi et. al., 2003; Rosenzweig et. al., 1995).

In view of the above background, there seems to be a fundamental need for understanding the performance of the rainfed sorghum system under different climate conditions. Analyzing

the statistics of rainfed sorghum would provide insights into the recent and current status of this important agricultural sector. Such an analysis will help in adopting adequate policies for the future.

Therefore, the objective of the current study is threefold: (1) to develop a Multi-Criteria Drought Index (MCDI) useful for assessing the drought state in the central and eastern parts of Sudan, taken as an example for intensive rainfed and mechanized agriculture, using station meteorological data, (2) to study the temporal resilience and vulnerability of mechanized sorghum cultivation under dry and wet years, using the developed MCDI and sorghum statistics measured on the ground, and (3) to examine the spatio-temporal state of agricultural productivity of the mechanized rainfed farming based on the MCDI and remotely-sensed vegetation indices for a case study. The ultimate goal of this research is to provide insights into the performance of sorghum cultivation in the mechanized rainfed system in Sudan and, therefore, to provide crucial knowledge to realize the opportunities and challenges for food security and sustainability of this system in the country. Previous studies carried out on rainfed sorghum farming in the study region include, among others, tillage practices and their impacts on sorghum yield (Willcocks and Twomlow, 1992), impacts of governmental policies on sorghum production (Elawad et. al., 2017), and factors determining the sowing date of sorghum (Bussmann et. al., 2016). Although these literature provide useful information about the major sorghum cultivation areas in Sudan, a comprehensive overview of the performance of this agricultural system is still lacking.

Sorghum is the main staple crop in Sudan, with at least 90% of the cultivated area is mainly under rainfed system (Elagib, 2014). To highlight the importance of the present investigation for Sudan, the status of sorghum production in general in Sudan is placed within the global production picture using the FAO (2018) sorghum statistics (harvested area, production, and yield) for several countries over the world. Among the top sorghum producing countries, Sudan is ranked third in terms of harvested area of sorghum, following India and Nigeria (Fig. 6.1a). However, with an area of 12% of the global harvested area of sorghum, Sudan is only producing 5.4% of the total global production on average. Despite the large harvested area of sorghum in Sudan, the low production ranks Sudan in the 7th place among the global sorghum producers (Fig. 6.1b). On average, with almost the same harvested area (Fig. 6.1a), the United States of America (USA) is producing fourfold the sorghum production in Sudan, and the yield level in the USA exceeds that in Sudan by more than 81% (Fig. 6.1c). The sorghum yield in the USA was highly improved due to the green revolution programs that started in the 1960s (Pingali,

2012). Comparison of the sorghum production in Sudan with that in a country of harsh socio-economic conditions like Ethiopia indicates a lower performance in the former country. With a harvested area of only 32% of that in Sudan, Ethiopia is producing around 86% of Sudan's total production of sorghum. To understand the reasons behind such a poor performance of sorghum production in Sudan, more detailed analysis and discussion are therefore given in the following sections.

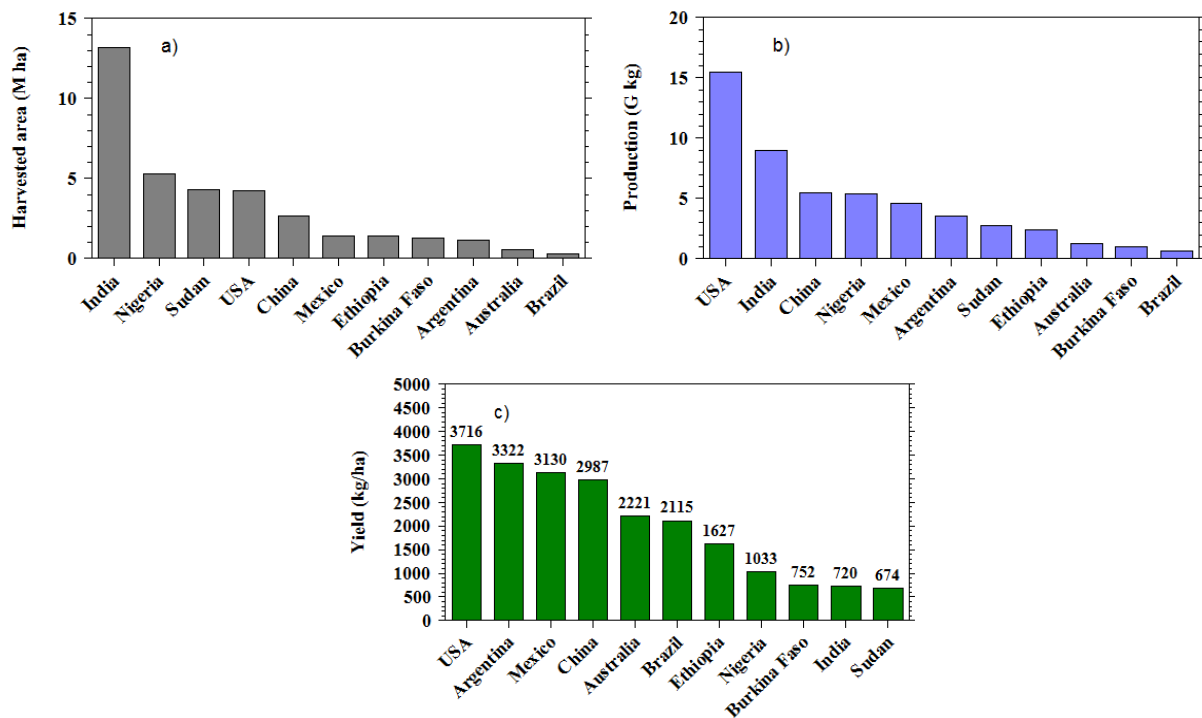


Fig. 6.1. Ranking of the top sorghum-producing countries in terms of (a) harvested area, (b) production and (c) yield. The data represent the multi-year averages (1961-2016) calculated from FAOSTAT data (<http://www.fao.org/faostat/en/#data/QC>). G = Giga.

6.2. Materials and methods

6.2.1. Study area

The study area consists of six states, namely Khartoum, Gezira, Kassala, El Gedaref, Sennar and Blue Nile, located in central and eastern Sudan (Fig. 6.2). Together, these six states occupy an area of 232,590.3 km². The region is characterized by arid and semi-arid climate with the average maximum temperature rises to more than 40 °C during April/May, the average minimum temperature drops to below 20 °C during January, and the median annual rainfall ranges between 87 in the northernmost part and 660 mm in the southwestern zone according to the 1971–2000 normals (Elagib, 2009). Wet conditions prevail during July to September in the arid part and extend longer from June to October in the semi-arid part (Elagib, 2009). Prominent

features of climatic changes in the region have been reported including increasing temperatures, droughts, rainfall variability, etc, during the last five decades which have brought about implications for the main human activities, such as farming and herding, resources, land use/cover changes, etc (Sulieman and Ahmed, 2013; Sulieman and Elagib, 2012; Elagib and Elhag, 2011; Elagib, 2010; Sulieman and Buchroithner, 2009; Elagib and Mansell, 2000).

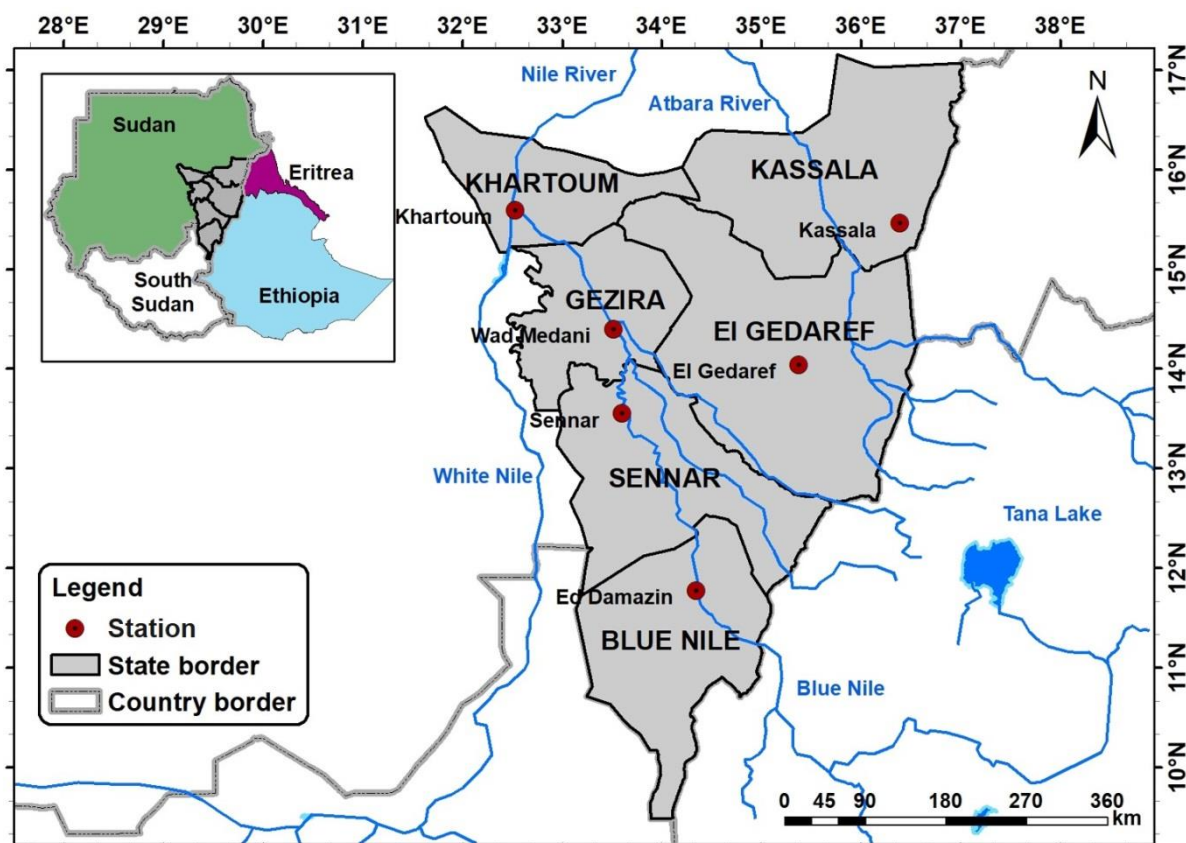


Fig. 6.2. Location map of the study area, regional states, and meteorological stations.

This area accommodates some of the major agricultural schemes in Sudan including rainfed and irrigated systems. Around one-third of the total production of sorghum in Sudan comes from El Gedaref State. While the six states were considered in the regional analysis, El Gedaref State was selected for more detailed analysis. Mechanization was introduced in El Gedaref in 1944 and spreaded southeast to other areas in the Blue Nile region in 1958/1959 (Mustafa, 2006). Although the purpose of the expansion was to take advantage of the vast potential of the rainfed area in this region and to overcome the problems facing the traditional rainfed farming (e.g. soil workability), rainfed farming in this region is still far beyond full mechanization as the use of machineries is confined only to some land preparation procedures (El Karouri, 2010). Semi-mechanized operations such as land preparation and sowing are carried out in farms larger than 420 ha (Bussmann et. al., 2016). With the mechanized farming accounting for about 65%

of the sorghum production in Sudan, three out of the five main contributing states in Sudan are located in the study region, namely El Gedaref, Sennar and Blue Nile, for which the records show that El Gedaref alone shares the largest contribution to the national sorghum production both in the mechanized rainfed sub-sector (45%) and in general (26%).

6.2.2. Data

The dataset used in the current study consists of climatic data (from stations and gridded data sources), sorghum statistics and satellite-based vegetation indices. The data on rainfed sorghum statistics, i.e. planted and harvested areas, production, and yield, come from only four out of the six states in the study region, namely Kassala, El Gedaref, Sennar, and Blue Nile. These data were obtained from MAF (2006) and CBS (2008) and updated from the Department of Agricultural Statistics, General Administration of Planning & Agricultural Economics of the Ministry of Agriculture and Forestry. These statistics were available from 1970 to 2016. Sorghum is selected for the current investigation because it is the major food crop cultivated in the region, as mentioned earlier. However, the capital of Sudan (Khartoum State) is not famous for cultivating this crop. Moreover, sorghum farming in Gezira State is overwhelmingly irrigated, and the available rainfed sorghum (traditional farming) data are not recognized on the records as mechanized. To obtain regional datasets for the sorghum statistics, the data for the four states were summed up. Finally, the sorghum yield was calculated as the ratio of regional sorghum production to the regional harvested sorghum area in the targeted states.

Part of the climate data consists of monthly temperature (maximum and minimum) and precipitation for the period 1941–2015 and was acquired from Sudan Meteorological Authority for six meteorological stations (Fig. 6.2). These stations are the main observing ones in the study area. One state (El Gedaref) was considered for further detailed analysis of the spatio-temporal variation of climate and vegetation productivity, using gridded data on climate elements, i.e. precipitation, temperature, and potential evapotranspiration, and vegetation index (Normalized Difference Vegetation Index, NDVI). The gridded data for El Gedaref State were acquired as shown in Table 6.1 and are described below. As reported earlier, sorghum is the major crop grown in El Gedaref State. Although masking the data for the sorghum areas alone is the best approach to reduce the uncertainty, unfortunately, there are no detailed data officially or readily available on the farm scale in Sudan. This information was confirmed by Mustafa (2006) for El Gedaref thus: “the data obtained from different sources [are] recorded on average for the whole region without in-depth details. The methods of keeping records on area grown, area harvested, costs, production, and yield are not regular, not systematic and only for a short

period” (Mustafa, 2006). Therefore, the present study attempted to relatively overcome this limitation as will be explained in the following section.

Tropical Precipitation Measuring Mission (TRMM 3B42) version 7 (Huffman et. al., 2007) of Multi-satellite Precipitation Analysis (TMPA) was used in this study. It is produced jointly by the United States National and Space Administration (NASA) and the Japan Aerospace Exploration Agency (JAXA). TRMM 3B42 v.7 is a blended product, which merges data from satellites with ground data from climate stations to obtain the final precipitation estimations. This precipitation product is widely used for many research purposes (Zulkafli et. al., 2014). TRMM provides precipitation estimations on different temporal domains (3 hourly, daily and monthly) on a spatial resolution of 0.25° from 1998 to the present. Daily precipitation data of TRMM 3B42 v.7 were processed online using GIOVANNI tool (Table 6.1).

Table 6.1. Characteristics of the gridded data used in the current study.

Variable	Data source	Spatial resolution	Time period	File format	Reference
Precipitation (P)	The Tropical Precipitation Measuring Mission (TRMM 3B42 v.7) Multi-satellite Precipitation Analysis (TMPA) https://giovanni.gsfc.nasa.gov/giovanni	0.25°	Monthly 2001- 2014	GeoTiff	Huffman et. al. (2007)
Potential evapotranspiration (PET)	Global Data Assimilation System (GLDAS) https://earlywarning.usgs.gov/fews/data/downloads	1.0°	Dekadal 2001- 2014	GeoTiff	Rodell et. al. (2004)
Temperature (T)	University of Delaware (UDel) version 4.01 https://www.esrl.noaa.gov/psd/data/gridded/data.UDel_AirT_Precip.html	0.5°	Monthly 2001- 2014	NetCDF	Willmott and Matsuura (2001)
Normalized Difference Vegetation Index (NDVI)	Moderate Resolution Imaging Spectroradiometer (MODIS) eMODIS Aqua NDVI https://earlywarning.usgs.gov/fews/data/downloads	250 m	Dekadal 2001- 2014	GeoTiff	Swets et. al. (1999)

Daily potential evapotranspiration (PET) were obtained from the website of Famine Early Warning System Networks (FEWS NET), as indicated in Table 6.1. These gridded data were produced using the climate variables output from the Global Data Assimilation Systems (GLDAS). PET data of this global product were calculated following the standard method of FAO Penman-Monteith for grass reference evapotranspiration, ETo (Allen et. al., 1998).

Terrestrial air temperature data were obtained from the public-domain product provided by the University of Delaware (UDel), as shown in Table 6.1. This product provides gridded temperature data derived from ground climate stations (Willmott and Matsuura, 2001). The production process used a combination of traditional interpolation and interpolation assisted

with Digital Elevation Model (DEM). To minimize the bias, this dataset went through an extensive validation process by the data providers (Willmott and Matsuura, 2001). For the current research, version 4.1 of this product was used. It provides monthly average data on air temperature with global coverage.

The Moderate Resolution Imaging Spectroradiometer (MODIS) satellite was used in this study as the source of NDVI data. This dataset is maintained by the United States Geological Survey (USGS) Earth Resources Observation and Science (EROS) Center. For the purpose of the current research, dekadal data (10-day composites) with a spatial resolution of 250 m for the years 2001 through 2014 were downloaded from the website of FEWS Net (Table 6.1).

6.2.3. Processing of gridded datasets

Processing of the gridded datasets, i.e. precipitation, PET, temperature, and NDVI, was done in Geographic Information System (GIS) environment using ArcGIS 10.3 software (ESRI, 2014). These data went through several processing procedures. The processing of PET data included restoring the original PET values by dividing the raster images by a factor of 100 using the “raster calculator” function in ArcGIS. The NDVI data were processed by removing the invalid raster values and applying the formula $(NDVI = (value - 100) / 100)$ on all the dekadal data to restore the NDVI values. Each of the processed precipitation, PET and NDVI data were summed up to produce seasonal values (June to October), and the monthly temperature raster files were averaged to produce average seasonal temperature. This five-month period represents the main growing season in the region (Elagib, 2014). All the seasonal images of the three variables along with the air temperature data from UDeI were clipped to the boundaries of El Gedaref State using the “Extract by mask” function in ArcGIS software.

To relatively overcome the limitation of unavailable data on specific sorghum farms, the present study considered the approach of masking the agricultural pixels alone with a threshold of $NDVI > 0.25$, as adopted by Al Zayed and Elagib (2017) for the Gezira Irrigation Scheme within the study area. However, the scale mismatch between NDVI and gridded meteorological data, i.e. precipitation, temperature, and potential evapotranspiration), does not allow such an extraction.

6.2.4. Drought assessment

Because long-term data over the period 1941–2015 that cover the full range of climatic elements for applying FAO Penman-Monteith are not available, the station data on temperature were used to calculate the ETo using the method developed by Hargreaves and Samani (1985)

and Hargreaves et. al. (1985), which is based on temperature. For this purpose, the values of extraterrestrial radiation for Sudan were taken from Elagib et. al. (1999). Using the precipitation and ETo data for the main growing season (June to October), the drought severity measured as the ratio of precipitation to ETo was calculated based on the concept of the aridity index (AI) of the United Nations Environment Programme (UNEP, 1992). This index has been used widely for drought studies for Sudan (Elagib, 2015, 2014, 2009; Elagib and Mansell, 2000). For the present work, a drought index was devised based partly on this ratio and partly on the drought risk index developed by Elagib (2014). Accordingly, three drought characteristics, namely drought severity (S), dry spell (DS) and time relative frequency of drought (TF), were used in a multiplication function to develop the MCDI:

$$\text{MCDI} = (1 - S) \times \text{DS} \times \text{TF} \quad (6.1)$$

where S is the ratio of the total precipitation to the total ETo for the growing season (June to October). S is subtracted from 1 since the drought risk (probability of drought occurrence) reduces with increasing S. If $S \geq 1$; then, the term $1 - S$ does not represent a dryness condition and is not considered in the calculation; DS is the ratio of the number of dry months to the total number of months (length) of the growing season in the given year; A month was considered dry if its UNEP AI was < 0.5 ; TF is the frequency of drought occurrences during the growing season (five months) over the whole study period 1941–2015; thus, it is a constant value for all the time series.

Each state MCDI was then standardized (SMCDI) after testing the normality of, and/or normalizing, the dataset of the given MCDI. To calculate a regional average time series of SMCDI, Thiessen polygons were constructed using GIS tools, as shown in figure 6.3. The regional SMCDI was validated by comparing it with the June-October regional Standardized Precipitation Index, SPI (McKee et. al., 1993). In this regard, the correlation between the two indices was investigated using the non-parametric Kendall tau correlation test (Kanji, 1993). Further validation was performed by comparing the synchronization and frequency of occurrence of drought and wet events as assessed by the two indices. The SPI time series was calculated following the same statistical procedure as described above for SMCDI, i.e. by testing the normality of, normalizing and/or standardizing the precipitation data. The development and use of the SMCDI in this study are justifiable for several reasons. First, the MDCI presented in Eq. (6.1) was tested for a large arid drought risk to food crops on both entire- and early-growing season scales (Elagib, 2015, 2014). Second, it was also able to capture the main drought events and El Nino – Southern Oscillation episodes that occurred in the region

(Elagib, 2014). Third, unlike other standardized drought indices (e.g. SPI; Standardized Precipitation Evapotranspiration Index, SPEI), it involves not only drought severity but also other drought characteristics, such as dry spells and time frequency of drought, as shown in Eq. (6.1).

For the spatial analysis of drought, the SMCDI was based on the gridded meteorological data. Each year was considered separately to calculate the MCDI, using the UNEP AI for all the pixels covering El Gedaref State, and to standardize the pixel MCDI based on the state-wide average and standard deviation of the MCDI for the given year.

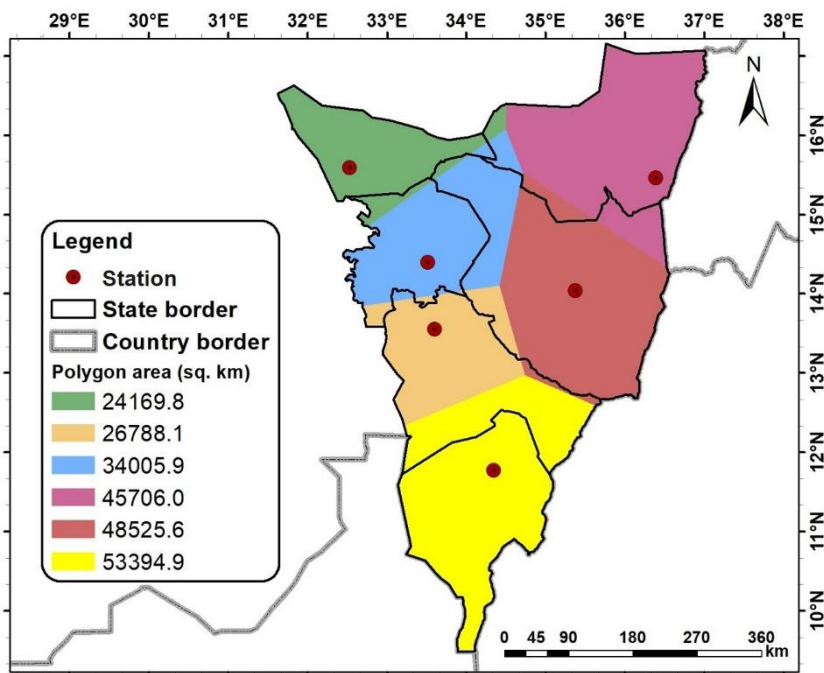


Fig. 6.3. Polygons represented by the meteorological stations as constructed by GIS.

6.2.5. Analysis of regime shift, vulnerability and resilience of sorghum production

To investigate the performance of sorghum production in the region under study, two approaches were followed. In the first approach, the regime shift analysis was performed over the study period using the Regime Shift Detector (RSD) software (Rodionov, 2004) in order to shed light on the significant change in the mean of sorghum statistics. The other approach utilized both the yield and SMCDI to classify the sorghum yield in terms of vulnerability and resilience during the dry and wet years. Simelton et. al. (2009) separated the vulnerable from the resilient cases by defining the former as years when significant harvest losses occurred despite only minor droughts, and the latter as years when harvest losses were minimal under a major drought. In the present study, six sorghum yield situations were explored, namely drought vulnerable (DV: yield loss under drought), drought resilient (DR: yield gain under drought),

near-normal climate resilient (NNR: yield gain under near-normal climatic condition), near-normal climate vulnerable (NNV: yield loss under near-normal climatic condition), wet vulnerable (WV: yield loss under wetness), and wet resilient (WR: yield gain under wet condition). It is worth mentioning that vulnerability (crop losses) could occur not only under extreme drought conditions, but also under extreme wet conditions due to oversaturation.

Without a prior removal of the effect of technology and other management measures taken by the farmers, using detrending techniques, one cannot use the yield data to establish a correlation with climatic elements, or infer the risk of climate (see for example, Elagib, 2015, 2014; Zhang, 2004; Nicholls, 1997). In other words, only the so-called “climatic yield” or the yield due to climate conditions can reflect such a crop yield-climate relationship. To do this, the trend in sorghum yield was removed over each regime shift period in the time series independently using linear regression to remove the non-climatic effects (e.g. technology, management, etc.); then, the resulting residuals were normalized by the linear regression to generate a dataset of yield anomalies or production levels (see Elagib (2014)). Negative anomalies refer to yield losses whereas positive anomalies indicate yield gains. Those anomalies were then compared with the SMCDI values considering three main climatic categories (drought, near normal and wet), each of which was further sub-divided to identify the years with sorghum vulnerability and resilience according to the six classes as defined earlier.

6.2.6. Vegetation productivity indices

Both the NDVI and Vegetation Condition Index (VCI) are used for drought detection and tracking; however, the former is “a better indicator of soil moisture than precipitation” (Nicholson et al., 1990) whereas the latter better portrays precipitation dynamics (Kogan, 1990). Since the study under evaluation herein concerns drought vulnerability of the farming system, the use of integrated NDVI (iNDVI), as a productivity index (Al Zayed and Elagib, 2017), over the potential growing season (June to October) is relevant rather than the decadal NDVI. To assess the vegetation or drought condition, the use of iNDVI also seems more appropriate than the average NDVI because it thus refers to vegetation or drought in terms of productivity. With reference to Al Zayed et al. (2015), the Modified Vegetation Condition Index (MVCI) was calculated on a spatial basis rather than temporally. This way, the MVCI can be used herein to assess the scalar, spatial ‘vegetation productivity drought’ for a particular year as follows:

$$MVCI = 100 \times \frac{iNDVI_i - iNDVI_{\min}}{iNDVI_{\max} - iNDVI_{\min}} \quad (6.2)$$

where $iNDVI_i$ is the integral (or sum) of the growing season decadal NDVI values of the present image pixel, and $iNDVI_{max}$ and $iNDVI_{min}$ are the maximum and the minimum $iNDVI_i$ s, respectively, of the given area under consideration. Note that MVCI qualitatively (rather than quantitatively) reveals the persistently dry or wet areas over the years (Al Zayed et al., 2015) in terms of growing-season vegetation productivity or greenness. Following Bhuiyan et al. (2017), the present study used the following classifications of indices for drought-related vegetation or moisture-related stresses to define the MVCI: $0 \leq$ Extreme drought < 10 ; $10 \leq$ Severe drought < 20 ; $20 \leq$ Moderate drought < 30 ; $30 \leq$ Mild drought < 40 ; No drought ≥ 40 . In the present research work, the analysis of vegetation productivity indices was confined to El Gedaref State case study.

6.2.7. Trend analysis

The Kendall tau correlation test (Kanji, 1993) was used whenever a decreasing or an increasing trend in a climatic or a vegetation index was necessary to be examined.

6.3. Results and discussion

6.3.1. Drought and wetness during the period 1941–2015

The three drought characteristics used to derive the MCDI for the six stations are shown in figure 6.4 based on the $AI < 0.5$ condition. The figure shows that three stations, namely Shambat, Wad Medani, and Kassala, are usually under drought, Sennar has a fluctuating drought and non-drought conditions, El Gedaref experiences drought only very infrequently while Ed Damazin is always under wet conditions. The dry spell over the growing season during the period 1941–2015 varies widely among the stations. Shambat has 4–5 dry months, Wad Medani and Kassala experience 2–5 dry months, El Gedaref indicates 0–4 dry months, Sennar shows 1–5 dry months and Ed Damazin reveals 0–3 dry months. The total cases of drought during the entire 75-year period range from 31% at Ed Damzin station to 95% at Shambat station. The above results reveal in general that the northern part of the study area is more vulnerable to drought than the southern part.

The developed regional SMCDI time series was divided into quantiles (using deciles) to classify the severity of drought into 10 main classes as shown in Table 6.2. However, an extra class, namely normal, was added in Table 6.2 to the main ten classes in case SMCDI is 0. Accordingly, a positive SMCDI indicates drought and vice versa, and the classes range from extreme drought to extremely wet. The SMCDI time series in figure (6.5a) that was compared with that of SPI in figure (6.5b) gave a Kendall tau of -0.749 at a significance level of 0.0001.

Furthermore, the SMCDI matched the SPI in the occurrence of 34 dry cases and 27 wet cases, i.e. 61 out of a total of 75 dry and wet events. This result indicates that the SMCDI is accurate in synchronizing 81.3% of the widely accepted SPI events. Both results thus indicate reasonable reliability of the developed SMCDI. Figure 6.5a reveals that until the end of the 1960s, there were only 5 drought years of mild to moderate severity and at least 11 severely to extremely wet years. The period extending from 1980 to 1991 witnessed consecutive drought conditions interrupted by only 2 wet years, viz. 1988 and 1989. Exceptionally heavy rainfall event in early August 1988 (Hulme and Trilsbach, 1989) was reported to cause severe flooding (Sutcliffe et. al., 1989). The 1980s represent the period notoriously known for the Sahel drought which culminated in the year 1984 (Hulme, 2001, 1990; Nicholson, 1985). During this period, a drought occurred with varying severities, i.e. 2 mild, 2 moderate, 2 severe and 1 extreme. Although the region somewhat recovered in the following two decades with 7 mildly to extremely wet years, still 12 drought years characterized this period, during which a 5-year long drought (2009–2013) took place. Extremely wet conditions occurred in the years 1999, 2007 and 2014. Evidence of devastating river flooding in for example 1998 and 2007 in Kassala State was reported by Amarnath et. al. (2016).

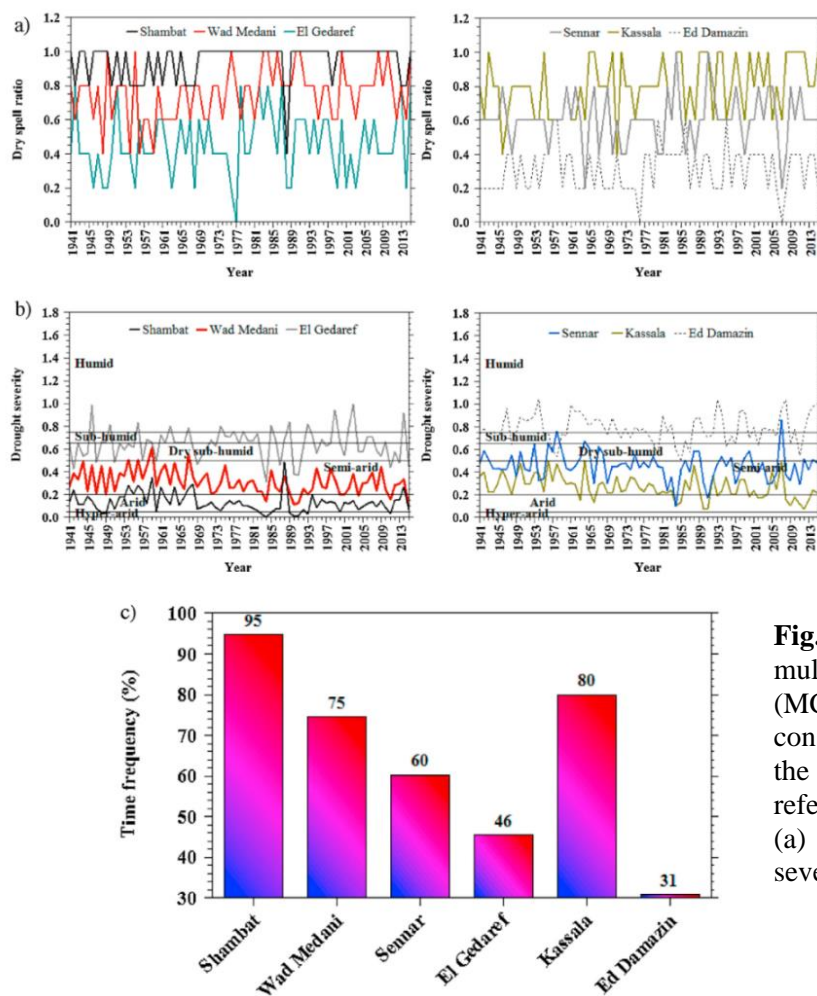


Fig. 6.4. Components of the multi-criterial drought index (MCDI) for the stations under consideration obtained using the ratio of rainfall to grass reference evapotranspiration: (a) Dry spell; (b) Drought severity; (c) Time frequency.

Table 6.2. Drought and wetness classes for the standardized multi-criteria drought index (SMCDI).

Class	Range
Extremely wet	< -0.69
Severely wet	-0.69 to < -0.41
Moderately wet	-0.41 to < -0.14
Mildly wet	-0.14 to < -0.04
Near normal (or incipient wet)	-0.04 to < 0
Normal	0
Near normal (or incipient drought)	> 0 to 0.11
Mild drought	> 0.11 to 0.34
Moderate drought	> 0.34 to 0.64
Severe drought	> 0.64 to 1.87
Extreme drought	> 1.87

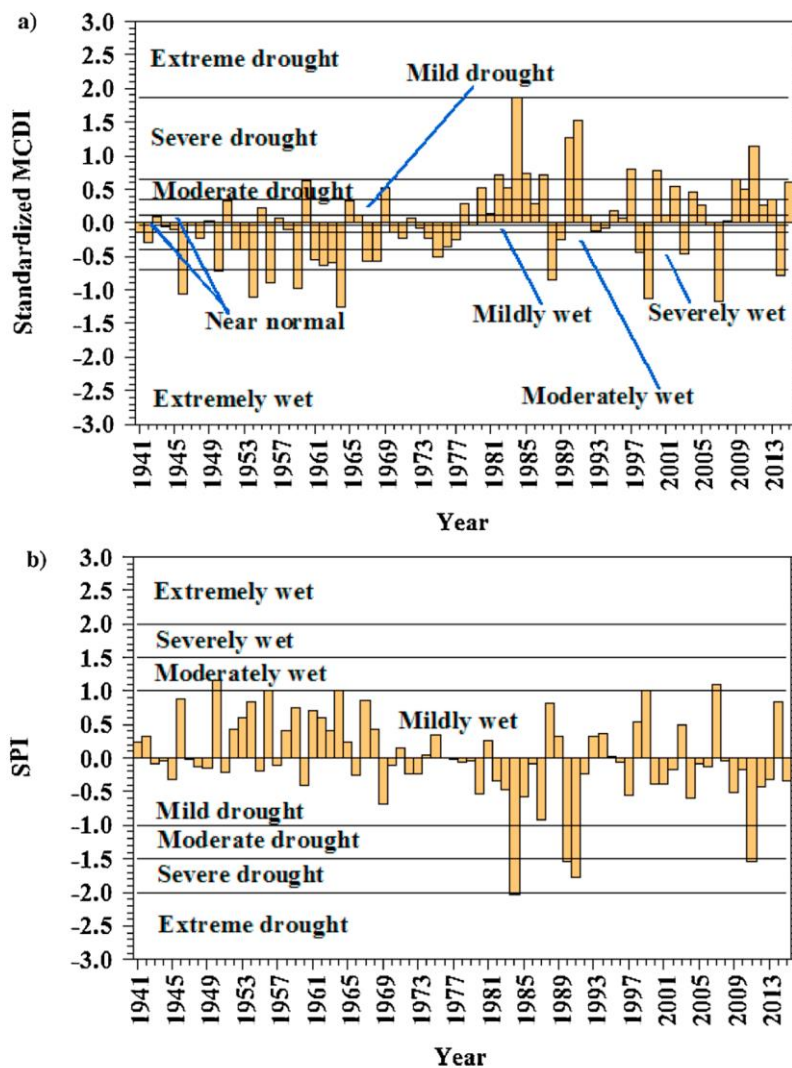


Fig. 6.5. Regional drought assessed by polygon-based average: (a) multi-criterial drought index (MCDI) compared to (b) Standardized Precipitation Index (SPI).

6.3.2. Performance of regional sorghum production during 1970–2016

The sorghum production statistics obtained during 1970–2016 are given in figure 6.6, with the regime shift means indicated on the time series and additionally summarized in Table 6.3. Three time series, namely planted area, harvested area, and yield, experienced significant changes in means in the early 1980s (1980 or 1982). The production also witnessed a significant change in the mid of this decade. These changes prominently concurred with the decade of the Sahel drought. Both the planted and harvested areas of sorghum have increased in the study region (Fig. 6.6 a and b). However, the former witnessed three different increases over the study period, with the greatest increase of 2.43 times being during the 1980s whereas the longest occurred over 18 years starting from 1991 (Table 6.3). The last shift in the mean sorghum planted area occurred towards the end of the first decade of the 21st century, i.e. in 2009. The harvested area had a prolonged shift in mean of 2.66 times over three and a half decades (Table 6.3; Fig. 6.6b). It is only until 2009 that a regime shift in the area lost at harvest occurred: from ~542,300 ha to ~1,690,100 ha (Table 6.3; Fig. 6.6c). On average, the ratio of the harvested-to-planted area indicates a drastic area loss at harvest of ~20% doubling to ~40% during the last decade and, additionally, with high variability from year to year (Fig. 6.4d). The average total production of sorghum increased from 743.7 million kg during the first 15 years to 1524.9 million kg, i.e. doubled during the next decade and a half (Fig. 6.6e and Table 6.3). Since 1999, the average production of sorghum decreased by 33%. This period reflects the distraction of the country's economic attention from agricultural production to the oil industry before the secession of South Sudan in 2011 where 75% of the explored oil existed. It is interesting to notice from figure 6.6e that, despite the varying levels of production from one year to another, there has been a tendency towards increasing levels again following the separation of the two countries. Finally, with all the above shifts in sorghum statistics, the yield levels have decreased significantly from 744.3 to 476.6 kg/ha since 1982.

6.3.3. Resilience and vulnerability of sorghum yield to climate during 1970-2015

Figure 6.7 shows the classification of the regional sorghum yield as being climate vulnerable or resilient over the 46-year study period (1970–2015). During the same period, 23 mild to extreme droughts and 17 mild to extreme wet cases can be identified (Fig. 6.5a). Based on the anomalies of sorghum yield and SMCIDI, 13 drought resilient years, 10 drought vulnerable years, 1 near-normal resilient years, 5 near-normal vulnerable years, 6 wet resilient years and 11 wet vulnerable years can be identified.

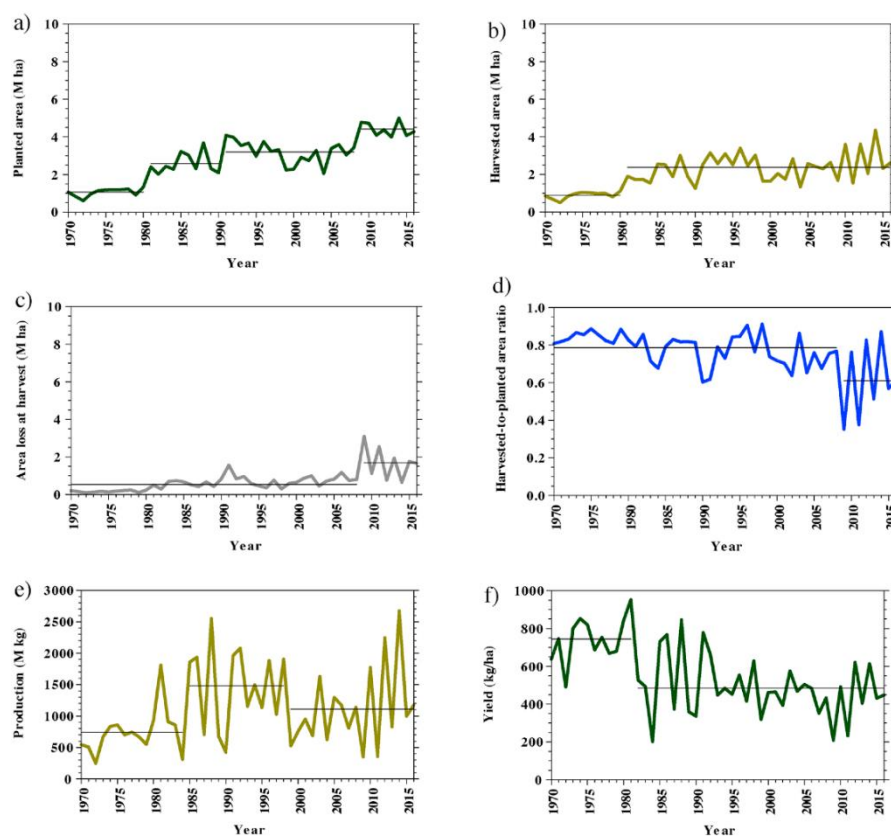


Fig. 6.6. Time series of particulars of mechanized sorghum farming and corresponding regime shift detection: (a) Planted area; (b) Harvested area; (c) Area lost at harvest; (d) Harvested-to-planted area ratio; (e) Production; (f) Yield. M = Million.

Table 6.3. Summary of results of the regime shift analysis.

Year	Length of shift (years)	Significance level, p	Ratio of present to past means	Mean
Planted area (1000 ha)				
1970	11			1061.0
1981	10	0.0001	2.43	2578.5
1991	18	0.0112	1.24	3193.5
2009	8	0.0001	1.38	4411.2
Harvested Area (1000 ha)				
1970	11			0893.7
1981	36	0.0001	2.66	2381.2
Area lost at harvest (1000 ha)				
1970	39			0542.3
2009	8	0.0064	3.16	1690.1
Production (million kg)				
1970	15			0743.7
1985	14	0.0010	2.00	1524.9
1999	18	0.1070	0.75	1017.3
Yield (kg/ha)				
1970	12			744.3
1982	35	0.0001	0.65	476.6

The occurrence of regional yield losses and gains under both dry and wet years suggests that the mechanized sorghum yield was highly variable in terms of vulnerability and resilience during the period of investigation. For instance, the yield of the regional mechanized rainfed sorghum was drought vulnerable in 1981–1984, 1995, 2000 and 2009, which were reported as salient meteorological drought years in the region according to Elagib (2009, 2014), Elagib and Elhag (2011) and Sulieman and Elagib (2012). However, years known to be dry on the record like 1970, 1990 and 1991 (Elagib (2014, 2009); Elagib and Elhag (2011); Sulieman and Elagib (2012)) are herein indicated as sorghum yield wet vulnerable in the first case but drought resilient in the other two cases. On the other hand, wet years like 1999, 2003 and 2006 in El Gedaref region (Sulieman and Elagib, 2012) or like 2003 and 2007 in Kassala State (Amarnath et. al., 2016) are classified herein for the regional sorghum yield as wet vulnerable (three years) or wet resilient (one year).

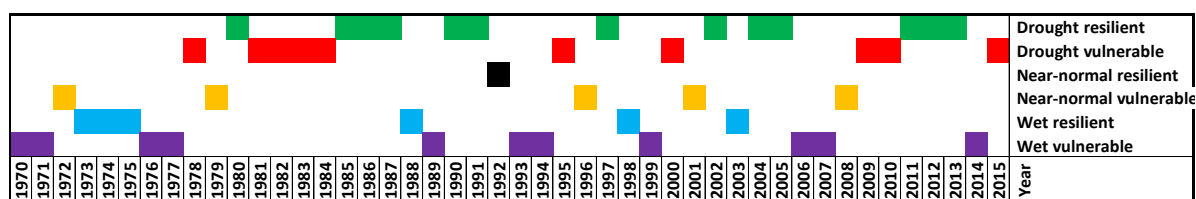


Fig. 6.7. The occurrence of drought and wetness resilience and vulnerability of sorghum.

The above findings indicate that sorghum production could, in fact, become vulnerable or resilient to both drought and wet conditions. Such results can be attributed to several factors. Although rainfall characteristics, such as onset (and in turn sowing date), distribution over the season and variability (Bussmann et. al., 2016; Elagib, 2015; Sulieman and Elagib, 2012) are in particular very important determinants of the crop yield. The instability of sorghum production can be influenced by several other factors that are perceived differently by farmers and agriculture experts and that have varying impacts from one year to another (Bussmann et. al., 2016). Among these factors, Bussmann et. al. (2016) identified degraded soil characteristics as a result of monoculture, limited crop rotation and neglected fallow periods, sorghum variety, weeds and parasites, and use of machinery, all of which in turn depend on socio-economic conditions, and finally institutional framework. Mustafa (2006) also elaborated on the factor of large fluctuations in agricultural inputs that affect production-related decisions and delay the agricultural development. These inputs include the financial constraints, as the majority of farmers depends on substantial amounts of loans to finance their agricultural activities and the high cost of labor, lack of infrastructures, absence of effective extension services and lack of knowledge about the use of technologies. Biro et. al. (2013) considers the rapid land use and land cover changes responsible for land degradation (change of the physical and chemical

properties of the soil) occurring in the agricultural areas. Even though farmers may be well aware of various forms of soil degradation that are taking place on their cultivated lands, the mitigation measures adopted by them may not be sufficient to restore the soil fertility (Sulieman and Buchroithner, 2009).

6.3.4. Case of El Gedaref State

6.3.4.1. Temporal variation in climatic factors and productivity indices

Figure 6.8a shows the time series of the areal average (2001–2014) of precipitation, temperature and potential evapotranspiration (PET) over the growing season (June to October) for El Gedaref State. Over this period, the precipitation and temperature show ups and downs but no significant trends could be found using the non-parametric Kendall tau correlation test. However, the figure clearly shows successive below-average precipitation (521.8 mm) from 2009 to 2013. Additionally, the PET is persistently increasing at a significant rate ($p=0.0012$), as per Kendall tau correlation test. Consecutively, the low P/PET ratio is recognizable over 2009–2013 (Fig. 8b) and indicates an overall semi-arid condition for the growing season. Years such as 2003 and 2007, which had high rainfall amounts and UNEP aridity indices, had noticeably high iNDVI values (Fig. 6.8c). Both the iNDVI and the sorghum yield (Fig. 6.8c and d, respectively) show decreasing trends, though insignificant, in El Gedaref State during the period spanning from 2001 through 2014. The decline in the sorghum yield/iNDVI could be attributed mainly to the drought conditions, especially during the years extending from 2009 through 2013 (Fig. 6.8b). In view of the approximate approach adopted in this study to extract the land use area of sorghum, more detailed quantitative analysis over a longer period is needed to support with confidence the use of iNDVI as a proxy for sorghum yield in this state.

6.3.4.2. Spatial variation in climatic and vegetation-related drought indices

The SMCDI-based spatial distribution of drought zones across El Gedaref State (Fig. 6.9) shows a northwest-to-southeast gradient of the dry-to-wet conditions in most of the years. However, there is still a remarkable spatial variation in the degree of drought condition from one year to another. Based on the areal average SMCDI, the year 2009 was the driest within the data period followed by the year 2003 when SMCDIs of only -0.17 and -0.18 were obtained, respectively. However, the latter year had the most spatially variable SMCDI values. It is worth mentioning here that the average value may not always be a good sign in arid areas. For instance, the state average iNDVI shows that the year 2003 had the highest value (iNDVI=5.78) within the study period followed by the year 2007 (iNDVI=5.58). In these two years, the most

unproductive part of the state in the northwest shows a diminishing zone of $iNDVI \leq 3$ (Fig. 6.10a).

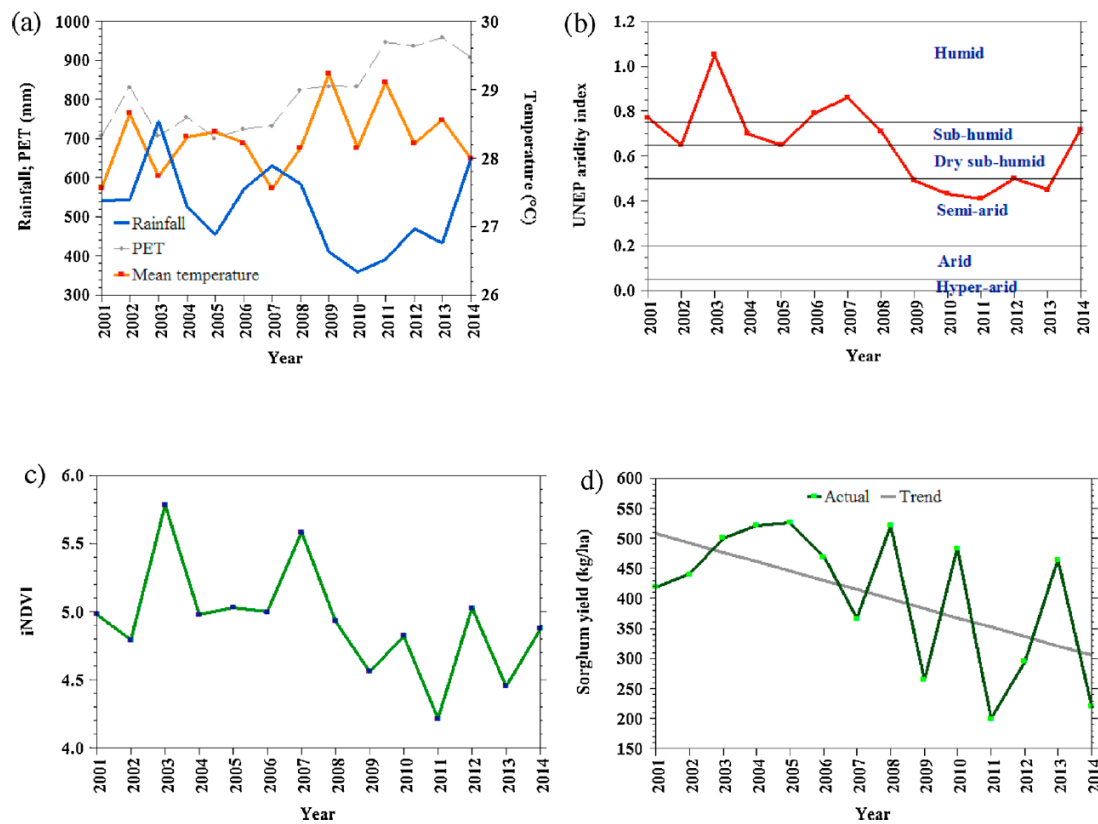


Fig. 6.8. Temporal areal average growing season (a) precipitation, temperature and potential evapotranspiration (PET) and (b) UNEP aridity index (AI), c) productivity index and d) sorghum yield for El Gedaref State.

Based on MVCI (Fig. 6.10b), the years 2003, 2007 and 2009 show area average MVCI values of 48% (best productivity conditions), 46% (second best productivity condition) and 37% (second worst productivity condition), respectively. Despite the variations in drought characterizations as obtained by the areal average values, the three indices, i.e. SMCDI, $iNDVI$, and MVCI, still show a consistent northwest-to-southeast gradient of drought to-wet conditions and productive-to-non-productive conditions. The areal averages of both $iNDVI$ and MVCI reflect low vegetation productivity (or noticeable drought conditions) during the last years of the investigation period, namely 2009-2014. As for $iNDVI$, all years except 2012 had $iNDVI$ of <5 . Using MVCI, values below 40% (drought) also characterized all the years except 2012. The year 2011 had the lowest $iNDVI$ (4.2) and MVCI (33%) within the period 2001–2014. These observations could be taken as signs of a drought vulnerable region for rainfed agriculture. During the study period, the area of El Gedaref State under mild to extreme droughts as assessed by SMCDI ranged from 20% in 2014 to 40% in 2003 with an average of 33% (Fig. 6.11).

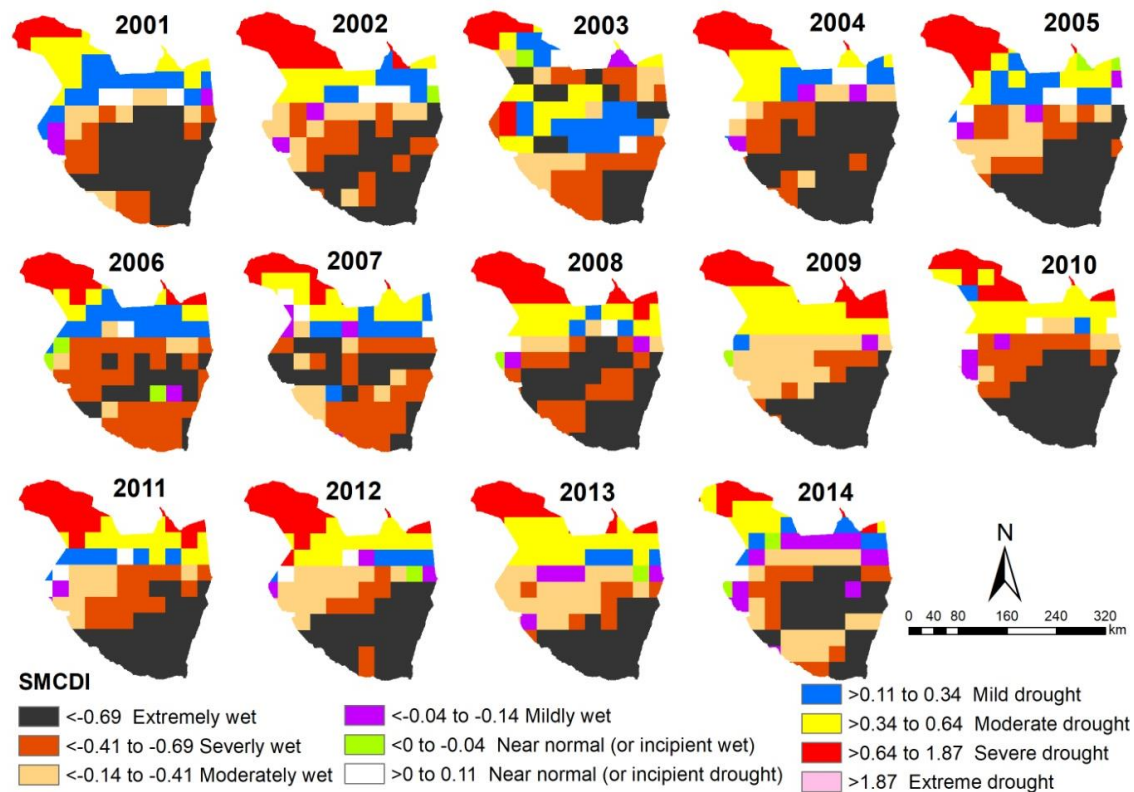


Fig. 6.9. Spatial distribution of drought zones in El Gedaref State assessed by the Standardized Multi-criteria Drought index (SMCDI) for the growing season.

During the same period, there seems to be a tendency towards intensifying low productivity conditions that can be inferred from the expanding area with $iNDVI < 5$ and $MVCI < 40\%$ (Fig. 6.11), though the positive trend direction investigated by Kendall tau test was not significant at $p=0.05$. The area corresponding to $iNDVI < 5$ ranged from 29% in 2003 to 72% in 2011. Based on $MVCI < 40\%$, the area reached 27% and 70%, also obtained in 2003 and 2011, respectively. The average area during 2001–2014 was found to be 54% and 52%, respectively for the $iNDVI$ and $MVCI$ thresholds. The incompatibility in the trends of the areas inferred from the drought index and the two vegetation indices is, at least partly, due to the fact that SMCDI was calculated for all land uses unlike the vegetation indices, which were based on only green areas ($NDVI < 0.25$), as explained earlier. The results of the analysis of the three indices, as described above, can be placed in the context of results based on ground observations of climatic and sorghum yield, as indicated in previous studies. They seem to have led to similar conclusions. For example, Sulieman and Elagib (2012) reported for El Gedaref State that the year 2009 was exceptionally characterized by high temperature, poor rainfall distribution over the growing season and low sorghum yield.

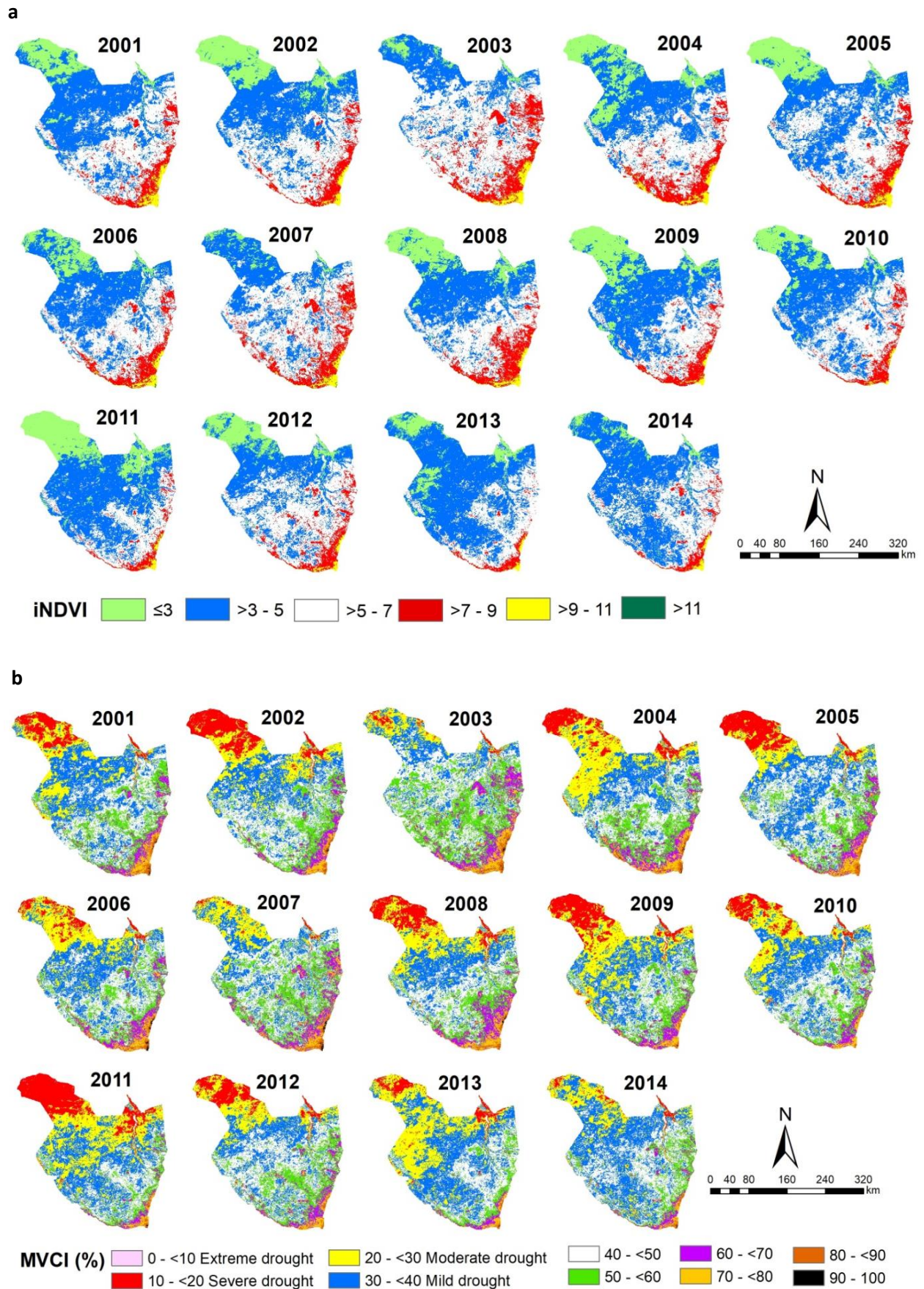


Fig. 6.10. Spatial distribution of vegetation indices across El Gedaref State for the growing season (June to October): a) productivity index (iNDVI) and b) Modified Vegetation Condition Index (MVCI).

The present results on lower productivity in 2011 and better conditions in 2012 are consistent with those reported by Hermance et. al. (2016), who classified the growing season of the two years as dry and relatively wet, respectively. For their study area in El Gedaref, Hermance et. al. (2016) also reported a lower height of sorghum plants in 2011 than that in 2012.

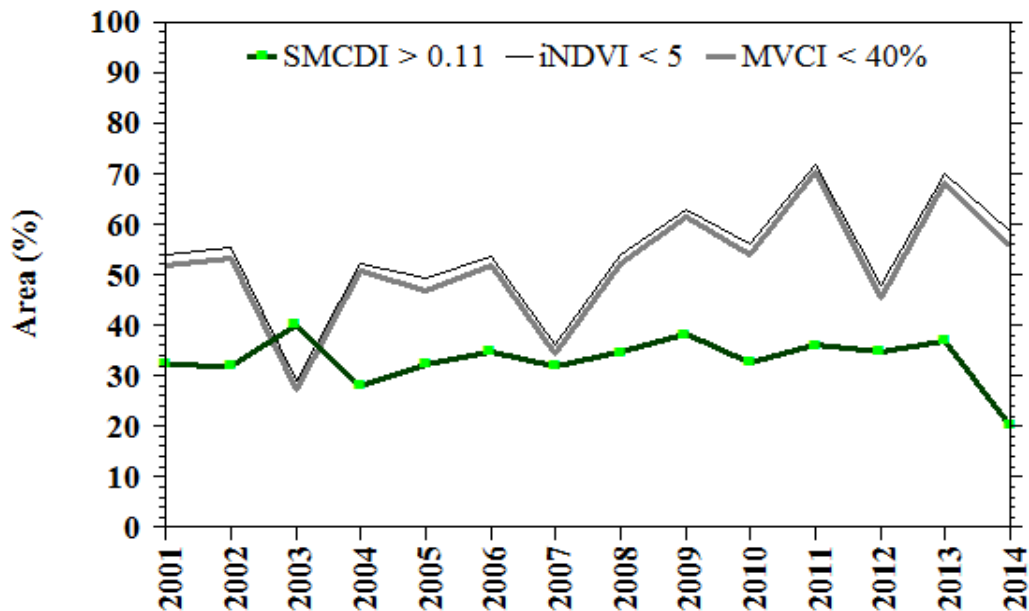


Fig. 6.11. Percentage area of El Gedaref State under drought and/or low productivity condition as measured by SMCDI > 0.11, iNDVI < 5 and MSCI < 40%.

6.3.4.3. Production level as a function of low precipitation

To investigate the effect of low total rainfall amount, i.e. drought, during June-October on the production level, the relationship between the two variables was established (Fig. 6.12). Obviously, low rainfall amount has a non-linear effect on the production level, with the best fit showing reduced effect of drought on sorghum production levels as the rainfall increases until an optimum amount of around 550 mm is reached. Beyond this optimum rainfall, the reduction in production level due to drought starts to magnify again. One can infer from the non-linearity and scatter of the points in this plot that factors other than just the total rainfall amount during the growing season play a role in defining the production level. In fact, Sulieman and Elagib (2012) gave an illustrative example of the prominent role played by the distribution of rain and rain days over the season in changing land use and land cover in El Gedaref region. This was exactly the reason why Elagib (2015, 2014) involved several drought characteristics, such as severity, frequency, and duration, in developing and applying a drought risk index for food crops.

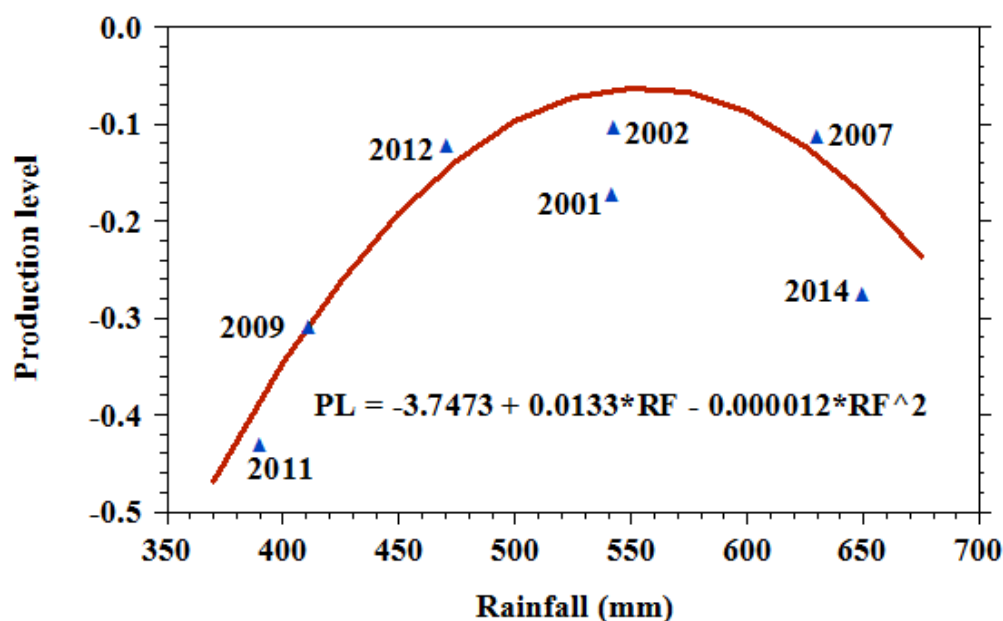


Fig. 6.12. Sorghum production level under drought versus low growing season (June to October) rainfall for El Gedaref State. PL is the production level and RF stands for rainfall.

6.4. Conclusion

The performance of the production of the main mechanized rainfed staple crop, i.e. sorghum, during the period 1970–2016 has been analyzed in relation to the prevalent moisture/drought conditions using diverse data observed on the ground and by remote sensing. A novel SMCDI together with other ground- and satellite-based meteorological and vegetation indices have all characterized the study area as spatiotemporally prone to drought and low productivity conditions.

As detected by regime shift analysis, a significant decrease in the sorghum-harvested area has manifested in the region despite the large agricultural extensification that is taking place. The total sorghum production increased during the period of the Sahel drought and doubled until the end of the last century when a drop occurred followed by strong ups and downs. Since the early 1980s, i.e. the date of peak Sahel drought, the average sorghum yield has decreased significantly by more than one-third its 1970s level. The current investigation has also characterized the mechanized rainfed sorghum production as variably vulnerable and resilient to drought, wet and normal moisture conditions. Since 1970, sorghum vulnerability has been as frequent as 57% of the years.

With the above findings in the backdrop, and given the fact that the economy, livelihood and food security of Sudan are mainly relying on agricultural activities, it can be concluded that the mechanized rainfed sorghum production in Sudan has yet performed below average.

Commensurate with a global awareness of advances in technology within the farming system (Lobell et al., 2011; Garcia et al., 1987), mechanization of rainfed sorghum in the study area has not yet been able to improve the production; rather, the increase in sorghum production remains significantly offset by the high dependence on a combination of physio-geographic, socio-economic and institutional factors.

This conclusion has its negative implications for food security in the country in the future. The decision making processes concerning the improvement of the sorghum agricultural sector, as recommended by Bussmann et. al. (2016), necessitates the understanding of the complexity of interdependence among the causes of such instability in the performance of mechanized rainfed sorghum production in the study area. There is a need to call for genuine intervention plans and policies toward improving the performance in the mechanized rainfed agriculture in Sudan, especially in terms of bridging the gap between the sorghum cultivated and harvested areas (or at least narrowing it) besides raising the yield. This study reiterates the recommendation put forth earlier by Bussmann et. al. (2016) that increasing recognition of rainfed agriculture is needed in Sudan to minimize the productivity losses that could lead to a series of consequences, including expanding the agricultural activities, increasing land degradation, conflict over resources, food insecurity and rural-urban migration. To reduce the sorghum vulnerability and increase the sorghum yield, several measures seem appropriate including improved technological packages, governmental incentives, infrastructure, basic services, and credit system (Mustafa, 2006). Foley et. al. (2011) suggest increasing the resilience of the food system for a cultivated planet through new practices. For India, Kumar et. al. (2018) stated that the categorization of rainfed agriculture and interventions should be based on agro-climatic conditions and hydro-meteorological parameters. Adopting this approach seems to be appropriate for the present study region. For instance, Sulieman and Buchroithner (2009) recommended the application of appropriate fertilizers, rotational cropping system and prolonged fallow periods.

Chapter 7

Synopsis, synthesis and perspectives



7.1. Synopsis

The current research was conducted to study the nexus between water, food, and climate in the NB region, using mainly EO datasets in addition to other primary and secondary data. In this area, agriculture is not only considered as the backbone of food security and the main source of livelihood for the local people but also as the main water consumer. Selecting the agriculture systems in Sudan as a central focus of the current research was due to the low performance of the rainfed and irrigated agriculture schemes which suggests huge potentials to contribute to water and food security in the NB region. This research followed a multi-disciplinary and multi-scale approach to identify potential synergies and trade-offs of the WFC Nexus within and across spatial scales. We investigated the nexus between the three systems on four different scales: (i) country, (ii) river basin, (iii) agriculture scheme and (iv) field. This approach is helpful to connect the strategic level (country) with operational levels (basin, scheme, and field). The analysis conducted in this research proved the usefulness of integrating different methodologies and datasets, especially EO datasets to identify and quantify these synergies and trade-offs. This integration has provided unprecedented spatial and temporal coverage that was not available for the study region. Besides, the current research suggested innovative approaches on how the EO dataset can be employed and augmented with other datasets for WFC Nexus analysis. Shedding lights on the potential interactions between the water, food and climate is critical for policy intervention that seeks to enhance water and food security under climate variability while ensuring the sustainability of natural resources.

7.2. Synthesis

The NPP, WUE, and CUE are important indicators to detect the behavior and functionality of vegetation, which represent the main source for food and major sink for the atmospheric CO₂ (Ardö, 2015; Zhao and Running, 2010). Comparing the magnitudes of the three indicators and their sensitivity and feedback to climate variation on the country scale (chapter 3), taking Sudan and Ethiopia as examples, provided essential knowledge that could lead to better policies for land cover management. The results of the current research showed that most land cover types in Sudan are characterized by relatively low annual precipitation and evapotranspiration levels and higher temperatures compared to Ethiopia. This difference in the prevailing climatic conditions is the main responsible factor of the varying magnitudes of NPP, WUE, and CUE calculated for the different land covers in the two countries (Liu et. al., 2016; Tang et. al., 2014). Generally, all the land cover types in Sudan exhibit lower

magnitudes in the three indicators compared to their counterparts in Ethiopia. This implies that the land cover types in Sudan are less efficient in terms of vegetation productivity and water/carbon use compared to those in Ethiopia. The noticeable increase in NPP, WUE, and CUE of the land cover types in Sudan in the years between 2009-2013 implies a relative enhancement in the vegetation conditions in these years, though their magnitude stills lower than those detected for Ethiopia.

The current investigation confirmed that climate variability and drought conditions have different effects on the different land cover types and the response of these land cover types to such variability is, to a large extent, controlled by the climate regime prevailing in the area in addition to other factors such as vegetation type, soil properties, water, and nutrient availability. The NPP in the studied land cover types showed relatively higher resistivity to drought in Sudan compared to those located in Ethiopia. This could be explained by the fact that vegetations that grow under climate stress might develop mechanisms (e.g. decreasing transpiration) to cope with such harsh climate conditions (Basu et. al., 2016; El-Sharkawy, 2007). The current research found that whereas the evergreen broadleaf forests and woody savannah in Ethiopia exhibit the highest NPP levels, savannah is the land cover with the highest NPP in Sudan. Savannah, grasslands and open shrublands are the most sensitive land cover types to drought, and a cumulative drought of a duration of three months is largely controlling the annual variability in NPP of these land cover types, especially in Ethiopia.

Duration of drought, its association with changes in temperature, timing and spatial extent of drought were found to control the impact of drought on vegetation NPP. Long-lasting drought conditions such as drought events in two successive years (e.g. 2001 and 2002) might induce a considerable decrease in NPP. Drought at the start of the season might lead to a larger reduction in NPP compared to a drought occurs at other stages of crop development. The lack of immediate response of vegetation to climate variability, especially in Sudan, might be a result of the intervention of other factors rather than climate (e.g. soil properties, nutrient availability, and technological solutions). Drought might increase WUE due to a decrease of water losses from the vegetation as a mechanism to cope with water stress conditions (Dong et al., 2011; Reichstein et al., 2002). This is evidenced by the case of NPP changes in Sudan during the dry year of 2009. CUE of the land covers in Ethiopia was found to be not regulated by water availability, as they show less inter-annual variability compared to those located in Sudan. These results have implications for food security and climate change mitigation in the two countries.

Adequate monitoring of precipitation is important for water and food security policies. Analysis of the regional setting in the larger NB region (chapter 2) emphasized the importance of the BNB, not only for the two riparian countries; i.e. Ethiopia and Sudan, but also for Egypt and the whole Nile River system. As the river basin is considered as the basic unit for water management (Newson, 1997; Teclaff, 1967; White, 1957), the BNB needs to be managed beyond the political boundaries. On the basin level, precipitation represents the main water source that needs to be monitored properly. Inadequate monitoring network of precipitation is seriously affecting the water management in the basin. Therefore, PPs could be considered as a potential alternative to ground monitoring network that has limited ground stations. However, they provide variable precipitation estimations and exhibit different spatial and temporal representations of precipitation on the basin scale. The results of the current analysis revealed large discrepancies between 17 studied PPs, which requires careful use of these products, preferably after bias correction.

Agriculture systems in the NB can be divided into two main types; i.e. irrigated and rainfed. Within the BNB, rainfed and irrigated schemes show low performance with low levels of yield in the main cereal crops (e.g. sorghum). Therefore, these schemes have a large room to produce more food from the same cultivated area and large potentialities to save water resources. In both sectors, the cultivated area shows a noticeable increase during the last few decades. However, this large horizontal expansion (extensification) in the cropland area did not couple with a parallel vertical development that includes substantial improvement in crop yield. The current research analyzed the performance of irrigated and rainfed schemes in the BNB, mainly those located in central and eastern Sudan and represent the main sorghum production area in the country. Assessing the performance of these schemes is critical to navigating the development and implementation of development pathways in the agriculture sector that aims at securing food production.

In the Gezira Irrigation Scheme, as an example of the irrigated sector, many factors of physical, socio-economic, and management nature are affecting the sorghum yield. Among all the studied factors, access to water, as represented by the location of farmland along tertiary canals, and farmer's financial status were found to be the most influential factors. It is believed that addressing some of the main influential factors would affect other factors, as many of them showed interlinkages. The identified controlling factors on crop yield could be considered as entry points for SI in the scheme. The developed conceptual framework for SI

presented in the current research aims not only at targeting crop yield enhancement but also at promoting a healthy environment, improved livelihood, and a growing economy.

Besides the low yield levels of sorghum, a drastic loss of area at harvest took place in the rainfed sector during the period 1970–2016. The yield gap and the losses at harvest, if reduced, have the potential to boost the total production of these schemes. Consequently, this would reduce the pressure on other important land covers types that are important for climate change mitigation and experiencing declining trends. As some of these land cover types are playing a key role as carbon sinks as sources for water production, preserving them is highly crucial for mitigating climate change. On the other hand, enhancing crop production in the rainfed sector would relieve some pressure on the limited river waters that are subject to transboundary conflict, as discussed in chapter 2.

7.3. Perspectives

7.3.1. Synergies and trade-offs on the country scale

- The low NPP, WUE, and CUE in the land cover types in Sudan compared to their counterparts in Ethiopia, especially for croplands, implies large rooms for improvement of vegetation productivity and efficiencies of water and carbon use in Sudan.
- The impact of climate variability on NPP is a good indicator of the anticipated impact on crop yield. Developing policies to cope with the impact of climate variability (e.g. improved seeds, climate insurance, and rainwater harvesting) would strengthen the abilities to face such external drivers.
- Some of the studied land cover types, especially the evergreen broadleaf forests, woody savannah and permanent wetlands in Ethiopia represent important sinks for CO₂, as exhibited by their high NPP and CUE levels. This suggests that a special focus should be given to protect these land cover types. Converting natural vegetation into croplands should be evaluated carefully and should take into consideration the vital functions these land cover paly in the carbon cycle.

7.3.2. Synergies and trade-offs on the river basin scale

- As a basic unit for water resources management, managing water in the BNB currently is lacking a basin perspective. This has its implications on water and food production in the basin. For example, water harvesting might increase the water availability in some

parts of the basin while relieving the pressure on the limited river water that is needed in other drier and more vulnerable parts of the basin to water stress.

- Precipitation is not only the main source of water in the BNB, but it also represents the most important source of water to sustain food production in the basin. Because most of the agricultural land in the BNB is under the rainfed system, inadequate monitoring of precipitation and its characteristics is responsible for large losses in crop yield and it is jeopardizing food security in the basin. For example, the unavailability of continuous precipitation monitoring may lead to wrong decisions regarding water availability and consequently, on agricultural field practices such as selecting the sowing date, which may result in serious implications on crop yield.
- The availability of the PPs could be considered as an approach to mitigate the disadvantage of weak ground precipitation monitoring. However, their performance over the basin in the studied timeframe is rather diverse and might also lead to wrong decisions regarding water resources management. For example, the total amount of precipitation falling annually over the BNB could be estimated by the annual average precipitation rate as calculated from any of the PPs. However, when the area of the basin (307,177 km²) is considered, this total amount could range between 202.58 (–32.25%) and 532.71 (+78.16%) billion m³ when the products of ARC 2.0 and ERA-Interim are used, respectively. This big difference requires a careful quality assessment of these products for water resources planning and management.
- The short duration of the rainy season (June-October) in the basin calls for water harvesting to be practiced to increase the water storage capacities. Water storage would play a key role in increasing water availability as it helps in transferring water temporally across seasons from wet to dry seasons (November-May) and spatially from dry to wet regions.

7.3.3. Synergies and trade-offs on irrigated scheme scale

- The Gezira scheme has large potentials that are still untapped. In the current research, it was calculated that the sorghum production in this scheme can be tripled if the yield gap between the actual and potential/attainable yields is bridged.
- Stabilizing the yield of sorghum and bridging the yield gap would provide more food without the need to cultivate additional land. The interventions should take into consideration the spatial and temporal dimensions of the yield gap.

- A paradigm shift towards SI in such underperforming schemes using the identified entry points and their proposed measures would maximize the crop production and would not only minimize the environmental problems related to agriculture activities but would also contribute to enhancing the socio-economic status of the local farmers.
- More efficient water management in the scheme would help in securing water resources to irrigate additional areas within and/or outside the scheme or to be used for other purposes.

7.3.4. Synergies and trade-offs on rainfed scheme scale

- The current performance of this system is below average, and it has experienced a steady decline in sorghum yield, high variability from year to year and substantial loss of area at harvest during the last decades. Enhancing the performance of the rainfed agriculture in Sudan would minimize the need for unsustainable extensification of agriculture that took place in this sector during the last few decades. Additionally, focusing on increasing crop yield under the rainfed system would minimize the need for using surface and groundwater in irrigation.
- The association of vulnerability and resilience of sorghum production with wet and dry conditions, respectively, indicates that non-climatic factors such as technological and socio-economic factors are playing key roles. The strong dependence of sorghum vulnerability and resilience on a combination of physio-geographic, socio-economic and institutional factors might hinder improving the production. However, at the same time, it offers an opportunity, if the interactions are well understood and properly addressed, to offset the impacts of climate variability on crop yield. Examples of such interventions include, for instance, improved technological packages, governmental policies, infrastructure and credit systems.

7.3.5. Synergies and trade-offs on the field scale

- The sorghum yield in the Gezira Scheme is affected by several field practices. It can be concluded that even small interventions at the field scale, like adjusting the sowing date or preparing the farmland early, could have positive impacts on the total production of the scheme. Many of these factors have synergies and trade-offs with each other. Therefore, addressing some of them might induce changes in other related factors. For example, securing water sources and early preparation of land would help farmers to adjust the sowing date, which could contribute to increasing the crop yield.

- The loss of area at harvest in the mechanized rainfed system has reached 1.69 million ha in the years post-2009, which represents approximately 40% of the total planted area. Solutions to reduce this on the field scale could boost the total production of sorghum in this system.

7.3.6. Cross-scale synergies and trade-offs

- Bridging the yield gap and increasing efficiency on a field scale and implementing SI in the underperforming agriculture schemes means more food to be produced and substantial savings in the water resources can be assured. The saved water in the irrigated system would increase water availability on a basin scale for other users or for cultivating more areas, which might enhance the overall water and food security situation in the country. This would contribute to enhancing food security in the NB basin through exports and to improve water security by water savings
- Rational use of natural resources in the riparian countries of the NB would minimize the transboundary conflict and would promote benefit sharing and cooperative management of the Nile waters beyond the political boundaries.

7.4. Final Remarks

Through the findings of this research, lights were shed on the interlinkages between water, food, and climate in the study region within and across spatial scales. Therefore, the results of this dissertation can assist to enhance our current understanding regarding the importance of the nexus approach to improve water and food security under climate variability and for mitigating climate change. A holistic way of systems management is more effective than the silo approach, which is characterized by governing each system in isolation from the other ones. The findings of the current study are useful for researchers, policy-makers and local farmers. For researchers, it provides innovative approaches on how EO data can be used to provide unprecedented knowledge on the interactions between water, food, and climate over time and space. The approaches can be transferred to many areas that share similar contexts. As many SDGs exhibit synergies and trade-offs (Kroll et. al., 2019), policy-makers should consider these interlinkages when planning and taking actions. This knowledge improves the understanding of how to benefit from the WFC Nexus synergies and how to reduce trade-offs. Mainly, it emphasizes on the importance of following a vertical development pathway that minimizes water use and cultivated land expansion. Although the horizontal expansion might help to fulfill SDG 2 on achieving zero hunger, this development pathway may have several

trade-offs that might affect the achievement of the other SDGs (e.g. water security (SDG 6) and mitigating climate change (SDG13)). For local farmers, it shows clearly that several field practices are contributing to the prevailing crop yield gap. Spreading knowledge among farmers regarding the best practices and increasing the rate of their adoption in operation is crucial to address the challenge of securing water and food security.

Despite the key information that this research has provided, many areas still need more research in the future. For instance, (i) due to the unavailability of crop maps for the agricultural schemes, it was not possible to detect the productivity level, WUE, and CUE for specific crops and the climate variability impacts on these parameters on specific crops, (ii) although the performance of many public-domain precipitation products was tested using traditional and data mining techniques, which could be considered as an innovative contribution of this research, employing these products in hydrological models would shed light on their performance in simulating hydrological system in the BNB, and (iii) The current research was not intended to provide a complete list of WFC synergies and trade-offs. Therefore, there might be others that can be identified using, perhaps, other types of data and different methodologies than those used in the current investigation.

References

- Abdi, A.M., Seaquist, J., Tenenbaum, D.E., Eklundh, L., Ardö, J., 2014. The supply and demand of net primary production in the Sahel. *Environ. Res. Lett.* 9, 111003.
- Abebe, M.A., 2014. Climate change, gender inequality, and migration in East Africa. *Wash. J. Environ. Law Policy* 4, 104–140.
- Abera, W., Brocca, L., Rigon, R., 2016. Comparative evaluation of different satellite rainfall estimation products and bias correction in the Upper Blue Nile (UBN) basin. *Atmos. Res.* 178–179, 471–483. <https://doi.org/10.1016/j.atmosres.2016.04.017>
- Abera, W., Formetta, G., Brocca, L., Rigon, R., 2017. Modeling the water budget of the Upper Blue Nile basin using the JGrass-NewAge model system and satellite data. *Hydrol. Earth Syst. Sci.* 21, 3145–3165. <https://doi.org/10.5194/hess-21-3145-2017>
- Abteu, W., Dessu, S.B., 2019. *The Grand Ethiopian Renaissance Dam on the Blue Nile*. Springer International Publishing AG, 173 pp.
- Abu-Zeid, M. A., and El-Shibini, F. Z. 1997. Egypt's High Aswan Dam. *Water Resources Development*, Vol. 13, No. 2, pp. 209–217.
- Adam, H.S., Abdelhadi, A.W., and Hata, T., 2002. Promotion of participatory water management in the Gezira scheme in Sudan. In: FAO – ICID, ed. *Irrigation advisory services and participatory extension in irrigation management*. Montreal, Canada, 21–28.
- Addinsoft, 2017. XLSTAT Version 19.4. <https://www.xlstat.com/en>.
- Adem, A., Tilahun, S.A., Ayana, E.K., Worqlul, A.W., Assefa, T.T., Dessu, S.B., Melesse, A.M., 2016. Climate change impact on sediment yield in the Upper Gilgel Abay catchment, Blue Nile Basin, Ethiopia. In: Melesse A.M., Abteu W., editors. *Landscape Dynamics, Soils and Hydrological Processes in Varied Climates*. Springer International Publishing; 2016. pp. 615–642.
- Adler, R.F., Gu, G., Hong, Y., Bowman, K.P., Stocker, E.F., 2007. The TRMM multisatellite precipitation analysis (TMPA): quasi-global, multiyear, combined-sensor precipitation estimates at fine scales. *J. Hydrometeorol.* 8, 38–55. <https://doi.org/10.1175/JHM560.1>.
- African Development Bank, 2000. Policy for integrated water resources management. Available online at: www.afdb.org/fileadmin/uploads/afdb/Documents/Policy-Documents/IWRM%20Policy%20Integrated%20Water%20Resources%20Management%20FINAL%20version%20%28highlights%20removed%29_April%2026%202000.pdf (Accessed on: 01.08.2019).
- Agutu, N.O., Awange, J.L., Zerihun, A., Ndehedehe, C.E., Kuhn, M., Fukuda, Y., 2017. Assessing multi-satellite remote sensing, reanalysis, and land surface models' products in characterizing agricultural drought in East Africa. *Remote Sens. Environ.* 194, 287–302. <https://doi.org/10.1016/J.RSE.2017.03.041>
- Ahlström, A., Raupach, M.R., Schurgers, G., Smith, B., Arneth, A., Jung, M., Reichstein, M., Canadell, J.G., Friedlingstein, P., Jain, A.K., Kato, E., Poulter, B., Sitch, S., Stocker, B.D., Viovy, N., Wang, Y.P., Wiltshire, A., Zaehle, S., Zeng, N., 2015. The dominant role of semi-arid ecosystems in the trend and variability of the land CO₂ sink. *Science* 348, 895–899.
- Ahmed, A.A., 2004. Sediment transport and watershed management component, Friend/Nile Project, Khartoum.
- Al Zayed, I.S., Elagib, N.A., 2017. Implications of non-sustainable agricultural water policies for the water-food nexus in large-scale irrigation systems: A remote sensing approach. *Adv. Water Resour.* 110, 408–422. <https://doi.org/10.1016/j.advwatres.2017.07.010>
- Al Zayed, I.S., Elagib, N.A., Ribbe, L., and Heinrich, J., 2015. Spatio-temporal performance of large-scale Gezira Irrigation Scheme, Sudan. *Agricultural Systems*, 133, 131–142. doi:10.1016/j.agry.2014.10.009
- Al Zayed, I.S., Elagib, N.A., Ribbe, L., Heinrich, J., 2016. Satellite-based evapotranspiration over Gezira Irrigation Scheme, Sudan: A comparative study. *Agric. Water Manag.* 177, 66–76. <https://doi.org/10.1016/j.agwat.2016.06.027>

- Al-Bakri, J., Suleiman, A., Abdulla, F., Ayad, J., 2011. Potential impact of climate change on rainfed agriculture of a semi-arid basin in Jordan. *Phys. Chem. Earth, Parts A/B/C* 36, 125–134. <https://doi.org/10.1016/J.PCE.2010.06.001>.
- Ali, Y.S.A., Paron, P., Crosato, A., & Mohamed, Y.A., 2017. Transboundary sediment transfer from source to sink using a mineralogical analysis. Case study: Roseires Reservoir, Blue Nile, Sudan. *International Journal of River Basin Management*, 1-15. doi.org/10.1080/15715124.2017.1411919
- Allam, M.M., Eltahir, E.A.B., 2019. Water-energy-food nexus sustainability in the upper Blue Nile (UBN) basin. *Front. Environ. Sci.* 7. <https://doi.org/10.3389/fenvs.2019.00005>
- Allen, R.G., Pereira, L.S., Raes, D., Smith, M., 1998. Crop evapotranspiration : guidelines for computing crop water requirements. FAO Irrigation and Drainage Paper 56. Food and Agriculture Organization of the United Nations p. 300.
- Amarnath, G., Alahacoon, N., Gismalla, Y., Mohammed, Y., Sharma, B.R., Smakhtin, V., 2016. Increasing early warning lead time through improved transboundary flood forecasting in the Gash River Basin, Horn of Africa. *Flood Forecast.* <https://doi.org/10.1016/B978-0-12-801884-2.00008-6>. Chapter 8, pp. 183–200.
- Amdihun, A., Gebremaria, E., Rebelo, L., Zeleke, G., 2014. Modeling Soil Erosion Dynamics in the Blue Nile (Abbay) Basin: A Landscape Approach. *Res. J. Environ. Sci.* 8, 243–258. doi.org/10.3923/rjes.2014.243.258
- Amitai, E., Llord, X., Sempere-Torres, D., 2009. Comparison of TRMM radar rainfall estimates with NOAA next-generation QPE. *J. Meteorol. Soc. Japan* 87A, 109–118. <https://doi.org/10.2151/Jmsj.87a.109>
- Amthor, J., 2000. The McCree–deWit–Penning de Vries–Thornley respiration paradigms: 30 years later. *Ann. Bot.* 86:1–20. <https://doi.org/10.1006/anbo.2000.1175>.
- Anand, S., 2019. Programming in R - Finding Optimal Number of Clusters [WWW Document]. URL <https://datascienceplus.com/finding-optimal-number-of-clusters/>
- Appelgren, B., Wulf Klohn, W., Alam, U., 2000. Water and agriculture in the Nile basin. Food and Agriculture Organization of the United Nations (FAO) - Land and Water Development Division, Rome. Available online at: www.fao.org/3/a-x8034e.pdf (Accessed on 10.07.2019).
- Ardö, J., 2015. Comparison between remote sensing and a dynamic vegetation model for estimating terrestrial primary production of Africa. *Carbon Balance Manag.* 10, 8. <https://doi.org/10.1186/s13021-015-0018-5>.
- Ashour, M.A., Aly, T.E., Abueleyon, H.M., 2019. Transboundary water resources “A comparative study”: The lessons learnt to help solve the Nile basin water conflict. *Limnol. Rev.* (2019) 19, 1: 3–14 DOI 10.2478/limre-2019-0001
- Ashouri, H., Hsu, K.-L., Sorooshian, S., Braithwaite, D.K., Knapp, K.R., Cecil, L.D., Nelson, B.R., Prat, O.P., Ashouri, H., Hsu, K.-L., Sorooshian, S., Braithwaite, D.K., Knapp, K.R., Cecil, L.D., Nelson, B.R., Prat, O.P., 2015. PERSIANN-CDR: Daily Precipitation Climate Data Record from Multisatellite Observations for Hydrological and Climate Studies. *Bull. Am. Meteorol. Soc.* 96, 69–83. <https://doi.org/10.1175/BAMS-D-13-00068.1>
- Ashton, P.J., 2002. Avoiding conflicts over Africa’s resources. *Royal Swedish Academy of Science* 31(3), 236–242.
- Asseng, S., Pannell, D.J., 2013. Adapting dryland agriculture to climate change: farming implications and research and development needs in Western Australia. *Clim. Change* 118, 167–181. <https://doi.org/10.1007/s10584-012-0623-1>.
- Augustin, H., Sudmanns, M., Tiede, D., Lang, S., Baraldi, A., 2019. Semantic Earth Observation Data Cubes. *Data* 4, 102. <https://doi.org/10.3390/data4030102>
- Ault, T.R., Cole, J.E., Overpeck, J.T., Pederson, G.T., Meko, D.M., Ault, T.R., Cole, J.E., Overpeck, J.T., Pederson, G.T., Meko, D.M., 2014. Assessing the risk of persistent

- drought using climate model simulations and paleoclimate data. *J. Clim.* 27:7529–7549. <https://doi.org/10.1175/JCLI-D-12-00282.1>.
- Awulachew, S. B., Demissie, S. S., Ragas, F., Erkossa, T., and Peden, D., 2012. Water management intervention analysis in the Nile Basin. in: Awulachew S.B., Smakhtin V., Molden D., and Peden D., 2012. *The Nile River Basin*. IWMI. Available online at: www.iwmi.cgiar.org/Publications/Books/PDF/H045322.pdf (Accessed on 15.07.2019).
- Awulachew, S., Rebelo, L.M., Molden, D., 2010. The Nile basin: Tapping the unmet agricultural potential of Nile waters. *Water Int.* 35, 623–654. <https://doi.org/10.1080/02508060.2010.513091>
- Awulachew, S.B., Smakhtin, V., Molden, D., Peden, D., 2012. *The Nile River Basin – Water, Agriculture, Governance and Livelihoods*, 1st ed. Routledge, London.
- Ayehu, G.T., Tadesse, T., Gessesse, B., Dinku, T., 2018. Validation of new satellite rainfall products over the Upper Blue Nile Basin, Ethiopia. *Atmos. Meas. Tech.* 11, 1921–1936. <https://doi.org/10.5194/amt-11-1921-2018>
- Ayyad, S., Al Zayed I. S., Ha, V.T.T., Ribbe, L., 2019. The Performance of Satellite-Based Actual Evapotranspiration Products and the Assessment of Irrigation Efficiency in Egypt. *Water*, 11(9), 1913. doi: <https://doi.org/10.3390/w11091913>
- Baez-Villanueva, O.M., Zambrano-Bigiarini, M., Beck, H.E., McNamara, I., Ribbe, L., Nauditt, A., Birkel, C., Verbist, K., Giraldo-Osorio, J.D., Xuan Thinh, N., 2020. RF-MEP: A novel Random Forest method for merging gridded precipitation products and ground-based measurements. *Remote Sens. Environ.* 239. <https://doi.org/10.1016/j.rse.2019.111606>
- Baez-Villanueva, O.M., Zambrano-Bigiarini, M., Ribbe, L., Nauditt, A., Giraldo-Osorio, J.D., Thinh, N.X., 2018. Temporal and spatial evaluation of satellite rainfall estimates over different regions in Latin-America. *Atmos. Res.* 213, 34–50. <https://doi.org/10.1016/J.ATMOSRES.2018.05.011>
- Bai, P., Liu, X., 2018. Evaluation of five satellite-based precipitation products in two gauge-scarce basins on the Tibetan Plateau. *Remote Sens.* 10. <https://doi.org/10.3390/RS10081316>
- Bajracharya, S.R., Palash, W., Shrestha, M.S., Khadgi, V.R., Duo, C., Das, P.J., Dorji, C., Bajracharya, S.R., Palash, W., Shrestha, M.S., Khadgi, V.R., Duo, C., Das, P.J., Dorji, C., 2015. Systematic Evaluation of Satellite-Based Rainfall Products over the Brahmaputra Basin for Hydrological Applications. *Adv. Meteorol.* 2015. <https://doi.org/10.1155/2015/398687>
- Barbier, E.B., 2013. *Economics, natural-resource scarcity and development*. London: Routledge.
- Barnes, J., 2017. The future of the Nile: climate change, land use, infrastructure management, and treaty negotiations in a transboundary river basin. *WIREs Clim Change*, 8:e449. doi: [10.1002/wcc.449](https://doi.org/10.1002/wcc.449)
- Basheer, M., Elagib, N.A., 2018. Sensitivity of Water-Energy Nexus to dam operation: A Water-Energy Productivity concept. *Sci. Total Environ.* 616–617, 918–926. <https://doi.org/10.1016/j.scitotenv.2017.10.228>
- Basheer, M., Elagib, N.A., 2019. Performance of satellite-based and GPCP 7.0 rainfall products in an extremely data-scarce country in the Nile Basin. *Atmos. Res.* 215, 128–140. <https://doi.org/10.1016/J.ATMOSRES.2018.08.028>
- Basheer, M., Wheeler, K.G., Ribbe, L., Majdalawi, M., Abdo, G., Zagona, E.A., 2018. Quantifying and evaluating the impacts of cooperation in transboundary river basins on the Water-Energy-Food nexus: The Blue Nile Basin. *Sci. Total Environ.* 630, 1309–1323. <https://doi.org/10.1016/J.SCITOTENV.2018.02.249>
- Bashir, M.A., Dawelbeit, M.I., Eltom, M.O., and Tanakamaru, H., 2015. Performance of different tillage implements and their effects on sorghum and maize grown in Gezira

- vertisols, Sudan. *International Journal of Scientific and Technology Research*, 4 (4), 237–242.
- Bashir, M.A., Tanakamaru, H., Tada, A., and Khalid, A.E., 2011. Remote sensing for assessing water management and irrigation performance in the arid environment of the Gezira scheme, Sudan. *Journal of Environmental Sciences and Engineering*, 5, 344–356.
- Bastiaanssen, W., Karimi, P., Rebelo, L.-M., Duan, Z., Senay, G., Muthuwatte, L., Smakhtin, V., 2014. Earth Observation Based Assessment of the Water Production and Water Consumption of Nile Basin Agro-Ecosystems. *Remote Sens.* 6, 10306–10334. doi.org/10.3390/rs61110306
- Basu, S., Ramegowda, V., Kumar, A., and Pereira, A., 2016. Plant adaptation to drought stress. *F1000Res.*, 5: F1000 Faculty Rev-1554. doi: 10.12688/f1000research.7678.1.
- Bauer, A. and Black, A.L., 1994. Quantification of the effect of soil organic matter content on soil productivity. *Soil Science Society of America Journal*, 58 (1), 185. doi:10.2136/sssaj1994.03615995005800010027x
- Bayissa, Y., Tadesse, T., Demisse, G., Shiferaw, A., 2017. Evaluation of satellite-based rainfall estimates and application to monitor meteorological drought for the upper Blue Nile Basin, Ethiopia. *Remote Sens.* 9:669. https://doi.org/10.3390/rs9070669.
- Bayissa, Y.A., Tadesse, T., Svoboda, M., Wardlow, B., Poulsen, C., Swigart, J., Van Andel, S.J., 2019. Developing a satellite-based combined drought indicator to monitor agricultural drought: a case study for Ethiopia. *GIScience Remote Sens.* 56, 718–748. https://doi.org/10.1080/15481603.2018.1552508
- Beck, H.E., van Dijk, A.I.J.M., Levizzani, V., Schellekens, J., Miralles, D.G., Martens, B., de Roo, A., 2017. MSWEP: 3-hourly 0.25° global gridded precipitation (1979–2015) by merging gauge, satellite, and reanalysis data. *Hydrol. Earth Syst. Sci.* 21, 589–615. https://doi.org/10.5194/hess-2016-236
- Beck, H.E., Wood, E.F., McVicar, T.R., Zambrano-Bigiarini, M., Alvarez-Garreton, C., Baez-Villanueva, O.M., Sheffield, J., Karger, D.N., 2019. Bias correction of global high-resolution precipitation climatologies using streamflow observations from 9372 catchments. *J. Clim.* https://doi.org/10.1175/jcli-d-19-0332.1
- Betrie, G.D., Mohamed, Y.A., van Griensven A., and Srinivasan, R., 2011. Sediment management modelling in the Blue Nile Basin using SWAT model. *Hydrol. Earth Syst. Sci.*, 15, 807–818. Available online at: www.hydrol-earth-syst-sci.net/15/807/2011/ doi:10.5194/hess-15-807-2011 (accessed 25.12.2019)
- Beyene, T., Lettenmaier, D.P., Kabat, P., 2010a. Hydrologic impacts of climate change on the Nile River Basin: implications of the 2007 IPCC scenarios. *Clim. Change* 100, 433–461. https://doi.org/10.1007/s10584-009-9693-0
- Bhuiyan, C., Saha, A.K., Bandyopadhyay, N., Kogan, F.N., 2017. Analyzing the impact of thermal stress on vegetation health and agricultural drought – a case study from Gujarat, India. *GIScience Remote Sens.* 54, 678–699. https://doi.org/10.1080/15481603.2017.1309737.
- Bicciato, F. and Faggi, P., 1995. Gezira Scheme between state and market: some remarks on the privatization of irrigation in Sudan. *GeoJournal*, 37 (1), 101–104. doi:10.1007/BF00814890
- Biro, K., Pradhan, B., Buchroithner, M., Makeschin, F., 2013. Land use/land cover change analysis and its impact on soil properties in the northern part of Gadarif region, Sudan. *L. Degrad. Dev.* 24, 90–102. https://doi.org/10.1002/ldr.1116.
- Birthal, P.S., Negi, D.S., Jha, and Singh, D., 2014. Income sources of farm households in India: determinants, distributional consequences and policy implications. *Agricultural Economics Research Review*, 27 (1), 37–48. doi:10.5958/j.0974-0279.27.1.003
- Bitew, M.M., Gebremichael, M., Ghebremichael, L.T., Bayissa, Y. a., 2012. Evaluation of satellite-based rainfall estimates and application to monitor meteorological drought for

- the Upper Blue Nile Basin, Ethiopia. *J. Hydrometeorol.* 13, 338–350. <https://doi.org/10.1175/2011JHM1292.1>
- Blackmore, D., and Whittington, D., 2008. Opportunities for Cooperative Water Resources Development on the Eastern Nile: Risks and Rewards. Nile Basin Initiative (NBI). Available online at: www.entospace.nilebasin.org/bitstream/handle/20.500.12351/173/19_JMP_Scoping_Study.pdf?sequence=1 (accessed on 20.07.2019).
- Blair, P. and Buytaert, W., 2016. Socio-hydrological modelling: a review asking why, what and how? *Hydrology and Earth System Sciences*, 20 (1), 443–478. doi:10.5194/hess-20-443-2016
- Bradford, J.B., Schlaepfer, D.R., Lauenroth, W.K., Yackulic, C.B., Duniway, M., Hall, S., Jia, G., Jamiyansharav, K., Munson, S.M., Wilson, S.D., Tietjen, B., 2017. Future soil moisture and temperature extremes imply expanding suitability for rainfed agriculture in temperate drylands. *Sci. Rep.* 7, 12923. <https://doi.org/10.1038/s41598-017-13165-x>.
- Bratchell, N., 1989. Cluster analysis. *Chemom. Intell. Lab. Syst.* 6, 105–125. [https://doi.org/10.1016/0169-7439\(87\)80054-0](https://doi.org/10.1016/0169-7439(87)80054-0)
- Breiman, L., Friedman, J., Stone, C.J., Olshen, R.A., 1984. Classification and regression trees. Belmont, CA: Wadsworth.
- Brooks, N., 2006. Cultural Responses to Aridity in the Middle Holocene and Increased Social Complexity. *Quaternary International*, 151, 29–49
- Brown, C., Lall, U., 2006. Water and economic development: The role of variability and a framework for resilience. *Nat. Resour. Forum* 30, 306–317.
- Burke, M., Lobell, D.B., and Turner, B.L., 2017. Satellite-based assessment of yield variation and its determinants in smallholder African systems. *Proceedings of the National Academy of Sciences of the United States of America*, 114 (9), 2189–2194. doi:10.1073/pnas.1616919114
- Burton, C., Rifai, S., Malhi, Y., 2018. Inter-comparison and assessment of gridded climate products over tropical forests during the 2015/2016 El Niño. *Philos. Trans. R. Soc. B Biol. Sci.* 373. <https://doi.org/10.1098/rstb.2017.0406>
- Bussmann, A., Elagib, N.A., Fayyad, M., and Ribbe, L., 2016. Sowing date determinants for Sahelian rainfed agriculture in the context of agricultural policies and water management. *Land Use Policy*, 52, 316–328. doi:10.1016/j.landusepol.2015.12.007
- Cao, Y., Zhang, W., Wang, W., 2018. Evaluation of TRMM 3B43 data over the Yangtze River Delta of China. *Sci. Rep.* 8, 5290. <https://doi.org/10.1038/s41598-018-23603-z>
- Casse, C., Gosset, M., Peugeot, C., Pedinotti, V., Boone, A., Tanimoun, B.A., Decharme, B., 2015. Potential of satellite rainfall products to predict Niger River flood events in Niamey. *Atmos. Res.* 163, 162–176. <https://doi.org/10.1016/j.atmosres.2015.01.010>
- CBS (Central Bureau of Statistics), 2008. Statistical Year Book for the Year 2007.
- Chapagain, T., Good, A., 2015. Yield and production gaps in rainfed wheat, barley, and canola in Alberta. *Front. Plant Sci.* 6, 990. <https://doi.org/10.3389/fpls.2015.00990>.
- Chen, S., Liu, H., You, Y., Mullens, E., Hu, J., Yuan, Y., Huang, M., He, L., Luo, Y., Zeng, X., Tang, G., Hong, Y., 2014. Evaluation of high-resolution precipitation estimates from satellites during July 2012 Beijing flood event using dense rain gauge observations. *PLoS One* 9, e89681. <https://doi.org/10.1371/journal.pone.0089681>
- Chen, T., Ren, L., Yuan, F., Yang, X., Jiang, S., Tang, T., Liu, Y., Zhao, C., Zhang, L., 2017. Comparison of Spatial Interpolation Schemes for Rainfall Data and Application in Hydrological Modeling. *Water* 9, 342. <https://doi.org/10.3390/w9050342>
- Chen, T., Van Der Werf, G.R., De Jeu, R.A.M., Wang, G., Dolman, A.J., 2013. A global analysis of the impact of drought on net primary productivity. *Hydrol. Earth Syst. Sci.* 17: 3885–3894. <https://doi.org/10.5194/hess-17-3885-2013>.

- Cheung, W.H., Senay, G.B., Singh, A., 2008. Trends and spatial distribution of annual and seasonal rainfall in Ethiopia. *Int. J. Climatol.* 28, 1723–1734. <https://doi.org/10.1002/joc.1623>
- Chintalapudi, S., Sharif, H.O., Xie, H., 2014. Sensitivity of distributed hydrologic simulations to ground and satellite based rainfall products. *Water (Switzerland)* 6, 1221–1245. <https://doi.org/10.3390/w6051221>
- Chipanshi, A.C., Chanda, R., Totolo, O., 2003. Vulnerability assessment of the maize and sorghum crops to climate change in Botswana. *Clim. Change* 61, 339–360. <https://doi.org/10.1023/B:CLIM.0000004551.55871.eb>
- Ciais, P., Bombelli, A., Williams, M., Piao, S.L., Chave, J., Ryan, C.M., Henry, M., Brender, P., Valentini, R., 2011. The carbon balance of Africa: synthesis of recent research studies. *Philos. Trans. A. Math. Phys. Eng. Sci.* 369:2038–2057. <https://doi.org/10.1098/rsta.2010.0328>
- Coffel, E. D., Keith, B., Lesk, C., Horton, R. M., Bower, E., Lee, J., & Mankin, J. S., 2019. Future hot and dry years worsen Nile Basin water scarcity despite projected precipitation increases. *Earth's Future*, 7, 967–977. doi. org/10.1029/2019EF001247
- Connif, R., 2017. The Vanishing Nile: A Great River Faces a Multitude of Threats. *Yale Environment* 360. Available online at: www.e360.yale.edu/features/vanishing-nile-a-great-river-faces-a-multitude-of-threats-egypt-dam (Accessed online at 09.11.2019).
- Conway, D., 2000. The Climate and Hydrology of the Upper Blue Nile River. *Geogr. J.* 166, 49–62. <https://doi.org/10.1111/j.1475-4959.2000.tb00006.x>
- Cosgrove, W.J., Loucks, D.P., 2015. Water management: Current and future challenges and research directions. *Water Resour. Res.* 51, 4823–4839. <https://doi.org/10.1002/2014WR016869>
- Dam, R.F., Mehdi, B.B., Burgess, M.S.E., Madramootoo, C.A., Mehuys, G.R., and Callum, I.R., 2005. Soil bulk density and crop yield under eleven consecutive years of corn with different tillage and residue practices in a sandy loam soil in central Canada. *Soil and Tillage Research*, 84 (1), 41–53. doi:10.1016/j.still.2004.08.006
- Davis, K.F., Gephart, J.A., Emery, K.A., Leach, A.M., Galloway, J.N., and D’Odorico, P., 2016. Meeting future food demand with current agricultural resources. *Global Environmental Change*, 39, 125–132. doi:10.1016/j.gloenvcha.2016.05.004
- Dee, D.P., Uppala, S.M., Simmons, A.J., Berrisford, P., Poli, P., Kobayashi, S., Andrae, U., Balmaseda, M.A., Balsamo, G., Bauer, P., Bechtold, P., Beljaars, A.C.M., van de Berg, L., Bidlot, J., Bormann, N., Delsol, C., Dragani, R., Fuentes, M., Geer, A.J., Haimberger, L., Healy, S.B., Hersbach, H., Hólm, E. V., Isaksen, L., Kållberg, P., Köhler, M., Matricardi, M., McNally, A.P., Monge-Sanz, B.M., Morcrette, J.-J., Park, B.-K., Peubey, C., de Rosnay, P., Tavolato, C., Thépaut, J.-N., Vitart, F., 2011. The ERA-Interim reanalysis: configuration and performance of the data assimilation system. *Q. J. R. Meteorol. Soc.* 137, 553–597. <https://doi.org/10.1002/qj.828>
- Degefu, D. M., and He, W., 2016. Water bankruptcy in the mighty Nile river basin. *Sustainable Water Resources Management*, 2 (1), 29-37.
- DeLucia, E.H., Drake, J.E., Thomas, R.B., Gonzalez-Meler, M., 2007. Forest carbon use efficiency: is respiration a constant fraction of gross primary production? *Glob. Chang. Biol.* 13:1157–1167. <https://doi.org/10.1111/j.1365-2486.2007.01365.x>
- Dessu, S., 2019. The battle for the Nile with Egypt over Ethiopia’s Grand Renaissance Dam has just begun. *Quartz Africa*. www.qz.com/africa/1559821/ethiopias-grand-renaissance-dam-battles-egypt-sudan-on-the-nile/ (Accessed on 09.11.2019).
- Devendra, C., 2012. Rainfed areas and animal agriculture in Asia: the wanting agenda for transforming productivity growth and rural poverty. *Asian-Australasian J. Anim. Sci.* 25, 122–142. <https://doi.org/10.5713/ajas.2011.r.09>

- Dinku, T., Ceccato, P., Grover-Kopec, E., Lemma, M., Connor, S.J., Ropelewski, C.F., 2007. Validation of satellite rainfall products over East Africa's complex topography. *Int. J. Remote Sens.* 28, 1503–1526. <https://doi.org/10.1080/01431160600954688>
- Dinku, T., Funk, C., Peterson, P., Maidment, R., Tadesse, T., Gadain, H., Ceccato, P., 2018. Validation of the CHIRPS satellite rainfall estimates over eastern Africa. *Q. J. R. Meteorol. Soc.* 144, 292–312. <https://doi.org/10.1002/qj.3244>
- Dittami, S., 2009. Online Calculator for Shapiro-Wilk Normality Test. <http://sdittami.altervista.org/shapiroTest/ShapiroTest.html>.
- Dong, G., Guo, J., Chen, J., Sun, G., Gao, S., Hu, L., Wang, Y., 2011. Effects of spring drought on carbon sequestration, evapotranspiration and water use efficiency in the Songnen Meadow Steppe in Northeast China. *Ecohydrology* 4, 211–224.
- Dong, W., Zhang, X., Wang, H., Dai, X., Sun, X., Qiu, W., and Yang, F., 2012. Effect of different fertilizer application on the soil fertility of paddy soils in red soil region of southern China. *PLoS One*, 7 (9), e44504. doi:10.1371/journal.pone.0044504
- Driscoll, P., Lecky, F., Crosby, M., 2000. An introduction to everyday statistics--2. *J. Accid. Emerg. Med.* 17, 274–81. <https://doi.org/10.1136/emj.17.4.274>
- Duan, Z., Liu, J., Tuo, Y., Chiogna, G., Disse, M., 2016. Evaluation of eight high spatial resolution gridded precipitation products in Adige Basin (Italy) at multiple temporal and spatial scales. *Sci. Total Environ.* 573, 1536–1553. <https://doi.org/10.1016/J.SCITOTENV.2016.08.213>
- El Karouri, M.O.H., 2010. Mechanized Rainfed Agriculture in the Sudan: Present Situation and Future Development, 1st ed. Al Hana Commercial Printing Press, Khartoum.
- Elagib, N.A., 2009. Assessment of drought across central Sudan using UNEP dryness ratio. *Hydrol. Res.* 40, 481. <https://doi.org/10.2166/nh.2009.016>.
- Elagib, N.A., 2010. Trends in intra-and inter-annual temperature variabilities across Sudan. *Ambio* 39, 413–429. <https://doi.org/10.1007/s13280-010-0042-3>.
- Elagib, N.A., 2013. Meteorological drought and crop yield in sub-Saharan Sudan. *Int. J. Water Resour. Arid Environ.* 2 (3), 164–171.
- Elagib, N.A., 2014. Development and application of a drought risk index for food crop yield in Eastern Sahel. *Ecological Indicators*, 43, 114–125. doi:10.1016/j.ecolind.2014.02.033
- Elagib, N.A., 2015. Drought risk during the early growing season in Sahelian Sudan. *Natural Hazards*, 79 (3), 1549–1566. doi:10.1007/s11069-015-1913-5
- Elagib, N.A., Alvi, S.H., Mansell, M.G., 1999. Day-length and extraterrestrial radiation for Sudan: a comparative study. *Sol. Energy Mater. Sol. Cells* 20, 93–109. <https://doi.org/10.1080/01425919908914348>.
- Elagib, N.A., Elhag, M.M., 2011. Major climate indicators of ongoing drought in Sudan. *J. Hydrol.* 409, 612–625. <https://doi.org/10.1016/j.jhydrol.2011.08.047>.
- Elagib, N.A., Khalifa, M., Rahma, A.E., Babker, Z., Gamaledin, S.I., 2019. Performance of major mechanized rainfed agricultural production in Sudan: Sorghum vulnerability and resilience to climate since 1970. *Agric. For. Meteorol.* 276–277, 107640. <https://doi.org/10.1016/J.AGRFORMET.2019.107640>
- Elagib, N.A., Mansell, M.G., 2000. Climate impacts of environmental degradation in Sudan. *GeoJournal* 50, 311–327. <https://doi.org/10.1023/A:1011071917001>.
- Elawad, S.M., Elkhiedir, E.E., Amassaib, M.A., Naim, A.M.El, 2017. Government policies and food security in Sudan (1970-2007): incentives, efficiencies and comparative advantage for sorghum producing in mechanised rain-fed subsector. *Acad. J. Life Sci.* 3, 12–17.
- Elnmer, A., Khadr, M., Tawfik, A., 2018. Using Remote Sensing Techniques for Estimating Water Stress Index for Central of Nile Delta, in: *IOP Conference Series: Earth and Environmental Science*. Institute of Physics Publishing. <https://doi.org/10.1088/1755-1315/151/1/012026>

- El-Sharkawy, M., 2007. Physiological characteristics of cassava tolerance to prolonged drought in the tropics: Implications for breeding cultivars adapted to seasonally dry and semiarid environments. *Braz. J. Plant Physiol.*, 19(4): 257-286. <https://doi.org/10.1590/S1677-04202007000400003>
- Environmental Protection Council (EPA), 2010. Africa Review Report On Drought And Desertification. United Nations Economic and Social Council. Available at: http://www.un.org/esa/sustdev/csd/csd16/rim/eca_bg3.pdf (accessed 5.12.2019).
- Erkossa, T., Stahr, K., and Gaiser, T., 2006. Effect of different methods of land preparation on runoff, soil and nutrient losses from a Vertisol in the Ethiopian highlands. *Soil Use and Management*, 21 (2), 253–259. doi:10.1111/j.1475-2743.2005.tb00132.x
- ESA, 2015. Satellite Earth observations in support of climate information challenges, CEOS Earth Observation handbook for COP21.
- ESRI, 2014. ArcGIS desktop. Redlands, CA: Environmental Systems Research Institute (ESRI). Available from: <https://www.esri.com/en-gb/about/overview> [Accessed 4 Nov. 2019].
- FAO, 2005. Irrigation in Africa in figures. AQUASTAT Survey 2005, FAO, Rome. Food and Agriculture Organization of the United Nations.
- FAO, 2011. Agricultural Water Use Projections in the Nile basin 2030: Comparison with the Food for Thought (F4T) Scenarios - Projections Reports. United Nations Food and Agriculture Organization (FAO). Available online at: www.fao.org/publications/card/en/c/355a7c33-bbce-5307-8169-9ba82bc3e522/ (Accessed on 07.10.2019).
- FAO, 2017. The future of food and agriculture - trends and challenges. Rome, Italy: Food and Agriculture Organization of the United Nations.
- FAO, 2018. FAOSTAT - Crop Production Data [WWW Document]. URL <http://www.fao.org/faostat/en/#data> (Accessed 3.1.19).
- FAO, IFAD, UNICEF, WFP, WHO, 2019. The State of Food Security and Nutrition in the World 2019. Safeguarding against economic slowdowns and downturns. Rome.
- FAOSTAT, 2017. Crop production data. Food and Agriculture Organization of the United Nations (FAO). Available online at: <http://www.fao.org/faostat/en/#data/QC>, (Accessed date: 3.1.2019).
- Fereres, E., Orgaz, F., Gonzalez-Dugo, V., 2011. Reflections on food security under water scarcity. *J. Exp. Bot.* 62, 4079–4086. <https://doi.org/10.1093/jxb/err165>.
- Fernández-Prieto, D., Van Oevelen, P., Su, Z., Wagner, W., 2012. Advances in Earth observation for water cycle science. *Hydrol. Earth Syst. Sci* 16, 543–549. <https://doi.org/10.5194/hess-16-543-2012>
- Fick, S. E. and Hijmans, R. J., 2017. Worldclim 2: New 1-km spatial resolution climate surfaces for global land areas. *International Journal of Climatology*. www.rmets.onlinelibrary.wiley.com/doi/full/10.1002/joc.5086 (Accessed online on 21.06.2019).
- Field, C.B., Randerson, J.T., and Malmström, C.M., 1995. Global net primary production: combining ecology and remote sensing. *Remote Sensing of Environment*, 51 (1), 74–88. doi:10.1016/0034-4257(94)00066-V
- Finger, R., 2011. Food security: close crop yield gap. *Nature*, 480 (7375), 39. doi:10.1038/480039e
- Foley, J.A., Ramankutty, N., Brauman, K.A., Cassidy, E.S., Gerber, J.S., Johnston, M., Mueller, N.D., O’Connell, C., Ray, D.K., West, P.C., Balzer, C., Bennett, E.M., Carpenter, S.R., Hill, J., Monfreda, C., Polasky, S., Rockstrom, J., Sheehan, J., Siebert, S., Tilman, D., Zaks, D.P.M., 2011. Solutions for a cultivated planet. *Nature* 478, 337–342. <https://doi.org/10.1038/nature10452>.

- Friedl, M.A., Sulla-Menashe, D., Tan, B., Schneider, A., Ramankutty, N., Sibley, A., Huang, X., 2010. MODIS collection 5 global land cover: algorithm refinements and characterization of new datasets. *Remote Sens. Environ.* 114:168–182. <https://doi.org/10.1016/j.rse.2009.08.016>.
- Fritz, S., See, L., Bayas, J.C.L., Waldner, F., Jacques, D., Becker-Reshef, I., Whitcraft, A., Baruth, B., Bonifacio, R., Crutchfield, J., Rembold, F., Rojas, O., Schucknecht, A., Van der Velde, M., Verdin, J., Wu, B., Yan, N., You, L., Gilliams, S., Mücher, S., Tetrault, R., Moorthy, I., McCallum, I., 2019. A comparison of global agricultural monitoring systems and current gaps. *Agric. Syst.* 168, 258–272. <https://doi.org/10.1016/j.agry.2018.05.010>
- Frolking, S., 1997. Sensitivity of spruce/moss boreal forest net ecosystem productivity to seasonal anomalies in weather. *J. Geophys. Res.* 102 (D24), 29053–29064.
- Funk, C., Peterson, P., Landsfeld, M., Pedreros, D., Verdin, J., Shukla, S., Husak, g., Rowland, J., Harrison, L., Hoell, A., and Michaelsen, J., 2015. The climate hazards infrared precipitation with stations—a new environmental record for monitoring extremes. *Scie. Data*, 2, 150066. doi:10.1038/sdata.2015.66
- Gabriele, S., Chiaravalloti, F., Procopio, A., 2017. Radar-rain-gauge rainfall estimation for hydrological applications in small catchments. *Adv. Geosci* 44, 61–66. <https://doi.org/10.5194/adgeo-44-61-2017>
- Gao, F., Zhang, Y., Ren, X., Yao, Y., Hao, Z., Cai, W., 2018. Evaluation of CHIRPS and its application for drought monitoring over the Haihe River Basin, China. *Nat. Hazards* 92, 155–172. <https://doi.org/10.1007/s11069-018-3196-0>
- Garcia, P., Offutt, S.E., Pinar, M., Changnon, S.A., Garcia, P., Offutt, S.E., Pinar, M., Changnon, S.A., 1987. Corn yield behavior: effects of technological advance and weather-conditions. *J. Clim. Appl. Meteorol.* 26, 1092–1102. [https://doi.org/10.1175/1520-0450\(1987\)026<1092:CYBEOT>2.0.CO;2](https://doi.org/10.1175/1520-0450(1987)026<1092:CYBEOT>2.0.CO;2).
- Ge, S., Zhu, Z., and Jiang, Y., 2018. Long-term impact of fertilization on soil pH and fertility in an apple production system. *Journal of Soil Science and Plant Nutrition*, 18 (1), 282–293.
- Gebrechorkos, S.H., Hülsmann, S., Bernhofer, C., 2018. Evaluation of multiple climate data sources for managing environmental resources in East Africa. *Hydrol. Earth Syst. Sci.* 22, 4547–4564. <https://doi.org/10.5194/hess-22-4547-2018>
- Gebrekiros, G., Araya, A., Yemane, T., 2015. Modeling impact of climate change and variability on Sorghum production in southern zone of Tigray, Ethiopia. *J. Earth Sci. Clim. Change* 07, 1–10. <https://doi.org/10.4172/2157-7617.1000322>.
- Gebremicael, T.G., Mohamed, Y.A., Betrie, G.D., van der Zaag, P., and Teferi, E., 2013. Trend analysis of runoff and sediment fluxes in the Upper Blue Nile basin: a combined analysis of statistical tests, physically-based models and landuse maps. *J. Hydrol.*, 482 (2013), pp. 57–68, 10.1016/j.jhydrol.2012.12.023
- Gelaro, R., McCarty, W., Suárez, M.J., Todling, R., Molod, A., Takacs, L., Randles, C.A., Darmenov, A., Bosilovich, M.G., Reichle, R., Wargan, K., Coy, L., Cullather, R., Draper, C., Akella, S., Buchard, V., Conaty, A., da Silva, A.M., Gu, W., Kim, G.-K., Koster, R., Lucchesi, R., Merkova, D., Nielsen, J.E., Partyka, G., Pawson, S., Putman, W., Rienecker, M., Schubert, S.D., Sienkiewicz, M., Zhao, B., Gelaro, R., McCarty, W., Suárez, M.J., Todling, R., Molod, A., Takacs, L., Randles, C.A., Darmenov, A., Bosilovich, M.G., Reichle, R., Wargan, K., Coy, L., Cullather, R., Draper, C., Akella, S., Buchard, V., Conaty, A., Silva, A.M. da, Gu, W., Kim, G.-K., Koster, R., Lucchesi, R., Merkova, D., Nielsen, J.E., Partyka, G., Pawson, S., Putman, W., Rienecker, M., Schubert, S.D., Sienkiewicz, M., Zhao, B., 2017. The Modern-Era Retrospective Analysis for Research and Applications, Version 2 (MERRA-2). *J. Clim.* 30, 5419–5454. <https://doi.org/10.1175/JCLI-D-16-0758.1>

- Ghasemi, A., Zahediasl, S., 2012. Normality tests for statistical analysis: a guide for nonstatisticians. *Int. J. Endocrinol. Metab.* 10 (2):486–489. <https://doi.org/10.5812/ijem.3505>.
- Gidey, E., Dikinya, O., Sebege, R., Segosebe, E., Zenebe, A., 2018. Analysis of the long-term agricultural drought onset, cessation, duration, frequency, severity and spatial extent using Vegetation Health Index (VHI) in Raya and its environs, Northern Ethiopia. *Environ. Syst. Res.* 7. <https://doi.org/10.1186/s40068-018-0115-z>
- Gillette, H.P., 1950. A creeping drought under way. *Water Sew. Works* 104–105.
- Gleason, C.J., Wada, Y., Wang, J., 2018. A Hybrid of Optical Remote Sensing and Hydrological Modeling Improves Water Balance Estimation. *J. Adv. Model. Earth Syst.* 10, 2–17. <https://doi.org/10.1002/2017MS000986>
- Godfray, H.C.J., Beddington, J.R., Crute, I.R., Haddad, L., Lawrence, D., Muir, J.F., Pretty, J., Robinson, S., Thomas, S.M., Toulmin, C., 2010. Food security: the challenge of feeding 9 billion people. *Science* 327, 812–818. <https://doi.org/10.1126/science.1185383>.
- Goovaerts, P., 2000. Geostatistical approaches for incorporating elevation into the spatial interpolation of rainfall. *J. Hydrol.* 228, 113–129. [https://doi.org/10.1016/S0022-1694\(00\)00144-X](https://doi.org/10.1016/S0022-1694(00)00144-X)
- Guo, H.D., Zhang, L., Zhu, L.W., 2015. Earth observation big data for climate change research. *Adv. Clim. Chang. Res.* 6, 108–117. <https://doi.org/10.1016/j.accre.2015.09.007>
- Habib, E., ElSaadani, M., Haile, A.T., Habib, E., ElSaadani, M., Haile, A.T., 2012a. Climatology-Focused Evaluation of CMORPH and TMPA Satellite Rainfall Products over the Nile Basin. *J. Appl. Meteorol. Climatol.* 51, 2105–2121. <https://doi.org/10.1175/JAMC-D-11-0252.1>
- Habib, E., Haile, A.T., Tian, Y., Joyce, R.J., Habib, E., Haile, A.T., Tian, Y., Joyce, R.J., 2012b. Evaluation of the High-Resolution CMORPH Satellite Rainfall Product Using Dense Rain Gauge Observations and Radar-Based Estimates. *J. Hydrometeorol.* 13, 1784–1798. <https://doi.org/10.1175/JHM-D-12-017.1>
- Hamm, N.A.S., Soares Magalhães, R.J., Clements, A.C.A., 2015. Earth Observation, Spatial Data Quality, and Neglected Tropical Diseases. *PLoS Negl. Trop. Dis.* 9, e0004164. <https://doi.org/10.1371/journal.pntd.0004164>
- Hargreaves, G.H., Samani, Z.A., 1985. Reference crop evapotranspiration from temperature. *Appl. Eng. Agric.* 1, 96–99. <https://doi.org/10.13031/2013.26773>.
- Hargreaves, G.L., Hargreaves, G.H., Riley, J.P., 1985. Agricultural benefits for Senegal River Basin. *J. Irrig. Drain. Eng.* 111, 113–124. [https://doi.org/10.1061/\(ASCE\)0733-9437\(1985\)111:2\(113\)](https://doi.org/10.1061/(ASCE)0733-9437(1985)111:2(113)).
- Harris, I., Jones, P.D., Osborn, T.J., Lister, D.H., 2014. Updated high-resolution grids of monthly climatic observations - the CRU TS3.10 Dataset. *Int. J. Climatol.* 34, 623–642. <https://doi.org/10.1002/joc.3711>
- Hassan, T.A., 2015. Economic analysis of factors affecting the farmer income under traditional farming system in South Darfur State – Sudan. *Journal of Agricultural Science and Engineering*, 1 (3), 114–119.
- Heinz, S., 1983. Sadd el-Ali, der Hochdamm von Assuan (Sadd el-Ali, the High Dam of Aswan). *Geowissenschaften in Unserer Zeit (in German)*. 1 (2): 51–85.
- Herman, A., Kumar, V.B., Arkin, P.A., Kousky, J. V., 1997. Objectively determined 10-day African rainfall estimates created for famine early warning systems. *Int. J. Remote Sens.* 18, 2147–2159. <https://doi.org/10.1080/014311697217800>
- Hermance, J.F., Sulieman, H.M., Mustafa, A.G., 2016. Predicting intra-seasonal fluctuations of NDVI phenology from daily rainfall in the East Sahel: a simple linear reservoir model. *Int. J. Remote Sens.* 37, 3293–3321. <https://doi.org/10.1080/01431161.2016.1196841>.

- Hilhorst, B., Burke, J., Hoogeveen, J., Fremken, K., Faures, J.-M., Gross, D., 2011. Information Products for Nile Basin Water Resources Management Synthesis Report. FAO Rome, Italy 130.
- Hirpa, F.A., Gebremichael, M., Hopson, T., Hirpa, F.A., Gebremichael, M., Hopson, T., 2010. Evaluation of High-Resolution Satellite Precipitation Products over Very Complex Terrain in Ethiopia. *J. Appl. Meteorol. Climatol.* 49, 1044–1051. <https://doi.org/10.1175/2009JAMC2298.1>
- Hoff, H., 2011. Background paper for the Bonn 2011 Nexus Conference: The water, energy and food security nexus. Stock. Environ. Institute, Stock.
- Holben, B.N., 1986. Characteristics of maximum-value composite images from temporal AVHRR data. *Int. J. Remote Sens.* 7:1417–1434. <https://doi.org/10.1080/01431168608948945>.
- Holben, B.N., 1986. Characteristics of maximum-value composite images from temporal AVHRR data. *International Journal of Remote Sensing*, 7 (11), 1417–1434. doi:10.1080/01431168608948945
- Holloway, R.E., Bertrand, I., Frischke, A.J., Brace, D.M., McLaughlin, M.J., Shepperd, W., 2001. Improving fertiliser efficiency on calcareous and alkaline soils with fluid sources of P, N and Zn. *Plant Soil* 236, 209–219. <https://doi.org/10.1023/A:1012720909293>
- Hong, Y., Hsu, K.-L., Sorooshian, S., Gao, X., 2004. Precipitation Estimation from Remotely Sensed Imagery Using an Artificial Neural Network Cloud Classification System. *Am. Meteorol. Soc.* 43, 1834–1852.
- Hu, Z., Hu, Q., Zhang, C., Chen, X., Li, Q., 2016. Evaluation of reanalysis, spatially interpolated and satellite remotely sensed precipitation data sets in central Asia. *J. Geophys. Res. Atmos.* 121, 5648–5663. <https://doi.org/10.1002/2016JD024781>
- Huang, L., Han, L., Liu, J., Wang, H., Chen, Z., 2017. A global examination of the response of ecosystem water-use efficiency to drought based on MODIS data. *Sci. Total Environ.* 601–602, 1097–1107.
- Huang, L., He, B., Chen, A., Wang, H., Liu, J., Lü, A., Chen, Z., 2016. Drought dominates the interannual variability in global terrestrial net primary production by controlling semi-arid ecosystems. *Sci. Rep.* 6, 24639.
- Huang, Y., Chen, Z. xin, Yu, T., Huang, X. zhi, Gu, X. Fa, 2018. Agricultural remote sensing big data: Management and applications. *J. Integr. Agric.* [https://doi.org/10.1016/S2095-3119\(17\)61859-8](https://doi.org/10.1016/S2095-3119(17)61859-8)
- Huffman, G.J., Adler, R.F., Morrissey, M.M., Bolvin, D.T., Curtis, S., Joyce, R., McGavock, B., Susskind, J., Huffman, G.J., Adler, R.F., Morrissey, M.M., Bolvin, D.T., Curtis, S., Joyce, R., McGavock, B., Susskind, J., 2001. Global Precipitation at One-Degree Daily Resolution from Multisatellite Observations. *J. Hydrometeorol.* 2, 36–50. [https://doi.org/10.1175/1525-7541\(2001\)002<0036:GPAODD>2.0.CO;2](https://doi.org/10.1175/1525-7541(2001)002<0036:GPAODD>2.0.CO;2)
- Huffman, G.J., Bolvin, D.T., Nelkin, E.J., Wolff, D.B., Adler, R.F., Gu, G., Hong, Y., Bowman, K.P., Stocker, E.F., Huffman, G.J., Bolvin, D.T., Nelkin, E.J., Wolff, D.B., Adler, R.F., Gu, G., Hong, Y., Bowman, K.P., Stocker, E.F., 2007. The TRMM Multisatellite Precipitation Analysis (TMPA): Quasi-Global, Multiyear, Combined-Sensor Precipitation Estimates at Fine Scales. *J. Hydrometeorol.* 8, 38–55. <https://doi.org/10.1175/JHM560.1>
- Huffman, G.J., Bolvin, D.T., Nelkin, E.J., Wolff, D.B., Adler, R.F., Gu, G., Hong, Y., Bowman, K.P., Stocker, E.F., Huffman, G.J., Bolvin, D.T., Nelkin, E.J., Wolff, D.B.,
- Hulme, M., 1990. The changing rainfall resources of Sudan. *Trans. Inst. Br. Geogr.* 15, 21. <https://doi.org/10.2307/623090>.
- Hulme, M., 2001. Climatic perspectives on Sahelian desiccation: 1973–1998. *Glob. Environ. Chang.* 11, 19–29. [https://doi.org/10.1016/S0959-3780\(00\)00042-X](https://doi.org/10.1016/S0959-3780(00)00042-X).

- Hulme, M., Trilsbach, A., 1989. The August 1988 storm over Khartoum: its climatology and impact. *Weather* 44, 82–90. <https://doi.org/10.1002/j.1477-8696.1989.tb06983.x>.
- Ibrahim, A.Z., Chamhuri, S., and Basri, A.T., 2013. Determining sources of income among paddy farmers in Muda irrigation area, Malaysia. *IOSR Journal of Humanities and Social Science (IOSR-JHSS)*, 17 (4), 100–105. doi:10.9790/0837-174100105
- Iqbal, A., Sadia, B., Khan, A.I., Awan, F.S., Kainth, R.A., Sadaqat, H.A., 2010. Biodiversity in the sorghum (*Sorghum bicolor* L. Moench) germplasm of Pakistan. *Genet. Mol. Res.* 9, 756–764. <https://doi.org/10.4238/vol9-2gmr741>.
- Ishag, K., Thornton, D., Tiffen, M., and Upton, M., 2007. Farm location and farmers' performance on the Hamza minor canal. *International Journal of Water Resources Development*, 7 (1), 2–15. doi:10.1080/07900629108722486
- Ito, A., Inatomi, M., 2012. Water-use efficiency of the terrestrial biosphere: a model analysis focusing on interactions between the global carbon and water cycles. *J. Hydrometeorol.* 13:681–694. <https://doi.org/10.1175/JHM-D-10-05034.1>.
- Jabloun, M., Sahli, A., 2012. WEAP-MABIA Tutorial - A Collection of Stand-alone Chapters to Aid in Learning the WEAP-MABIA Module. Available online at: https://www.bgr.bund.de/EN/Themen/Wasser/Projekte/abgeschlossen/TZ/Acsad_dss/tutorial_weap-mabia.pdf?__blob=publicationFile&v=2, (Accessed date: 13 November 2017).
- Jolliffe, I.T., Cadima, J., 2016. Principal component analysis: a review and recent developments. *Philos. Trans. A. Math. Phys. Eng. Sci.* 374, 20150202. <https://doi.org/10.1098/rsta.2015.0202>
- Joyce, R.J., Janowiak, J.E., Arkin, P.A., Xie, P., Joyce, R.J., Janowiak, J.E., Arkin, P.A., Xie, P., 2004. CMORPH: A Method that Produces Global Precipitation Estimates from Passive Microwave and Infrared Data at High Spatial and Temporal Resolution. *J. Hydrometeorol.* 5, 487–503. [https://doi.org/10.1175/1525-7541\(2004\)005<0487:CAMTPG>2.0.CO;2](https://doi.org/10.1175/1525-7541(2004)005<0487:CAMTPG>2.0.CO;2)
- Kaba, E., Philpot, W., Steenhuis, T., Tana Getis–Ord Gi, L., 2014. Evaluating suitability of MODIS-Terra images for reproducing historic sediment concentrations in water bodies: Lake Tana, Ethiopia. *Int. J. Appl. Earth Obs. Geoinf.* 26, 286–297. <https://doi.org/10.1016/j.jag.2013.08.001>
- Kanji, G.K., 1993. 100 Statistical Tests, first. ed. SAGE Publications, London, California, New Delhi.
- Karimi, P., Bastiaanssen, W.G.M., Molden, D., 2013. Water Accounting Plus (WA+)-a water accounting procedure for complex river basins based on satellite measurements. *Hydrol. Earth Syst. Sci* 17, 2459–2472. <https://doi.org/10.5194/hess-17-2459-2013>
- Karimi, P., Bastiaanssen, W.G.M., 2015. Spatial evapotranspiration, rainfall and land use data in water accounting – part 1: review of the accuracy of the remote sensing data. *Hydrol. Earth Syst. Sci.* 19:507–532. <https://doi.org/10.5194/hess-19-507-2015>.
- Karimi, P., Bastiaanssen, W.G.M., Molden, D., Cheema, M.J.M., 2013. Basin-wide water accounting based on remote sensing data: an application for the Indus Basin. *Hydrol. Earth Syst. Sci.* 17, 2473–2486. <https://doi.org/10.5194/hess-17-2473-2013>
- Keith, B., Enos, J., Cadets, G. B., Simmons, G., Copeland, D., and Cortizo, M., 2013. Limits to population growth and water resource adequacy in the Nile river basin, 1994–2100. In: *Proceedings of the 31st international conference of the system dynamics society, Cambridge*, 21–25 July 2013.
- Khalifa, M., Elagib, N.A., Ribbe, L., and Schneider, K., 2018. Spatio-temporal variations in climate, primary productivity and efficiency of water and carbon use of the land cover types in Sudan and Ethiopia. *Science of the Total Environment*, 624, 790–806. doi:10.1016/j.scitotenv.2017.12.090

- Kidd, C., 2001. Satellite rainfall climatology: a review. *Int. J. Climatol.* 21, 1041–1066. <https://doi.org/10.1002/joc.635>
- Kim, U., and Kaluarachchi, J.J., 2009. Climate change impacts on water resources in the upper Blue Nile river basin, Ethiopia. *Journal of the American Water Resources Association* 45 (6), 1361–1378.
- Kim, U., Kaluarachchi, J. J., Smakhtin, V. U., 2008. Climate change impacts on hydrology and water resources of the Upper Blue Nile River Basin, Ethiopia. Colombo, Sri Lanka: International Water Management Institute. 27p (IWMI Research Report 126)
- Kim, U., Kaluarachchi, J.J., Smakhtin, V.U., 2008. Climate change impacts on hydrology and water resources of the Upper Blue Nile River Basin, Ethiopia. IWMI Res. Reports.
- Kimenyi, M. S., and Mbaku, J. M., 2015. The limits of the new “Nile Agreement”. www.brookings.edu/blog/africa-in-focus/2015/04/28/the-limits-of-the-new-nile-agreement/ (Accessed on 09.11.2019).
- Kimes, P.K., Liu, Y., Neil Hayes, D., Marron, J.S., 2017. Statistical significance for hierarchical clustering. *Biometrics* 73, 811–821. <https://doi.org/10.1111/biom.12647>
- Kite, G.W., Pietroniro, A., 1996. Remote sensing applications in hydrological modelling. *Hydrol. Sci. J. Hydrometeorol.* 563. <https://doi.org/10.1080/02626669609491526>
- Knapp, A.K., Smith, M.D., 2001. Variation among biomes in temporal dynamics of aboveground primary production. *Science* 291:481–484. <https://doi.org/10.1126/science.291.5503.481>.
- Knol, A.B., Briggs, D.J., Lebet, E., 2010. Assessment of complex environmental health problems: Framing the structures and structuring the frameworks. *Sci. Total Environ.* 408, 2785–2794. <https://doi.org/10.1016/J.SCITOTENV.2010.03.021>
- Kogan, F.N., 1990. Remote sensing of weather impacts on vegetation in non-homogeneous areas. *Int. J. Remote Sens.* 11, 1405–1419. <https://doi.org/10.1080/01431169008955102>.
- Kotu, B.H., Alene, A., Manyong, V., Hoeschle-Zeledon, I., Larbi, A., 2017. Adoption and impacts of sustainable intensification practices in Ghana. *International Journal of Agricultural Sustainability*, 15 (5), 539–554. doi:10.1080/14735903.2017.1369619
- Kowalik, W., Dabrowska-Zielinska, K., Meroni, M., Raczka, T.U., and de Wit, A., 2014. Yield estimation using SPOT-VEGETATION products: a case study of wheat in European countries. *International Journal of Applied Earth Observation and Geoinformation*, 32, 228–239. doi:10.1016/j.jag.2014.03.011
- Kraus, E.B., 1977. Subtropical droughts and cross-equatorial energy transports. *Mon. Weather Rev.* 105, 1009–1018.
- Kroll, C., Warchold, A., and Prashan, P., 2019. Sustainable Development Goals (SDGs): Are we successful in turning trade-offs into synergies? *Palgrave Commun* 5, 140. <https://doi.org/10.1057/s41599-019-0335-5>
- Kuglitsch, F.G., Reichstein, M., Beer, C., Carrara, A., Ceulemans, R., Granier, A., Janssens, I.A., Koestner, B., Lindroth, A., Loustau, D., Matteucci, G., Montagnani, L., Moors, E.J., Papale, D., Pilegaard, K., Rambal, S., Rebmann, C., Schulze, E.D., Seufert, G., Verbeeck, H., Vesala, T., Aubinet, M., Bernhofer, C., Foken, T., Grünwald, T., Heinesch, B., Kutsch, W., Laurila, T., Longdoz, B., Miglietta, F., Sanz, M.J., Valentini, R., 2008. Characterisation of ecosystem water-use efficiency of European forests from eddy covariance measurements. *Biogeosci. Discuss.* 5:4481–4519. <https://doi.org/10.5194/bgd-5-4481-2008>.
- Kukul, M.S., Irmak, S., 2018. Climate-driven crop yield and yield variability and climate change impacts on the U.S. Great plains agricultural production. *Sci. Rep.* 8, 3450. <https://doi.org/10.1038/s41598-018-21848-2>.

- Kumar, M.D., Reddy, V.R., Narayanamoorthy, A., Bassi, N., James, A.J., 2018. Rainfed areas: poor definition and flawed solutions. *Int. J. Water Resour. Dev.* 34, 278–291. <https://doi.org/10.1080/07900627.2017.1278680>.
- Kummu, M., Guillaume, J.H.A., de Moel, H., Eisner, S., Flörke, M., Porkka, M., Siebert, S., Veldkamp, T.I.E., Ward, P.J., 2016. The world's road to water scarcity: shortage and stress in the 20th century and pathways towards sustainability. *Sci. Rep.* 6, 38495. <https://doi.org/10.1038/srep38495>
- Kuyper, T.W. and Struik, P.C., 2014. Epilogue: global food security, rhetoric, and the sustainable intensification debate. *Current Opinion in Environmental Sustainability*, 8, 71–79. doi:10.1016/j.cosust.2014.09.004
- Lal, R., 2008. Managing soil water to improve rainfed agriculture in India. *J. Sustain. Agric.* 32, 51–75. <https://doi.org/10.1080/10440040802121395>.
- Lazarus, S., 2018. Is Ethiopia taking control of the River Nile? www.edition.cnn.com/2018/10/19/africa/ethiopia-new-dam-threatens-egypt-water/index.html (Accessed online at 09.11.2019).
- Lemma, E., Upadhyaya, S., and Ramsankaran, R., 2019. Investigating the performance of satellite and reanalysis rainfall products at monthly timescales across different rainfall regimes of Ethiopia. *International Journal of Remote Sensing*, 40 (10), 4019–4042. doi:10.1080/01431161.2018.1558373
- Lenney, M.P., Woodcock, C.E., Collins, J.B., Hamdi, H., 1996. The status of agricultural lands in Egypt: The use of multitemporal NDVI features derived from Landsat TM. *Remote Sens. Environ.* 56, 8–20. [https://doi.org/10.1016/0034-4257\(95\)00152-2](https://doi.org/10.1016/0034-4257(95)00152-2)
- Levy, M.C., Cohn, A., Lopes, A.V., Thompson, S.E., 2017. Addressing rainfall data selection uncertainty using connections between rainfall and streamflow. *Sci. Rep.* 7, 219. <https://doi.org/10.1038/s41598-017-00128-5>
- Li, R., 2005. Transboundary Water Conflicts in the Nile Basin. *Water Encyclopedia*. doi.org/10.1002/047147844X.wr152
- Li, Z., Chen, Y., Wang, Y., Fang, G., 2016. Dynamic changes in terrestrial net primary production and their effects on evapotranspiration. *Hydrol. Earth Syst. Sci.* 20: 2169–2178. <https://doi.org/10.5194/hess-20-2169-2016>.
- Liang, W., Yang, Y., Fan, D., Guan, H., Zhang, T., Long, D., Zhou, Y., Bai, D., 2015. Analysis of spatial and temporal patterns of net primary production and their climate controls in China from 1982 to 2010. *Agric. For. Meteorol.* 204:22–36. <https://doi.org/10.1016/j.agrformet.2015.01.015>.
- Licker, R., Johnston, M., Foley, J.A., Barford, C., Kucharik, C.J., Monfreda, C., Ramankutty, N., 2010. Mind the gap: how do climate and agricultural management explain the ‘yield gap’ of croplands around the world? *Glob. Ecol. Biogeogr.* 19, 769–782. <https://doi.org/10.1111/j.1466-8238.2010.00563.x>.
- Ligaray, M., Kim, H., Sthiannopkao, S., Lee, S., Cho, K., Kim, J., 2015. Assessment on Hydrologic Response by Climate Change in the Chao Phraya River Basin, Thailand. *Water* 7, 6892–6909. <https://doi.org/10.3390/w7126665>
- Liu, J., Yang, H., Gosling, S.N., Kummu, M., Flörke, M., Pfister, S., Hanasaki, N., Wada, Y., Zhang, X., Zheng, C., Alcamo, J., Oki, T., 2017. Water scarcity assessments in the past, present, and future. *Earth's Futur.* 5, 545–559. <https://doi.org/10.1002/2016EF000518>
- Liu, Y., Xiao, J., Ju, W., Zhou, Y., Wang, S., Wu, X., 2015. Water use efficiency of China's terrestrial ecosystems and responses to drought. *Sci. Rep.* 5, 13799.
- Lobell, D.B., 2013. The use of satellite data for crop yield gap analysis. *Field Crops Research*, 143, 56–64. doi:10.1016/j.fcr.2012.08.008
- Lobell, D.B., Ortiz-Monasterio, J.I., Asner, G.P., Naylor, R.L., and Falcon, W.P., 2005. Combining field surveys, remote sensing, and regression trees to understand yield variations in an irrigated wheat landscape. *Agronomy Journal*, 97, 241–249.

- Lobell, D.B., Schlenker, W., Costa-Roberts, J., 2011. Climate trends and global crop production since 1980. *Science* 333, 616–620. <https://doi.org/10.1126/science.1204531>.
- Loos, J., Abson, D.J., Chappell, M.J., Hanspach, J., Mikulcak, F., Tichit, M., and Fischer, J., 2014. Putting meaning back into “sustainable intensification”. *Frontiers in Ecology and the Environment*, 12 (6), 356–361. doi:10.1890/130157
- Luo, X., Wu, W., He, D., Li, Y., Ji, X., 2019. Hydrological Simulation Using TRMM and CHIRPS Precipitation Estimates in the Lower Lancang-Mekong River Basin. *Chinese Geogr. Sci.* 29, 13–25. <https://doi.org/10.1007/s11769-019-1014-6>
- Lynch, C., 2008. How do your data grow? *Nature* 455, 28–29. <https://doi.org/10.1038/455028a>
- MAF (Ministry of Agriculture and Forestry), 2006. Time series of cropped areas and yield according to the states and irrigation methods (1970/71–004/05).
- Mahgoub, B.O., Mirghani, O.A., and Ali, S.A.E., 2017. Optimizing the cropping pattern in Gezira Scheme, Sudan. *International Journal of Scientific and Research Publications*, 7 (2), 22.
- Maidment, R.I., Grimes, D., Allan, R.P., Tarnavsky, E., Stringer, M., Hewison, T., Roebeling, R., Black, E., 2014. The 30 year TAMSAT African Rainfall Climatology And Time series (TARCAT) data set. *J. Geophys. Res. Atmos.* 119, 10,619–10,644. <https://doi.org/10.1002/2014JD021927>
- Maidment, R.I., Grimes, D., Black, E., Tarnavsky, E., Young, M., Greatrex, H., Allan, R.P., Stein, T., Nkonde, E., Senkunda, S., Misael, & E., Alcántara, U., 2017. Data Descriptor: A new, long-term daily satellite-based rainfall dataset for operational monitoring in Africa Background and Summary. *Nat. Publ. Gr.* 4. <https://doi.org/10.1038/sdata.2017.63>
- Manikandan, S., 2011. Measures of central tendency: Median and mode. *J. Pharmacol. Pharmacother.* 2, 214–5. <https://doi.org/10.4103/0976-500X.83300>
- Masih, I., Maskey, S., Mussá, F.E.F., Trambauer, P., 2014. A review of droughts on the African continent: a geospatial and long-term perspective. *Hydrol. Earth Syst. Sci* 18, 3635–3649. <https://doi.org/10.5194/hess-18-3635-2014>
- McCartney, M. P., Alemayehu, T., Easton, Z. M., and Awulachew, S. B., 2012. Simulating current and future water resources development in the Blue Nile River Basin. In Awulachew S.B., Smakhtin V., Molden D. and Peden D. (Eds.). *The Nile River Basin: water, agriculture, governance and livelihoods*. Abingdon, UK: Routledge - Earthscan. pp.269-291.
- McDonnell, R.A., 2008. Challenges for Integrated Water Resources Management: How Do We Provide the Knowledge to Support Truly Integrated Thinking? *Int. J. Water Resour. Dev.* 24, 131–143. <https://doi.org/10.1080/07900620701723240>
- Mckee, T.B., Doesken, N.J., Kleist, J., 1993. The relationship of drought frequency and duration times scales. 8th Conference on Applied Climatology 179–184.
- Medlyn, B.E., 2011. Comment on “Drought-induced reduction in global terrestrial net primary production from 2000 through 2009”. *Science* 333, 1093d.
- Mekonnen, D.F., Disse, M., 2018. Analyzing the future climate change of Upper Blue Nile River basin using statistical downscaling techniques. *Hydrol. Earth Syst. Sci* 22, 2391–2408. <https://doi.org/10.5194/hess-22-2391-2018>
- Meroni, M., Verstraete, M.M., Rembold, F., Urbano, F., Kayitakire, F., 2014. A phenology-based method to derive biomass production anomalies for food security monitoring in the Horn of Africa. *International Journal of Remote Sensing*, 35 (7), 2472–2492. doi:10.1080/01431161.2014.883090
- Metcalf, D.B., Meir, P., Aragão, L.E.O.C., Lobo-do-Vale, R., Galbraith, D., Fisher, R.A., Chaves, M.M., Maroco, J.P., da Costa, A.C.L., de Almeida, S.S., Braga, A.P., Gonçalves, P.H.L., de Athaydes, J., da Costa, M., Portela, T.T.B., de Oliveira, A.A.R., Malhi, Y., Williams, M., 2010. Shifts in plant respiration and carbon use efficiency at a large-scale

- drought experiment in the eastern Amazon. *New Phytol.* 187:608–621. <https://doi.org/10.1111/j.1469-8137.2010.03319.x>.
- Metsalu, T., Vilo, J., 2015. ClustVis: a web tool for visualizing clustering of multivariate data using Principal Component Analysis and heatmap. *Nucleic Acids Res.* 43, W566–W570. <https://doi.org/10.1093/nar/gkv468>
- Meze-Hausken, E., 2004. Contrasting climate variability and meteorological drought with perceived drought and climate change in northern Ethiopia. *Clim. Res.* 27, 19–31. <https://doi.org/10.2307/24868730>
- Michelson, D.B., 2004. Systematic correction of precipitation gauge observations using analyzed meteorological variables. *J. Hydrol.* 290, 161–177. <https://doi.org/10.1016/j.jhydrol.2003.10.005>
- Misra, A.K., 2014. Climate change and challenges of water and food security. *Int. J. Sustain. Built Environ.* <https://doi.org/10.1016/j.ijsbe.2014.04.006>
- Mlengera, N., Wanjala, N., Tegambwage, W., Kakema, T., Kayeke, J., Ndunguru, A., 2015. Promotion of labour saving rice mechanization technologies in rain-fed low land and irrigated ecologies of Tanzania and Kenya. *J. Nat. Sci. Res ISSN.* www.iiste.org.
- Mmbando, G., Kleyer, M., Mmbando, G.A., Kleyer, M., 2018. Mapping Precipitation, Temperature, and Evapotranspiration in the Mkomazi River Basin, Tanzania. *Climate* 6, 63. <https://doi.org/10.3390/cli6030063>
- Mohamed, H.I., Ahmed, E.E., Abbas, O.M., Mohamed, A.E., 2010. Water allocation and optimization of minor canal operation. *Agricultural and Biology Journal of North America*, 1 (5), 1031–1043. doi:10.5251/abjna.2010.1.5.1031.1043
- Monteith, J.L., 1965. Evaporation and environment. *Symp. Soc. Exp. Biol.* 19, 205–234.
- Montesarchio, V., Orlando, D., Del Bove, D., Napolitano, F., Magnaldi, S., 2015. Evaluation of optimal rain gauge network density for rainfall-runoff modelling, in: *AIP Conference Proceedings*. AIP Publishing LLC, p. 190004. <https://doi.org/10.1063/1.4912473>
- Mu, Q., Heinsch, F.A., Zhao, M., Running, S.W., 2007. Development of a global evapotranspiration algorithm based on MODIS and global meteorology data. *Remote Sens. Environ.* 111:519–536. <https://doi.org/10.1016/j.rse.2007.04.015>.
- Mu, Q., Zhao, M., Running, S.W., 2011. Improvements to aMODIS global terrestrial evapotranspiration algorithm. *Remote Sens. Environ.* 115:1781–1800. <https://doi.org/10.1016/j.rse.2011.02.019>.
- Multsch, S., Elshamy, M. E., Batarseh, S., Seid, A. H., Fredea, H. G., and Breuerac L., 2017. Improving irrigation efficiency will be insufficient to meet future water demand in the Nile Basin. *Journal of Hydrology: Regional Studies*, 12, 315-330.
- Mustafa, R.H., 2006. Risk Management in the Rain-fed Sector of Sudan : Case Study, Gedaref Area Eastern Sudan. GEB-IDN/3679. Justus-Liebig-Universitat Gießen.
- Newson, M., 1997. Land, Water and Development. Sustainable Management of River Basin Systems. Routledge, London and New York
- Nicholls, N., 1997. Increased Australian wheat yield due to recent climate trends. *Nature* 387, 484–485. <https://doi.org/10.1038/387484a0>.
- Nicholson, S.E., 1985. Sub-saharan rainfall 1981–84. *J. Clim. Appl. Meteorol.* 24, 1388–1391. [https://doi.org/10.1175/1520-0450\(1985\)024<1388:SSR>2.0.CO;2](https://doi.org/10.1175/1520-0450(1985)024<1388:SSR>2.0.CO;2).
- Nicholson, S.E., Davenport, M.L., Malo, A.R., 1990. A comparison of the vegetation response to rainfall in the Sahel and East Africa, using normalized difference vegetation index from NOAA AVHRR. *Clim. Change* 17, 209–241. <https://doi.org/10.1007/BF00138369>.
- Nile Basin Initiative (NBI), 2012. State of the River Nile Basin Report. Nile Basin Initiative.
- NOAA, 2016. Global Analysis for Annual 2015. NOAA, National Centers for Environmental Information, State of the Climate Available online at. <http://www.ncdc.noaa.gov/sotc/global/201513>, (Accessed date: 15 December 2016).

- Novella, N.S., Thiaw, W.M., 2013. African rainfall climatology version 2 for famine early warning systems. *J. Appl. Meteorol. Climatol.* 52, 588–606. <https://doi.org/10.1175/JAMC-D-11-0238.1>
- Noy-Meir, I., 1973. Desert Ecosystems: Environment and Producers. *Annu. Rev. Ecol. Syst.* 4, 25–51. <https://doi.org/10.1146/annurev.es.04.110173.000325>
- Oestigaard, T., 2012. Water Scarcity and Food Security along the Nile Politics, population increase and climate change. *Current African Issues* 49. Nordiska Afrikainstitutet, Uppsala. Available online at: www.files.ethz.ch/isn/152248/FULLTEXT01-5.pdf (accessed on 19.07.2019).
- Onencan, A., Enserink, B., Van de Walle, B., and Chelang, J., 2016. Coupling Nile Basin 2050 scenarios with the IPCC 2100 projections for climate-induced risk reduction. *Procedia Engineering* 159 (2016) 357 – 365
- Oshunsanya, S.O., 2013. Crop yields as influenced by land preparation methods established within Vetiver Grass Alleys for sustainable agriculture in Southwest Nigeria. *Agroecology and Sustainable Food Systems*, 37 (5), 578–591. doi:10.1080/21683565.2012.762439
- Osman, I.S., Schultz, B., Osman, A., Suryadi, F.X., 2017. Effects of different operation scenarios on sedimentation in irrigation canals of the Gezira Scheme, Sudan. *Irrigation and Drainage*, 66 (1), 82–89. doi:10.1002/ird.v66.1
- Panda, S.S., Ames, D.P., and Panigrahi, S., 2010. Application of vegetation indices for agricultural crop yield prediction using neural network techniques. *Remote Sensing*, 2 (3), 673–696. doi:10.3390/rs2030673
- Pande, S. and Savenije, H.H.G., 2016. A sociohydrological model for smallholder farmers in Maharashtra, India. *Water Resources Research*, 52 (3), 1923–1947. doi:10.1002/2015WR017841
- Pande, S. and Sivapalan, M., 2017. Progress in socio-hydrology: a meta-analysis of challenges and opportunities. *Wiley Interdisciplinary Reviews: Water*, 4 (4), e1193. doi:10.1002/wat2.1193
- Pardo-Igúzquiza, E., 1998. Optimal selection of number and location of rainfall gauges for areal rainfall estimation using geostatistics and simulated annealing, *Journal of Hydrology*. [https://doi.org/10.1016/S0022-1694\(98\)00188-7](https://doi.org/10.1016/S0022-1694(98)00188-7)
- Peerzada, A.M., Ali, H.H., and Chauhan, B.S., 2017. Weed management in sorghum [*Sorghum bicolor* (L.) Moench] using crop competition: a review. *Crop Protection*, 95, 74–80. doi:10.1016/j.cropro.2016.04.019
- Pei, F., Li, X., Liu, X., Lao, C., 2013. Assessing the impact of drought on net primary productivity in China. *J. Environ. Manag.* 114, 362–371.
- Peña-Arancibia, J.L., van Dijk, A.I.J.M., Renzullo, L.J., Mulligan, M., Peña-Arancibia, J.L., Dijk, A.I.J.M. van, Renzullo, L.J., Mulligan, M., 2013. Evaluation of Precipitation Estimation Accuracy in Reanalyses, Satellite Products, and an Ensemble Method for Regions in Australia and South and East Asia. *J. Hydrometeorol.* 14, 1323–1333. <https://doi.org/10.1175/JHM-D-12-0132.1>
- Peng, D., Zhang, B., Wu, C., Heute, A.R., Gonsamo, A., Lei, L., Ponce-Campos, G.E., Liu, X., Peters, A.J., Walter-Shea, E.A., Ji, L., Vina, A., Hayes, M., and Svoboda, M.D., 2002. Drought monitoring with NDVI-based standardized vegetation index. *Photogrammetric Engineering and Remote Sensing*, 68 (1), 71–75.
- Pingali, P.L., 2012. Green revolution: impacts, limits, and the path ahead. *Proc. Natl. Acad. Sci. U. S. A.* 109, 12302–12308. <https://doi.org/10.1073/pnas.0912953109>.
- Potopová, V., Štěpánek, P., Možný, M., Türkott, L., Soukup, J., 2015. Performance of the standardised precipitation evapotranspiration index at various lags for agricultural drought risk assessment in the Czech Republic. *Agric. For. Meteorol.* 202, 26–38.

- Powledge, F., 2010. Food, hunger, and insecurity. *BioScience*, 60 (4), 260–265. doi:10.1525/bio.2010.60.4.3
- Pradhan, P., Fischer, G., van Velthuis, H., Reusser, D.E., Kropp, J.P., 2015. Closing yield gaps: how sustainable can we be? *PLOS One*, 10 (6), e0129487. doi:10.1371/journal.pone.0129487
- Pretty, J., Toulmin, C., Williams, S., 2011. Sustainable intensification in African agriculture. *Int. J. Agric. Sustain.* 9 (1), 5–24. <https://doi.org/10.3763/ijas.2010.0583>.
- Prince, S.D., Goward, S.N., 1995. Global primary production: a remote sensing approach. *J. Biogeogr.* 22(4):815–835. <https://doi.org/10.2307/2845983>.
- Quan, M. and Liang, J., 2017. The influences of four types of soil on the growth, physiological and biochemical characteristics of *Lycoris aurea* (L' Her.) Herb. *Scientific Reports*, 7, 43284. doi:10.1038/srep43284
- R Core Team, 2008. R: A Language and Environment for Statistical Computing. R Found. Stat. Comput. Vienna, Austria. ISBN 3-900051-07-0, URL <http://www.R-project.org>.
- Rahman, M., 2012. Water Security: Ethiopia–Egypt Transboundary Challenges over the Nile River Basin. *Journal of Asian and African Studies*, 48(1) 35–46. doi.org/10.1177/0021909612438517
- Ramoelo, A., Majazi, N., Mathieu, R., Jovanovic, N., Nickless, A., Dziki, S., 2014. Validation of global evapotranspiration product (MOD16) using flux tower data in the African savannah, South Africa. *Remote Sens.* 6:7406–7423. <https://doi.org/10.3390/rs6087406>.
- Rasul, G., 2014. Food, water, and energy security in South Asia: A nexus perspective from the Hindu Kush Himalayan region☆. *Environ. Sci. Policy* 39, 35–48. <https://doi.org/10.1016/J.ENVSCI.2014.01.010>
- Ray, D.K., Mueller, N.D., West, P.C., Foley, J.A., Meybeck, A., 2013. Yield trends are insufficient to double global crop production by 2050. *PLoS One* 8, e66428. <https://doi.org/10.1371/journal.pone.0066428>.
- Reichert, J.M., Akiyoshi, L.E., Suzuki, S., Reinert, J., Horn, R., and Hå, I., 2009. Reference bulk density and critical degree-of compactness for no-till crop production in subtropical highly weathered soils. *Soil & Tillage Research*, 102, 242–254. doi:10.1016/j.still.2008.07.002
- Reichstein, M., Tenhunen, J.D., Rouspard, O., ourcival, J., Rambal, S., miglietta, F., peressotti, A., pecchiari, M., tirone, G., valentini, R., 2002. Severe drought effects on ecosystem CO₂ and H₂O fluxes at three Mediterranean evergreen sites: revision of current hypotheses? *Glob. Chang. Biol.* 8:999–1017. <https://doi.org/10.1046/j.1365-2486.2002.00530.x>.
- Rienecker, M.M., Suarez, M.J., Gelaro, R., Todling, R., Bacmeister, J., Liu, E., Bosilovich, M.G., Schubert, S.D., Takacs, L., Kim, G.-K., Bloom, S., Chen, J., Collins, D., Conaty, A., da Silva, A., Gu, W., Joiner, J., Koster, R.D., Lucchesi, R., Molod, A., Owens, T., Pawson, S., Pegion, P., Redder, C.R., Reichle, R., Robertson, F.R., Ruddick, A.G., Sienkiewicz, M., Woollen, J., Rienecker, M.M., Suarez, M.J., Gelaro, R., Todling, R., Julio Bacmeister, Liu, E., Bosilovich, M.G., Schubert, S.D., Takacs, L., Kim, G.-K., Bloom, S., Chen, J., Collins, D., Conaty, A., Silva, A. da, Gu, W., Joiner, J., Koster, R.D., Lucchesi, R., Molod, A., Owens, T., Pawson, S., Pegion, P., Redder, C.R., Reichle, R., Robertson, F.R., Ruddick, A.G., Sienkiewicz, M., Woollen, J., 2011. MERRA: NASA's Modern-Era Retrospective Analysis for Research and Applications. *J. Clim.* 24, 3624–3648. <https://doi.org/10.1175/JCLI-D-11-00015.1>
- Robinson, L.W., Ericksen, P.J., Chesterman, S., and Worden, J.S., 2015. Sustainable intensification in drylands: what resilience and vulnerability can tell us. *Agricultural Systems*, 135, 133–140. doi:10.1016/j.agsy.2015.01.005
- Rockström, J., Karlberg, L., Wani, S.P., Barron, J., Hatibu, N., Oweis, T., Bruggeman, A., Farahani, J., Qiang, Z., 2010. Managing water in rainfed agriculture—the need for a

- paradigm shift. *Agric. Water Manag.* 97, 543–550. <https://doi.org/10.1016/J.AGWAT.2009.09.009>.
- Rockström, J., Williams, J., Daily, G., Noble, A., Matthews, N., Gordon, L., Wetterstrand, H., DeClerck, F., Shah, M., Steduto, P., de Fraiture, C., Hatibu, N., Unver, O., Bird, J., Sibanda, L., Smith, J., 2017. Sustainable intensification of agriculture for human prosperity and global sustainability. *Ambio*, 46 (1), 4–17. doi:10.1007/s13280-016-0793-6
- Rodell, M., Houser, P.R., Jambor, U., Gottschalck, J., Mitchell, K., Meng, C.-J., Arsenault, K., Cosgrove, B., Radakovich, J., Bosilovich, M., Entin, J.K., Walker, J.P., Lohmann, D., Toll, D., 2004. The global land data assimilation system. *Bull. Am. Meteorol. Soc.* 85, 381–394. <https://doi.org/10.1175/BAMS-85-3-381>.
- Rodionov, S.N., 2004. A sequential algorithm for testing climate regime shifts. *Geophys. Res. Lett.* 31 <https://doi.org/10.1029/2004GL019448>. n/a-n/a.
- Romilly, T.G., Gebremichael, M., 2011. Evaluation of satellite rainfall estimates over Ethiopian river basins. *Hydrol. Earth Syst. Sci.* 15, 1505–1514. <https://doi.org/10.5194/hess-15-1505-2011>
- Rosenzweig, C., Gangadhar Rao, D., Katyal, J.C., Sinha, S.K., Srinivas, K., 1995. Impacts of climate change on sorghum productivity in India: simulation study. *Climate change and agriculture: analysis of potential international impacts American Society of Agronomy*, pp. 325–337. <https://doi.org/10.2134/asaspecpub59.c17>.
- Roth, V., Lemann, T., Zeleke, G., Subhatu, A.T., Nigussie, T.K., Hurni, H., 2018. Effects of climate change on water resources in the upper Blue Nile Basin of Ethiopia. *Heliyon* 4, e00771. <https://doi.org/10.1016/J.HELIYON.2018.E00771>
- Rulli, M.C., Savoria, A., and D’Odorico, P., 2013. Global land and water grabbing. *Proceedings of the National Academy of Sciences of the United States of America (PNAS)*, 110 (3) 892–897. doi.org/10.1073/pnas.1213163110
- Saber, M., Yilmaz, K., 2016. Bias Correction of Satellite-Based Rainfall Estimates for Modeling Flash Floods in Semi-Arid regions: Application to Karpuz River, Turkey. *Nat. Hazards Earth Syst. Sci. Discuss.* 1–35. <https://doi.org/10.5194/nhess-2016-339>
- Sahlu, D., Moges, S.A., Nikolopoulos, E.I., Anagnostou, E.N., Hailu, D., 2017. Evaluation of High-Resolution Multisatellite and Reanalysis Rainfall Products over East Africa. *Adv. Meteorol.* 2017, 1–14. <https://doi.org/10.1155/2017/4957960>
- Sahoo, A.K., Sheffield, J., Pan, M., Wood, E.F., 2015. Evaluation of the Tropical Rainfall Measuring Mission Multi-Satellite Precipitation Analysis (TMPA) for assessment of large-scale meteorological drought. *Remote Sens. Environ.* 159, 181–193. <https://doi.org/10.1016/J.RSE.2014.11.032>
- Salih, A.A.M., Elagib, N.A., Tjernström, M., Zhang, Q., 2018. Characterization of the Sahelian-Sudan rainfall based on observations and regional climate models. *Atmos. Res.* 202, 205–218. <https://doi.org/10.1016/J.ATMOSRES.2017.12.001>
- Salman M.A.S., 2013. The Nile Basin Cooperative Framework Agreement: a peacefully unfolding African spring?, *Water International*, 38 (1), 17–29, DOI: 10.1080/02508060.2013.744273
- Samanta, A., Costa, M.H., Nunes, E.L., Vieira, S.A., Xu, L., Myneni, R.B., 2011. Comment on “Drought-induced reduction in global terrestrial net primary production from 2000 through 2009”. *Science* 333 (6064), 1093c.
- Schmidhuber, J., Tubiello, F.N., 2007. Global food security under climate change. *Proc. Natl. Acad. Sci. U. S. A.* 104, 19703–19708. <https://doi.org/10.1073/pnas.0701976104>.
- Schneider, U., Becker, A., Finger, P., Meyer-Christoffer, A., Rudolf, B., Ziese, M., 2011. GPCC Full Data Reanalysis Version 6.0 at 0.5°: Monthly Land-Surface Precipitation from Rain-Gauges built on GTS-based and Historic Data. https://doi.org/10.5676/DWD_GPCC/FD_M_V7_050

- Schut, M., van Asten, P., Okafor, C., Hicintuka, C., Mapatano, S., Nabahungu, N.L., Kagabo, D., Muchunguzi, P., Njukwe, E., Dontsop-Nguezet, P.M., Sartas, M., and Vanlauwe, B., 2016. Sustainable intensification of agricultural systems in the Central African Highlands: the need for institutional innovation. *Agricultural Systems*, 145, 165–176. doi:10.1016/j.agsy.2016.03.005
- Sebastiani, P., Perls, T.T., 2016. Detection of Significant Groups in Hierarchical Clustering by Resampling. *Front. Genet.* 7, 144. <https://doi.org/10.3389/fgene.2016.00144>
- Senay, G.B., Asante, K., Artan, G., 2009. Water balance dynamics in the Nile Basin. *Hydrol. Process.* n/a-n/a. <https://doi.org/10.1002/hyp.7364>
- Senay, G.B., Velpuri, N.M., Bohms, S., Demissie, Y., Gebremichael, M., 2014. Understanding the hydrologic sources and sinks in the Nile Basin using multisource climate and remote sensing data sets. *Water Resour. Res.* 50, 8625–8650. <https://doi.org/10.1002/2013WR015231>
- Setegn, S. G., Rayner, D., Melesse, A. M., Dargahi, B., Srinivasan, R., and Wörman, A., 2011. Climate Change Impact on Agricultural Water Resources Variability in the Northern Highlands of Ethiopia A.M. Melesse (ed.), Nile River Basin, Springer Science+Business Media B.V. DOI 10.1007/978-94-007-0689-7_12. www.cnn.com/2018/10/19/africa/ethiopia-new-dam-threatens-egypts-water/index.html (Accessed online on 09.11.2019)
- Seyoum, W.M., 2018. Characterizing water storage trends and regional climate influence using GRACE observation and satellite altimetry data in the Upper Blue Nile River Basin. *J. Hydrol.* 566, 274–284. <https://doi.org/10.1016/j.jhydrol.2018.09.025>
- Shaghaghian, M.R., Abedini, M.J., 2013. Rain gauge network design using coupled geostatistical and multivariate techniques. *Sci. Iran.* 20, 259–269. <https://doi.org/10.1016/j.scient.2012.11.014>
- Shahin, M., 1993. An overview of reservoir sedimentation in some African river basins, in: *Proceedings of Sediment Problems: Strategies for Monitoring, Prediction and Control*, Yokohama, July 1993, LAHS Publ. no. 217, 93–100.
- Shapiro, S.S. and Wilk, M.B., 1965. An analysis of variance test for normality (complete samples). *Biometrika*, 52 (3/4), 591. doi:10.1093/biomet/52.3-4.591
- Shaver, G.R., Canadell, J., Chapin, F.S., Gurevitch, J., Harte, J., Henry, G., Ineson, P., Jonasson, S., Melillo, J., Pitelka, L., Rustad, L., 2000. Global warming and terrestrial ecosystems: a conceptual framework for analysis. *Bioscience* 50:871. [https://doi.org/10.1641/0006-3568\(2000\)050\[0871:GWATEA\]2.0.CO;2](https://doi.org/10.1641/0006-3568(2000)050[0871:GWATEA]2.0.CO;2).
- Sheffield, J., Goteti, G., Wood, E.F., Sheffield, J., Goteti, G., Wood, E.F., 2006. Development of a 50-Year High-Resolution Global Dataset of Meteorological Forcings for Land Surface Modeling. *J. Clim.* 19, 3088–3111. <https://doi.org/10.1175/JCLI3790.1>
- Sheffield, J., Wood, E.F., Pan, M., Beck, H., Coccia, G., Serrat-Capdevila, A., Verbist, K., 2018. Satellite Remote Sensing for Water Resources Management: Potential for Supporting Sustainable Development in Data-Poor Regions. *Water Resour. Res.* <https://doi.org/10.1029/2017WR022437>
- Siam, M.S., Eltahir, E.A.B., 2017. Climate change enhances interannual variability of the Nile river flow. *Nat. Clim. Chang.* 7, 350–354. <https://doi.org/10.1038/nclimate3273>
- Siddique-E-Akbor, A.H.M., Hossain, F., Sikder, S., Shum, C.K., Tseng, S., Yi, Y., Turk, F.J., Limaye, A., Siddique-E-Akbor, A.H.M., Hossain, F., Sikder, S., Shum, C.K., Tseng, S., Yi, Y., Turk, F.J., Limaye, A., 2014. Satellite Precipitation Data–Driven Hydrological Modeling for Water Resources Management in the Ganges, Brahmaputra, and Meghna Basins. *Earth Interact.* 18, 1–25. <https://doi.org/10.1175/EI-D-14-0017.1>
- Siderius, C., Van Walsum, P.E.V., Roest, C.W.J., Smit, A.A.M.F.R., Hellegers, P.J.G.J., Kabat, P., Van Ierland, E.C., 2016. The role of rainfed agriculture in securing food production in

- the Nile Basin. *Environ. Sci. Policy* 61, 14–23. <https://doi.org/10.1016/J.ENVSCI.2016.03.007>.
- Simelton, E., Fraser, E.D.G., Termansen, M., Forster, P.M., Dougill, A.J., 2009. Typologies of crop-drought vulnerability: an empirical analysis of the socio-economic factors that influence the sensitivity and resilience to drought of three major food crops in China (1961–2001). *Environ. Sci. Policy* 12, 438–452. <https://doi.org/10.1016/J.ENVSCI.2008.11.005>.
- Sivapalan, M., Savenije, H.H.G., and Blöschl, G., 2012. Socio-hydrology: a new science of people and water. *Hydrological Processes*, 26 (8), 1270–1276. doi:10.1002/hyp.8426
- Smith, P., Bustamante, M., Ahammad, H., Clark, H., Dong, H., Elsiddig, E.A., Haberl, H., Harper, R., House, J., Jafari, M., Masera, O., Mbow, C., Ravindranath, N.H., Rice, C.W., Robledo Abad, C., Romanovskaya, A., Sperling, F., Tubiello, F., 2014. Agriculture, forestry and other land use (AFOLU). 2014. In: Edenhofer, O., Pichs-Madruga, R., Sokona, Y., Farahani, E., Kadner, S., Seyboth, K., Adler, A., Baum, I., Brunner, S., Eickemeier, P., Kriemann, B., Savolainen, J., Schlömer, S., von Stechow, C., Zwickel, T., Minx, J.C. (Eds.), *Climate Change 2014: Mitigation Of Climate Change. Contribution of Working Group III to the Fifth Assessment Report of the Intergovernmental Panel on Climate Change*. Cambridge University Press, Cambridge, United Kingdom and New York, NY, USA Available online at: https://www.ipcc.ch/pdf/assessment-report/ar5/wg3/ipcc_wg3_ar5_chapter11.pdf, (Accessed date: 13 November 2017).
- Song, Q., Fei, X., Zhang, Y., Sha, L., Liu, Y., Zhou, W., Wu, C., Lu, Z., Luo, K., Gao, J., Liu, Y., 2017. Water use efficiency in a primary subtropical evergreen forest in Southwest China. *Sci. Rep.* 7, 43031. <https://doi.org/10.1038/srep43031>.
- Song, X., Li, W., Ma, D., Wu, Y., Ji, D., 2018. An Enhanced Clustering-Based Method for Determining Time-of-Day Breakpoints Through Process Optimization. *IEEE Access* 6, 29241–29253. <https://doi.org/10.1109/ACCESS.2018.2843564>
- Sorooshian, S., Hsu, K.-L., Gao, X., Gupta, H. V., Imam, B., Braithwaite, D., Sorooshian, S., Hsu, K.-L., Gao, X., Gupta, H. V., Imam, B., Braithwaite, D., 2000. Evaluation of PERSIANN System Satellite-Based Estimates of Tropical Rainfall. *Bull. Am. Meteorol. Soc.* 81, 2035–2046. [https://doi.org/10.1175/1520-0477\(2000\)081<2035:EOPSSSE>2.3.CO;2](https://doi.org/10.1175/1520-0477(2000)081<2035:EOPSSSE>2.3.CO;2)
- Steffen, W., Broadgate, W., Deutsch, L., Gaffney, O., and Ludwig, C., 2015. The trajectory of the Anthropocene: the great acceleration. *The Anthropocene Review*, 2 (1), 81–98. doi:10.1177/2053019614564785
- Steffen, W., Crutzen, P.J., and McNeill, J.R., 2007. The Anthropocene: are humans now overwhelming the great forces of nature? *Ambio*, 36 (8), 614–621. doi:10.1579/0044-7447(2007)36[614:TAAHNO]2.0.CO;2
- Steffen, W., Noone, K., Lambin, E., Lenton, T.M., Scheffer, M., Folke, C., Schellnhuber, H.J., Wit, C.A. De, Hughes, T., Leeuw, S. Van Der, Rodhe, H., Snyder, P.K., Costanza, R., Svedin, U., Falkenmark, M., Karlberg, L., Corell, R.W., Fabry, V.J., Hansen, J., Walker, B., Liverman, D., Richardson, K., Crutzen, P., Foley, J., 2009. Planetary Boundaries : Exploring the Safe Operating Space for Humanity. *Ecol. Soc.* 14.
- Stöckle, C.O., Donatelli, M., Nelson, R., 2003. CropSyst, a cropping systems simulation model. *Eur. J. Agron.* 18 (3–4):289–307. [https://doi.org/10.1016/S1161-0301\(02\)00109-0](https://doi.org/10.1016/S1161-0301(02)00109-0).
- Su, Z., Dorigo, W., Fernández, D., Fernández-Prieto, F., Van Helvoirt, M., Hungershofer, K., De Jeu, R., Parinussa, R., Timmermans, J., Roebeling, R., Schröder, M., Schröder, S., Schulz, J., Van Der Tol, C., Stammes, P., Wagner, W., Wang, L., Wang, P., Wolters, E., 2010. Earth observation Water Cycle Multi-Mission Observation Strategy (WACMOS). *Hydrol. Earth Syst. Sci. Discuss* 7, 7899–7956. <https://doi.org/10.5194/hessd-7-7899-2010>

- Sudmanns, M., Tiede, D., Lang, S., Bergstedt, H., Trost, G., Augustin, H., Baraldi, A., Blaschke, T., 2019. Big Earth data: disruptive changes in Earth observation data management and analysis? *Int. J. Digit. Earth* 1–19. <https://doi.org/10.1080/17538947.2019.1585976>
- Sulieman, H.M., Ahmed, A.G.M., 2013. Monitoring changes in pastoral resources in eastern Sudan: a synthesis of remote sensing and local knowledge. *Pastor. Res. Policy Pract.* 3, 22. <https://doi.org/10.1186/2041-7136-3-22>.
- Sulieman, H.M., Buchroithner, M.F., 2009. Degradation and abandonment of mechanized rain-fed agricultural land in the Southern Gadarif region, Sudan: the local farmers' perception. *L. Degrad. Dev.* 20, 199–209. <https://doi.org/10.1002/ldr.894>.
- Sulieman, H.M., Elagib, N.A., 2012. Implications of climate, land-use and land-cover changes for pastoralism in eastern Sudan. *J. Arid Environ.* 85, 132–141. <https://doi.org/10.1016/j.jaridenv.2012.05.001>.
- Sultan, B., Roudier, P., Quirion, P., Alhassane, A., Muller, B., Dingkuhn, M., Ciaï, P., Guimberteau, M., Traore, S., Baron, C., 2013. Assessing climate change impacts on sorghum and millet yields in the Sudanian and Sahelian savannas of West Africa. *Environ. Res. Lett.* 8, 014040. <https://doi.org/10.1088/1748-9326/8/1/014040>.
- Sun, B., Zhao, H., Wang, X., 2016. Effects of drought on net primary productivity: roles of temperature, drought intensity and duration. *Chin. Geogr. Sci.* 26 (2), 270–282.
- Sun, Q., Miao, C., Duan, Q., Ashouri, H., Sorooshian, S., Hsu, K.-L., 2018. A Review of Global Precipitation Data Sets: Data Sources, Estimation, and Intercomparisons. *Rev. Geophys.* 56, 79–107. <https://doi.org/10.1002/2017RG000574>
- Sutcliffe, J. V. and Parks, Y. P., 1999. *The Hydrology of the Nile*. Oxfordshire: The International Association of Hydrological Science (IAHS).
- Sutcliffe, J.V., Dugdale, G., Milford, J.R., Sutcliffe, J.V., Mdlford, J.R., 1989. The Sudan floods of 1988. *Hydrol. Sci. J. Des. Sci. Hydrol.* 34, 355–364. <https://doi.org/10.1080/02626668909491339>.
- Swain, A., 2011. Challenges for water sharing in the Nile basin: changing geo-politics and changing climate. *Hydrol. Sci. J.* 56, 687–702. <https://doi.org/10.1080/02626667.2011.577037>
- Swets, D., Reed, B.C., Rowland, J., Marko, S.E., 1999. A weighted least-squares approach to temporal NDVI smoothing. *ASPRS Annual Conference: from Image to Information*.
- Tadesse, T., Demisse, G.B., Zaitchik, B., Dinku, T., 2014. Satellite-based hybrid drought monitoring tool for prediction of vegetation condition in Eastern Africa: A case study for Ethiopia. *Water Resour. Res.* 50, 2176–2190. <https://doi.org/10.1002/2013WR014281>
- Tan, C., Erfani, T., Erfani, R., Tan, C.C., Erfani, T., Erfani, R., 2017. Water for Energy and Food: A System Modelling Approach for Blue Nile River Basin. *Environments* 4, 15. <https://doi.org/10.3390/environments4010015>
- Tang, R., Shao, K., Li, Z.-L., Wu, H., Tang, B.-H., Zhou, G., Zhang, L., 2015. Multiscale validation of the 8-day MOD16 evapotranspiration product using flux data collected in China. *IEEE J. Sel. Top. Appl. Earth Obs. Remote Sens.* 8, 1478–1486.
- Tang, X., Li, H., Desai, A.R., Nagy, Z., Luo, J., Kolb, T.E., Oliosio, A., Xu, X., Yao, L., Kutsch, W., Pilegaard, K., Köstner, B., Ammann, C., 2014. How is water-use efficiency of terrestrial ecosystems distributed and changing on Earth? *Sci. Rep.* 4, 7483. <https://doi.org/10.1038/srep07483>.
- Tarnavsky, E., Grimes, D., Maidment, R., Black, E., Allan, R.P., Stringer, M., Chadwick, R., Kayitakire, F., Tarnavsky, E., Grimes, D., Maidment, R., Black, E., Allan, R.P., Stringer, M., Chadwick, R., Kayitakire, F., 2014. Extension of the TAMSAT Satellite-Based Rainfall Monitoring over Africa and from 1983 to Present. *J. Appl. Meteorol. Climatol.* 53, 2805–2822. <https://doi.org/10.1175/JAMC-D-14-0016.1>

- Teclaff, L. A., 1967. *The River Basin in History and Law*. Martinus Nijhoff, The Hague, The Netherlands.
- Teferi, E., Uhlenbrook, S., Bewket, W., 2015. Inter-annual and seasonal trends of vegetation condition in the Upper Blue Nile (Abay) Basin: dual-scale time series analysis. *Earth Syst. Dyn.* 6, 617–636. <https://doi.org/10.5194/esd-6-617-2015>
- Tekeli, A., Tekeli, Emre, A., 2017. Exploring Jeddah Floods by Tropical Rainfall Measuring Mission Analysis. *Water* 9, 612. <https://doi.org/10.3390/w9080612>
- Thiemig, V., Rojas, R., Zambrano-Bigiarini, M., Levizzani, V., De Roo, A., 2012. Validation of Satellite-Based Precipitation Products over Sparsely Gauged African River Basins. *J. Hydrometeorol.* 13, 1760–1783. <https://doi.org/10.1175/JHM-D-12-032.1>
- Thies, B., Bendix, J., 2011. Satellite based remote sensing of weather and climate: Recent achievements and future perspectives. *Meteorol. Appl.* <https://doi.org/10.1002/met.288>
- Thompson, P.B., 2007. Agricultural sustainability: what it is and what it is not. *International Journal of Agricultural Sustainability*, 5 (1), 5–16. doi:10.1080/14735903.2007.9684809
- Thorndike, R.L., 1953. Who belongs in the family? *Psychometrika* 18, 267–276. <https://doi.org/10.1007/BF02289263>
- Tian, H., Chen, G., Liu, M., Zhang, C., Sun, G., Lu, C., Xu, X., Ren, W., Pan, S., Chappelka, A., 2010. Model estimates of net primary productivity, evapotranspiration, and water use efficiency in the terrestrial ecosystems of the southern United States. *For. Ecol. Manag.* 259, 1311–1327.
- Tian, H., Lu, C., Chen, G., Xu, X., Liu, M., Ren, W., Tao, B., Sun, G., Pan, S., Liu, J., 2011. Climate and land use controls over terrestrial water use efficiency in monsoon Asia. *Ecohydrology* 4:322–340. <https://doi.org/10.1002/eco.216>
- Tilman, D., 1999. Global environmental impacts of agricultural expansion: the need for sustainable and efficient practices. *Proceedings of the National Academy of Sciences of the United States of America*, 96 (11), 5995–6000. doi:10.1073/pnas.96.11.5995
- Tittonell, P. and Giller, K.E., 2013. When yield gaps are poverty traps: the paradigm of ecological intensification in African smallholder agriculture. *Field Crops Research*, 143, 76–90. doi:10.1016/j.fcr.2012.10.007
- Tomás, R., Li, Z., 2017. Earth Observations for Geohazards: Present and Future Challenges. *Remote Sens.* 9, 194. <https://doi.org/10.3390/rs9030194>
- Tramblay, Y., Thiemig, V., Dezetter, A., Hanich, L., 2016. Evaluation of satellite-based rainfall products for hydrological modelling in Morocco. *Hydrol. Sci. J.* 61, 2509–2519. <https://doi.org/10.1080/02626667.2016.1154149>
- Tuinstra, M.R., 2008. Food-grade sorghum varieties and production considerations: a review. *J. Plant Interact.* 3, 69–72. <https://doi.org/10.1080/17429140701722770>
- Turner, D.P., Ritts, W.D., Cohen, W.B., Gower, S.T., Running, S.W., Zhao, M., Costa, M.H., Kirschbaum, A.A., Ham, J.M., Saleska, S.R., Ahl, D.E., 2006. Evaluation of MODIS NPP and GPP products across multiple biomes. *Remote Sens. Environ.* 102:282–292. <https://doi.org/10.1016/j.rse.2006.02.017>
- UN-DESA, 2019. *World population prospects 2019*. <https://population.un.org/wpp/>
- UNEP, 1992. *World Atlas of Desertification*. London/New York/Melbourne/Auckland.
- UNESCO, 2019. *The United Nations World Water Development Report 2019 - Leaving no one behind*. Paris.
- UNECA, 2016. *The Demographic Profile of African Countries*. Economic Commission for Africa Addis Ababa, Ethiopia Available online at: http://www.uneca.org/sites/default/files/PublicationFiles/demographic_profile_rev_april_25.pdf (Accessed 11 June 2017).
- Valentini, R., Arneeth, A., Bombelli, A., Castaldi, S., Cazzolla Gatti, R., Chevallier, F., Ciais, P., Grieco, E., Hartmann, J., Henry, M., Houghton, R.A., Jung, M., Kutsch, W.L., Malhi, Y., Mayorga, E., Merbold, L., Murray-Tortarolo, G., Papale, D., Peylin, P., Poulter, B.,

- Raymond, P.A., Santini, M., Sitch, S., Laurin, G.V., Van Der Werf, G.R., Williams, C.A., Scholes, R.J., 2014. A full greenhouse gases budget of Africa: synthesis, uncertainties, and vulnerabilities. *Biogeosciences* 11:381–407. <https://doi.org/10.5194/bg-11-381-2014>.
- Valverde, P., De Carvalho, M., Serralheiro, R., Maia, R., Ramos, V., Oliveira, B., 2015. Climate change impacts on rainfed agriculture in the Guadiana river basin (Portugal). *Agric. Water Manag.* 150, 35–45. <https://doi.org/10.1016/j.agwat.2014.11.008>.
- Van Der Molen, M.K., Dolman, A.J., Ciais, P., Eglin, T., Gobron, N., Law, B.E., Meir, P., Peters, W., Phillips, O.L., Reichstein, M., Chen, T., Dekker, S.C., Doubková, M., Friedl, M.A., Jung, M., Van Den Hurk, B.J.J.M., De Jeu, R.A.M., Kruijt, B., Ohta, T., Rebel, K.T., Plummer, S., Seneviratne, S.I., Sitch, S., Teuling, A.J., Van Der Werf, G.R., Wang, G., 2011. Drought and ecosystem carbon cycling. *Agric. For. Meteorol.* 151:765–773. <https://doi.org/10.1016/j.agrformet.2011.01.018>.
- Vanuytrecht, E., Raes, D., Steduto, P., Hsiao, T.C., Fereres, E., Heng, L.K., Vila, M.G., Moreno, P.M., 2014. AquaCrop: FAO's crop water productivity and yield response model. *Environ. Model. Softw.* 62 (2014):351–360. <https://doi.org/10.1016/j.envsoft.2014.08.005>.
- Vergara, H., Hong, Y., Gourley, J.J., Anagnostou, E.N., Maggioni, V., Stampoulis, D., Kirstetter, P.-E., 2013. Effects of Resolution of Satellite-Based Rainfall Estimates on Hydrologic Modeling Skill at Different Scales. *J. Hydrometeorol.* 15, 593–613. <https://doi.org/10.1175/JHM-D-12-0113.1>
- Vicente-Serrano, S.M., Beguería, S., López-Moreno, J.I., 2010. A multiscale drought index sensitive to global warming: the standardized precipitation evapotranspiration index. *J. Clim.* 23:1696–1718. <https://doi.org/10.1175/2009JCLI2909.1>.
- Villarini, G., Mandapaka, P. V., Krajewski, W.F., Moore, R.J., 2008. Rainfall and sampling uncertainties: A rain gauge perspective. *J. Geophys. Res.* 113, D11102. <https://doi.org/10.1029/2007JD009214>
- Voisin, N., Wood, A., Dennis, L., 2007. Evaluation of Precipitation Products for Global Hydrological Prediction. *J. Hydrometeorol.* 9, 388–407.
- Wang, Q., Tenhunen, J., Quoc D.N., Reichstein, M., Vesala, T., and Keronen, P., 2004. Similarities in ground- and satellite-based NDVI time series and their relationship to physiological activity of a Scots pine forest in Finland. *Remote Sensing of Environment*, 93, 225–237. doi:10.1016/j.rse.2004.07.006
- Webb, P., Stordalen, G.A., Singh, S., Wijesinha-Bettoni, R., Shetty, P., and Lartey, A., 2018. Hunger and malnutrition in the 21st century. *BMJ (Clinical Research ed.)*, 361, k2238. doi:10.1136/bmj.k2238
- Wheeler, K. G., Basheer, M., Mekonnen, Z. T., Eltoun, S. O., Mersha, A., Abdo, G. M., Zagona, E. A., Hall, J. W., and Dadson, S. J., 2016. Cooperative filling approaches for the Grand Ethiopian Renaissance Dam. *Water International*, 41 (4), 611-634. Doi.org/10.1080/02508060.2016.1177698
- White, G. F., 1957. A perspective of river basin development. *Law and Contemporary Problems*, 22(2), 156–187.
- Wilhite, D., Glantz, M.K., 1985. Understanding the drought phenomenon: The role of definitions. Drought Mitigation Center Faculty Publications (Paper 20).
- Willcocks, T.J., Twomlow, S.J., 1992. An evaluation of sustainable cultural practices for rainfed sorghum production on Vertisols in east Sudan. *Soil Tillage Res.* 24, 183–198. [https://doi.org/10.1016/0167-1987\(92\)90100-P](https://doi.org/10.1016/0167-1987(92)90100-P).
- Williams, C.A., Hanan, N.P., Neff, J.C., Scholes, R.J., Berry, J.A., Denning, A.S., Baker, D.F., 2007. Africa and the global carbon cycle. *Carbon Balance Manag.* 2 (3).
- Williams, M.A.J., 2009. Human Impact on the Nile Basin: Past, Present, Future. In: Dumont H.J. (eds) *The Nile. Monographiae Biologicae*, vol 89. Springer, Dordrecht

- Willmott, C.J., Matsuura, K., 2001. Terrestrial air temperature and precipitation: Monthly and annual time series (1950–1999). Center for Climatic Research, University of Delaware Available online at: http://climate.geog.udel.edu/~climate/html_pages/README.ghcn_ts2.html, (Accessed date: 12 July 2016).
- Woldegebriel, E., Smit, H., and Alex, B., 2012. Water distribution changes in Tuweir minor canal, Gezira Scheme. *Nile Basin Water Science & Engineering Journal*, 5 (2), 11–22.
- Woldesenbet, T.A., Elagib, N.A., Ribbe, L., Heinrich, J., 2017. Gap filling and homogenization of climatological datasets in the headwater region of the Upper Blue Nile Basin, Ethiopia. *Int. J. Climatol.* 37, 2122–2140. <https://doi.org/10.1002/joc.4839>
- World Bank, 1990. *The Gezira Irrigation Scheme in Sudan - objectives, design, and performance*. Washington, DC: World Bank.
- Worqlul, A.W., Dile, Y.T., Ayana, E.K., Jeong, J., Adem, A.A., Gerik, T., 2018. Impact of Climate Change on Streamflow Hydrology in Headwater Catchments of the Upper Blue Nile Basin, Ethiopia. *Water*, 10, 120; doi:10.3390/w10020120
- Wu, Y., 2017. Country-level net primary production distribution and response to drought and land cover change. *Sci. Total Environ.* 574, 65–77.
- Xiao, J., Sun, G., Chen, J., Chen, H., Chen, S., Dong, G., Gao, S., Guo, H., Guo, J., Han, S., Kato, T., Li, Y., Lin, G., Lu, W., Ma, M., McNulty, S., Shao, C., Wang, X., Xie, X., Zhang, X., Zhang, Z., Zhao, B., Zhou, G., Zhou, J., 2013. Carbon fluxes, evapotranspiration, and water use efficiency of terrestrial ecosystems in China. *Agric. For. Meteorol.* 182–183:76–90. <https://doi.org/10.1016/j.agrformet.2013.08.007>.
- Xie, P., Janowiak, J.E., Arkin, P.A., Adler, R., Gruber, A., Ferraro, R., Huffman, G.J., Curtis, S., Xie, P., Janowiak, J.E., Arkin, P.A., Adler, R., Gruber, A., Ferraro, R., Huffman, G.J., Curtis, S., 2003. GPCP Pentad Precipitation Analyses: An Experimental Dataset Based on Gauge Observations and Satellite Estimates. *J. Clim.* 16, 2197–2214. <https://doi.org/10.1175/2769.1>
- Xue, J., Su, B., 2017. Significant remote sensing vegetation indices: A review of developments and applications. *J. Sensors*. <https://doi.org/10.1155/2017/1353691>
- Yang, X., Blower, J.D., Bastin, L., Lush, V., Zabala, A., Masó, J., Cornford, D., Díaz, P., Lumsden, J., 2013. An integrated view of data quality in Earth observation. *Philos. Trans. A. Math. Phys. Eng. Sci.* 371, 20120072. <https://doi.org/10.1098/rsta.2012.0072>
- Yang, Y., Guan, H., Batelaan, O., McVicar, T.R., Long, D., Piao, S., Liang, W., Liu, B., Jin, Z., Simmons, C.T., 2016. Contrasting responses of water use efficiency to drought across global terrestrial ecosystems. *Sci. Rep.* 6, 23284. <https://doi.org/10.1038/srep23284>.
- Yee, S.H., Bradley, P., Fisher, W.S., Perreault, S.D., Quackenboss, J., Johnson, E.D., Bousquin, J., Murphy, P.A., 2012. Integrating Human Health and Environmental Health into the DPSIR Framework: A Tool to Identify Research Opportunities for Sustainable and Healthy Communities. *Ecohealth* 9, 411–426. <https://doi.org/10.1007/s10393-012-0805-3>
- Yihdego, Y., Khalil, A., Salem, H.S., 2017. Nile River's Basin Dispute: Perspectives of the Grand Ethiopian Renaissance Dam (GERD). *Global Journal of HUMAN-SOCIAL SCIENCE: B Geography, Geo-Sciences, Environmental Science & Disaster Management* 17 (2). Available online at: www.researchgate.net/publication/317372179_Nile_River's_Basin_Dispute_Perspectives_of_the_Grand_Ethiopian_Renaissance_Dam_GERD (Accessed 06.01.2020).
- Yilmaz, K.K., Hogue, T.S., Hsu, K.-L., Sorooshian, S., Gupta, H. V, Wagener, T., 2005. Intercomparison of Rain Gauge, Radar, and Satellite-Based Precipitation Estimates with Emphasis on Hydrologic Forecasting. *J. Hydrometeorology* 6, 497–517.

- Yim, O., Ramdeen, K.T., 2015. Hierarchical Cluster Analysis: Comparison of Three Linkage Measures and Application to Psychological Data. *Quant. Methods Psychol.* 11, 8–21. <https://doi.org/10.20982/tqmp.11.1.p008>
- Yletyinen, J., 2009. Holocene climate variability and cultural changes at River Nile and its Saharan surroundings. *Institutionen för naturgeografi och kvartärgeologi*. Stockholm. <https://www.diva-portal.org/smash/get/diva2:400169/FULLTEXT01.pdf>
- Yoffe S., 2002. Basins at Risk: Conflict and cooperation over international freshwater resources. Ph.D. Dissertation, Oregon State University, Corvallis, 97 pp.
- Yoon, S.-S., Phuong, A.T., Bae, D.-H., Yoon, S.-S., Phuong, A.T., Bae, D.-H., 2012. Quantitative Comparison of the Spatial Distribution of Radar and Gauge Rainfall Data. *J. Hydrometeorol.* 13, 1939–1953. <https://doi.org/10.1175/JHM-D-11-066.1>
- Zambelli, A.E., 2016. A data-driven approach to estimating the number of clusters in hierarchical clustering. *F1000Research* 5. <https://doi.org/10.12688/f1000research.10103.1>
- Zambrano-Bigiarini, M., 2011. Goodness-of-fit Measures to Compare Observed and Simulated Values with hydroGOF.
- Zambrano-Bigiarini, M., Baez-Villanueva, O.M., 2019. Characterizing meteorological droughts in data scarce regions using remote sensing estimates of precipitation, in: Maggioni, V., Massari, C. (Eds.), *Extreme Hydroclimatic Events and Multivariate Hazards in a Changing Environment - A Remote Sensing Approach*. Elsevier.
- Zambrano-Bigiarini, M., Nauditt, A., Birkel, C., Verbist, K., Ribbe, L., 2017. Temporal and spatial evaluation of satellite-based rainfall estimates across the complex topographical and climatic gradients of Chile. *Hydrol. Earth Syst. Sci. Discuss.* 0, 1–43. <https://doi.org/10.5194/hess-2016-453>
- Zappia, L., 2019. Visualise Clusterings at Different Resolutions. <https://cran.r-project.org/web/packages/clustree/clustree.pdf>
- Zhang, J., 2004. Risk assessment of drought disaster in the maize-growing region of Songliao Plain, China. *Agric. Ecosyst. Environ.* 102, 133–153. <https://doi.org/10.1016/J.AGEE.2003.08.003>
- Zhang, Y., Xu, M., Chen, H., Adams, J., 2009. Global pattern of NPP to GPP ratio derived from MODIS data: effects of ecosystem type, geographical location and climate. *Glob. Ecol. Biogeogr. Ecol. Biogeogr.* 18:280–290. <https://doi.org/10.1111/j.1466-8238.2008.00442.x>
- Zhang, Z., Moran, M.S., Zhao, X., Liu, S., Zhou, T., Ponce-Campos, G.E., Liu, F., 2014. Impact of prolonged drought on rainfall use efficiency using MODIS data across China in the early 21st century. *Remote Sens. Environ.* 150, 188–197.
- Zhao, M., Heinsch, F.A., Nemani, R.R., Running, S.W., 2005. Improvements of the MODIS terrestrial gross and net primary production global data set. *Remote Sens. Environ.* 95:164–176. <https://doi.org/10.1016/j.rse.2004.12.011>
- Zhao, M., Running, S.W., 2010. Drought-induced reduction in global terrestrial net primary production from 2000 through 2009. *Science* 329:940–943. <https://doi.org/10.1126/science.1192666>
- Zhao, M., Running, S.W., 2011. Response to comments on “drought-induced reduction in global terrestrial net primary production from 2000 through 2009”. *Science* 80 (333): 1093. <https://doi.org/10.1126/science.1199169>
- Zulkaflī, Z., Buytaert, W., Onof, C., Manz, B., Tarnavsky, E., Lavado, W., Guyot, J.-L., 2014. A comparative performance analysis of TRMM 3B42 (TMPA) versions 6 and 7 for hydrological applications over Andean–Amazon River Basins. *J. Hydrometeorol.* 15, 581–592. <https://doi.org/10.1175/JHM-D-13-094.1>

Appendices



Appendix A: Chapter 2

Table S2.1. List of data sources used to produce maps, tables, and graphs

No.	Data source	Website
1	GADM	www.gadm.org/index.html
2	WorldClim	www.worldclim.org/version2
3	GlobCover	www.due.esrin.esa.int/page_globcover.php
4	FAOSTAT	www.fao.org/faostat/en/#data/QC
5	AQUASTAT	www.fao.org/nr/water/aquastat/data/query/index.html?lang=en
6	World Bank database	www.data.worldbank.org/indicator
7	UN DESA population	www.population.un.org/wpp/Download/Standard/Population/

Appendix B: Chapter 3

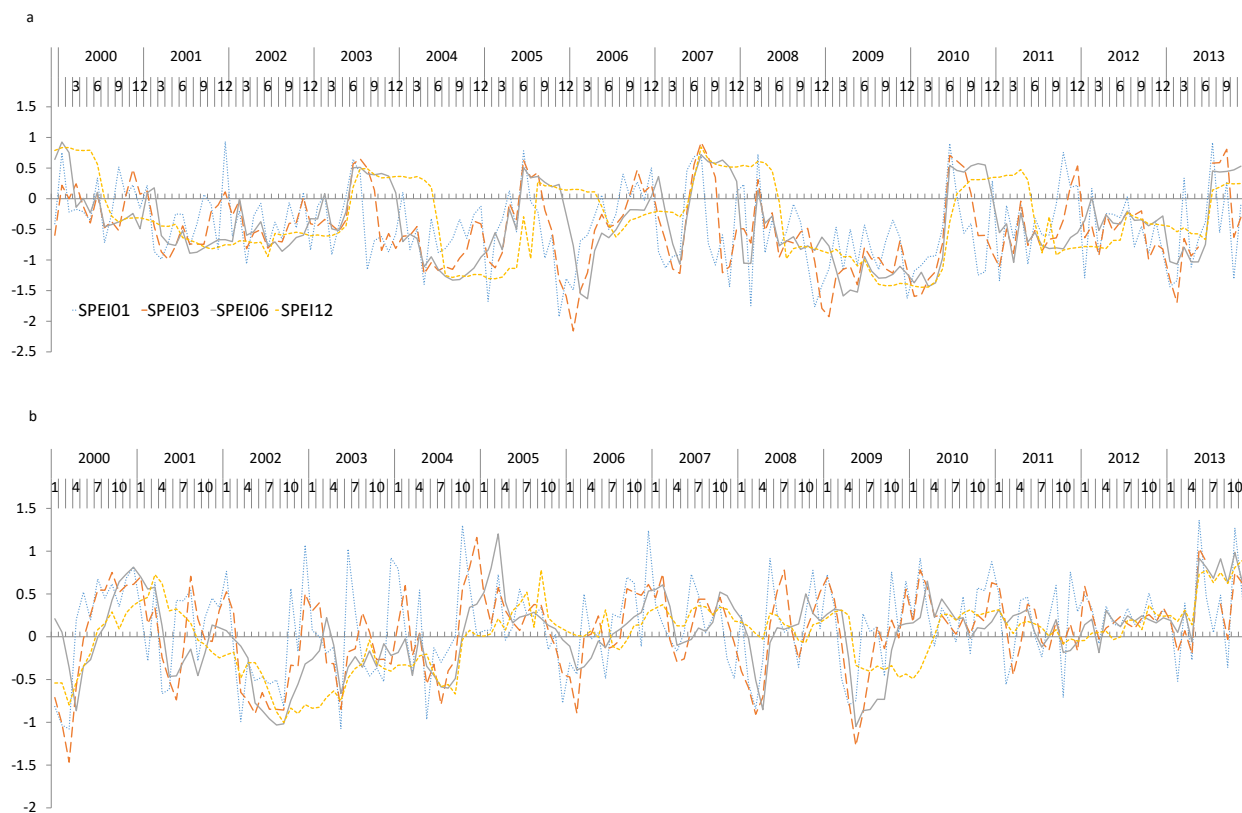


Fig. S3.1. Monthly time series of SPEI for (a) Sudan and (b) Ethiopia, with different time steps: 1, 3, 6 and 12 months.

	Precipitation	Temperature	SPEI01	SPEI03	SPEI06	SPEI12
CS	0.58	-0.05	0.70	0.73	0.68	0.53
CNV	0.65	-0.12	0.66	0.77	0.60	0.54
C	0.57	0.01	0.51	0.66	0.49	0.35
DBF	0.57	0.01	0.51	0.66	0.49	0.35
EBF	0.09	0.39	0.54	0.47	0.48	0.42
G	0.82	0.06	0.69	0.73	0.65	0.58
MF	0.20	0.35	0.51	0.59	0.51	0.47
OS	0.49	0.05	0.84	0.81	0.77	0.53
PW	0.68	0.53	0.33	0.63	0.35	0.19
S	0.41	0.11	0.42	0.93	0.46	0.38
WS	0.39	0.28	0.55	0.77	0.51	0.38

Values in bold are significant at $p=0.05$

Fig. S3.2. Spearman values of correlating NPP with precipitation, temperature, and SPEI with different time steps (1, 3, 6 and 12) for land cover types in Ethiopia.

	Precipitation	Temperature	SPEI01	SPEI03	SPEI06	SPEI12
C&NV	0.40	0.13	0.06	-0.09	0.06	-0.20
C	0.14	0.42	0.02	0.07	0.16	-0.03
G	0.30	0.43	0.09	0.04	0.16	-0.07
OS	0.34	0.41	-0.35	-0.22	-0.01	-0.24
S	0.20	0.43	-0.01	0.09	-0.04	-0.20
WS	0.20	0.35	-0.11	-0.15	-0.28	-0.39

Values in bold are significant at p=0.05

Fig. S3.3. Spearman values of correlating NPP with precipitation, temperature and SPEI with different time steps (1, 3, 6 and 12) for land cover types in Sudan.

		NDVI	Temperature	Precipitation	SPEI01	SPEI03	SPEI06	SPEI12
Sudan	Croplands	0.90	-0.42	0.68	0.32	0.58	0.22	0.09
	Grasslands	0.91	-0.33	0.58	0.29	0.59	0.20	0.02
Ethiopia	Croplands	0.95	-0.56	0.25	0.19	0.27	0.05	0.05
	Grasslands	0.93	-0.11	0.49	0.01	0.06	0.06	0.12

Values in bold are significant at p=0.05

Fig. S3.4. Spearman values of correlating intra-annual variation of GPP of croplands and shrublands in Sudan and Ethiopia with NDVI, temperature, precipitation, and SPEI with a drought of 1, 3, 6 and 12 months time scales. The correlation is conducted for years 2007 and 2009.

	Precipitation	Temperature	SPEI01	SPEI03	SPEI06	SPEI12
C&NV	0.28	0.33	-0.15	-0.07	0.10	-0.07
C	0.08	0.46	-0.02	0.01	0.09	-0.11
G	0.26	0.43	0.08	0.04	0.14	-0.07
OS	0.32	0.44	-0.40	-0.19	0.01	-0.25
S	0.20	0.52	-0.04	0.07	-0.07	-0.29
WS	0.17	0.38	-0.24	-0.14	-0.30	-0.42

Values in bold are significant at p=0.05

Fig. S3.5. Spearman values of correlating WUE and SPEI with a drought of 1, 3, 6 and 12 months time scales for land cover types in Sudan.

	Precipitation	Temperature	SPEI01	SPEI03	SPEI06	SPEI12
CS	0.42	-0.01	0.75	0.71	0.71	0.60
CNV	0.63	-0.27	0.67	0.82	0.61	0.59
C	0.39	-0.12	0.47	0.58	0.51	0.42
DBF	0.39	-0.12	0.47	0.58	0.51	0.42
EBF	0.34	0.04	0.74	0.72	0.72	0.64
G	0.62	-0.16	0.67	0.78	0.66	0.58
MF	0.11	0.45	0.58	0.66	0.55	0.41
OS	0.42	-0.10	0.92	0.75	0.91	0.68
PW	0.56	0.46	0.23	0.57	0.25	0.08
S	0.21	0.57	0.31	0.75	0.28	0.02
WS	0.51	0.17	0.73	0.91	0.69	0.65

Values in bold are significant at p=0.05

Fig. S3.6. Spearman values of correlating WUE and SPEI with a drought of 1, 3, 6 and 12 months time scales for Land cover types in Ethiopia.

	Precipitation	Temperature	SPEI01	SPEI03	SPEI06	SPEI12
C&NV	0.27	0.30	-0.07	-0.17	0.02	-0.13
C	-0.03	0.48	-0.10	-0.03	0.03	-0.07
G	0.22	0.49	0.02	-0.05	0.07	-0.14
OS	0.19	0.48	-0.32	-0.40	-0.14	-0.28
S	0.19	0.45	-0.02	0.02	-0.12	-0.27
WS	0.17	0.37	-0.09	-0.16	-0.30	-0.40

Values in bold are significant at p=0.05

Fig. S3.7. Spearman values of correlating CUE and SPEI with a drought of 1, 3, 6 and 12 months time scales for Land cover types in Sudan.

	Precipitation	Temperature	SPEI01	SPEI03	SPEI06	SPEI12
CS	0.51	-0.06	0.70	0.66	0.67	0.52
CNV	0.51	-0.02	0.73	0.85	0.61	0.56
C	0.24	0.21	0.26	0.31	0.22	-0.09
DBF	0.24	0.21	0.26	0.31	0.22	-0.09
EBF	0.20	0.22	0.60	0.56	0.55	0.43
G	0.56	-0.09	0.75	0.82	0.74	0.66
MF	-0.01	0.41	0.25	0.37	0.25	0.34
OS	0.28	-0.01	0.93	0.72	0.89	0.63
PW	-0.35	-0.38	0.01	0.27	0.01	0.02
S	-0.02	0.48	0.13	0.80	0.13	-0.06
WS	0.44	0.38	0.63	0.83	0.60	0.45

Values in bold are significant at p=0.05

Fig. S3.8. Spearman values of correlating CUE and SPEI with a drought of 1, 3, 6 and 12 months time scales for Land cover types in Ethiopia.

Appendix C: Chapter 4

Table S4.1. Summarized review of the previous studies conducted to compare different Public-domain precipitation products in the Blue Nile Basin (BNB) region.

	Author(s)	Area of study	PPs used	Temporal domain	Main findings
1	Abera et al. (2016)	UBNB	TRMM 3B42, CMORPH, TAMSAT, SM2R-CCI, and CFSR	daily (2003-2012)	<ul style="list-style-type: none"> • CMORPH, TAMSAT, and SM2R-CCI outperform SM2R-CCI and CFSR • PPs performs better in the high lands than over the lowlands
2	Allam et al. (2016)	UBNB	CRU TS 3.0, TRMM 3B43, GPCP	annual (2002-2012)	<ul style="list-style-type: none"> • TRMM 3B43 is the best performing PP
3	Ayehu et al. (2018)	UBNB	CHIRPS, TAMSAT 3.0; ARC 2.0	dekadal; monthly (2000-2015)	<ul style="list-style-type: none"> • CHIRPS showed better performance compared to ARC 2 and TAMSAT 3 • CHIRPS showed less dependency with elevation
4	Basheer et al. (2018)	LBNB	ARC 2.0, CHIRPS 2.0, PERCIANN-CDR, TAMSAT	Daily (1999-2007)	<ul style="list-style-type: none"> • ARC 2.0 shows the best performance compared to the other three PPs.
5	Fenta et al. (2018)	UBNB	TAMSAT, CHIRPS, ARC	daily; dekadal; monthly; seasonal (1995-2010)	<ul style="list-style-type: none"> • The three products are underestimating rainy events • TAMSAT showed better performance • all the products underestimate moderate and heavy rain rates
6	Gebremichael et al. (2014)	UBNB	CMORPH, TRMM 3B42, TRMM 3B42 RT	3-hourly (2012-2013)	<ul style="list-style-type: none"> • All the 3 PPs tend to overestimate the mean precipitation rate at the lowland plain sites but underestimate it at the highland mountain site. • The products are influenced by elevation • PPs are better representing the Q in hydrological modeling when they are first calibrated independently • All the products underestimate the precipitation compared to the rain gauges values
7	Lakew et al. (2017)	Gilgel Abbay (UBNB)	CMORPH, TRMM 3B42, ECMWF	daily (2000-2011)	<ul style="list-style-type: none"> • CMORPH and TRMM 3B42 RT are outperforming PERSIANN • CMORPH and TRMM 3B42 RT give good estimations for precipitation at highlands and overestimating precipitation at low lands • The elevation is influencing the performance of these products
8	Romilly and Gebremichael (2011)	UBNB	CMORPH, PERSIANN, TRMM 3B42	annual (2003-2007)	<ul style="list-style-type: none"> • CMORPH and TRMM 3B42 RT are outperforming PERSIANN • CMORPH and TRMM 3B42 RT give good estimations for precipitation at highlands and overestimating precipitation at low lands • The elevation is influencing the performance of these products
9	Sahlu et al. (2016)	UBNB	GPM (IMERG), CMORPH	wet season: daily and hourly (2014)	<ul style="list-style-type: none"> • The two products are approximately equivalent in performance • GPM (IMERG) showed relatively better performance compared to CMORPH. • The products are moderately underestimated precipitation.
10	Sahlu et al. (2017)	UBNB	TRMM, CMORPH, PERSIANN, ECMWF ERA Interim, MSWEP	daily (2000-2013)	<ul style="list-style-type: none"> • CMORPH showed the best performance during the wet season • MSWEP outperforms ERA-Interim
11	Valley et al. (2014)	UBNB	CMORPH, TMPA-RT v7, TMPA-RP v7.	seasonal (2012-2013)	<ul style="list-style-type: none"> • Elevation plays a role in the variation in performance of the products • The products are underestimated and overestimate precipitation at the low and high elevation areas, respectively • Underestimation of heavy rains and overestimation of the light rain are detected
12	Worqlul et al. (2014)	UBNB	TRMM 3B42, MPEG, CFSR	daily (2010)	<ul style="list-style-type: none"> • MPEG and CFSR are better performing than TRMM 3B42 • While TRMM 3B42 is unbiased, MAPEG and CFSR are systematically underestimating and overestimating P, respectively

Appendix D: Chapter 5

S5.1. Gezira Irrigation Scheme and Field survey

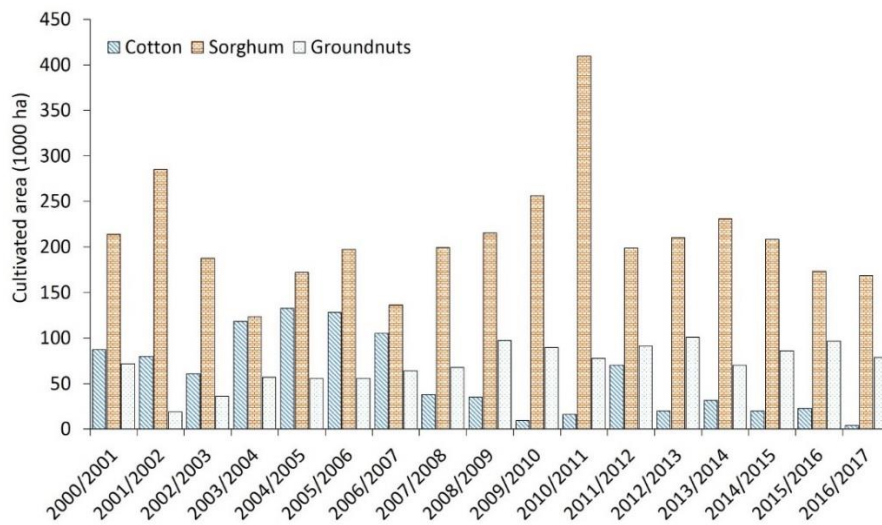


Fig. S5.1. The cultivated area of the main summer crops in the Gezira Scheme for the seasons 2000/2001 – 2016/2017.



Fig. S5.2. Problems in the irrigation canals in the Gezira Scheme: (a) weeds, (b) siltation, (c) improper maintenance resulted in different levels in the canals and (d) broken water gates.



Fig. S5.3. Main crops in the Gezira Scheme: (a) cotton, (b) groundnuts (c) sorghum and (d) chickpea during the 2017/2018 season.

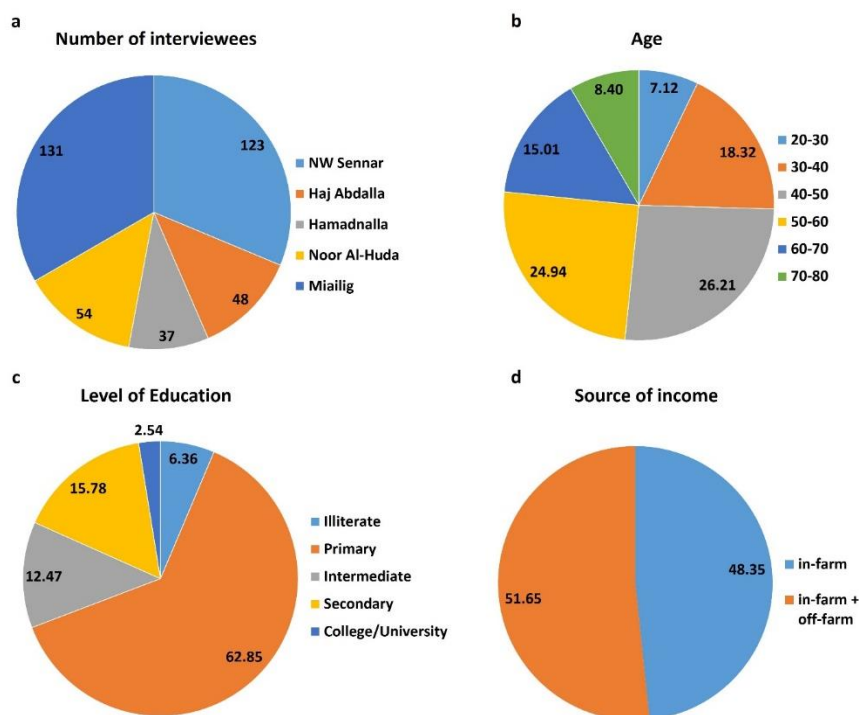


Fig. S5.4. Summary of socio-economic characteristics of the respondent farmers: (a) the number of interviewees in each block, (b) age, (c) level of education and (c) source of income. Values inside the pie charts b, c, and d are in percentage.

S5.2. Consistency of iNDVI and iFAPAR datasets

The data on iNDVI and iFAPAR indicators exhibited a significant positive correlation between the two indices ($p < 0.01$) at the pixel level. While the Spearman's Rho (ρ) value of correlating multi-year average (2001-2016) of iNDVI and iFAPAR was 0.72, correlating the maximum value composites of iNDVI and iFAPAR revealed expectedly lower ρ of 0.4 (Fig. S5.5). Using all pixel values for the years 2001-2016, the relative frequency distribution shows similar patterns but differences in the actual relative frequency values between the two indicators (Fig. S5.6). CV values of the time series of the two indicators were found to be 32% and 30% for iNDVI and iFAPAR, respectively. However, the difference between the two population variances using *T*-test was found to be significant. On the other hand, CVs for all pixel values of maximum iNDVI and maximum iFAPAR were around 14% and 18% for the two datasets, respectively (Fig. S5.7). The result of *F*-test showed a significant difference between the two population variances. The maximum iNDVI and iFAPAR share some similarities in their spatial distribution (Fig. S5.8). The differences in the spatial distribution could be attributed mainly to the difference in their spatial resolution. These results indicate that the two indicators are independent. Therefore, one should take the magnitude of the productivity gap derived by using them with caution.

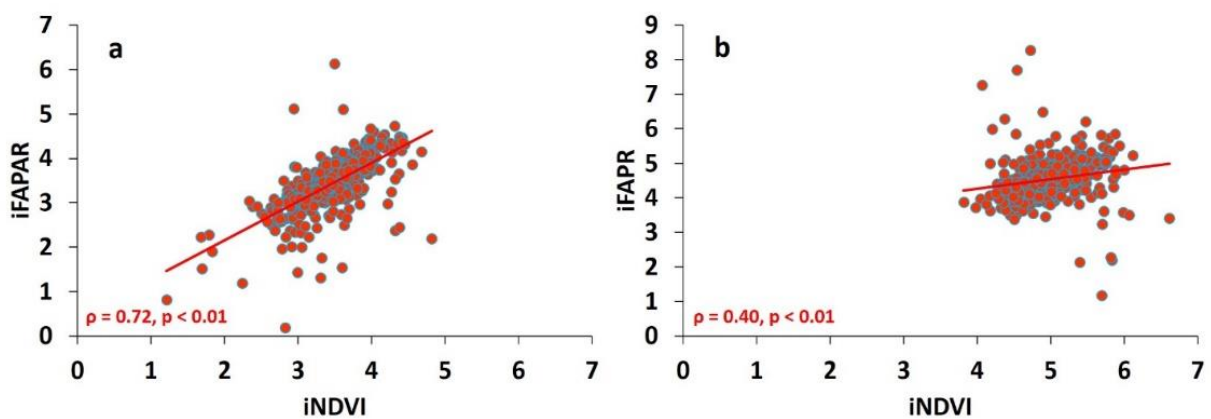


Fig. S5.5. Correlation between iNDVI and iFAPAR: (a) multi-year average (2001-2016), and (b) maximum value composite.

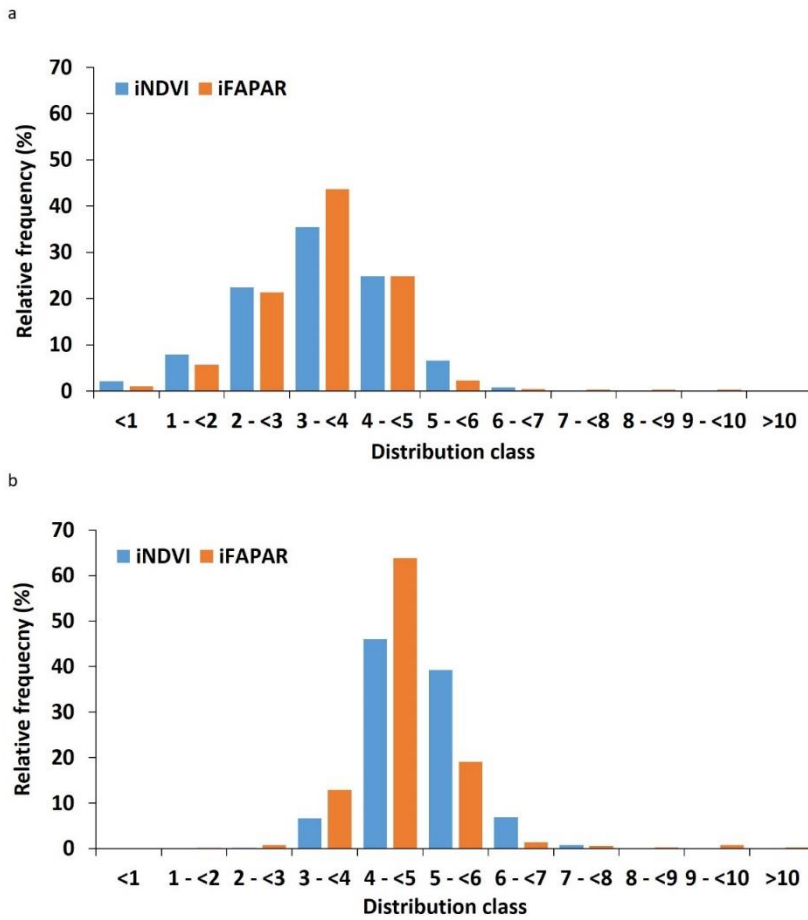


Fig. S5.6. Relative frequency distribution of all pixel values of (a) multi-year average and (b) maxima of iNDVI and iFAPAR over the whole Gezira Scheme for the period 2001-2016.

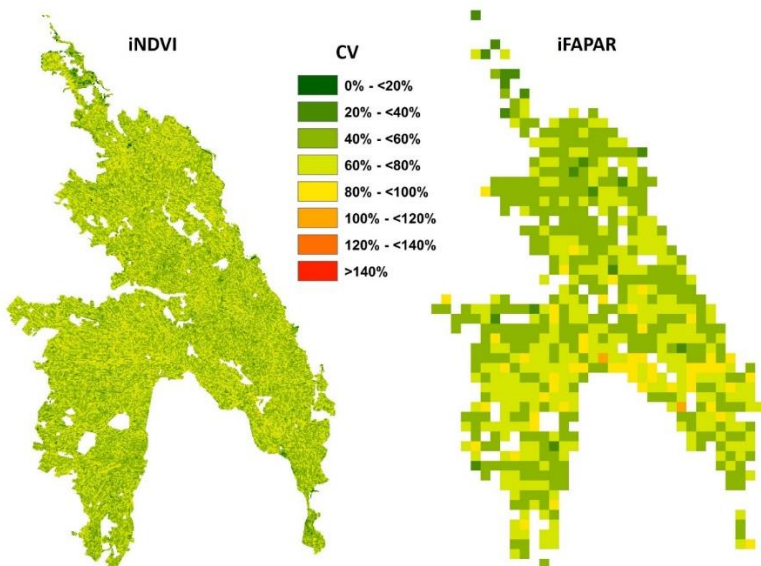


Fig. S5.7. Spatial distribution of coefficient of variation (CV) of iNDVI and iFAPAR for the period 2001-2016 over the Gezira Scheme.

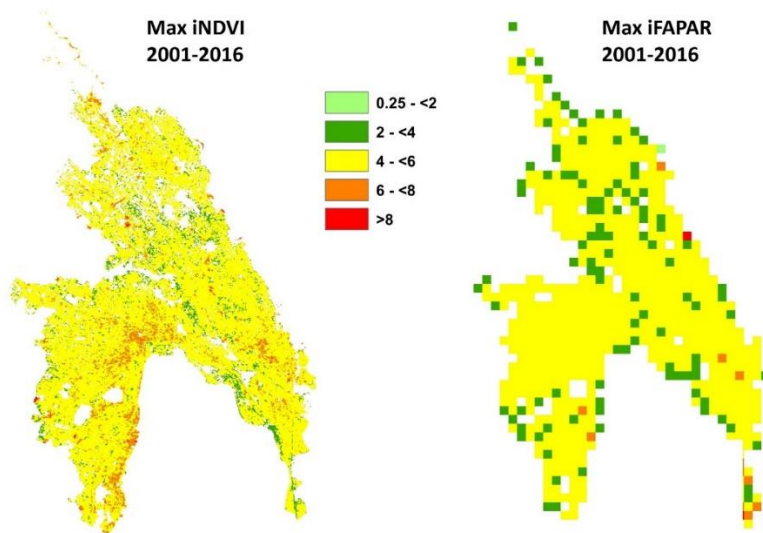


Fig. S5.8. Maximum productivity levels created from the iNDVI and iFAPAR datasets for the years 2001-2016 using the Maximum Value Composite (MVC) method.

S5.3. Cultivated area and sorghum yield in Gezira Scheme during 2015 and 2016

Taking the years 2015 and 2016 as examples of low and high productivity levels, respectively, it could be noted that while there are no large differences in the cultivated areas of sorghum, large differences in the average yield were detected for the two years (Fig. S5.9).

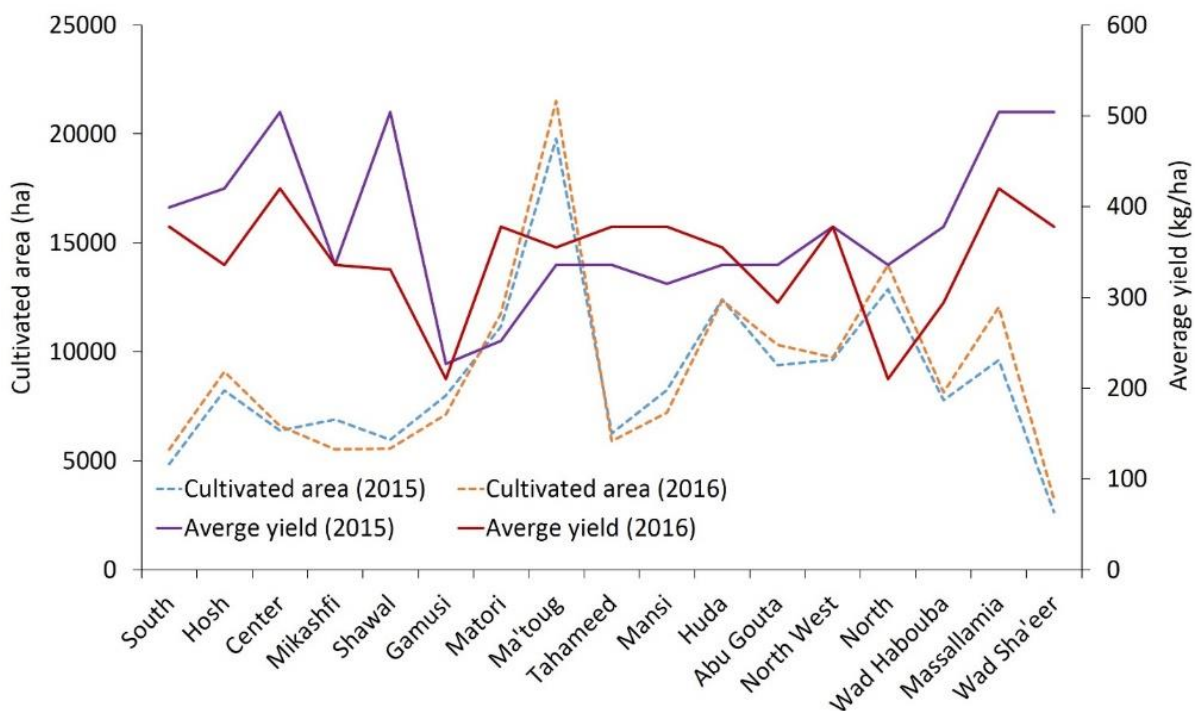


Fig. S5.9. Comparison between the cultivated area and average yield of sorghum for years 2015 and 2016 at the level of administrative groups.

	Average yield	Source of income	Age	No. household members	Experience in agriculture	Farm size	Location along tertiary canal	No. irrigation event	Seed density	Frequency of fertilizer application	Quantity of fertilizer	First irrigation	Sowing date	Land preparation
Average yield	1	0.62**	0.1	0.12*	0.05	0.16**	-0.56**	0.27**	-0.01	0.40**	0.47**	-0.16**	-0.22**	-0.22**
Source of income		1	0.06	0.06	0.01	0.17**	-0.34**	0.22**	-0.1	0.27**	0.30**	0.01	-0.12*	-0.14**
Age			1	0.10*	0.51**	0.13**	-0.04	-0.02	0.09	0.04	0.04	-0.09	-0.08	-0.07
No. household members				1	0.09	0.06	-0.07	0.06	0.06	0.08	0.09	-0.05	-0.02	-0.03
Experience in agriculture					1	0.09	0.01	0.02	0.03	0.02	0.04	-0.02	-0.1	-0.07
Farm size						1	-0.16**	0.06	-0.03	0.08	0.15**	-0.03	-0.07	-0.06
Location along tertiary canal							1	-0.46**	-0.04	-0.30**	-0.37**	0.11*	0.12*	0.08
No. irrigation event								1	0.02	0.19**	0.14**	-0.01	0.02	0.03
Seed density									1	0.04	0.02	-0.08	0.04	0.02
No. of application										1	0.66**	-0.04	-0.01	-0.06
Quantity											1	-0.12*	-0.14**	-0.17**
First irrigation												1	0.01	0.03
Sowing date													1	0.93**
Land preparation														1

* Correlation is significant at p level of 0.05
 ** Correlation is significant at p level of 0.01

Fig. S5.10. Matrix of spearman’s Rho (ρ) values shows the degree of correlation between the main average sorghum yield, socio-economic factors and field practices of farmers.

Appendix E: Erklärung

Ich versichere, dass ich die von mir vorgelegte Dissertation selbständig angefertigt, die benutzten Quellen und Hilfsmittel vollständig angegeben und die Stellen der Arbeit – einschließlich Tabellen, Karten und Abbildungen –, den anderen Werken im Wortlaut oder dem Sinn nach entnommen sind, in jedem Einzelfall als Entlehnung kenntlich gemacht habe; dass diese Dissertation noch keiner anderen Fakultät oder Universität zur Prüfung vorgelegen hat; dass sie – abgesehen von unten angegebenen Teilpublikationen – noch nicht veröffentlicht worden ist sowie, dass ich eine solche Veröffentlichung vor Abschluss des Promotionsverfahrens nicht vornehmen werde. Die Bestimmungen der Promotionsordnung sind mir bekannt. Die von mir vorgelegte Dissertation ist von Prof. Dr. Karl Schneider betreut worden.

Köln, den 23.03.2020

Folgende Teilpublikationen liegen vor:

	Title of publication	Type of publication	My contribution
1	Khalifa, M. , Thomas, S., Ribbe, L., 2020. The Nile River Basin, in: Schmandt, J., North, G., Ward, G., Kibaroglu, A., (eds). Sustainability of engineered rivers in arid lands: Challenge and Response. Cambridge University Press (In preparation).	Book chapter	<ul style="list-style-type: none"> - Participated in designing the chapter - Processing and visualizing gridded and other public-domain datasets - Assisting in data analysis and literature review - Writing major sections of the chapter
2	Khalifa, M. , Elagib, N.A., Ribbe, L., Schneider, K., 2018. Spatio-temporal variations in climate, primary productivity and efficiency of water and carbon use of the land cover types in Sudan and Ethiopia. <i>Science of the Total Environment</i> , 624, 790–806.	Original paper	<ul style="list-style-type: none"> - Concept development and study design - Data processing - Data analysis - Results interpretation - Writing the first draft of the manuscript
3	Khalifa, M. , Korres, W., Saif, S., Elagib N.A., Baez-Villanueva O.M., Bahseer, M., Ayyad, S., Ribbe L., Schneider K., 2020. Consistency of public-domain precipitation products: coupling traditional validation approaches with data mining techniques.	Original paper	<ul style="list-style-type: none"> - Concept development and study design - Data processing - Data analysis - Results interpretation - Writing the first draft of the manuscript
4	Khalifa, M. , Elagib, N.A., Bashir, M.A., Ribbe, L., Schneider, K., 2020. Exploring socio-hydrological determinants of crop yield in under-performing irrigation schemes: Pathways for sustainable intensification. <i>Hydrological Sciences Journal</i> , 55 (2), 153-168.	Original paper	<ul style="list-style-type: none"> - Concept development and study design - Field survey - Data processing - Data analysis - Results interpretation - Writing the first draft of the manuscript
5	Elagib, N.A., Khalifa, M. , Rahma, A.E., Babker, Z., Gamaledin, S.I., 2019. Performance of major mechanized rainfed agricultural production in Sudan: Sorghum vulnerability and resilience to climate since 1970. <i>Agricultural and Forest Meteorology</i> , 276–277, 107640.	Original paper	<ul style="list-style-type: none"> - Participated in concept development and study design - Processing of remote sensing data - Engaged in data analysis - Participated in results interpretation - Participated in writing the manuscript

Appendix F: Curriculum Vitae (CV)

MUHAMMAD KHALIFA

ACADEMIC QUALIFICATIONS

- **Doctor of Philosophy (Ph.D.) in Science**
– May 2020 (expected)

Institute of Geography, University of Cologne

- **Master of Science (double degree) -**
2012

Institute for Technology and Resources
Management in the Tropics and Subtropics (ITT),
Cologne University of Applied Sciences, Cologne,
Germany and University of Jordan, Jordan

- **Master of Science - 2010**

Earth and Environmental Sciences Department
Sana'a University, Yemen

- **Bachelor of Science - 2004**

Earth and Environmental Sciences Department
Sana'a University, Yemen

AREAS OF EXPERTISE

- Water-Food-Climate Nexus
- Remote sensing applications
- GIS analysis and modeling
- Data mining and data analysis
- Climate variability and land cover changes
- Hydrological and crop modeling
- Geology and Environment

KEY SKILLS

- Processing and analyzing remote sensing data of various formats (e.g. Tiff, NetCDF, HDF)
- Hydrological modeling
- Statistical analysis
- Planning and organizing field works
- Good writing and presentation skills

OTHER SKILLS

Languages: Arabic (Native), English (Fluent), German (Basic)

Computer skills: GIS (ArcGIS, QGIS), remote sensing (ENVI, ERDAS), water allocation modeling (WEAP, RIBASIM), Crop modeling (MABIA, Cropwat, AquaCrop, APSIM), Data mining (Orange), hydrological modeling (HBV, VIC), statistical analysis and data processing (R, SPSS, XLSTAT), Image processing (CorelDraw), and Microsoft office package (Word, Excel, PowerPoint, Access).

ADDITIONAL TRAINING

- Effective poster presentation and improving presentation skills
- Scientific writing and publishing
- Hydrological modeling
- Spatio-temporal data analysis using R
- Remote sensing for drought assessment and water balance studies
- Preparation of remote sensing training

COMMUNITY SERVICES

- Reviewer for:
 - Science of the Total Environment (Elsevier)
 - Arid Land Research and Management (Taylor and Francis)
 - Hydrological Sciences Journal (Taylor and Francis)
 - Advances in Meteorology (Hindawi)
 - Scientific Reports (Nature)
 - Remote Sensing (MDPI)
- Lead author of the Global Environment Outlook (GEO6) report for youth - Africa and Global Editions, UN Environment.
- Participate in organizing scientific sessions on water assessment and modeling in the Water Security and Climate Change (WSCC2017) conference, Cologne, Germany and organizing and moderating a session on water-energy nexus in WSCC2019, San Luis Potosi, Mexico.

PUBLICATIONS AND PRESENTATIONS

Key publications:

1. **Khalifa M.**, Korres, W., Saif, S., Elagib N.A., Baez-Villanueva O.M., Bahseer, M., Ribbe L., Schneider K., 2020. Consistency of public-domain precipitation products over the Blue Nile Basin: coupling traditional validation approaches with data mining techniques (Submitted).
2. **Khalifa M.**, Thomas S., Ribbe L., 2020. The Nile River Basin, in: Schmandt, J., North, G., Ward, G., Kibaroglu, A., (eds). Sustainability of engineered rivers in arid lands: Challenge and Response. Cambridge University Press (In preparation).
3. Elagib N.A., **Khalifa, M.**, Rahma, A.E., Babker Z., and Gamaledin S.I., 2019. Performance of major mechanized rainfed agricultural production in Sudan: Sorghum vulnerability and resilience to climate since 1970. *Agricultural and Forest Meteorology*, 276-277.
4. **Khalifa M.**, Elagib N.A., Bashir M.A., Ribbe L., Schneider K., 2020. Exploring socio-hydrological determinants of crop yield in under-performing irrigation schemes: Pathways for sustainable intensification, *Hydrological Sciences Journal*, 55 (2), 153-168.
5. Aboelnga H.T., **Khalifa M.**, McNamara I., Ribbe L., and Sycz J., 2018. Water-Energy-Food Nexus - A Review of Nexus Literature and ongoing Nexus Initiatives for Policymakers. German Agency for International Cooperation (GIZ).
6. **Khalifa M.**, Elagib N.A., Ribbe L., Schneider K., 2018. Spatio-temporal variations in climate, primary productivity and efficiency of water and carbon use of the land cover types in Sudan and Ethiopia. *Science of the Total Environment*, 624, 790-806.

Selected presentations in conferences, seminars and workshops

1. **Khalifa, M.**, and Ribbe, L., 2020. Assessing multi-satellite products in characterizing drought in the Blue Nile Basin. the 2nd International Water Conference on Water Resources in Arid Areas (WRAA 2020), Muscat, Oman. March 16-19, 2020 (Oral presentation).
2. Ayyad, S., **Khalifa, M.**, 2019. Vertical or horizontal growth? Food production in the Nile Basin – An outlook from water and land perspectives. Water Security and Climate Change Conference, San Luis Potosi, Mexico, 28-30 October 2019 (Oral presentation)
3. Ribbe, L., **Khalifa, M.**, Basheer M., Ayyad S., Nauditt A., and Babker. Z., 2018. Water-Energy-Food Nexus Accounting for the Eastern Nile Basin. American Geophysical Union (AGU), 2018 Fall Meeting, 10-14 December 2018, Washintgon DC., USA (poster presentation).
4. **Khalifa, M.**, 2017. Impact of climate variability on water and food and its role in migration. Regional workshop on international migration from the Horn of Africa to Sudan and from there onwards, Gedaref. 27-30 November 2017 (Oral presentation)
5. **Khalifa, M.**, 2017. Tools for water accounting: A comparison of rainfall data from open sources. Water balance and accounting for the Eastern Nile using advanced tools workshop, Khartoum. 13-18 November 2017 (Oral presentation).
6. **Khalifa, M.**, 2017. Crop yield gap: a challenge and opportunity for food security, case of Sudan. Water Security and Climate Change Conference, Cologne, 18-21 September 2017 (Poster presentation)